School of Pharmacy and Biomedical Sciences

Ageing and Mesothelioma Drive Lipid Accumulation and Dysfunction in Dendritic Cells and Macrophages

Mohd Sheeraz

This thesis is presented for the Degree of

Doctor of Philosophy

of

Curtin University

May 2022

Declaration

To the best of my knowledge and belief this contains no material previously published by any other person except where due acknowledgement has been made.

This thesis contains no material which has been accepted for the award of any other degree or diploma in any university.

Human Ethics The research presented and reported in this thesis was conducted in accordance with the National Health and Medical Research Council National Statement on Ethical Conduct in Human Research (2007) – updated March 2014. The proposed research study received human research ethics approval from the Curtin University Human Research Ethics Committee (EC00262), Approval Number # HRE2017-0823.

Animal Ethics The research presented and reported in this thesis was conducted in compliance with the National Health and Medical Research Council Australian code for the care and use of animals for scientific purposes 8th edition (2013). The proposed research study received animal ethics approval from the Curtin University Animal Ethics Committee, #Approval number #AEC_2016_04.

Signature: …….

Date: ……

Acknowledgements

Firstly, thank you to my supervisors, Associate Professor Delia Nelson, Dr Connie Jackaman, and Associate Professor Cyril Mamotte for your continuous support, guidance, and mentorship, and for sharing your extensive knowledge and expertise. I am really appreciative of all your effort, dedication, and enthusiasm you have devoted to my studies. Thank you also for not only guiding me through my studies, but looking out for my health and well-being as well. I could not have asked for kinder, more caring supervisors and I will be forever grateful for everything you have done for me.

Thank you to Associate Professor Elizabeth Watkin, the chairperson of my thesis committee, for your help and support.

I would like to acknowledge Curtin University for providing the scholarships that assisted me throughout my PhD. I would also like to acknowledge the School of Pharmacy and Biomedical Sciences, the Curtin Health Innovation Research Institute (CHIRI), and the Curtin University Animal Facility for providing the resources which enabled me to complete my project, and to the staff in these departments for their technical guidance and expertise. I would also like to thank our collaborators, Dr Rodrigo Carlessi from Curtin University.

To the current members especially Wei Khei and Lelinh Duong, and previous members of the Nelson laboratory group especially Joanne Gardner, thank you for all of the support, friendship, laughter, and memorable moments over the years. You made all of the early mornings, late nights, and long days enjoyable. You have all been wonderful and I am truly lucky to have been part of such an amazing group, and to have made lifelong friendships. Thank you also to my friends and colleagues from the School of Pharmacy and Biomedical Sciences and CHIRI for your smiles and kind words. In particular, to my lab partner Wahed, I am so glad to have had you by my side through this journey. It has been so much fun sharing a desk with you, working side by side in the lab. Thank you for making me smile and helping me to overcome challenges, and for always being there.

I would also like to thank my team members at Fiona Stanley Hospital who supported me and encouraged me.

Last, but certainly not least, a massive thank you to Sana and my parents for their constant love, care, support, encouragement, and confidence in me, not just in my studies, but in all aspects of my life. Completing my PhD is as much your success as it is mine. Thank you for always being there, taking care of me, and giving me the best of what life has to offer. I am privileged to have both of you as parents, and there are not enough words to express my gratitude. Thank you from the bottom of my heart.

Abstract

The immune system can protect us from cancer however, tumours modulate immune function to enable cancer progression. Moreover, age-related changes may contribute to increased cancer incidence in the elderly. Previous studies have examined the effect of age and mesothelioma separately on macrophages and dendritic cells (DCs). This is the first study to examine the combined effect of age and mesothelioma on macrophages and DCs. This study also examined the effect of soluble factors from mesothelioma tumour cells (using conditioned media) on metabolic processes in murine bone marrow-derived DCs and human monocyte-derived DCs (MoDCs), as DCs regulate T cells with effector function against cancerous cells. Thus, this thesis aimed to: (i) examine changes to murine macrophage subsets in young and elderly mice with mesothelioma; (ii) examine changes to DC subsets in young versus elderly mice with mesothelioma; and (iii) investigate metabolic changes induced by mesothelioma in human and murine DCs by comparing the glycolytic and mitochondrial profiles of healthy DCs to DCs exposed to mesothelioma-derived soluble factors.

This thesis showed that healthy ageing (i) had no effect on lipid levels and costimulatory molecule expression levels in macrophages, (ii) the percentage of major histocompatibility complex (MHC-I^+) DCs increased in dLNs and alongside increased expression of MHC-II in spleens and BM suggesting maintenance or even improved ability of DCs to prime $CD8^+$ and $CD4^+$ T cells.

This thesis also showed that when ageing hosts have mesothelioma (i) there is an increase in lipid accumulation in macrophages that is associated with upregulated CD36 and CD147 expression. This was not associated with changes to CD80 and CD40 expression but was associated with decreased MHC-I and MHC-II suggesting a reduced capacity to activate tumour infiltrating $CD8^+$ and $CD4^+$ T cells, (ii) all tumour infiltrating DC subsets reduce MHC-II expression with the percentage of MHC-I^+ pDCs significantly reduced in elderly tumours relative to young tumours. All other DC subsets trended towards decreased MHC-I which may represent a strategy used by tumours to escape CTL recognition, especially if these DC migrate to LNs.

The final part of the study examined changes in cellular metabolism measured using Seahorse technology. When activated by bacterial lipopolysaccharide (LPS), DCs

demonstrated a metabolic switch characterized by an increased extracellular acidification rate and a progressive loss of oxidative phosphorylation suggesting a metabolic transition towards Warburg metabolism, commonly associated with immune cell activation. In contrast, mesothelioma exposed DCs demonstrated a simultaneous increase in glycolysis and oxidative phosphorylation. High mitochondrial respiration and glycolytic capacity represent a characteristic profile of tolerogenic DCs.

To summarise, the study found that ageing and mesothelioma upregulate expression of the scavenger receptors CD36 and CD147 which is associated with increased lipid accumulation in macrophages and DCs. MHC-I and MHC-II expression decreased in all tumour-associated macrophages (TAMs) and tumour-associated DCs, suggesting a reduced capacity to activate tumour infiltrating $CD8^+$ and $CD4^+$ T cells, thereby providing an advantage for mesothelioma in elderly hosts. DCs exposed to mesothelioma-derived factors were skewed more towards a tolerogenic state by simultaneously upregulating glycolysis and OXPHOS which could account for DC/macrophage dysfunction in elderly hosts with mesothelioma.

Contents

List of Tables

List of Figures

List of supplementary figures

List of Appendices

List of abbreviation

ADP	Adenosine diphosphate
APCs	Antigen presenting cells
APS	Ammonium Persulfate
BCA	Bicinchoninic acid
BM	Bone marrow
CDP	Common dendritic cell progenitor
cDC	Conventional DC
cMOP	Common monocyte progenitor
CMP	Common myeloid progenitor
CSFR-1	Colony stimulating factor receptor 1
CTLA	Cytotoxic T-lymphocyte-associated protein
CXCL	C-X-C motif chemokine ligand
DC	Dendritic cell
dLN	Draining lymph node
EDTA	Ethylenediaminetetraacetic acid
ERK	Extracellular signal regulated kinase
ETC	Electron transport chain
FAO	Fatty acid oxidation
FAS	Fatty acid synthesis
FCS	Fetal calf serum
FCCP	Carbonyl cyanide-4(trifluoromethoxy) phenylhydrazone
FLT3	Fms like tyrosine kinase 3
GAPDH	Glyceraldehyde 3-phosphate dehydrogenase

GCR	Glucocorticoid receptor
G-CSF	Granulocyte-colony stimulating factor
GM-CSF	Granulocyte-macrophage colony-stimulating factor
GMP	Granulocyte macrophage progenitor
GPT	Glutamic pyruvic transaminase
HK	Hexokinase
HRP	Horseradish peroxidase
ICOS	Inducible co-stimulatory molecule
IDO	Indoleamine 2-3 dexoygenase
IFN-γ	Interferon-γ
IL	Interleukin
IRF	Interferon regulatory factor
JAK2	Janus kinase
LCs	Langerhans cells
LDH	Lactate dehydrogenase
LDL	Low density lipoproteins
LDLr	Low density lipoprotein receptor
LOX	Lectin type oxidised LDL receptor
LN	Lymph node
LPS	Lipopolysaccharides
M-CSF	Macrophage colony-stimulating factor
mDCs	Myeloid DCs
MDP	Macrophage dendritic cell progenitor
MDSC	Myeloid-derived suppressor cell
MHC	Major Histocompatibility Complex
MoDC	Monocyte-derived dendritic cell
MPS	Mononuclear phagocyte system
Msr	Macrophage scavenger receptor
NADH	Nicotinamide adenine dinucleotide
NF-κB	Nuclear factor-kappa B

NK	Natural killer
OCR	Oxygen consumption rate
OXPHOS	Oxidative phosphorylation
PBMCs	Peripheral blood mononuclear cells
PBS	Phosphate-buffered saline
PD-1	Programmed cell death protein 1
PD-L1	*Programmed death-ligand 1*
PEP	Phosphoenolpyruvate
PFK	Phosphofructokinase
PGC-1β	PPARγ coactivator-1β
PK	Pyruvate kinase
PPAR-γ	Peroxisome proliferator-activated receptor γ
PPP	Pentose phosphate pathway
ROS	Reactive oxygen species
SDS-PAGE Electrophoresis	Sodium Dodecyl Sulphate Polyacrylamide Gel
SP	Specificity protein
STAT	Signal transducer and activation of transcription
TAMs	Tumour-associated macrophages
TBS	Tris-buffered saline
TCA	Tricarboxylic acid
TCM	Tumour conditioned media
TEMED	Tetramethylethylenediamine
TLR-4	Toll-like receptor-4
TGF	Transforming growth factor
TNF	Tumour necrosis factor
TYK	Tyrosine kinase
VLDLr	Very low-density lipoprotein receptor
YS	Yolk sac

This page has been left blank intentionally

Chapter 1: Introduction

1.1 Introduction

Mesothelioma is one of the most aggressive forms of cancer that develops from cells of the mesothelium, a protective lining that covers many internal organs [1, 2]. About 70% cases of mesothelioma are caused by exposure to asbestos [3, 4]. Other possible causes of mesothelioma, such as radiation exposure and viral infections are under debate. Mesothelioma in its early stages is difficult to diagnose as there are no clinical symptoms therefore it is usually diagnosed at advanced stages [5]. Current treatments for mesothelioma include standard clinical therapeutic approaches such as surgery, radiotherapy and chemotherapy [4]. Only a minority of the patients are eligible for surgery, and limited clinical studies make it hard to draw definite conclusions on the survival benefit of surgery in mesothelioma [6-8]. Radiotherapy may be used to prevent local tumour outgrowth at intervention sites These sites arise mostly from invasive pleural interventions to facilitate diagnosis or alleviate symptoms from malignant pleural effusions [9]. However, mesothelioma cells can seed along the intervention site tract resulting in the formation of painful and unsightly subcutaneous metastasis. As a result, radiotherapy is used to try to prevent these procedure tract metastases from developing [10]. Currently, the only treatment for mesothelioma that has proven to be successful is chemotherapy, however often only a life extension of 3-10 months is achieved [11].

There is increasing evidence that this cancer is susceptible to immunotherapy with studies examining anti-mesothelioma immune responses with or without therapy in young and elderly hosts [12-17]. Evidence that the immune system plays a role in human mesothelioma development/progression has been shown by Anraku [18] and Yamada [19] who demonstrated that $CD8^+$ T cell infiltration into human mesothelioma is associated with better outcomes. However, Uijie et al [20] showed that tumour $CD4^+$ T cell infiltration is associated with better survival in epithelioid mesothelioma. Both studies show that the immune system recognizes progressing mesothelioma. As a result, there is an increasing interest in cancer immunotherapy to treat mesothelioma. Several studies have been conducted in mouse models of mesothelioma.

One approach tested was using DC-based immunotherapy to amplify the anti-tumour response [21-23]. Hegmans et al found that mesothelioma outgrowth was prevented by immunizing mice with tumour lysate pulsed DCs [24]. Other immunotherapy approaches include checkpoint blockade using anti-PD-L1 monoclonal antibodies [25], anti-CTLA-4 monoclonal antibodies [26], or both [25]. Tan et al demonstrated that CTLA-4 alone had minimal efficacy, better results were seen in combination with PD-1, leading to 60% complete remission [25]. Earlier studies in our group using young mice demonstrated increased CTL activity driven by IL-2 combined with an agonist anti-CD40 monoclonal antibody [27, 28]. However, mesothelioma often presents in the elderly population with a median age of presentation of 68 years for peritoneal mesothelioma and 74 years for pleural mesothelioma [29]. In our group, Duong et al showed that IL-2/CD40 immunotherapy led to full mesothelioma regression in young mice with a 90% survival rate, while the survival rate in elderly mice reduced to 38%. Interestingly, that study also showed that macrophages interfered with responses in elderly, but not young mice. Macrophage depletion improved responses to IL-2/CD40 immunotherapy [30]. These studies show that macrophages in the elderly function differently to younger hosts.

There are two types of immune responses; innate and adaptive (acquired) responses [31]. The innate response involves barriers such as the skin [32] as well as cells such as dendritic cells (DCs), macrophages and natural killer (NK) cells. DCs and macrophages are antigen presenting cells (APCs) that form an important link between the innate and acquired immune responses [33, 34].

Most of our current understanding of macrophages and DCs, which are a part of mononuclear phagocyte system (MPS), come from studies using murine models and adult humans [35]. These cell types play an important role in the induction and maintenance of immune responses. Macrophages were first described by Ilya Metchnikoff in 1882 [36], while DCs were discovered by Ralph Steinman in 1970 [37]. DCs were initially proposed to be distinct from macrophages [38] and defined as "*dendritic-shaped cells that can process and present antigen to activate naive T cells*" [39], however, it is now clear that other cells can be dendritic in appearance and that not all DCs are dendritic or immunostimulatory [40]. The role of macrophages and DCs in mesothelioma progression remains unclear and is the focus of this thesis

1.1.1. Development of macrophages

Macrophages were first discovered by Ilya Metchnikoff in the late 19th century [36] and they were cells that phagocytose particulate material and microbes as well as regulate the activation of T and B lymphocytes [41]. Macrophages can be activated by a large range of factors including lipopolysaccharides (LPS) via Toll-like receptor-4 (TLR-4) which has been confirmed as a transmembrane receptor with an extracellular LPS binding domain [42], or cytokines such as interferon-γ (IFN-γ) [43]. Mantovani and colleagues grouped macrophages as M1 and M2 cells based on selective markers [44]. M1 macrophages include IFN-γ + LPS-activated cells [45]. M2 cells include interleukin-4 (IL-4) or IL-13-activated cells [46].

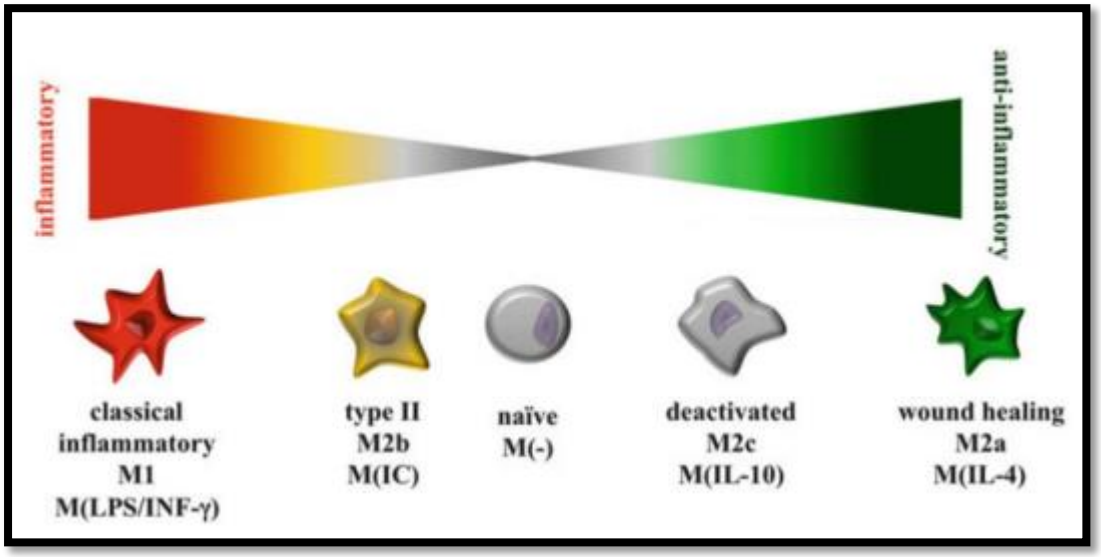

Figure 1.1: Macrophage activation states

Image taken from: Macrophages: Origin, Functions and Bio intervention. Book editor Kloc, Malgorzata [47]

It is now recognised that macrophage activation states represent a continuum ranging from pro-inflammatory or M1-like macrophages to anti-inflammatory or M2-like macrophages (Figure 1.1) [48]. M2 cells have been further subdivided into other activation states such as M2a or alternatively activated cells (induced by IL-4 or IL-13; sitting at the far right of the continuum shown in Figure 1.1); M2b, induced by TLRs agonists (like LPS); and M2c, induced by glucocorticoid hormones or IL-10 [44]. Figure 1.1 depicts the M2b (or type II) and M2c types lying between

inflammatory and anti-inflammatory macrophages [47]. Before they were named M2b cells, Moser and Anderson had previously reported distinct phenotypes that were different to M1 and M2 cells and induced by LPS plus anti-ovalbumin antibody (OVA) IgG/OVA immune complex or anti-sheep erythrocyte IgG/erythrocytes immune complex [44, 49]. M2b activation in human macrophages and monocytes is driven by FcγRII (CD32) [50] and in terms of function, M2b macrophages are reported to represent the only example of macrophages that crosstalk with B cells [51].

Inflammatory macrophages M1-like cells are also known as classically activated macrophages, whilst anti-inflammatory M2-like macrophages are also known as wound healing macrophages and these activation states form two extreme parts of a continuum [52, 53]. Resting macrophages corresponds to naïve macrophages (unstimulated/not activated) and represent the centre of the continuum [54].

Key characteristics of M1-like inflammatory macrophages are expression of co-stimulatory molecules such as CD40, CD80 and CD86 and secretion of pro-inflammatory cytokines such as IL-6, IL-1βα and TNF-α [55] that relate to their primary anti-microbial and anti-tumour function. In contrast, key characteristics of M2-like anti-inflammatory macrophages is the expression of surface markers such as CD206, CD163 and secretion of anti-inflammatory molecules such as IL-10, TGF-β [56] that relate to their primary wound healing/tissue repair function. However, M2-like macrophages can also promote tumour growth by recruiting regulatory T cells and Thelper-2 (Th2) cells to induce a suppressive environment.

In this study, the terms M1-like and M2-like macrophages will be used to represent inflammatory and anti-inflammatory macrophages respectively, whilst M0 macrophages will be used to represent cells most likely to represent resting or naïve macrophages based on lack of expression of the maturation markers chosen for the study as per our group's reference [57] The term M3 macrophages will be used to represent intermediate M1/M2 populations per our group's reference [57]; this is discussed in more detail in chapter 3 - section 3.1.

1.1.1.1 Development of macrophages in mice

There are at least three sources the MPS is derived from. The first source is the yolk sac (YS) that produces F4/80 bright resident macrophages which populate all tissues and persist throughout life (shown in Figure 1.2) [58]. These cells are mainly regulated by colony stimulating factor receptor 1 (CSFR-1). CSFR-1 is a transmembrane tyrosine kinase receptor, expressed on most of the mononuclear phagocytic cells [58]. It is also known as macrophage CSFR-1 (M-CSFR) which together with its ligand CSF-1L plays a role in the differentiation and proliferation of myeloid cells, in particular the macrophage lineage [59, 60]. The second source is fetal liver which is less defined but has been shown to contribute to adult langerhans cells (LCs) possibly via a progenitor derived from yolk sac. The third source is the bone marrow (BM) that gives rise to circulating monocytes, F4/80^{low} macrophages and DCs [58]. In this lineage, Ly6C^{+} monocytes under the regulation of fms like tyrosine kinase 3 (FLT3) give rise to classical DCs. Ly6C^{+} monocytes also give rise to F4/80^{low} macrophages. The role of circulating macrophages as well as the contribution of fetal liver to adult tissue macrophages is still unknown.

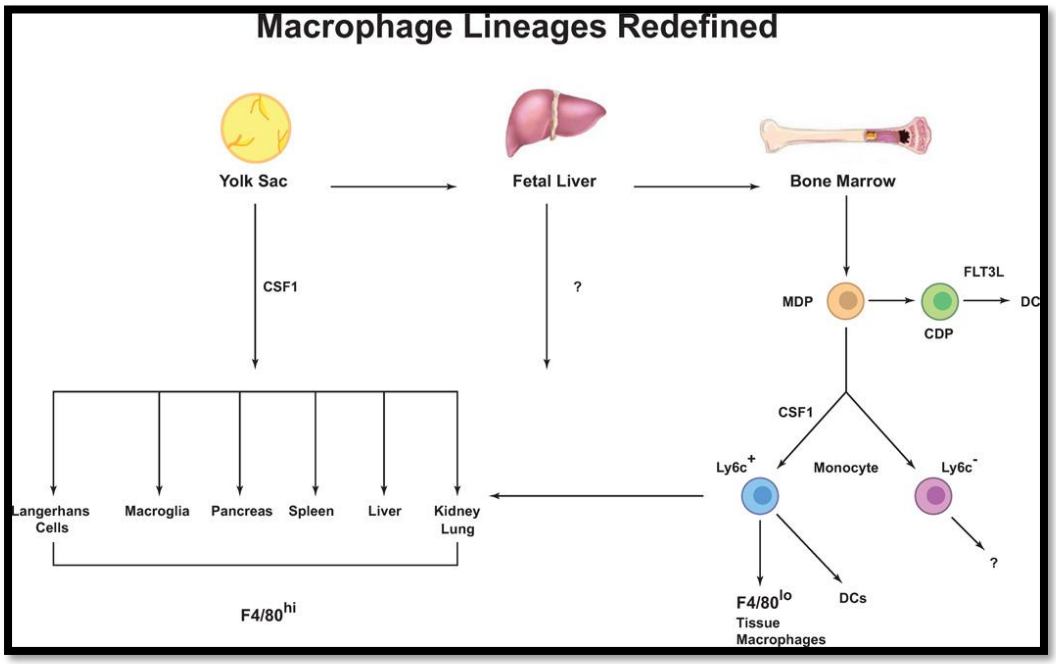

Figure 1.2: Macrophage lineages in mice

Yolk sac, fetal liver and BM are the three sources of the MPS. Yolk sac macrophages persist throughout life as F4/80 bright resident macrophages. Fetal liver populations are less defined while BM give rise to circulating monocytes and their progeny, F4/80^{low} macrophages and DCs. **Image** from "Macrophage biology in development, homeostasis and disease" [58].

1.1.2 Macrophage Subpopulations

Macrophages are highly plastic cells that can change their physiology in response to different environmental factors. These changes give rise to different macrophage populations having distinct functions [48]. On a linear scale, macrophages can be divided into two main groups. One end of the scale represents M1 macrophages, also known as classically activated or inflammatory macrophages, and the other end represents M2 macrophages, also known as alternatively activated macrophages or anti-inflammatory macrophages [61].

1.1.2.1 M1 macrophages

These macrophages induce pro-inflammatory immune responses. Pro-inflammatory signals may include interleukin-1 (IL-1), IL-12, tumour necrosis factor alpha (TNF-α), interferon gamma (IFN-γ) [62]. One of the three main M1 stimuli is granulocyte-macrophage colony-stimulating factor (GM-CSF) which is produced by various cell types including macrophages [51]. The GM-CSF receptor recruits Janus kinase (JAK2), which leads to activation of signal transducer and activation of transcription 5 (STAT5), extracellular signal regulated kinase (ERK), as well as nuclear translocation of interferon regulatory factor 5 (IRF-5) and nuclear factor-kappa B (NF-κB) upon binding [63]. Complement and antibody mediated phagocytosis, antigen presentation, leukocyte chemotaxis and adhesion are all enhanced by GM-CSF. GM-CSF also induces macrophage and monocyte production of granulocyte-colony stimulating factor (G-CSF), IL-8, IL-6, IL-1β and tumour necrosis factor (TNF). Another M1 stimulus is IFN-γ which is produced by a number of cells including NK cells and macrophages. The third main M1 stimulus is LPS which is recognised by TLR-4. Recently it has been shown that LPS can also be recognised by a TLR-4 independent mechanism that leads to inflammasome activation [64]. TLR-4 activation can lead to production of high levels of pro-inflammatory cytokines such as IL-6, TNF, IL-12 and IL-1β, as well as chemokines such as C-X-C motif chemokine ligand (CXCL)-10, CXCL11 and increased antigen presentation molecules (MHC) and co-stimulatory molecules, such as CD80 and CD86. IFN-γ and TLR-4 signalling share many of the same regulators as the GM-CSF pathway. However, whilst LPS and IFN-

γ activated macrophage gene profiles may show some overlap, they are not enough to be considered homologous. Other M1 stimuli include TNF, IL-6 and IL-1β.

1.1.2.2 M2 macrophages

These macrophages are also known as alternatively activated macrophages. There are five main M2 stimuli. One is IL-4 which is produced by basophils, eosinophils, Th2 cells and macrophages and is recognised by IL-4Rα1 which pairs up with a common gamma chain that enables IL-4 binding, or with the IL-13Rα1 chain that enables IL-4 or IL-13 binding. JAK1 and JAK3 are activated by receptor binding which activates STAT6 activation and translocation [51]. IL-4 decreases phagocytosis and induces macrophage fusion [65].

M2 cells can be further subdivided into M2a or alternatively activated cells (induced by IL-4 or IL-13); M2b, induced by TLRs agonists (like LPS) and M2c, induced by glucocorticoid hormones or IL-10 [44]. Glucocorticoids and IL-10 are M2 stimuli. Adrenal glands secrete glucocorticoid hormones which are metabolised by cellular enzymes in macrophages.

Active glucocorticoids diffuse through the lipophilic membrane and bind the glucocorticoid receptor (GCR) alpha, that leads to nuclear translocation of the complex. Monocyte spreading, adherence, apoptosis and phagocytosis are all affected by glucocorticoids. Studies have shown that M1 macrophages produce mainly IL-12 and low levels of IL-10, while M2 macrophages produces significant amount of IL-10 but no IL-12 [51, 66]. IL-10 has multifunctional roles. It acts as an immune-regulatory cytokine with anti-angiogenic and immunosuppressive functions and is produced not just by macrophages but also by NK cells and T lymphocytes [67]. IL-10 has two transmembrane protein receptors, IL-10RA and IL-10RB [68]. Both receptors contain each intra-cellular, trans-membrane and extra-cellular domains and belong to the class-II receptor family [68]. IL-10RA has a greater affinity for IL-10 and binding of IL-10 to IL-10RA leads to JAK1 and tyrosine kinase-2 (TYK2) phosphorylation. JAK1 phosphorylates STAT-3. After phosphorylation STAT-3 translocate to the nucleus and activates transcription of cell-cycle progression and anti-apoptotic genes [67, 68].

Macrophage colony-stimulating factor (M-CSF), a tyrosine kinase transmembrane receptor, is another M2 stimulus. M-CSF binding leads to activation of ERK, autophosphorylation, receptor dimerization, phosphatidylinositol 3-kinase, phospholipase C, and eventually specificity protein (SP1) transcription factor nuclear localization. The key role of M-CSF is highlighted by M-CSF mutant mice as they have reduced levels of selected macrophages and monocytes [69].

1.1.2.3 M3 macrophages

Jackaman et al. defined the M3 phenotype as macrophages that did not polarize into M1 or M2-like cells when exposed to tumour-derived factors [70]. Others have shown that M1 macrophages can switch into M3 macrophages by activation reprogramming pathways and simultaneously inhibiting transcription factors of M2 phenotype such as SMAD3, STAT3 and STAT6 [71].

1.1.3 Macrophages, cancer and mesothelioma

Macrophages play a dual role in cancer where they can either promote or reverse cancer progression [72]. During the last 10 years, many studies have suggested a tumour-supporting role for macrophages in cancer. High tumour grade and shorter survival in many cancers (such as breast cancer, pancreatic cancer, glioblastoma, renal cell carcinoma, head and neck cancer and lymphoma) have been correlated with tumour-associated macrophages (TAMs) in human tumours [73-78]. Repolarisation of macrophages to acquire pro-inflammatory signatures, including IL-12 and TNF-α secretion, have been associated with increased survival in mice and humans with diverse forms of cancer [79] (Figure 1.3).

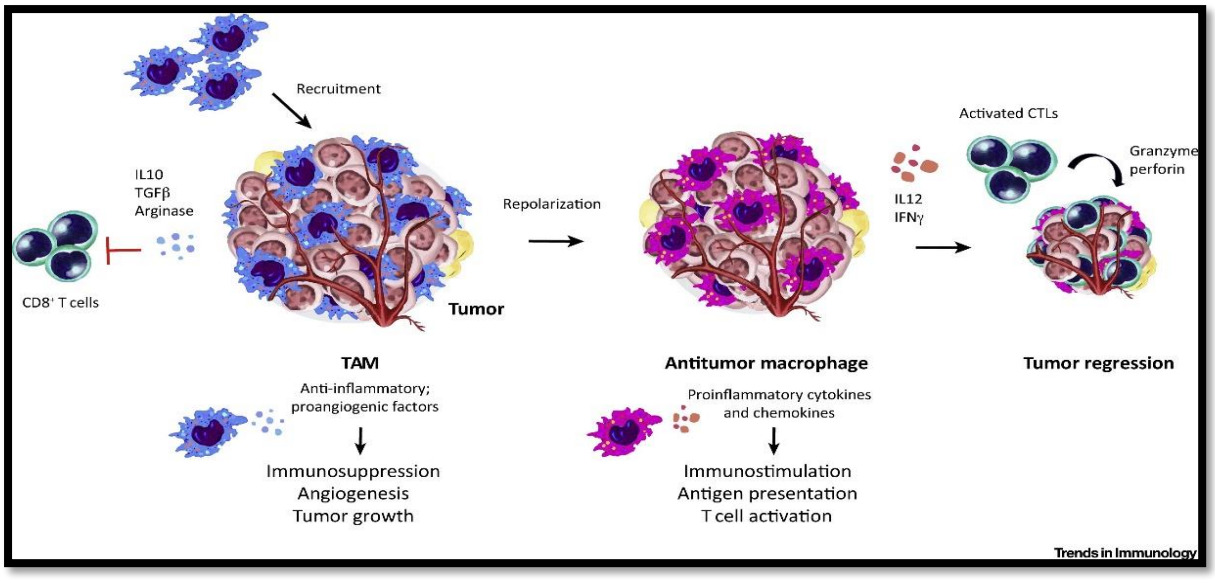

Figure 1.3: Macrophages: Adaptable cells that can promote or reverse tumour progression

Tissue resident precursors or bone marrow derived precursors give rise to macrophages that accumulate in tumours. In tumours, they can adopt a tumour-promoting phenotype and induce angiogenesis, immunosuppression, tumour growth and metastasis. Strategies are being developed to improve tumour therapies that include (i) blocking TAM recruitment; (ii) repolarising TAMs into an immunostimulatory phenotype; and (iii) activating cytotoxic T lymphocyte (CTL) by upregulating antigen presentation machinery. Abbreviations used: Transforming growth factor (TGF)-β, interferon (IFN)-γ. **Image** from "Targeting tumour-associated macrophages in cancer" [72].

1.1.3.1 Macrophages in mesothelioma

Mesothelioma was identified by Klemperer and Rabin and the term entered the medical literature in 1931 [80]. In 1960, the link between mesothelioma and asbestos fibres was recognised and published in Lancet [81]. Multiple studies have confirmed the association between asbestos exposure and the subsequent development of mesothelioma via inhalation, intrapleural, subcutaneous or intraperitoneal inoculation with asbestos fibres [82-85]. Macrophages infiltrate the pleural space of the lungs to phagocytose inhaled asbestos fibres [86]. Reactive oxygen species (ROS) are generated in an effort to clear asbestos fibres which causes DNA damage to nearby cells. This leads to increased recruitment of immune cells and production of inflammatory cytokines at sites of inflammation [87-90]. Since asbestos fibres are large in size, macrophages fail to clear it. This results in continuous secretion of pro-inflammatory cytokines and continued generation of ROS, a process called "frustrated phagocytosis" [91]. Asbestos fibres can also directly penetrate cells and injure

chromosomes in addition to the release of pro-carcinogenic and pro-inflammatory substances [92].

In the mesothelioma microenvironment, TAMs constitute a majority of the cellular population suggesting a crucial role in tumour progression [93]. Established human mesothelioma cell lines and normal human mesothelial cells produce large quantities of cytokines including G-CSF, GM-CSF, IL-8 and IL-6. [94, 95]. These cytokines recruit myeloid-derived suppressor cell (MDSC) and monocytes to the tumour mass, where they differentiate into macrophages. Little is known regarding the phenotype and function of these macrophages although it is clear that mesothelioma cells can shift mature macrophages towards the M2 phenotype [96-98]. TAMs have been associated with decreased MHC-II, leading to impaired antigen presentation in tumours [99, 100]. Similarly, a study on DCs revealed mesothelioma drove lipid accumulation which was associated with impaired antigen presentation [101]. Hence, this study examined lipid accumulation in mesothelioma-exposed macrophages and whether this also is associated with dysfunctional antigen presentation.

1.1.4 Development of DCs from bone marrow precursors

DCs were first discovered by Steinman and Cohn in 1973 [102]. These stellate cells are potent APCs that play a key role in the initiation of immune responses [103]. DCs stimulate naïve T cells and hence play a pivotal role in the generation of adaptive immune responses [103]. DCs are also critical for the induction of immunological tolerance [104]. We now know that DCs are a heterogenous population that comprise of many subsets and can be divided into conventional/myeloid DCs (cDCs/mDCs) and plasmacytoid DCs (pDCs) which arise from progenitors in the BM [105, 106].

1.1.4.1 DC progenitors in mice

A series of DC progenitors have been identified in mice and humans. In mice, a macrophage dendritic cell progenitor (MDP) originates from a common myeloid

progenitor (CMP) that lacks megakaryocyte, lymphoid and granulocyte potential [107]. Two pathways originate from MDP, one leads to the production of monocytes and the other towards generating DCs [108]. MDPs later give rise to a common dendritic cell progenitor (CDP), as shown in (Figure 1.4). CDPs lose monocyte potential and bifurcate to produce pDCs or cDCs [109]. CDPs give rise to pre-DCs which are progenitors to pre-DC1, pre-DC2 and pre-pDCs. Pre-DC1 and pre-DC2 differentiate into cDC1 which express $CD8^+$ or $CD103^+$ and cDC2 that express $CD11b^+$ respectively. Pre-pDCs on the other hand give rise to pDCs [109].

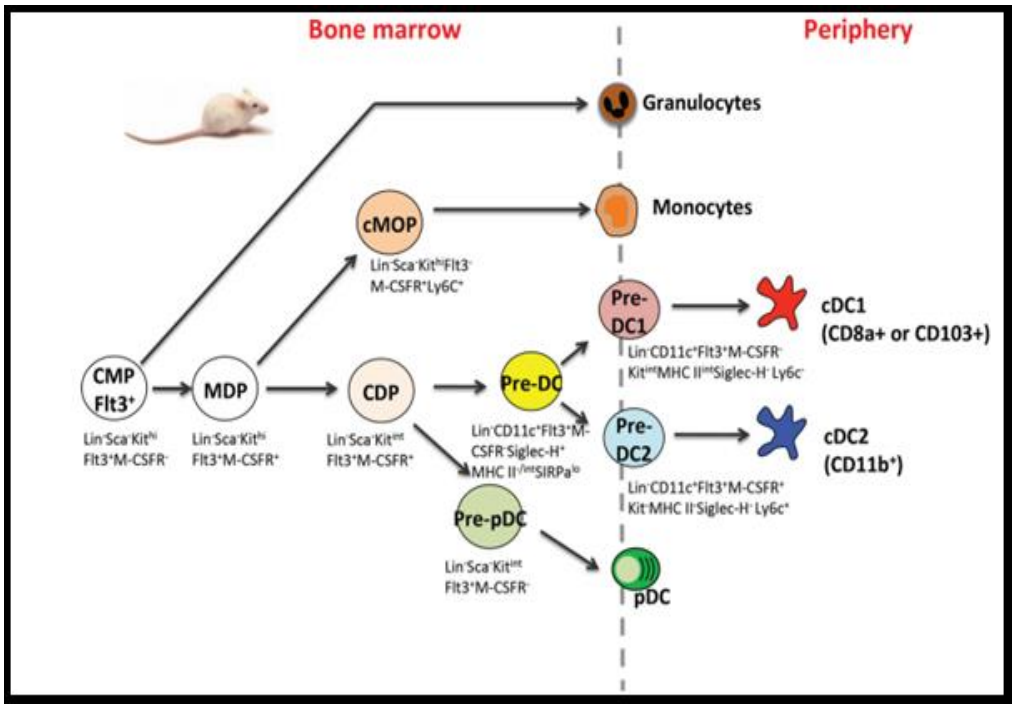

Figure 1.4: DC progenitors in mice

The phenotype and relationship of DC progenitors in mice. Image from: Dendritic Cell **Image** from "Development – History, Advances, and Open Questions" [108]

1.1.4.2 DC progenitors in humans

Lee and colleagues isolated distinct human granulocyte macrophage progenitor (GMPs) subpopulations using cytokine receptor expression with one population equivalent to CMPs in mice having granulocyte, monocyte and DC potential, called GMDP (Figure 1.5). Human GDMP give rise to MDP cells that produce monocytes via a common monocyte progenitor (cMOP) and DCs via CDPs. The latter generate pre-cDCs which are present in blood, BM and peripheral organs [108].

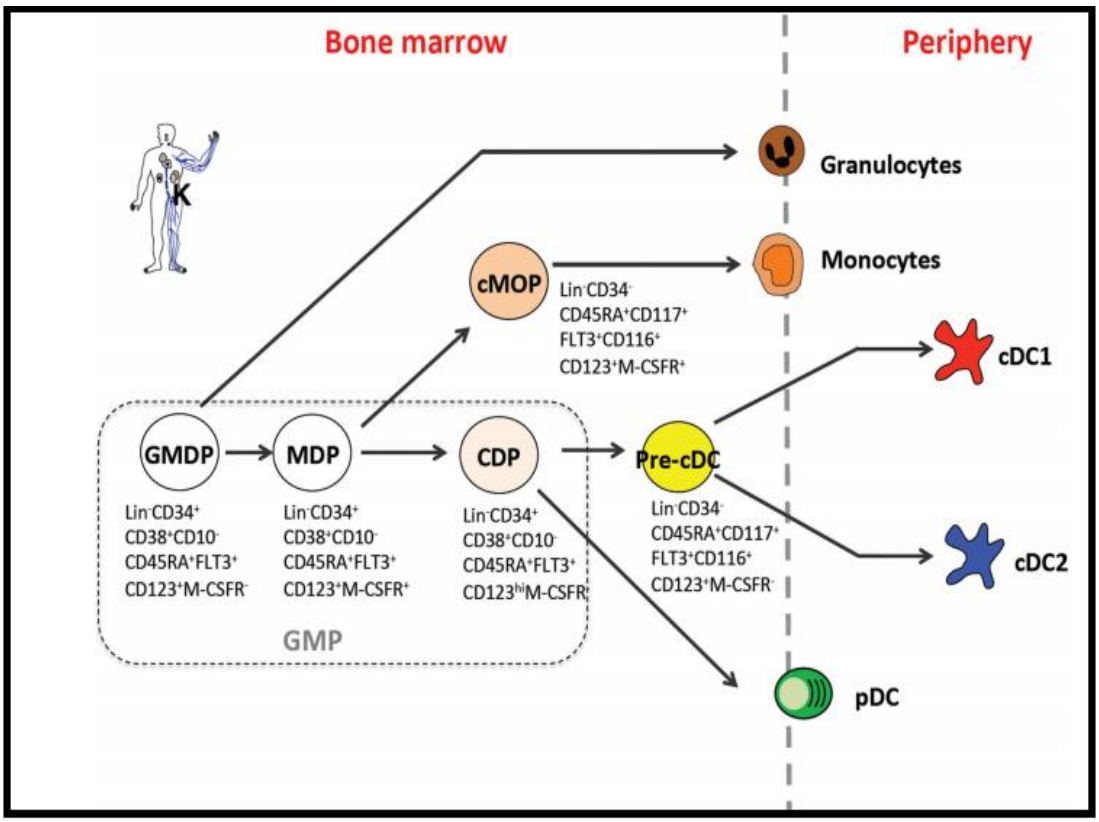

Figure 1.5: DC progenitors in Human

Shows the phenotype and relationship of DC progenitors in human. **Image** from "Cell Development – History, Advances, and Open Questions" [108].

1.1.5 Dendritic cells subpopulations

In the mid-1990s, the significance of DC diversity became clear. Two different murine DC subsets based on the presence or absence of CD8 were identified that have distinct immune functions [110]. These findings were later extended to non-lymphoid tissues, where $CD8^+$ DC equivalents were discovered that do not express CD8 but were recognised by expression of the integrin, CD103 [111].

Recently, a new DC population has been discovered that morphologically resembles plasma cells, but when exposed to viral stimuli produces large quantities of IFN-α and differentiates into immunogenic DCs that prime T cells against viral antigens. This population was named pDCs to differentiate them from Steinman's DCs, the latter were renamed as cDCs [112].

1.1.5.1 Murine plasmacytoid dendritic cells (pDCs)

pDCs represent a small subset (0.3-.05%) of the DC population and are found in lymphoid and non-lymphoid tissues [113]. Their concentration varies depending on the tissue site [114]. Recent studies have shown common developmental origins and genetic similarity between pDCs and cDCs; however, in pDCs, the E protein transcription factor (E2-2) has been shown to control lineage commitment and the pDC gene expression program [115].

pDCs develop in the BM and represent 1-2% of the DC population in mice. The development of cDCs and pDCs depends on Flt3 ligand (Flt3L) and its receptor Flt3 suggesting both cell types have common progenitors [116]. Recently Shortman and colleagues identified a common progenitor called CDP in Flt3L cultures and *in-vivo* [117]. pDCs accumulate mainly in lymphoid tissues via the circulation and express low levels of MHC-II, the integrin CD11c and co-stimulatory molecules. In the steady state, pDCs express high levels of TLR-7 and -9, enabling them to sense viral nucleic acids and respond by production of large quantities of IFN-α and IFN-β, making them important mediators of anti-viral immunity [118]. There are many phenotypic and functional similarities between murine and human pDCs [119]. pDCs of both mice and humans express predominantly TLR-7 and TLR-9 and both produce high levels of IFN-α [120]. In humans, pDCs and B cells express TLR-9 and as a result respond to TLR-9 ligands. Other effects of TLR-9 ligands seem to be indirectly dependent on factors produced by pDC and B cells [121]. This is different from mice, as most DC subsets, as well as macrophages, express TLR-9 [121].

1.1.5.2 Murine classical DCs (cDCs)

cDCs refer to all DCs other than pDCs. They represent the major DC population in most lymphoid and non-lymphoid tissues. cDCs have a heightened ability to sense tissue injuries and to capture and process antigens for presentation to T lymphocytes [105]. cDCs have a distinctive potential to perform these functions because of the following attributes. First is their critical location in non-lymphoid tissues and in the spleen where they continuously acquire blood and tissue antigens [122]. Secondly, they are highly specialised APCs that can efficiently present endogenous as well as exogenous antigen through MHC-I and MHC-II pathways respectively [123]. Third,

they demonstrate a superior ability to prime naïve T cell responses [124]. They can also present exogenous non-cytosolic antigens through the MHC-I pathway by a process called cross-presentation [125], which is critical in protecting the body from intracellular pathogens such as viruses and from tumours [126]. cDCs degrade engulfed material slowly, controlling lysosomal degradation to preserve peptides for T cell recognition [127].

cDCs can be sub-divided into cDC1 expressing $CD8\alpha^+$ and $CD103^+$ or cDC2 expressing $CD11b^+$. Both subpopulations can be found in BM, spleen and lymph nodes (LNs) as well as non-lymphoid tissue [128]. cDC1 that express CD8α or cD103 play an important role in cross-presentation to $CD8^+$ T cells that is critical for immunity against cancer [129-132]. cDC2 expressing CD11b promote $CD4^+$ T cell differentiation into subsets specialising in anti-fungal, -viral or - helminth immunity [133, 134]. cDCs have a central role in T cell activation and hence have been implicated in the development of T cell-mediated inflammatory, allergic, autoimmune and anti-tumour responses [135].

In murine models of cancer, DC-based therapies to modulate T cell activation have been very successful, however more work is needed to make these therapies work in humans [136]. In contrast to murine studies, human DC studies are often focussed on circulating DCs including MoDCs generated from blood $CD14^+$ monocytes [137]. Human blood $CD141^+$ and $CD1c^+$ monocytes were identified and aligned with murine cDC1 and cDC2 respectively [138-140].

1.1.6 cDCs in non-lymphoid tissue

Depending on the organ, DCs represent 1-5% of tissue cells and consist of two major subsets: $CD103^+CD11b^-$ and $CD11b^+$ cDCs.

1.1.6.1 $CD103^+CD11b^-$ cDC

This subset is the equivalent of $CD8^+$ cDCs in lymphoid tissue in function and origin [111, 141]. Their proportion rarely exceeds 20-30% of total cDCs and they mainly populate connective tissues. $CD103^+CD11b^-$ cDC are enriched in Peyer's patches in

the intestines and express low levels of MHC-II but co-express CD8. They lack macrophage markers such as CD11b, F4/80, C-X3-C motif receptor 1 (CX3CR1), CD115 and CD172a [142].

1.1.6.2 CD11b$^+$ classical DCs

CD11b$^+$ cDCs often lack the integrin CD103. CD11b$^+$ cells mostly consist of a mixture of macrophages and cDCs. CD11b$^+$ DCs are best characterised by expression of CD172a and express a more mature phenotype. CD11b$^+$ DCs also produce high levels of CD4$^+$ T cell attractant chemokines, such as CCL22 and CCL17 [143]. CD11b$^+$ cDCs arise from cDC-restricted precursors and monocytes [144].

1.1.6.3 Tissue migratory DCs

These DCs represent non-lymphoid tissue DCs that have migrated via the lymphatics to tissue draining LNs (dLN) [145]. Most tissue migratory cDCs die in LNs but some access the blood by exiting through efferent lymphatics and play a role in immune responses and tolerance [146]. In response to inflammatory signals, non-lymphoid tissue cDCs migration increases through afferent lymphatics to the T cell areas of LNs [147] . C-C chemokine receptor (CCR)-7 controls DC migration to LNs [148]. In the steady state, migratory DCs have high MHC-II expression and low CD11c expression. DC migration is often associated with maturation which is characterised by upregulation of MHC-II complexes and co-stimulatory molecules. During inflammation, these DCs produce inflammatory cytokines and upregulate co-stimulatory molecules that drives adaptive immunity [149].

1.1.6.4 Lymphoid organ-resident DCs

Lymphoid tissue resident cDCs differentiate and remain within lymphoid tissues. They constitute all splenic cDCs and mainly comprise of two subsets: CD8$^+$ cDCs and CD11b$^+$ cDCs [110].

1.1.6.5 $CD8^+$ cDCs

These DCs represent 20-40% of splenic and LN cDCs. $CD8^+$ cDCs express CD8α but not CD8αβ, the latter is commonly expressed by $CD8^+$ T cells [110]. They do not express CD11b or other macrophage markers, but instead express high levels of Flt3 and proliferate in response to Flt3L [150]. Lymphoid tissue resident $CD8^+$ cDCs are phenotypically immature in the steady state compared to tissue migratory cDCs that arrive in a mature state in LNs [110]. The transcriptome of $CD8^+$ cDCs matches that of non-lymphoid tissue $CD103^+$ cDCs and is different from $CD11b^+$ cDCs.

Summarising the above section:

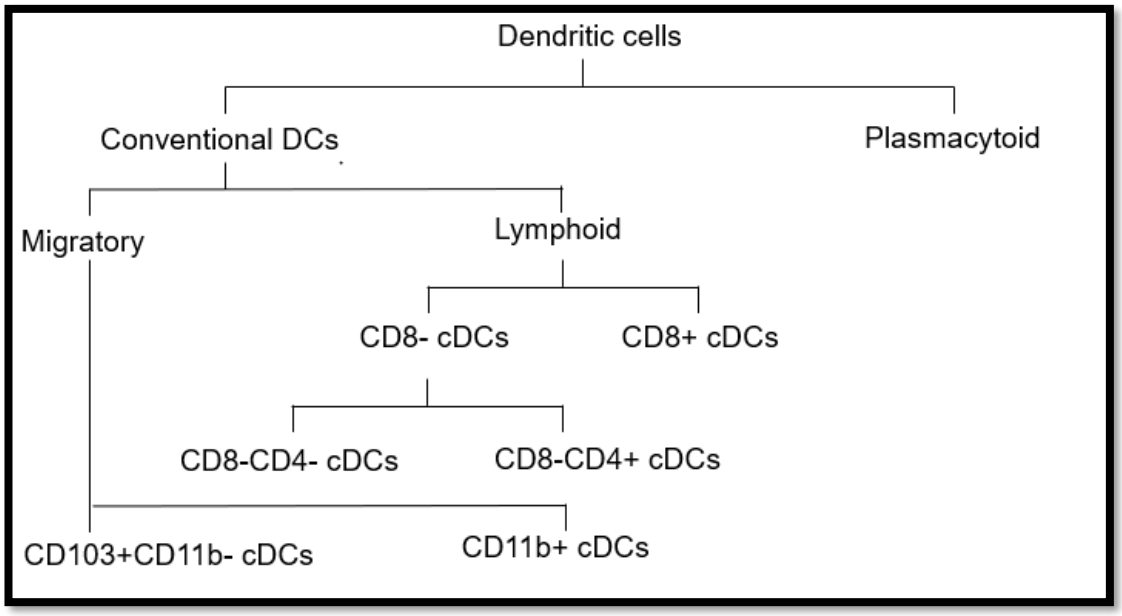

Figure 1.6 : DC subsets
Shows different DC subsets in mice

1.1.7 DCs used in the study

Steinman first isolated DCs from murine spleen [151] but now DC precursors can be isolated from many tissues and induced to differentiate into functional DCs [152-156]. When derived from different sources or at different differentiation stages, the biological characteristics of DCs are quite distinct [157]. BM has easy accessibility and abundant DC precursors and hence has become a major source of DCs. In the

present study, hematopoietic precursor cells were obtained from the BM of C57BL/6J mice and BMDCs were induced by GM-CSF and IL-4 *in vitro* for 7 days.

Murine DCs have stellate morphology and high antigen presentation capacity and activating naïve T cells. They express CD11c on their surface and the antigen presenting molecules, MHC class II [38, 105, 158-160]. With advancing technology, such as transcriptional profiling, mass cytometry and flow cytometry, there is an increase in the characteristics to identify and classify DC subsets [105, 161, 162]. Recently it has been shown that other cell types also share some features typically used to identify DCs [105, 162]. For example, macrophages/monocytes [163-166], natural killer cells [167], activated T cells [168] and B cells [168, 169] also express CD11c. On the other hand, DCs can express markers such as CD14 which is a lipopolysaccharide co-receptor [170] and F4/80 which is a member of the epidermal growth factor-seven transmembrane receptor family [171-173]. Macrophages/monocytes can also prime naïve T cells, but they are not as effective as DCs [174-176]. Ontogenic studies have reported that DCs have a distinct development lineage thus providing a strong evidence that monocytes/macrophages and DCs are distinct cell types [159, 177-179]. Transcriptional studies have further shown that genetic profiles are different for DC subsets and macrophages [105, 180-183]. Thus, for antigen presentation, CD11c could still be considered with $CD11c^+$ DCs being most effective APCs [106, 184]. For this study, FMO control for CD11c is used to gate the positive population (Figure 2.6).

For human studies, monocyte derived DCs were used as these cells show similarities in morphology, physiology and function to conventional myeloid DCs. They are generated by the stimulation of monocytes from healthy donors using GM-CSF and IL-4 (chapter 2, section 2.3.5).

1.1.8 DCs, cancer and mesothelioma

Despite the self-origin of tumours, they can still induce immune responses. T cells and B cells can mediate these responses, however T cells are important because they can lyse tumour cells [185, 186]. In many cancer patients, spontaneous T cell responses have been shown to occur frequently, and molecular studies have helped identify tumour antigens that are recognised by T cells [187]. The immunogenicity of a tumour depends on its antigenicity [188] in the context of MHC molecules presenting peptides

recognised by T cells. The existence of tumour-specific peptides could be explained by genetic mechanisms. Cancer germline genes such as melanoma associated antigens (MAGE) encode tumour specific antigens in some tumour types [189]. Mutations (mostly point mutations) can also lead to the generation of new tumour specific peptides as a result of a modified peptide sequence. Oncogenic viruses such as Epstein-Barr virus (EBV) and human papilloma virus (HPV) that induce tumour formation can also encode antigenic peptides that are seen as tumour-associated peptides [187]. Large scale projects such as Immunoprofiler Initiative and The Cancer Genome Atlas have been designed to identify tumour-infiltrating immune cells by direct observation or through gene-expression signatures [190-192]. DCs constitute a small population within tumours but are critical for the initiation of antigen specific immunity and tolerance [193].

DCs present tumour-associated antigens to T cells on MHC-I and MHC-II molecules. To effectively prime anti-tumour immunity further positive signalling through co-stimulatory molecules (such as CD40, CD80) and soluble factors (such as IL-12) are required [194]. There are also inhibitory mechanisms in place that limit T cell activation which are mediated by molecules such as cytotoxic T-lymphocyte-associated protein 4 (CTLA-4), inducible co-stimulatory molecule (ICOS), indoleamine 2-3 dexoygenase (IDO), programmed death-ligand 1 (PD-L1), and programmed cell death protein 1 (PD-1) [195] (Figure 1.6).

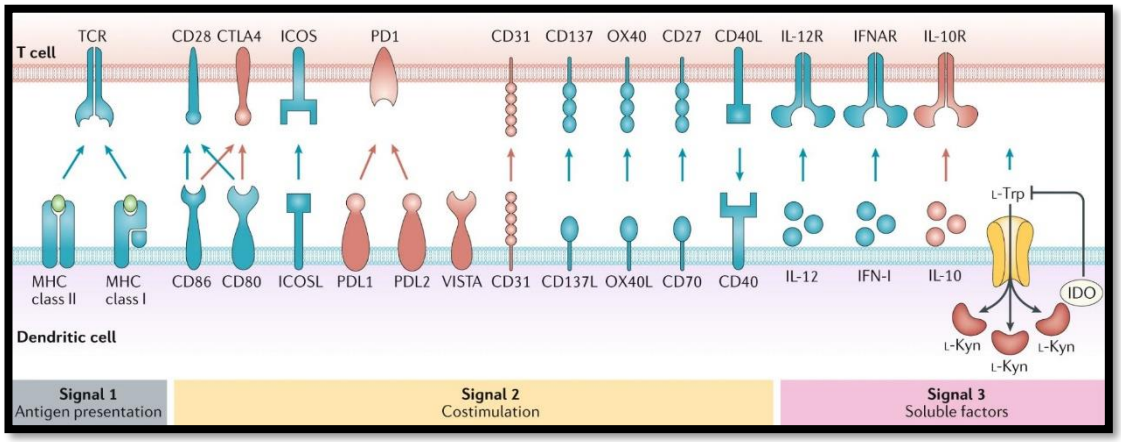

Figure 1.7: Induction of T cell mediated immunity or tolerance by DCs

DCs present tumour antigens on MHC-I and MHC-II molecules alongside co-stimulatory molecules to effectively prime anti-tumour immunity. **Image** from "Dendritic cells in cancer immunology and cancer immunotherapy" [195].

1.1.8.1 Dendritic cell in mesothelioma

Earlier studies by our group have shown decreased numbers of circulating mDC1 cells, mDC2 cells and pDCs in mesothelioma patients relative to their healthy age-matched counterparts [196]. Blood monocytes in mesothelioma patients were found to have a reduced ability to differentiate into MoDCs indicated by a reduced ability to process antigen and reduced expression of co-stimulatory molecules, such as CD80, CD40 and CD86 [197]. Another study by our group examined the effect of mesothelioma on DC lipid content, phenotype and function [198] and found that mesothelioma-exposed immature MoDCs have increased lipid content relative to control DCs; this was associated with reduced antigen processing ability. Another study by the group examined T cell responses to mesothelioma tumours in ageing hosts and showed faster tumour growth in elderly relative to young mice which was associated with increased pro-inflammatory cytokines and exacerbated cancer cachexia [199]. However, a gap in knowledge remains, and that is the combined effect of ageing and mesothelioma on lipid accumulation and DC dysfunction. This thesis addresses this gap and also examines mesothelioma-induced changes in DC metabolism

1.1.9 Cancer, immune cells and immunometabolism

Cancers are highly diverse, and a range of immune cell populations can be found in human tumour tissue including DCs, macrophages and T cells. Cancer cells have the ability to maintain and eventually increase glycolysis and high glucose uptake, leading to a decrease of intra-tumoural glucose levels [200-202]. This decrease in glucose levels can induce extensive metabolic reprogramming in local immune cells. For example, low glucose can prevent the production of IFN-γ, a key T-cell effector molecule in tumour-infiltrating $CD8^+$ T cells [203]. Macrophages and DCs in tumour are also likely to be affected by the tumour microenvironment. These APCs play an important role in initiating and regulating immune responses. The latter are determined by the activation status of macrophages and DCs. It is now clear that different stages of immune cell activation and function depend on different metabolic pathways that are determined by the bioenergetic and biosynthetic needs of the cell [204-206]. The following pathways are involved in cellular metabolism.

1.1.9.1 Glycolysis

Glycolysis is an energy generating pathway that occurs in the cytoplasm and breaks glucose down into 2 three carbon compounds (Figure 1.7). Glycolysis plays an important role in generating adenosine triphosphate (ATP) without requiring oxygen. There are 10 steps involved in glycolysis, five of which constitute a preparatory phase and five are in the payoff phase generating a net gain of two ATP and two nicotinamide adenine dinucleotide (NADH). Glycolysis is not a linear reaction, and instead many intermediate metabolites of glycolysis branch into other metabolic pathways [207]. Glucose-6-phosphate, the first intermediate of glycolysis, is also used for pentose phosphate pathway (PPP) and glycogen synthesis, as well as acting as the glycolytic intermediate for glyceraldehyde-3-phosphate, through which glycerol generates fatty acids and triglycerides.

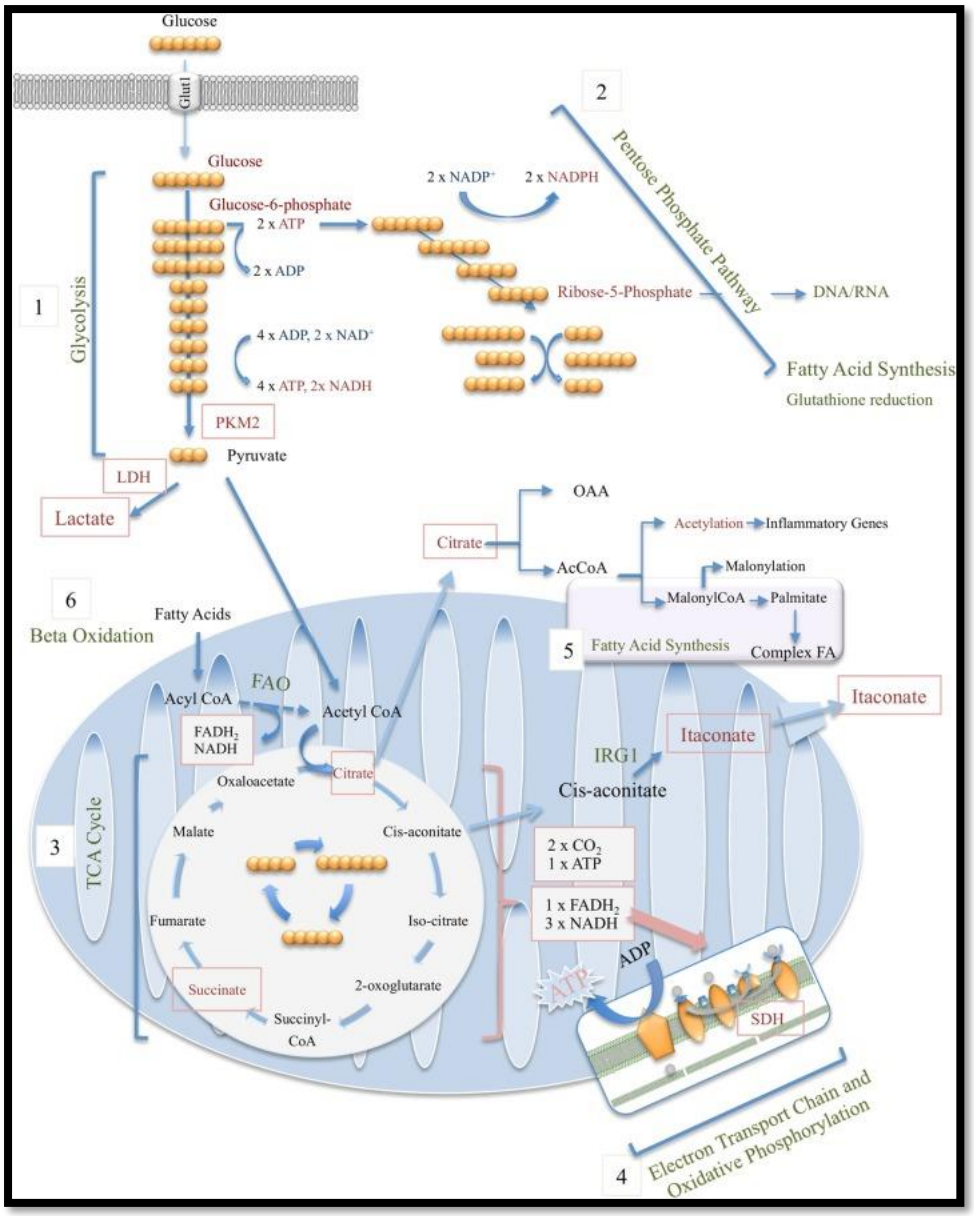

Figure 1.8: Overview of metabolic pathways

Glycolysis (1), pentose phosphate pathways (PPP) (2), tricarboxylic acid (TCA) cycle (3), electron transport chain (ETC) and oxidative phosphorylation (OXPHOS) (4), fatty acid synthesis (FAS) (5) and beta oxidation (fatty acid oxidation) (6): **Image** from "Metabolic Modulation in Macrophage Effector Function" [207].

Each reaction in glycolysis is catalysed by its own enzyme (Figure 1.8). Hexokinase (HK) catalyses the first step in the glycolytic cycle [208]. In this step, glucose is phosphorylated at C-6 to yield glucose-6-phosphate. ATP acts as the phosphoryl donor. The rate of glycolysis is highly dependent on HK activity [209]. This step not just activates glucose but also restricts glucose in cells. Phosphofructokinase (PFK) is the most important rate limiting enzyme as it catalyses the conversion of ATP and fructose-6-phosphate to fructose 1,6-bisphosphate and adenosine diphosphate

(ADP)[210]. Pyruvate kinase (PK) catalyses one of the irreversible steps of glycolysis by transferring a phosphate group from phosphoenolpyruvate (PEP) to ADP, resulting in one molecule of ATP and one molecule of pyruvate. PK has two isoenzymes, PKM 1 and PKM 2. Lactate dehydrogenase catalyses the interconversion of lactate and pyruvate and concomitantly interconversion of nicotinamide adenine dinucleotide from the oxidised (NAD^+) to the reduced state (NADH). Glyceraldehyde 3-phosphate dehydrogenase (GAPDH) catalyses the 6^{th} step in the glycolysis cycle. A study has shown that increased GAPDH gene expression is associated with increased cell proliferation [211] and increased GAPDH alongside increased hexokinase activity has been associated with increased glycolytic activity in macrophages [212].

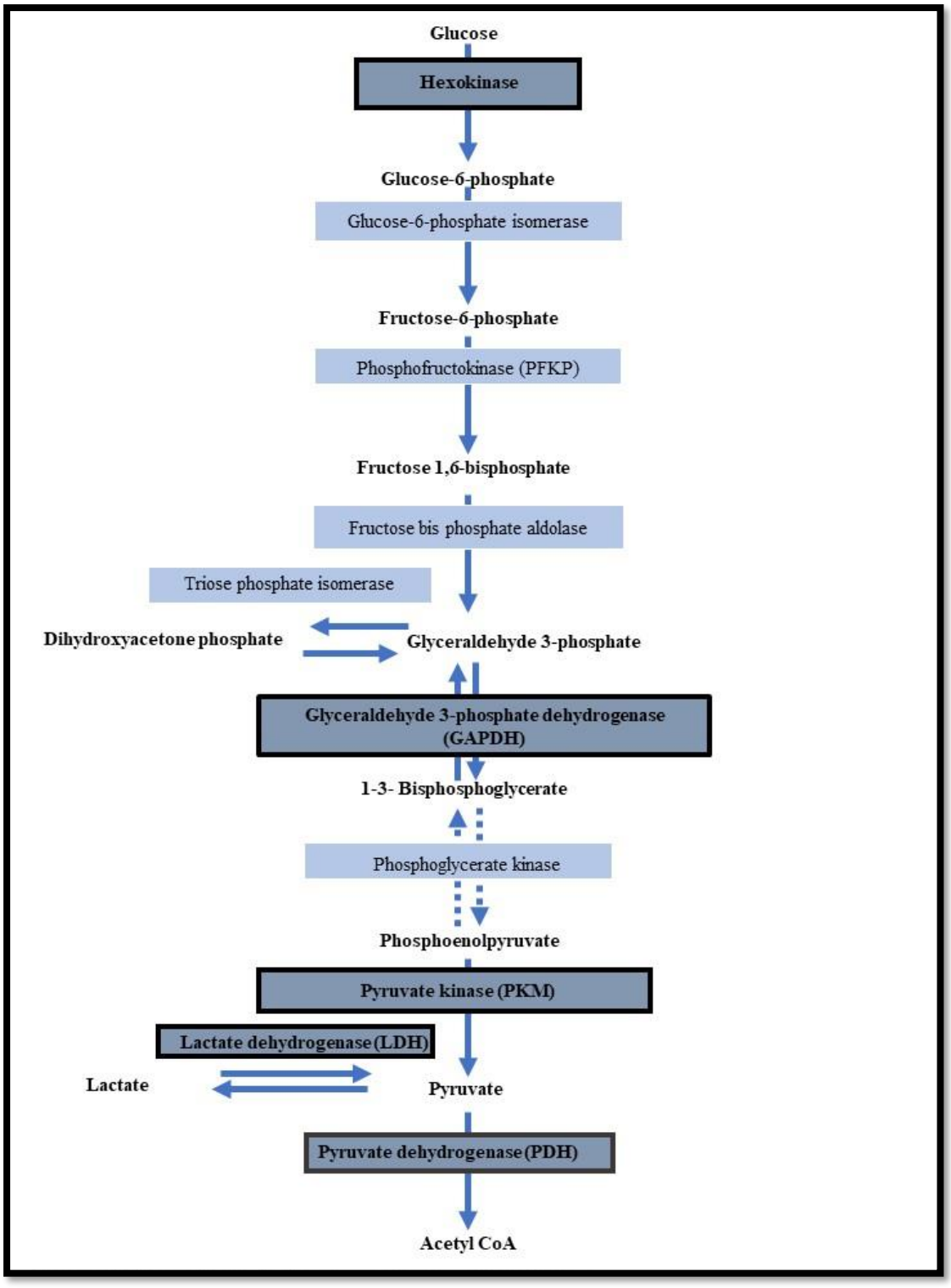

Figure 1.9: Enzymes involved in the glycolytic pathway

Key enzymes involved in the glycolytic pathway are shown. Those examined using western blotting are bolded and highlighted.

The end product of glycolysis is pyruvate that enters the mitochondria to undergo oxidative decarboxylation by the enzyme, pyruvate dehydrogenase (PDH), and serve as the major source of acetyl-CoA, that enters the tricarboxylic acid cycle (TCA), also known as citric acid cycle. Under high energy demand, pyruvate can be converted into lactate by lactate dehydrogenase (LDH) that can act as another primary source of carbon fuelling the TCA cycle [213].

Glycolysis is upregulated in M1 macrophages, and this upregulation has been associated with the pro-inflammatory M1 phenotype. In contrast, M2 macrophages have been shown to employ oxidative phosphorylation (OXPHOS) as their main energy source of ATP to support their metabolic demands [214, 215]. OXPHOS generates 36 molecules of ATP, which is much more than glycolysis (2 molecules of ATP per molecule of glucose) however, glycolysis is faster and produces biosynthetic intermediates that can be utilised in other pathways, such as PPP, which are crucial for macrophage activation and effector functions [216, 217].

1.1.9.2 The pentose phosphate pathway (PPP)

The PPP takes place in the cytosol and can be divided into two stages. The first is an oxidative phase which generates NADH phosphate (NADPH) and the second is a non-oxidative phase where 5 carbon sugars are synthesised. Glucose-6-phosphate generated from the first step in glycolysis feeds anabolic PPP that generates 5 ribose phosphate and pentoses for nucleic acid production and serves as the major source of NADPH. NADPH acts as a reducing power for a range of anabolic and synthetic pathways [207].

1.1.9.3 The tricarboxylic acid cycle (TCA)

During sufficient oxygen conditions, glucose is catabolised through glycolysis producing pyruvate and lactate that enter the TCA cycle where by-products from this cycle donate electrons into the electron transport chain (ETC) to produce a further theoretical yield of 36 ATP molecules per glucose molecule. The TCA cycle is

followed by the ETC, and lastly, proton gradient established as a result of the ETC drives the OXPHOS of ADP to ATP.

Pyruvate formed through glycolysis enters the TCA cycle after being decarboxylated into acetyl Co-A by the PDH complex. The TCA involves a series of oxidising reactions where each acetyl Co-A is converted into two molecules of water and carbon dioxide. One lap around the TCA cycle generates one ATP (2 per molecule of glucose). Most of the energy produced through the TCA cycle is stored as NADH and flavin adenine dinucleotide ($FADH_{2)}$ that produce large amounts of ATP in subsequent reactions of ETC and OXPHOS [207]. The TCA cycle occurs in the presence of oxygen.

The next phase of cellular respiration involves the transfer of high energy electrons within NADH and $FADH_2$ to a set of membrane bound enzymes in the mitochondrion which is called the ETC.

1.1.9.4 The electron transport chain (ETC)

NADH and $FADH_2$ from the TCA cycle are important electron donors during OXPHOS that occurs in the ETC of the mitochondria. The translocation of protons across the inner mitochondrial membrane, driven by a series of enzyme complexes, enables the generation of ATP by the ATP synthase complex.

1.1.9.5 Fatty acid oxidation and synthesis

The fatty acid oxidation (FAO) pathway converts fatty acids into intermediates that can feed into other pathways such as OXPHOS to generate more ATP. Fatty acid synthesis utilises products from other pathways to produce fatty acid chains which could be further condensed to complex lipids (phospholipids) that could be components of cellular structures [218].

Like glycolysis, many of the key intermediates of the TCA cycle serve as precursors in biosynthetic pathways. In inflammatory macrophages, many significant changes occur in the TCA cycle. Citrate not only fuels fatty acid synthesis but also serves as a

precursor of itaconate, which is one of the most highly induced metabolites in LPS-activated macrophages [207]. LPS-activated macrophages have been linked with increase in fatty acids. [219, 220]. Macrophages associated with atherosclerosis are commonly called foam cells and LPS-activated macrophages have been associated with increased accumulation of cholesterol esters and triglycerides that contribute to the pathogenesis of chronic inflammatory diseases [221, 222]. De novo synthesis of fatty acids is largely responsible for this increased lipid accumulation as well, as increases in many key enzymes involved in glycerol lipid synthesis including Lipin 1, glutamic pyruvic transaminase (GPT3) is seen, which may contribute to increased lipid accumulation. Along with an increase in lipid accumulation and synthesis, LPS-activated macrophages decrease in fatty acid oxidation (FAO) [223]. To summarise, macrophages have been shown to uptake lipids through different pathways and enzymes which leads to their dysfunction. The effect of mesothelioma on lipid accumulation by macrophages and DCs was examined in this study.

1.1.10 Metabolic processes in macrophages and DCs

As discussed above, M1 macrophages, or classically activated macrophages, use glycolytic pathways to produce most of their ATP while alternatively activated macrophages M2 macrophages utilise OXPHOS. Therefore, M2 macrophages maintain the forward flow of electrons obtained within NADH and $FADH_2$ through the ETC and generate ATP via ATP synthase [220]. Exposure of macrophages with IL-4 upregulates OXPHOS via the transcription factor STAT6 and the PPARγ coactivator-1β (PGC-1β). Over expression of PGC-1β can lead to a reduction of pro-inflammatory cytokines and knockdown of PGC-1β leads to impaired traits of alternative activation such as promotion of FAO and arginase activity [224]. Citrate from the TCA cycle acts as the substrate for fatty acid synthesis which uses fatty acid synthase to catalyse citrate in a series of reactions. Pro-inflammatory functions of macrophages have been closely linked with fatty acid synthesis, as many studies have shown that there is an increase in fatty acids and citrate in LPS-activated macrophages [219, 220].

Increased mitochondrial biogenesis has been observed in human monocyte-derived DCs. DCs generated in response to GM-CSF and IL-4 is accompanied by increased

expression of peroxisome proliferator-activated receptor γ (PPAR-γ) [225]. PPAR-γ is a key transcription factor in controlling lipid metabolism and PPAR-γ receptor is a master regulator of mitochondrial biogenesis [226]. Rotenone, an electron transport chain inhibitor, has been shown to block DC differentiation upon inhibition of mitochondrial respiration in monocytes [227] suggesting active mitochondrial biogenesis occurs during DC differentiation.

Edward et al have shown a significant correlation between increased synthase activity and DC differentiation as citrate subsequently gives rise to α-ketoglutarate in the TCA cycle but is also a precursor for FA synthesis [228]. DC development and differentiation of monocytes into DCs has been shown to be dependent on FA synthesis [229]. This shows that DC differentiation processes are dependent on metabolic pathways integrating mitochondrial function with synthesis of fatty acids.

1.1.11 Lipid accumulation in macrophages and dendritic cells

Several studies have shown that lipid accumulation causes DC and macrophage dysfunction [101, 230-235]. Fu et al. [236] and Herber et al. [101] have shown that radiation and tumours respectively cause lipid accumulation in DCs that leads to low expression of co-stimulatory molecules and reduced cytokine secretion. These lipid laden DCs had a reduced capacity to process antigens and were unable to effectively stimulate allogenic T cells. Studies in macrophages have shown that lipid accumulation influences their phenotype and blunts their pro-inflammatory immune responses [235, 237, 238]. Macrophages facilitate the uptake of lipids mainly through scavenger receptors leading to the formation of foam cells [239]. Earlier studies in the group by Gardner et al. investigated the lipid accumulation in mesothelioma in young mice. The studies found higher lipid accumulation and reduced numbers of cross-presenting $CD8\alpha^{+}CD4^{-}$ DCs. This was associated with decreased T cell proliferative response to tumour antigen presentation in draining lymph nodes [240]. Other studies have shown lipid laden iMoDCs (monocyte-derived dendritic cell) to have reduced CD1a expression which could further lead to decreased presentation of tumour-associated lipid antigens and reduced activation of lipid-specific T cells [241, 242]. Lipid accumulation in response to combined effects of ageing and mesothelioma have not been looked before which is the main focus of this thesis.

1.1.11.1 Mechanism of lipid accumulation in DCs

Scavenger receptors play an important role in the intracellular transport of lipids and constitute a large family of proteins. There are 8 classes of scavenger receptors ranging from class A to class H. [243]. Lymphoma tumour explant supernatants induce significant upregulation of the macrophage scavenger receptor 1 (Msr 1 also known as SR-A) in DCs. Msr-1 is predominantly found in macrophages, monocytes and DCs in both humans and mice [244]. Similar effects have been seen with colon carcinomas and melanoma [101]. CD36, also known as SR-B, is a type B scavenger receptor while CD68 is a type D scavenger receptor [243]. CD68 has been known to play a minor role in the uptake of oxidised lipoproteins by macrophages [245]. Earlier work by Gardner et al. has shown that with ageing, expression levels of CD36 (a scavenger receptor), CD68 (a member of scavenger receptor supergene family 5), very low density lipoprotein receptor (VLDLr) and low density lipoprotein receptor (LDLr) significantly increased in different DC subsets that may be responsible for increased lipid accumulation [246].

1.1.11.2 Mechanism of lipid accumulation in macrophages

Macrophages take up low density lipoproteins (LDL), very low-density lipoproteins (VLDL) and oxidised lipoproteins via phagocytosis, micropinocytosis and pathways mediated by scavenger receptors such as CD36, scavenger receptor class B type 1 (SR-B1), scavenger receptor class A type 1 (SR-A1) and lectin type oxidised LDL receptor 1 (LOX-1) [247].

1.1.12 Project aims

Macrophages and DCs likely change in response to their microenvironment during DCs ageing and when a tumour is present. Previous studies have examined the effect of age and mesothelioma separately on macrophages and DCs. This is the first study to examine the combined effect of age and mesothelioma on macrophages and DCs.

Thus, this thesis aimed to:

1. Examine changes to murine macrophage subsets in young and elderly mice with mesothelioma by comparing:
    A) Macrophages obtained from young mice (2-5 months, equivalent to 16-18 human years) and elderly mice (20–24 months, equivalent to 60-70 human years).
    B) Macrophages obtained from BM, spleen, lymph nodes and tumour.
    C) Lipid accumulation and markers of macrophage function.

2. Examine changes to DC subsets in young versus elderly mice with mesothelioma by comparing:
    A) BM, spleen, lymph nodes and tumour
    B) Lipid accumulation and markers of DC function.

3. Investigating metabolic changes induced by mesothelioma in human and murine DCs by comparing the glycolytic and mitochondrial profiles of healthy DCs to DCs exposed to mesothelioma-derived soluble factors.

Thesis hypothesis

Mesothelioma drives lipid accumulation in DCs and macrophages leading to their dysfunction; this is exacerbated with ageing

Chapter 2: Material and methods

2.1 Cell culture

2.1.1 Tumour cell lines, cell culture and maintenance

The two tumour cell lines used in this study were JU77 human mesothelioma cells and AE17 murine mesothelioma cells. The JU77 cell line was established from a pleural effusion of a patient with a confirmed disease diagnosis [248]. The AE17 cell line is a confirmed murine malignant mesothelioma cell line which was derived from the peritoneal cavity of C57BL/6J mice injected with asbestos fibres [249]. RPMI 1640 (Life Technologies, Victoria, Australia) media containing 10% fetal calf serum (FCS; ThermoScientific Victoria, Australia), 10 μg/ml streptomycin (Penicillin-Streptomycin; Life Technologies), 100 units/ml penicillin and 2 mM L-glutamax (Life Technologies), which is referred as complete RPMI 1640 (cRPMI) media was used to maintain both the cell lines. All cells were maintained at 37ºC in a 5% CO_2 atmosphere.

2.1.2 Generating tumour conditioned media

To mimic a tumour microenvironment, tumour conditioned media was generated using AE17 and Ju77 mesothelioma cell lines. Tumour conditioned media (TCM) contains factors secreted by tumour cells such as cytokines, metabolites and growth factors [250]. To generate TCM, tumour cell lines were first thawed in cRPMI and then gradually weaned into complete serum-free media (SFM; Invitrogen, USA). Weaning was performed in different stages. Firstly, Ju77/AE17 cells cultured in cRPMI media were split into 25% SFM + 75% cRPMI media after reaching 80-90% confluency. This cycle continued as Ju77/AE17 cells were successively weaned into 50% SFM + 50% cRPMI media, 75% SFM + 25% cRPMI media and then 100% SFM. To maintain consistency, cells were left in SFM for 72 hours until the media turned yellow when supernatant was collected, centrifuged at 300 g for 5 minutes to remove any dead cells and stored at -80ºC for future use (Figure 2.1).

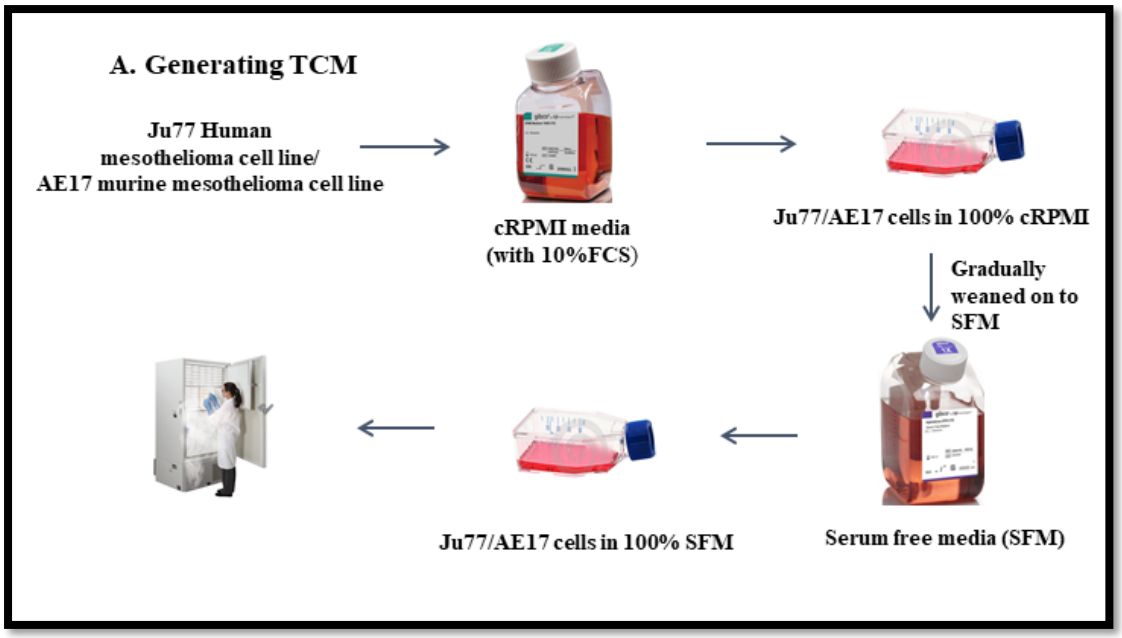

Figure 2.1: Generating AE17/ Ju77 tumour conditioned media

2.1.3 Passaging tumour cell lines

JU77 and AE17 tumour cell lines were grown to approximately 80-90% confluency before passaging. Both cells lines were adherent and required trypsinisation with or without ethylenediaminetetraacetic acid (EDTA) during passage. For passaging, medium was removed from confluent cells and the monolayer was washed using phosphate-buffered saline (PBS; Life Technologies). After removal of PBS, 1 ml of trypsin (Life Technologies) +/- EDTA (EDTA; Life Technologies) was added to cells for 3 minutes at 37ºC and 5% CO_2 to release adherent cells. AE17 cells were detached from tissue culture flasks using 0.25% trypsin only as the use of EDTA on AE17 cells interferes with their ability to form tumours in mice (unpublished laboratory observations). 0.25% trypsin-EDTA (Life Technologies) was used to detach JU77 cells from tissue culture flasks. Once cells were detached, cRPMI media was added to neutralise trypsin [251]. Cells were centrifuged at 300 g for 5 minutes, resuspended in cRPMI media and seeded into new tissue culture plates or flasks (Becton Dickinson, California, USA).

2.1.4 Freezing and thawing of cells

Trypan blue was used for cell viability and quantification. 10 µl of 0.4% trypan blue solution (Sigma-Aldrich, USA) was mixed with 10 µl of cells following which 10 µl of the mixture was loaded onto a haemocytometer and dead (blue stained) and viable (unstained) cells were counted. Cells were centrifuged and resuspended in a freezing mixture consisting of 10% dimethyl sulfoxide (DMSO; Sigma-Aldrich, USA) and 90% FCS at a concentration of 1 x 10^6 cells/ml and aliquoted into cryovials at 1 ml/vial for storage at -80ºC.

Frozen cells were thawed in a 37ºC water bath and transferred to 50 ml tubes with cRPMI media containing an FCS underlay added in a dropwise manner. Cells were centrifuged to remove DMSO at 300 g for 5 minutes, resuspended in cRPMI media, transferred to tissue culture flasks or plates and cultured at 37ºC in a 5% CO_2 atmosphere.

2.2 Human Studies

2.2.1 Human ethics approval

This study was approved by the Curtin University Human Research Ethics Committee (approval number HRE2017-0823).

2.2.2 Volunteer recruitment

Healthy volunteers aged between 20-35 years were recruited by word of mouth within the Curtin Health Innovation Research Institute (CHIRI), Curtin University, Perth. An information leaflet was provided to the volunteers prior to obtaining signed consent. Volunteer health status was evaluated via a questionnaire (refer to appendix).

2.2.3 Whole blood sample collection

Whole blood samples (50 ml) were collected from volunteers via venepuncture into five 10 ml K_2EDTA [252]) vacutainers (Becton Dickinson) and transported to the laboratory for immediate processing.

2.2.4 PBMCs isolation via density gradient centrifugation

Peripheral blood mononuclear cells (PBMCs) obtained from whole blood samples were evenly divided between two 50 ml tubes. PBS containing 2 mM EDTA (Sigma-Aldrich, USA) was added to make a total volume of 35 ml per tube. 15 ml of Ficoll-paque PLUS (GE healthcare, New South Wales, Australia) was added into a new 50ml tube and overlaid with 35 ml of diluted blood and centrifuged at 400 g for 40 minutes at 20ºC without brakes. After centrifugation, the PBMC layer was carefully collected with a sterile transfer pipette, resuspended in 50 ml of PBS/EDTA and washed 4 times. The first wash was at 300 g for 10 minutes at 20ºC with full acceleration and brakes. The second and third washes were performed at 200 g for 10 minutes each at 20ºC with full acceleration and brakes to remove platelets. The final wash was at 120 g for 10 minutes at 20ºC. PBMCs were then resuspended in cRPMI media and aliquoted into 6 well plates at a concentration of 5 x 10^6 cells per well.

2.2.5 In-vitro generation of human monocyte-derived dendritic cells

Monocyte-derived dendritic cells (MoDCs) were prepared as per Romani et al. [253] and Sallusto et al. [137]. Briefly, PBMCs were allowed to adhere to wells for 2-3 hours in cRPMI media at 37ºC and 5% CO_2, after which non-adherent cells were removed. To differentiate the monocytes into DCs; the remaining adherent cells were cultured for 7 days in cRPMI media supplemented with 80 ng/ml human granulocyte-macrophage colony-stimulating factor (GM-CSF; Shenandoah Biotechnology, Pennsylvania, USA), 10 ng/ml recombinant human interleukin (IL)-4 (Shenandoah Biotechnology) and 10 µg/ml Polymyxin B (Sigma-Aldrich) to neutralize any endotoxin [253], [137], [254]. cRPMI media containing the relevant growth factors was replaced at day 3 and day 6.

2.2.6 Human MoDC stimulation with LPS and /or exposure to tumour conditioned media

Human MoDCs were cultured in 6 well plates at a concentration of 5 x 10^6 cells per well, under the following conditions: (i) cRPMI media only (unstimulated/non-tumour exposed controls), (ii) cRPMI media supplemented with 1 µg/ml LPS (Sigma Aldrich) to activate MoDCs and induce their maturation (mature MoDC controls), and (iii) a

mixture of 50% JU77 TCM and 50% cRPMI media as tumour-exposed tests. After 24 hours, MoDCs were collected by gentle pipetting with a sterile transfer pipette for analysis via flow cytometry, seahorse technology or western blotting (Figure 2.2).

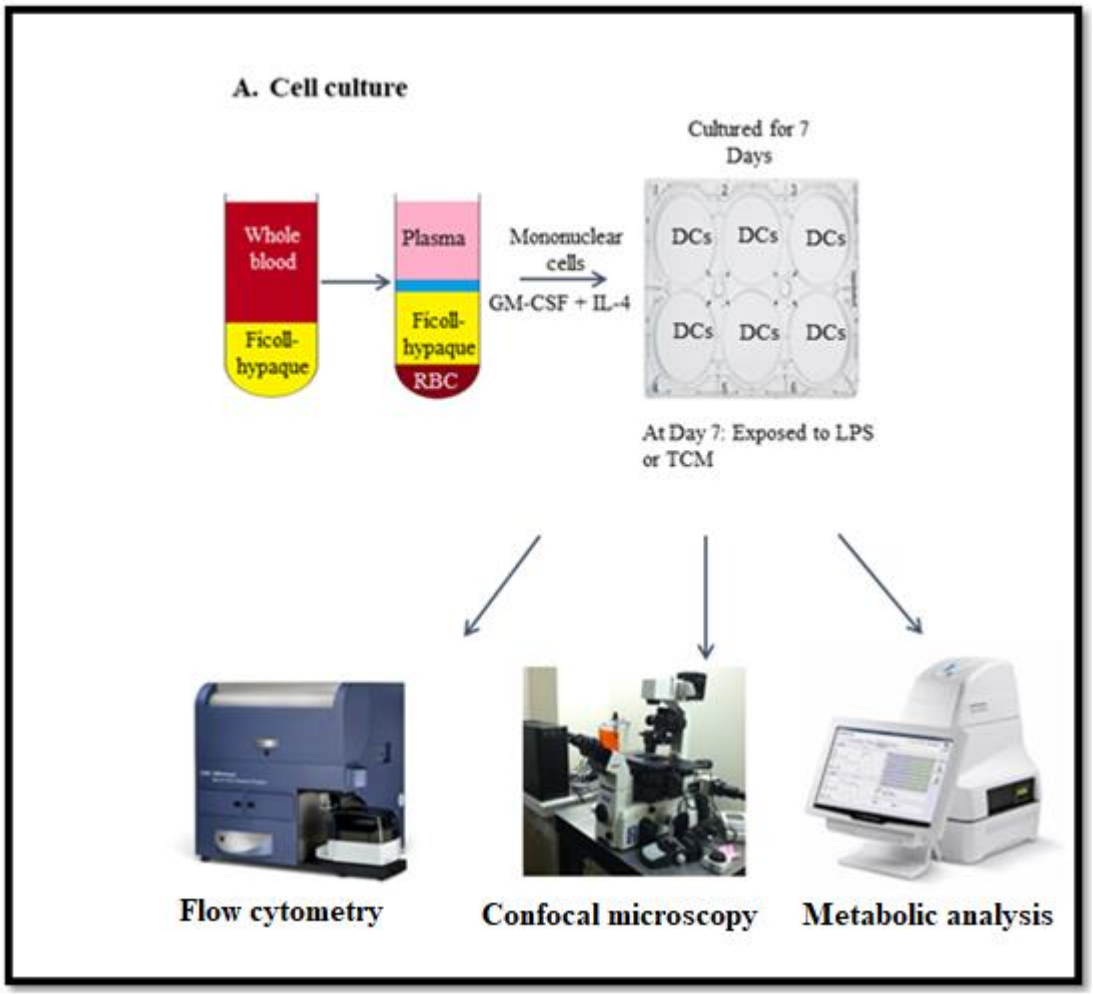

Figure 2.2: Cell culture and experimental analysis

2.2.7 Western blot analysis

Sodium Dodecyl Sulphate Polyacrylamide Gel Electrophoresis (SDS-PAGE) was used to run multiple protein samples. Ten percent resolving gel as per Table 2.1 was poured in between two clean glass plates clamped in a gasket and propanol (Ajax Finechem, Thermo Fisher Scientific) poured along the top to remove air bubbles. Once the resolving gel had polymerised, propanol was poured off before addition of 5% stacking gel. A 10 well comb was placed carefully to prevent air bubbles forming in the stacking gel. Once gels had polymerised, plates were clamped into running buffer

(25 mM Tris Base (Life Technologies) with 192 mM glycine (Bioland Scientific LLC), and gel glycerol (Biochemicals) at 50%, pH 6.5). Cell lysates were diluted 1:4 in sample buffer (Novex, Life Technologies) and NuPage sample reducing agent (ThermoFisher Scientific) and boiled for 5 minutes. The amount of lysate to be loaded was determined using a bicinchoninic acid protein assay (BCA; Thermo Scientific). 3 µg of the molecular marker ladder (Bio-Rad) was loaded to provide a standard for molecular weights. The system was initially run at 80 V through the stacking gel then increased to 120 V until the dye front had reached the end of the plate. Protein transfer to a nitrocellulose membrane (Bio-Rad) was followed by electrophoresis. The gel and membrane were soaked in transfer buffer (25 mM Tris Base, 192 mM glycine, 20% methanol) then layered between blotting paper before being placed in the transfer system. Proteins were transferred at 250 mA for 1 hour and 15 minutes and Ponceau-S staining (Sigma-Aldrich) used to confirm successful protein transfer. Blots were then blocked in 3% bovine serum albumin (BSA; Amresco) in 1x Tris-buffered saline (TBS)-Tween solution (20 mM Tris Base, 140 mM NaCl, 0.05% Tween 20, pH 7.4). Primary rabbit antibody solutions (diluted as per Table 2.3) in 3% BSA in TBS-Tween (0.02% sodium azide was added to ensure long term use), were added to the membrane and incubated overnight at 4ºC. 5 ml of primary antibody was added to 15 ml tubes; this volume is used to ensure the blots are fully immersed as they face upwards when inserted inside the 15 ml tubes. The blots were washed 3 times in SNAPid (EMD Millipore Corporation) to remove any unbound primary antibody. Blots were then incubated with a secondary polyclonal goat anti-rabbit antibody (Dako, Denmark) which is conjugated with horseradish peroxidase (HRP) prepared at a 1:2000 dilution in TBS-Tween solution for 30 minutes. Blots were washed 3 times with TBS-Tween before detection using enhanced chemiluminescence (ECL) substrate for the detection of HRP on immunoblots [255]. Visualization and quantitative densitometry analysis were performed with Molecular Imager® Gel Doc™ XR System v5.2.1 (Bio-Rad Laboratories, Hercules, CA, USA).

Table 2.1 Composition of gels used in SDS PAGE protein separation. (For 1 gel)

Reagent	10% Resolving gel	5% Stacking gel
Acrylamide Stock (40%) (Invitrogen)	2ml	0.25ml
1.25mM Bis-Tris buffer pH 6.5 (Invitrogen)	2.25ml	0.71ml
Gel glycerol (Biochemicals)	1.9ml	0ml
Milli-Q H_20 (Baxter water)	1.9ml	1.04ml
10% Ammonium Persulfate (APS; Invitrogen)	50 µl	25 µl
Tetramethylethylenediamine (TEMED; Invitrogen)	5 µl	2.5 µl

Table 2.2: Solutions used in preparation of western blot

Running buffer	Transfer buffer	10x TBS	Primary antibody	Secondary antibody
Trizma base (Sigma) 3.03g	Milli-Q H_20	NaCl, 87.5g	1:1000 in TBST in 3% BSA	1:2000 in TBST in 3% BSA (anti-rabbit)
Glycine 14.4g	1x Tris glycine Methanol, 20%	Trizma base, 21.1g		

Table 2.3: Antibody dilutions used in western blot

Antibodies	Dilutions	Supplier	Catalog number	Molecular weight (kDa)
Beta Actin (13E5) Rabbit mAb	1:2000	Cell Signalling Technology	4970	45
Glyceraldehyde 3-phosphate dehydrogenase	1:1000	Cell Signalling Technology	5174	37

(GAPDH) (D16H11) XP Rabbit mAb				
Hexokinase I (C35C4) Rabbit mAb	1:1000	Cell Signalling Technology	2024	102
Hexokinase II (C64G5) Rabbit mAb	1:1000	Cell Signalling Technology	2867	102
Lactate dehydrogenase A (LDHA) (C4B5) Rabbit mAb	1:1000	Cell Signalling Technology	3582	37
Pyruvate dehydrogenase (C54G1) Rabbit mAb	1:1000	Cell Signalling Technology	3205	43
Pyruvate kinase I and II (C103A3) Rabbit mAb	1:1000	Cell Signalling Technology	3190	60
Pyruvate kinase II (D78A4) XP Rabbit mAb	1:1000	Cell Signalling Technology	4053	60

2.2.8 Seahorse metabolic analysis

The Seahorse (Seahorse XFe96 Analyzer, Agilent) preparation station was turned on 24 hours before performing the assay and set at 37ºC in a 0% CO_2 atmosphere. Hydrated XFe96 sensor cartridges were placed in the seahorse preparation station for 24 hours with a calibrant solution and on the day of assay, they were inserted into the instrument to initiate the calibration process. Basal media containing Dulbecco's Modified Eagle's Medium (DMEM; Sigma), 2mM L-glutamax (Gibco), 1mM pyruvate (Sigma) and 3 ml/l phenol red (Sigma) was prepared fresh on the day of the assay, warmed at 37ºC in a water bath and adjusted to pH 7.4. Basal media was aliquoted as follows: (i) 50 ml for washing cells and for the glycolysis stress test

(media was left as is with no glucose added), (ii) 24 ml for the mitochondrial stress test with glucose (Sigma) added to make a final concentrate on of 2.5 mM glucose

2.2.9 Dendritic cell preparation for the seahorse assay

MoDCs were lifted off six well plates by gentle pipetting using sterile transfer pipettes and centrifuged at 300 g for 5 minutes. The supernatant was removed, and pellets were resuspended in basal media, washed 3 times at 300 g for 5 minutes each and cell quantification was performed. Cells were seeded in a seahorse XF-96 cell culture microplate at 7 x 10^4 cells per well with 8 replicates for each condition. On the day of the stress tests and seahorse analysis, culture media was changed to basal media containing 2.5 mM glucose, 1 mM sodium pyruvate and without bicarbonate for the mitochondrial stress test [256]. The same media was also used for the glycolytic stress test but without glucose. Cells were then incubated in the seahorse preparation station set at 37ºC in a non-CO_2 incubator. Each sample was subjected to a glycolytic stress test and a mitochondrial stress test.

2.2.10 Aliquoting drugs into seahorse ports

A multi-channel pipette was used to load two ports at a time with 10 µl tips that fit the small port openings. Tips were placed against the side of the well, about halfway down the well, to avoid creating bubbles when dispensing drug solutions. 25 µl of each drug solution was aliquoted into the respective ports while the remaining ports were aliquoted with 25 µl of basal seahorse media. These drugs are diluted 8, 9, 10 times when injected into the wells due to the volumes already present in the relevant wells in a Seahorse XF96 culture plate. Therefore, stock solutions are made at concentrations that are 8, 9 and 10 -fold higher than the intended working concentration, this is shown in "x-conc" column [257]. Drug concentrations are shown in Tables 2.4 and 2.5.

For the glycolytic stress test (Figure 2.3), the first injection was 1 µg/ml LPS to measure DC responses to LPS. The second injection was a saturating concentration of glucose. Cells use the glycolytic pathway to catabolise glucose to pyruvate producing nicotinamide adenine dinucleotide (NADH), adenosine triphosphate (ATP), water and protons. Extracellular acidification rate (ECAR), which is a measure of the rate of

glycolysis is rapidly increased upon the extrusion of protons into the medium [258]. Oligomycin, the third injection, is an ATP synthase inhibitor. Oligomycin inhibits mitochondrial ATP production and shifts energy production towards glycolysis with a subsequent increase in ECAR, enabling cells to reach their maximum glycolytic capacity [258]. The final injection is 2-deoxy-glucose (2-DG), a glucose analog that competitively inhibits glucose hexokinase, an enzyme in the glycolytic cycle, this prevents glycolysis. The resulting decrease in ECAR produced as a result of 2-DG confirms that the ECAR produced in the experiment is due to glycolysis [259].

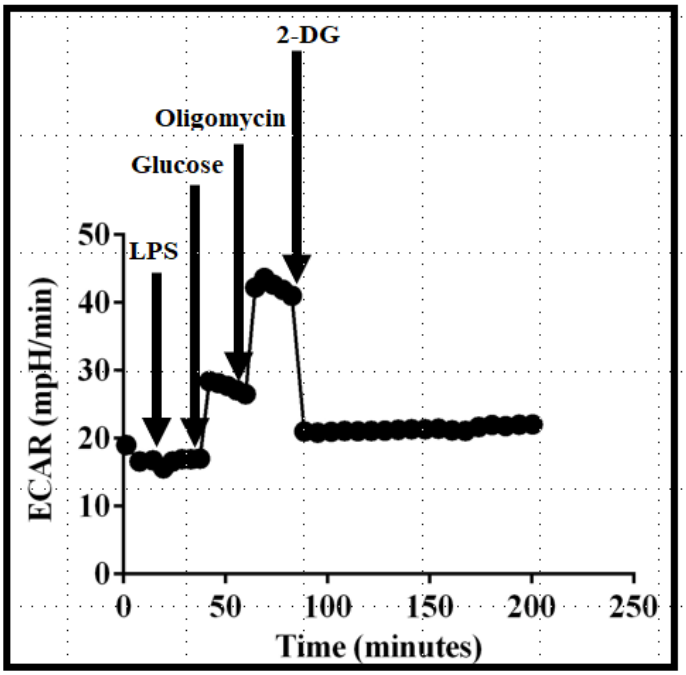

Figure 2.3: Glycolytic stress test injections strategy

For the mitochondrial stress test (Figure 2.4), oligomycin is used after LPS. This inhibits ATP synthase (complex V as seen in Figure 2.5) and decreases the oxygen consumption rate (OCR), a measure of mitochondrial respiration. The next injection is the uncoupling agent, carbonyl cyanide-4(trifluoromethoxy) phenylhydrazone (FCCP) [260]. FCCP allows the free flow of electron through the electron transport chain (ETC) and the maximum consumption of oxygen by cells, thus, measuring the maximum rate of respiration. The final injection is a mixture of rotenone and antimycin A that abrogate mitochondrial respiration by blocking complex I and

complex III of the electron transport chain (Figure 2.5) thus enabling the calculation of non-mitochondrial respiration driven by processes outside the mitochondria. [261].

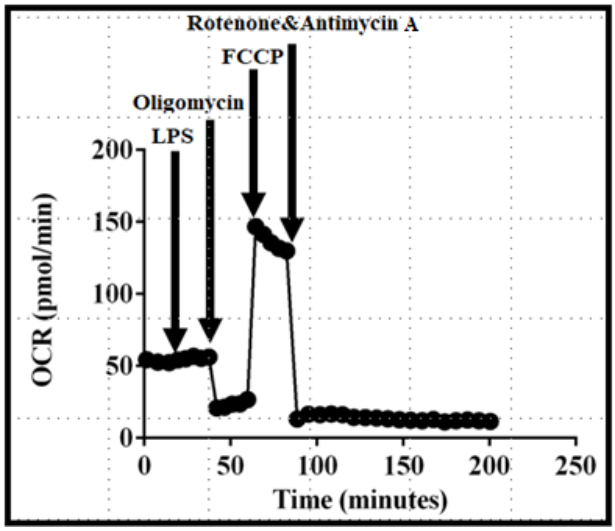

Figure 2.4: Mitochondrial stress test injections strategy

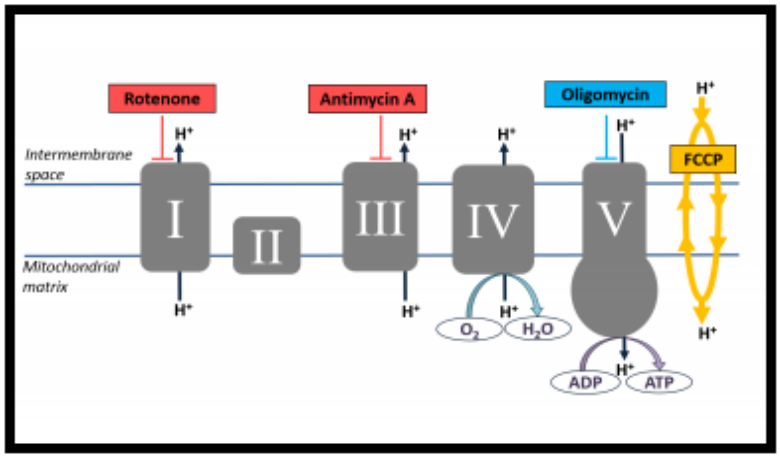

Figure 2.5: Mitochondrial stress test modulators that inhibits complexes of the electron transport chain [262]

Table 2.4: Glycolysis stress test drug calculations (Prepared in Seahorse media (DMEM) 0mM glucose)

Port	Drug	Stock conc.		Final conc.		x conc.	Final vol. (µl)	Volume of stock (µl)	Volume of media (µl)
A	LPS	1000	µg/ml	1	µg/ml	8	1000.0	8.0	992.0
B	Glucose (Sigma)	2498	mM	25	mM	9	1000.0	90.1	909.9
C	Oligomycin (Sigma)	5000	µM	1.5	µM	10	1000.0	3.0	997.0
D	2-DG (Sigma)	1M (use as it is)						1000	0

Table 2.5: Mitochondrial stress test drug calculations (Prepare in Seahorse media (DMEM) 2.5mM glucose)

Port	Drug	Stock conc.		Final conc.		x conc.	Final vol. (µl)	volume of stock (µl)	Volume of media (µl)
A	LPS	1000	µg/ml	1	µg/ml	8	1000.0	8.0	992.0
B	Oligomycin (Sigma)	5000	µM	1.5	µM	9	1000.0	2.7	997.3
C	FCCP (sigma)	5000	µM	1.5	µM	10	1000.0	3.0	997.0
D	Antimycin A (Sigma)	5000	µM	2.5	µM	11	1000.0	5.5	991.8
	Rotenone (Sigma)	5000	µM	1.25	µM			2.8	

2.2.11 Mito-Tracker Flow Staining

MoDCs lifted off 6 well plates were washed twice and equally distributed in a 24 well plate before staining with 10 nM Mito-Tracker Green (Thermo Fisher Scientific) and Mito-Tracker Deep Red (Thermo Fisher Scientific) for 45 minutes at 37ºC. Cells were then washed in PBS at 300 g for 5 minutes at 4ºC, resuspended in 120 µl of PBS and data acquired for flow cytometric analysis using a LSR Fortessa (BD Biosciences). Unstained cells were used to determine the optimal photomultiplier tube (PMT) voltages on the flow cytometer, single stained cells were included as compensation controls and a minimum of 10,000 cells/sample were collected for analysis.

2.3 Murine Studies

2.3.1 Mice and tumour growth

Curtin University Animal Ethics Committee (AEC) approved this project (AEC approval numbers: AEC_2012_21 and AEC_2016_05); all experiments were performed in accordance with the Australian Code of Practice. Female mice C57BL/6J mice 6 to 8 weeks old (equivalent to 14-20 human years) and 18 months old (equivalent to 60-70 human years) were obtained from the Animal Resources Centre, Perth and maintained under standard animal housing conditions at the Curtin University Animal Facility. For studies involving healthy mice, any mouse with an enlarged spleen, lymph nodes and/or liver was excluded. For studies involving tumour-bearing mice, mice were injected with 5×10^5 AE17 tumour cells in 100 µl of PBS, subcutaneously in the right flank, by Dr. Connie Jackaman, Curtin University and tumour growth monitored regularly. Micro-callipers were used to measure tumour size. The maximum tumour size allowed was 140 mm^2 in accordance with AEC ethics approval.

2.3.2 Collection and processing of murine samples

Methoxyflurane (Medical Developments International, Victoria, Australia) was used to anaesthetise mice prior to euthanasia by cervical dislocation. Lymph nodes (LN), bone marrow (BM) and spleens were collected from healthy (non-tumour bearing) mice whilst spleens, BM, tumour, and tumour draining lymph nodes were collected

from AE17-tumour bearing mice. Frosted glass slides were used to gently disaggregate tumours, lymph nodes and spleens into single cell suspensions. BM was flushed from tibiae and femurs using fluorescence-activated cell sorting (FACS) buffer (1x PBS/1% normal calf serum (NCS, ThermoScientific)/1% bovine serum albumin (BSA, Sigma-Aldrich) in a 0.5 ml insulin syringe. Samples were then centrifuged at 300 g for 5 minutes, supernatants removed, cells resuspended in FACS buffer and washed once by centrifuging at 300 g for 5 minutes.

2.3.3 Staining protocol

Prior to staining, an Fc block (CD16/32) diluted 1:200 in FACS buffer was used to prevent the Fc portion of the staining antibodies binding FcyRIII and FcyRII potentially resulting in false positives [263]. Antibody staining panels used for identifying murine DCs and macrophages are shown in Tables 2.6 and 2.7, respectively. 20 µl of Fc block was added per well and cells incubated for 30 minutes in the dark at 4°C. Cells were then washed twice with 200 µl of FACS buffer by centrifugation at 300 g for 2 minutes at 4°C and stained with 20 µl per well of the primary antibodies diluted in FACS buffer (as per Table 2.6 and 2.7) for 30 minutes in the dark at 4°C. Cells were again washed twice with 200 µl of FACS buffer by centrifugation at 300 g for 2 minutes at 4°C. After the second wash, cells were stained with 20 µl per well of the secondary antibodies (diluted in FACS buffer; Table 2.6) for 30 minutes in the dark at 4°C. Cells were then washed once with FACS buffer and once with PBS by centrifugation at 300 g for 2 minutes at 4°C. After washing, cells were stained with Zombie (diluted in PBS, Table 2.6) for 15 minutes in the dark at 4°C, washed twice with PBS before being stained with Bodipy dye (diluted in PBS, Table 2.6) for 15 minutes in the dark at 4°C. Zombie NIR is an amine reactive fluorescent dye which is permeant to cells with a compromised membrane, but is non-permeant to live cells and is used to asses dead versus live cells [264]. A further two washes were performed with FACS buffer at 300 g for 2 minutes at 4°C when cells were resuspended in 200 µl of FACS buffer before flow cytometric analysis on a BD LSR Fortessa (BD).

2.3.4 Flow cytometry control and gating

Unstained cells were used to determine the optimal photomultiplier tube (PMT) voltages on the flow cytometer for each fluorochrome, taking into account potential sample autofluorescence. Single-stained cells were used as compensation controls to account for fluorescence spillover. Fluorescence minus one (FMO) controls were performed for molecules with specific fluorochromes that demonstrated spreading or spillover on the single stain profile and the cells of interest could not be resolved. FMO controls were performed for key markers because of limited resources. The FMOs used were MHC-I conjugated to PerCP-Cy5.5, MHC-II conjugated to AF700, BODIPY FL dye with similar excitation and emission to fluorescein (FITC), and CD11c conjugated to BV605 during staining optimisation (Figure 2.6). FMO controls included all antibody conjugates present in the test sample except one and were used as gating controls [265]. The antibodies conjugated to fluorochrome markers used are shown in Tables 2.8 and 2.9 for the macrophage and DC staining panels respectively. The study used Ly6C and Ly6G instead of GR-1 in macrophage panel because Shawn et al demonstrated that for flow cytometry, Ly6C/Ly6G are superior to GR-1 for identifying different subsets of macrophages/monocytes [266]. The study further showed that interactions between anti-F4/80 antibody and anti-GR-1 antibody lead to poor discrimination of $F4/80^{+}$ and $F4/80^{-}$ cells, however this is not the problem when co-incubated with other markers conjugated to same fluorochrome [266]. A dump gating channel using the following three markers Zombie NIR, CD3 (expressed on T cells) [267] and NK1.1 (expressed on natural killer cells, [268]) was used to exclude dead cells, T cells and NK cells for macrophage and DC flow cytometric analyses.

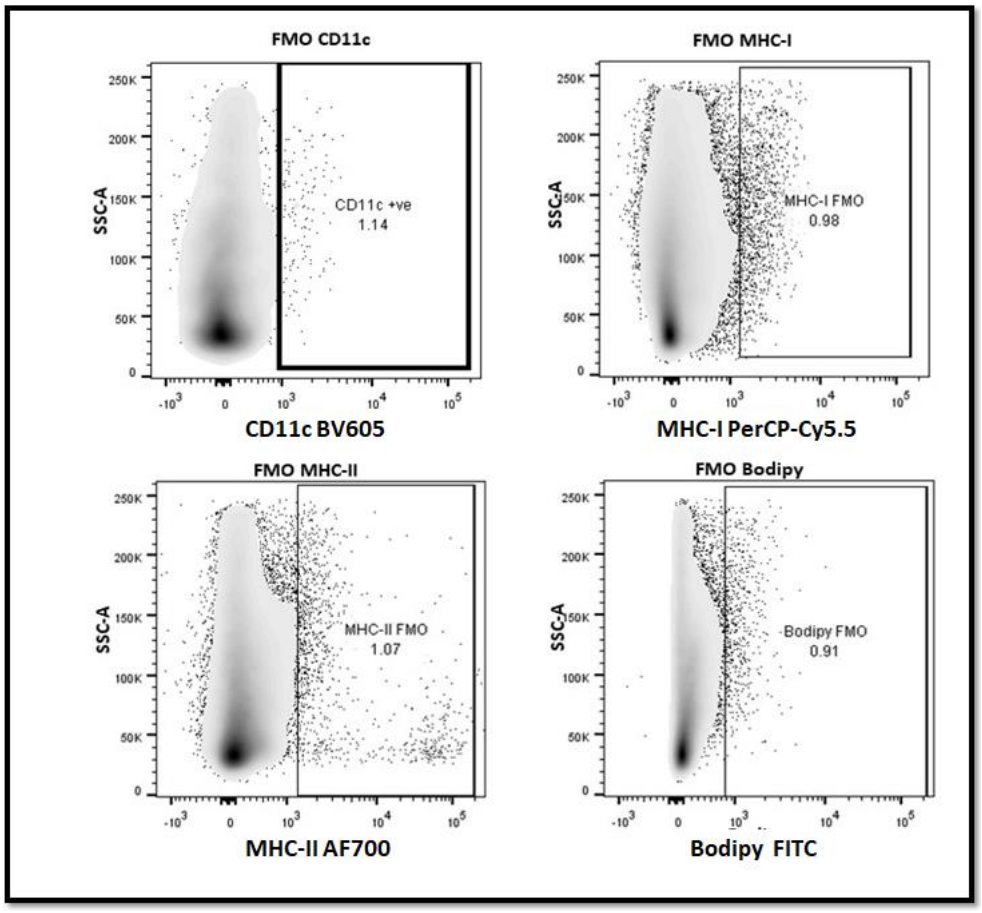

Figure 2.6: FMO controls used in the study

Filter	Antibody	Dilution
V_450/50	CD80-BV421	1:200
V_525/50	Ly6C Biotin + SA V500	1:200(Ly6C) SA V500: 1:500
V_605/12	CD11c BV605	1:100
V_655/8	CX3CR1-BV650	1:200
V_780/60	Ly6G-BV785	1:200
B_530/30	Bodipy FITC	1:200
B_575/26	F4/80 PE	1:100
B_695/40	MHC Class I-PerCP-Cy5.5	1:200
B_780/60	CD11b PE-Cy7	1:500
R_670/14	CD40 APC	1:200
R_730/45	MHC II AF700	1:200
R_780/60	CD3-APC Cy7, NK1-APC Cy7,ZOMBIE NIR	CD3-APC 1:100, Zombie NIR: 1:400 NK1-APC:1:100

Table 2.6: The macrophage staining panel and dilutions used

This table shows the flow panel designed for ex-vivo analysis of murine macrophages. Controls used were unstained cells and single stains. A dump channel was included that consisted of Zombie NIR (to exclude dead cells), CD3 and NK1.1 (to exclude T cells and NK cells). For staining optimization purposes, controls included pooled samples from young healthy mice, young tumour-bearing mice, old healthy mice and old tumour-bearing mice.

Filter	Antibody	Dilution
V_450/50	CD80-BV421	1:200
V_525/50	B220 Biotin + SA V500	1:200(B220) SA V500: 1:500
V_605/12	CD11c BV605	1:100
V_655/8	CD4 BV650	1:100
V_780/60	MHC II BV785	1:200
B_530/30	Bodipy FITC	1:200
B_575/26	GR1 PE	1:200
B_695/40	MHC Class I-PerCP-Cy5.5	1:200
B_780/60	CD11b PE-Cy7	1:500
R_670/14	CD40 APC	1:200
R_730/45	MHC II AF700	1:200
R_780/60	CD3-APC Cy7, NK1-APC Cy7,ZOMBIE NIR	CD3-APC 1:100, Zombie NIR: 1:400 NK1-APC:1:100

Table 2.7: Dendritic cell panel

The table shows the dendritic cell panel designed for ex-vivo analysis of murine samples and the antibody dilutions used for the study.

2.3.5 Generating murine bone marrow-derived dendritic cells and macrophages

Frozen murine BM cells were transferred to a 37°C water bath until approximately 50% thawed when 0.5 ml media from a 50 ml tube containing cRPMI media and 10% FCS was added and the media gently mixed until the cells were fully thawed and transferred to 50 ml tube (containing cRPMI media and 10% FCS) in a dropwise manner using a transfer pipette. Cells were centrifuged at 300 g for 5 minutes and supernatant discarded. Cells were gently resuspended using a serological pipette in 10 ml warmed cRPMI media and again, centrifuged at 300 g for 5 minutes and supernatant discarded. Cells were counted and cultured in 6 well plates (BD plates) at

1-5 x 10^6 cells/ml (depending on number of wells required) with cRPMI media supplemented with 20 ng/ml murine GM-CSF (Shenandoah Biotechnology, Pennsylvania, USA), 20 ng/ml recombinant murine IL-4 (Shenandoah Biotechnology) and 10 μg/ml Polymyxin B (Sigma-Aldrich). At day 3 or 4, supernatants were removed, and cells resuspended in 2 ml of cRPMI media supplemented with GM-CSF and IL-4. Media was changed again on day 5 or 6 supplemented with growth factors and cells were ready for stimulation on day 7 with LPS or AE17 TCM. Alternatively, to differentiate the BM cells into macrophages, a similar protocol was followed however cells were cultured for 7 days in cRPMI media supplemented with 50 ng/ml murine macrophage colony-stimulating factor (M-CSF; Shenandoah Biotechnology, Pennsylvania, USA). Media was changed along with growth factors on day 3 and day 6 and cells were ready for stimulation on day 7 with LPS or AE17 TCM.

2.3.6 Bodipy staining for immunohistochemistry and confocal microscopy

Cells were removed from the 6 well plates and washed with 2 ml PBS. After washing, cells were seeded on a 96 well Falcone black/clear bottom plates and fixed with 2% paraformaldehyde for 15 minutes at room temperature in dark. After fixation, cells were washed twice with 2 ml of FACS buffer. Bodipy 493/503 (diluted 1:1000 in PBS to a final concentration of 1 μg/ml) was added for 15 minutes on ice in the dark. Three washes of 5 minutes each were performed, and cells were finally left in PBS for imaging. DAPI (1:1000 was included in the first wash to counterstain nucleus). BODIPY or boron dipyrromethene is a class of UV absorbing molecules which demonstrates a sharp emission peak [269]. The chemical formula of BODIPY is $C_{13}H_{15}BF_2N_2$ and targets lipid molecules [269]. BODIPY FL has a similar excitation and emission to fluorescein (FITC) [270] and hence was used on the FITC channel.

Nikon A1+ point scanning confocal microscope with NIS elements software (Nikon instruments, Tokyo, Japan) was used to scan the images using a Plan Apo 40x objective lens (NA 0.95) with sequential laser scanning using 405 nm (450/50 filter for DAPI), 488nm (525/50 filter for Bodipy 493/503). Settings were compared to unstained negative controls. Approximately four images were taken from each sample. Images were analysed using NIS elements advanced research software (Nikon).

Table 2.8: Murine DC panel

Antigen/ Target Molecule	Fluorochrome / Conjugate	Supplier	Dilution	Catalog number	Antibody concentration (mg/ml)
B220	Biotin	Biolegend	1:200	128003	0.1
Neutral lipids	Bodipy - dye	Thermo Fisher Scientific	1:200	D3922	1 µg/ml for imaging and 0.5 µg/ml for flow cytometry
CD3	APC/Cy7	Biolegend	1:100	100222	0.02
CD4	BV650	Biolegend	1:200	100545	0.04
CD8	AF700	Biolegend	1:200	344724	0.04
CD11b	BUV395	Becton Dickinson	1:100	563553	0.02
CD11c	BV605	Biolegend	1:100	117334	0.02
CD36	APC	Biolegend	1:100	102611	0.02
CD80	BV421	Becton Dickinson	1:200	562611	0.04
CD86	PE-Cy7	Biolegend	1:200	105013	0.04
CD147	PE	Biolegend	1:100	123707	0.02
GR-1	PE CF594	Biolegend	1:100	108451	0.02
MHC-I	PerCP-Cy5.5	Biolegend	1:200	116515	0.04
MHC-II	BV785	Biolegend	1:200	107645	0.04
NK1.1	APC/Cy7	Biolegend	1:100	108723	0.02
Steptavidin-V500	Binds to Biotin	Becton Dickinson	1:200	561419	0.1
Zombie	NIR	Biolegend	1:400	423105	Reconstituted in 100µl of DMSO

Table 2.9:Macrophage cell panel for the ageing mouse experiments

Antigen/ Target molecule	Fluorochrome/ Conjugate	Supplier	Dilution	Catalog number	Antibody concentration (mg/ml)
Neutral lipids	Bodipy Dye	Thermo Fisher Scientific	1:200	D3922	1 μg/ml for imaging and 0.5 μg/ml for flow cytometry
CD8	AF700	Biolegend	1:200	344724	0.04
CD11b	BUV395	Becton Dickinson	1:100	563553	0.02
CD11c	BV605	Biolegend	1:100	117334	0.02
CD36	APC	Biolegend	1:100	102611	0.02
CD80	BV421	Becton Dickinson	1:200	562611	0.04
CD86	PE-Cy7	Biolegend	1:200	105013	0.04
CD147	PE	Biolegend	1:100	123707	0.02
CX3CR1	BV650	Biolegend	1:200	149033	0.04
F4/80	PE CF594	Becton Dickinson	1:100	565613	0.02
Ly6C	Biotin	Biolegend	1:200	128003	0.04
Ly6G	BV785	Biolegend	1:200	127645	0.04
MHC-I	PerCP-Cy5.5	Biolegend	1:200	116515	0.4
MHC-II	BV785	Biolegend	1:200	107645	0.4
Zombie	NIR	Biolegend	1:400	423105	Reconstituted in 100μl of DMSO

Table 2.10: Molecules examined in this study and their expression and functions

Molecules	Other names	Expression and functions
B220	CD45R	BM precursors, thymocytes, B cells, activated T cells, natural killer (NK) cells and plasmacytoid (pDCs)
		Lymphocyte proliferation, differentiation and activation [167, 271-278]
CD4	T4	DCs, macrophages, monocytes, thymocytes, T helper (Th) cells
	L3T4	
		Promotes Th1 cell migration by binding IL-16
		Functions as a T cell co-receptor by binding MHC-II, assisting T cell receptor (TCR) antigen recognition and T cell activation [279-288]
CD8α	T8	DCs, thymocytes, NK cells and cytotoxic T cells
	Lyt2	
	Ly-2	Its function on DCs is unknown
		Functions as a T cell co-receptor, binds MHC-I, assists TCR antigen recognition and T cell activation [286, 287, 289-292]
CD11b	Macrophage-1 antigen (Mac-1)	DCs, macrophages, monocytes, granulocytes, B, T and NK cells
	Integrin αM	Mediates cell migration and adhesion, phagocytosis of particles opsonized with complement component iC3b, binds fibrinogen, neutrophil cytotoxicity
	Complement receptor 3 (CR3)	

		Associates with CD18 (β2 integrin), binds intercellular adhesion molecule (ICAM)-1, 2, and 4 [106, 293-300]
CD11c	Integrin αX CR4 subunit p150	DCs, macrophages, monocytes, NK cells, T cells, B cells and neutrophils Mediates monocyte migration, binds LPS and fibrinogen, activating immune cells Associates with CD18 (β2 integrin), binds Intercellular Adhesion Molecule 1 and 4 (ICAM) to mediate adhesion, phagocytosis of particles opsonized with complement component iC3b [167, 301-315]
CD36	SCARB3 GP88 GPIIIB, GPIV	Platelets, erythrocytes and monocytes Imports fatty acids inside cells and is a member of the class B scavenger receptor family of cell surface proteins [316-318]
CD40	BP50 TNFRSF5	DCs, macrophages, monocytes, T and B cells, platelets, endothelial cells, tumour cells, epithelial cells. Co-stimulatory molecule: on B cells binds CD40L on $CD4^+$ T cells, promoting B cell proliferation, survival and antibody production; on DCs binds CD40L on $CD4^+$ Tcells, leading to DC and T cell activation [319-330]
CD80	B7-1 B7 BB1	DCs, macrophages, monocytes, NK cells B and T cells

		Co-stimulatory molecule: binds cytotoxic T-lymphocyte associated protein (CTLA)-4 and programmed death-ligand 1 (PD-L1)on T cells, inhibiting T cells, binds CD28 on T cells, leading to T cell activation, proliferation and cytokine production [331-341]
CD86	B7-2 B70	DCs, macrophages, monocytes, NK, T and B cells Co-stimulatory molecule: binds CTLA-4 on T cells, leading to T cell inhibition, binds CD28 on T cells, leading to T cell activation, proliferation and cytokine production [331-341]
CD147	Extracellular matrix metalloproteinase inducer (EMMPRIN)	Human metastatic tumours, epithelial cells, endothelial cells and leukocytes. Fetal, neuronal, lymphocyte and extracellular matrix development, promotes matrix metalloprotease (MMP) secretion from fibroblasts, interacts physically with α3β1 integrin at points of cell-cell contact [342-346]
CX3CR1	Fractalkine receptor or G-protein coupled receptor 13 (GPR13)	Lymphocytes and monocytes Binds chemokine CX3CL1, major role in survival of monocytes [347]
F4/80	EMR1	Murine macrophages and human eosinophils Mature mouse cell surface glycoprotein expressed at high levels on various macrophages [348-350]

Galectin-9	Ecalectin	DCs, macrophages, T cells, endothelial and epithelial cells, regulatory T cells (Tregs), intestine, stomach, lungs, tumour cells, liver Induces apoptosis and promotes Tregs as a lectin which binds B-galactosidase, binds T-cell immunoglobulin and mucin-domain containing **(**TIM)-3 on $CD8^+$ T cells and $CD4^+$ Th1 cells. Mediates cell-cell adhesion, cell-extracellular matrix interactions, migration and proliferation. Also plays a role in angiogenesis, brain development and pathogenesis of autoimmune conditions and cancer, binds microbial carbohydrates [351-363]
GR-1	Ly6C/Ly6G	Macrophages, monocytes, granulocytes, myeloid-derived suppressor cells (MDSCs), pDCs, BM cells Ly6C mediates adhesion and homing of $CD8^+$ T cells. It may play a role in neutrophil migration, although the function of Ly6G is unclear [364-371]
MHCI	Humans: HLA-A, -B, and -C Mice: H2-D, -K, -L	All nucleated cells Antigen-presenting molecule that presents peptides to $CD8^+$ TCR [372, 373]
MHCII	Humans: HLA-DR, -DQ, and -DP Mice: I-A, I-E	DCs, macrophage, B cells Antigen-presenting molecule that presents peptides to $CD4^+$ TCR [372, 373]

2.3.7 Data analysis

Statistical significance was calculated using GraphPad PRISM 6 (GraphPad Software Inc, California, USA). For flow analysis, student's t-test, Wilcoxon Signed Rank Test and Mann-Whitney U-test are used for comparison between two samples. Kruskal Wallis Test is used to make multiple comparisons followed by an additional ad hoc Dunn's Test. For western blotting, Image Lab 6.0.1 was used to process the images.

Chapter 3: Examining the effects of mesothelioma and ageing on murine macrophages

3.1 Introduction

A fully functioning immune system is crucial in maintaining health; however, the immune system deteriorates with advancing age which likely contributes to increased susceptibility to infections, autoimmunity and cancer in the ageing population [374]. The innate immune system provides the first line of defence against infection, and macrophages are central effector cells of the innate immune system. Macrophages may also play an essential role in inflammageing, which is defined by age-related low-grade inflammation on account of increasing tissue damage and reduced tissue repair capacity [375]. Several studies have examined macrophages in ageing livers [376-379], and chronic diseases [380-382], and shown that whilst macrophages are essential for healing and maintenance of tissue homeostasis [383], they could also promote tissue dysfunction and inflammation [235, 384].

Although tumour-associated macrophages (TAMs) constitute a large proportion of total tumour cellularity and stimulate critical steps in tumour progression the contribution of age to the numbers and function of TAMs is not yet well understood. This is because most cancer-related preclinical studies only use young adult mice, and human studies have mostly not dichotomised the effect of age in terms of immune responses to cancer with or without treatment [385-388]. A previous study by our group looked at macrophages in tumours from elderly versus young adult hosts and showed that tumours grew faster in elderly mice compared with young mice which coincided with increased TAMs [30]. That study also looked at the effect of ageing and cancer on lymphoid and tumour macrophages and found that macrophages in aged mice showed altered responses to pro- and anti-inflammatory stimuli which corresponded with decreased T cell anti-tumour responses [389-391]. However, the combined impact of ageing and cancer, in particular mesothelioma, on macrophages requires further investigation.

In diseases such as atherosclerosis, lipid accumulation has been shown to be a contributing factor to macrophage dysfunction [392]. Similarly, it has been shown that TAMs accumulate cytoplasmic lipid droplets in colorectal cancer [393], while a study

in ovarian cancer has shown that increased cholesterol influx in TAMs promotes interleukin (IL)-4-mediated reprogramming, that includes inhibition of IFNγ gene expression thereby inhibiting the pro-inflammatory macrophage phenotype [394-396]. There are no data relating to the effect of mesothelioma and ageing on macrophages and lipid uptake, therefore this is addressed here.

Macrophages are versatile and depending on their activation states can perform various functions in different anatomical locations [397, 398]. Arnold et al examined skeletal muscle injury and used in vivo tracing methods to analyze macrophage subsets recruited to the injured site [399]. The authors found that they could distinguish macrophages into $CX3CR1^{lo}/Ly6C^{+}$ and $CX3CR1^{hi}/Ly6C^{-}$ cells, with the former expressing a pro-inflammatory profile and the latter expressing an anti-inflammatory profile [399]. Their results showed that $CX3CR1^{lo}/Ly6C^{+}$ macrophages express IL-1β which is a pro-inflammatory molecule [400] while $CX3CR1^{hi}/Ly6C^{-}$ macrophages express IL-10, an anti-inflammatory cytokine [401]. Geissmann et al, also showed that CX3CR1 expression could be used to distinguish monocyte/macrophage sub-populations [402]. That study showed low expression of CX3CR1 expression in an inflammatory subset and high expression in tissue resident monocytes [402]. In the cancer setting, Movahedi et al. looked at different macrophage subsets in murine tumours such as mammary carcinoma, mammary adenocarcinoma, and Lewis Lung carcinoma and found that tumour-monocyte populations mostly consisted of $Ly6C^{hi}$ and $CX3CR1^{low}$ monocytes [403]. The study classified macrophages based on expression of Ly6C and CX3CR1 [403] and found that $Ly6C^{hi}CX3CR1^{int}$ cells dominated the tumour-infiltrating monocyte pool while $Ly6C^{low}CX3CR1^{hi}$ cells formed a small population.

Classification of monocytes on the basis of Ly6C and CX3CR1 expression has also been reviewed by Arnold and Chazaud, Moser, Shi & Palmer, Gordon & Taylor and Jeong & Jung [397, 404-406]. Arnold and Chazaud studied monocyte/macrophage phenotypes and function during skeletal muscle repair in $CX3CR1^{GFP/+}$ mice. That study demonstrated enhanced recruitment of $CX3CR1^{lo}/Ly6C^{+}$ cells with a pro-inflammatory profile in injured muscles. Those cells later switched phenotype to become anti-inflammatory $CX3CR1^{hi}/Ly\text{-}6C^{-}$ cells [399]. Jeong and Jung reviewed the role of pro-inflammatory cells characterized by expression of $Ly6C^{hi}CX_3CR1^{low}$ populations while anti-inflammatory cells were characterised by

$Ly6C^{low}CX_3CR1^{hi}$ populations [406]. Similarly, Shi and palmer showed that $Ly6C^{hi}$ monocytes give rise to pro-inflammatory macrophages while $Ly6C^{low}$ monocytes differentiate into alternatively activated macrophages and promote wound healing [407].

Chemokines control the migration of myeloid cells and CX3CR1 is a chemokine receptor and a member of the seven transmembrane G-protein coupled receptor family [408]. Monocytes arise from hematopoietic stem cells in bone marrow (BM) and are released into the bloodstream to colonise peripheral organs [407]. With maturation, BM monocytes elevate CX3CR1 levels [408, 409]. CX3CR1 has been shown to mediate retention of monocytes in the BM [409] and modulate inflammatory responses that include monocyte homeostasis and macrophage phenotype and function [410]. Geissmann et al showed that CX3CR1 is expressed in low levels in classical circulatory monocytes with higher expression seen in non-classical monocytes [402]. As mentioned above, CX3CR1 levels are inversely correlated with Ly6C in blood monocytes[409] and macrophages [411]. In inflammatory diseases such as liver fibrosis and cardiovascular disorders, CX3CR1 and its ligand CX3CL1 have been shown to control migration and recruitment of immune cells [412-414]. However, the precise role of CX3CR1 and how it regulates different TAM subtypes is still unknown.

Ly6C has long been used to identify various myeloid populations [415]. $Ly6C^{+}$ monocyte/macrophage populations display distinct proliferative and inflammatory profiles [399]. BM monocytes released into circulation when recruited into inflammatory lesions can differentiate into macrophages and DCs. These monocytes also show differential expression of chemokine receptors such as C-C-Chemokine Receptor type 2 (CCR2) and CX3CR1 [177, 397]. A subset of $Ly6C^{+}$ monocytes have been shown to differentiate into M1-like cells and initiate inflammatory responses [416]. Bain et al, demonstrated that $Ly6C^{hi}$ monocytes differentiating into $CX3CR1^{hi}$ monocytes acquire anti-inflammatory genes alongside increased expression of CD163, CD206 and TGFβR2,and downregulation of pro-inflammatory genes including CCR2, IL6 and iNOS [417]. $Ly6C^{hi}$ and $Ly6C^{low}$ macrophages can play pro-tumoral or anti-tumoral roles depending on context [418-424]. For example, in early stages of inflammatory arthritis, $Ly6C^{-}$ monocytes can differentiate into M1-like macrophages. In later stages, these cells can re-polarise into M2-like macrophages, promoting resolution of joint inflammation [425].

Therefore, Ly6C^{hi} and CX3CR1^{low} expression may be considered to represent classical inflammatory monocytes in mice, whereas non-classical alternative monocytes are represented by Ly6C^{low} and CX3CR1^{high} expression [426]. Our group has previously used these markers to distinguish macrophages subsets [28, 427]. Therefore, to extend our previous studies, this thesis used the same markers and gating strategy to identify macrophages subsets in the context of ageing and mesothelioma. This chapter examines the combined effect of ageing and mesothelioma on murine macrophage subsets, focussing on changes to lipid content, molecules associated with lipid uptake and antigen-presentation.

3.2 Results

3.2.1 Mesothelioma elevates lipid levels in murine macrophages in-vitro

The first series of experiments investigated the effects of AE17 mesothelioma tumour conditioned media (TCM) on bone marrow (BM)-derived murine macrophages. BM cells obtained from young adult C57BL/6J healthy mice (2-5 months old) were cultured in media supplemented with murine macrophage colony-stimulating factor (M-CSF) that was refreshed on day 3 and day 6. Macrophages were exposed to 50% TCM (chapter 2, section 2.1.2) on day 7 for 24 hours, while 50% of SFM was also added to control wells to match TCM-exposed wells. The cells were then stained with Bodipy to detect intracellular neutral lipids and surface MHC-I and MHC-II molecules which present peptides to CD8$^+$ T cells and CD4$^+$ T cells respectively [428, 429], and analysed by flow cytometry. The gating strategy is shown in Figure 3.1 A-C. No changes were observed in the percentage of cells positive for bodipy, MHC-I or MHC-II (3.1 D-F). However, lipid levels measured by MFI significantly increased in TCM-exposed macrophages relative to unexposed macrophages (Figure 3.1G). Although surface MHC-I expression levels appeared to decrease, differences to controls did not reach statistical significance (Figure 3.1H). On the other hand, there was a statistically significant reduction of surface MHC-II expression levels (MFI) implying a reduced capacity to activate tumour-infiltrating CD4$^+$ T cells (Figure 3.1I). This increase in lipid content in mesothelioma-exposed macrophages was visualised and confirmed through staining with Bodipy and images recorded with Nikon confocal microscope (Figure 3.2). However, the study did not used negative control of DAPI which is

essential to determine the background autofluorescence. The study used split filters and unexposed DCs to set up the instrument.

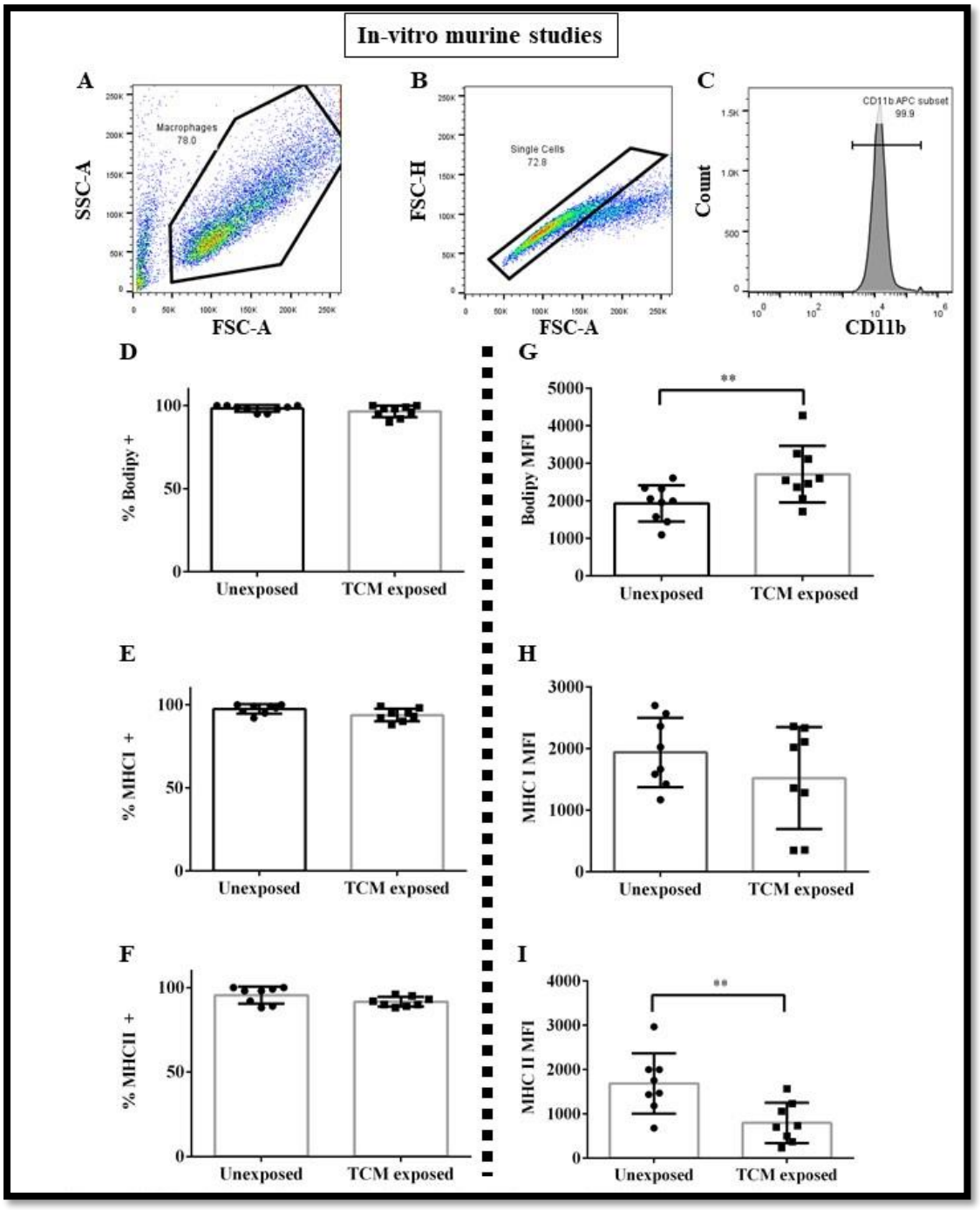

Figure 3.1: Mesothelioma increases lipid content and decreases MHC-I/II in macrophages

Macrophages generated from bone marrow (BM) taken from healthy mice (aged 2-5 months) were left untreated or exposed to AE17 mesothelioma-derived tumour conditioned media (TCM) before being stained with Bodipy to measure neutral lipids; MHC-I, an antigen presenting molecule that presents peptides to $CD8^+$ T cells; and MHC-II, that presents peptides to $CD4^+$ T cells. Large cells **(A),** single cells **(B)** and $CD11b^+$ cells **(C)** were gated. **D**, **E** and **F** show percent of cells positive for Bodipy, MHC-I and MHC-II respectively. **G, H and I** show expression levels measured as MFI of Bodipy, MHC-I and MHC-II. Data shown as mean ± SEM, n = 8. ** = $p<0.005$. Statistical significance assessed by a Wilcoxon signed-rank test.

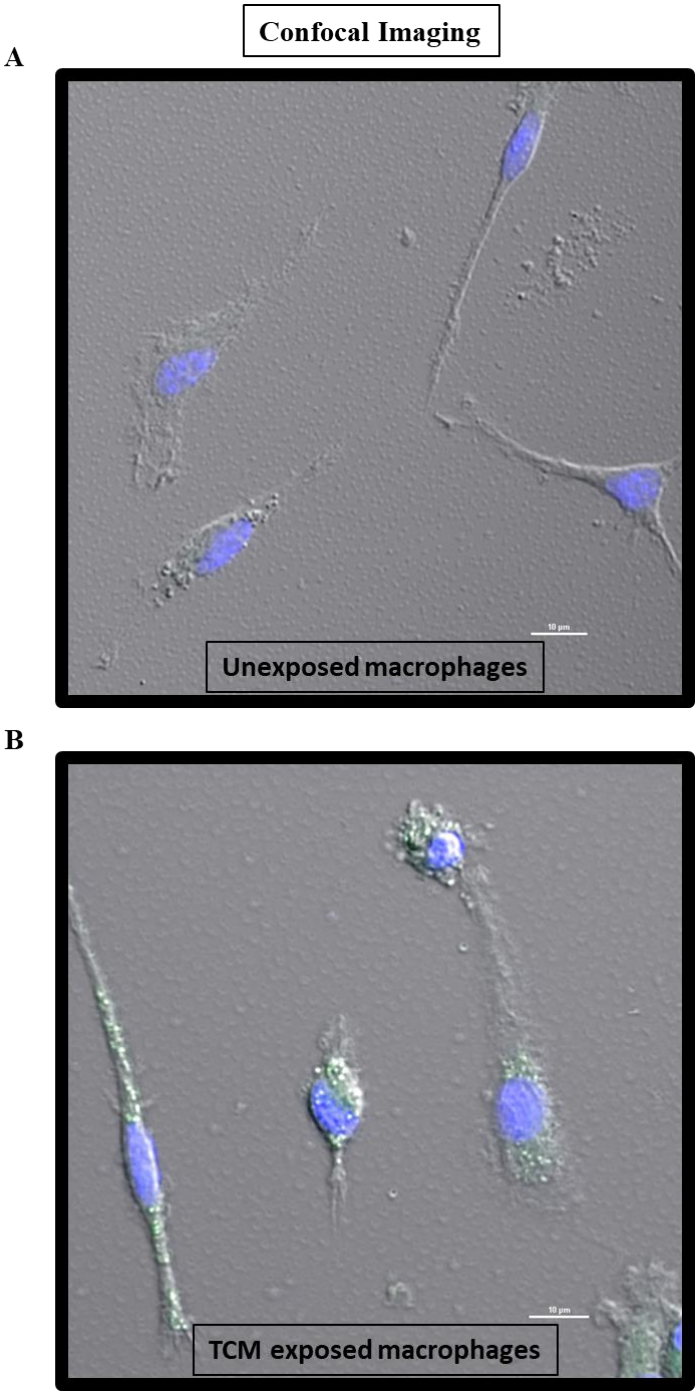

Figure 3.2: Mesothelioma increases lipid content in TCM exposed macrophages

Macrophages generated from BM taken from healthy mice (aged 2-5 months) were left untreated or exposed to TCM. Unexposed macrophages (A) and TCM-exposed macrophages (B) were cultured on glass bottom plates before being stained with Bodipy (green) and DAPI (nucleus, blue). After fixation the cells were visualised using a Nikon A1^{+} confocal microscope.

3.2.2 Examining the effects of ageing and mesothelioma on murine macrophages *in-vivo*

The effect of ageing with or without mesothelioma tumours on $CD11b^+F4/80^+$ cells in BM, spleens, dLNs and tumours in young versus old mice was examined using flow cytometry as per Figure 3.3.

3.2.3 $CD11b^+F4/80^+$ macrophages increase in lymphoid organs with ageing

Healthy ageing did not affect $CD11b^+F4/80^+$ BM cell proportions which remained the same in young healthy (YH) versus old healthy (OH) BM macrophages (Figure 3.4). Also, the presence of mesothelioma did not induce any changes in the proportions of BM macrophages relative to their aged matched heathy counterparts, i.e. there was no change in the percentage of $CD11b^+F4/80^+$ cells between young tumour-bearing (YT) versus YH mice or in old tumour-bearing (OT) versus OH mice (Figure 3.4). In contrast, an effect of age and mesothelioma was observed as $CD11b^+F4/80^+$ cell proportions in BM macrophages, as their numbers were significantly increased in OT and OH mice compared to YT mice (Figure 3.4A). The increase in $CD11b^+F4/80^+$ cell proportions in old mice in BM might be to supply cancer-promoting macrophages [430].

Whilst there was a significant increase in $CD11b^+F4/80^+$ splenic cell proportions in OH mice compared to YT mice (Figure 3.4B), the data is difficult to interpret as no other differences were seen.

In lymph nodes, healthy ageing led to a significant increase in $CD11b^+F4/80^+$ cell proportions in OH compared to YH mice. Also, tumour and ageing led to a significant increase in $CD11b^+F4/80^+$ cell proportions in OT compared to YT mice (Figure 3.4C). This increase in macrophage proportions with healthy ageing and with ageing and tumour may compensate for their reduced function, as speculated in another study [431].

There were no differences between the proportions of $CD11b^+F4/80^+$ TAMs in OT compared to YT mice in tumour tissue (Figure 3.4D). The highest percentage of

$CD11b^{+}F4/80^{+}$ cells (nearly 40-60%) was observed in tumours compared to other lymphoid organs, which correlates with studies showing increased macrophage proportions in tumours [432, 433].

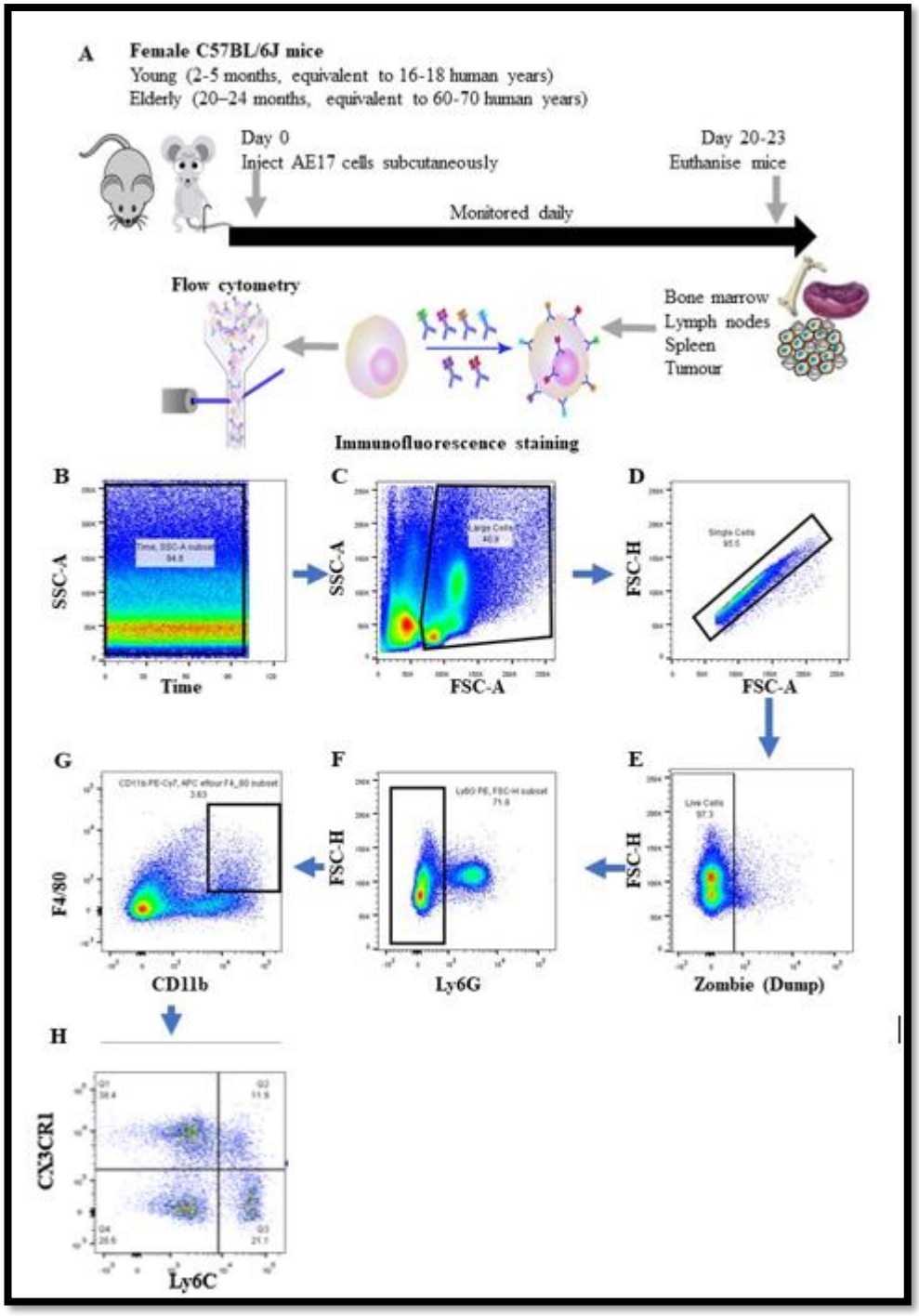

Figure 3.3: The experimental approach and flow cytometric gating strategy to isolate different macrophage subsets based on expression of Ly6C and CX3CR1

(A) Young and old C57BL/6J mice were inoculated with $5x10^5$ AE17 cells in 100µl of PBS on day 0 and monitored daily until tumours reached $120mm^2$ when BM, tumours, draining lymph nodes (dLNs) and spleens were collected and stained with fluorescently-labelled antibodies to detect macrophage

subpopulations using flow cytometry. The gating strategy included selection by time (**B)**, size (**C)** and single cells (**D)** live cells **(E)**, neutrophils were excluded using Ly6G staining **(F)**, before $CD11b^+$ and $F4/80^+$ macrophages (**G**) were identified. $Ly6C^-CX3CR1^-$ (M0) macrophages, $Ly6C^+CX3CR1^-$ (M1-like macrophages), $Ly6C^-CX3CR1^+$ (M2-like macrophages) and $Ly6C^+CX3CR1^+$ (M3 macrophages) subsets were identified based on $Ly6C^+$ and CX3CR1 expression (**H**).

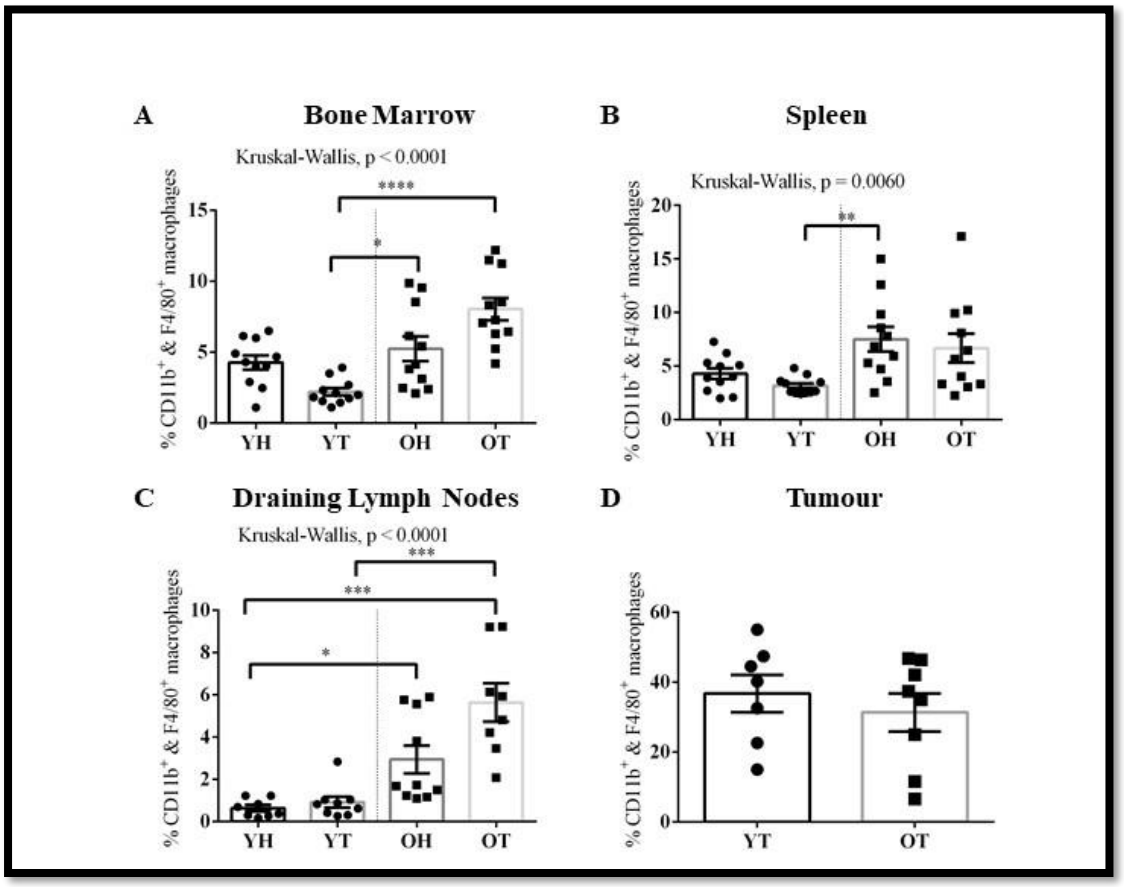

Figure 3.4: $CD11b^+F4/80^+$ macrophages increase in old healthy and tumour bearing mice

BM, spleens, dLNs and tumours from young healthy (YH), young tumour-bearing (YT), old healthy (OH) and old tumour-bearing mice (OT) were stained and $CD11b^+F4/80^+$ macrophages selected as described in Figure 3.3. The proportion of $CD11b^+F4/80^+$ macrophages in BM **(A)**, spleens **(B)**, LNs **(C)** and tumours **(D)** are shown as mean ± SEM, n = 10-11 mice in each group. * = $p<0.05$, ** = $p<0.005$, *** = $p<0.0005$, **** = $p<0.0001$. Statistical significance for three or more than three groups was assessed by Kruskal-Wallis test followed by post hoc Dunn's test while Mann Whitney U test is used to compare two groups.

3.2.4 Examining the effect of age and tumour in BM macrophage subsets

This study further looked at different macrophage subsets such as $Ly6C^{-}CX3CR1^{-}$ (M0 macrophages); $Ly6C^{+}CX3CR1^{-}$ (M1-like macrophages); $Ly6C^{-}CX3CR1^{+}$ (M2-like macrophages); and $Ly6C^{+}CX3CR1^{+}$ (M3 macrophage) subpopulations (Figures 3.5A and B). This thesis describes M0 macrophages as cells that have not differentiated into M1-like pro-inflammatory cells or M2-like anti-inflammatory cells based on expression of the molecules chosen for this study. It is not clear what these cells are, although one possibility is that they are recent arrivals that have not yet responded to tumour-derived factors. In tumours, macrophages can adopt multiple phenotypes ranging from classically activated M1-like cells to alternatively activated M2-like cells [434]. $Ly6C^{+}CX3CR1^{-}$ (M1-like macrophages) are anti-tumourigenic as they release pro-inflammatory cytokines such as IL-6, IL-1β and tumour necrosis factor (TNFα) and have high antigen presentation capacity [435]. On the other hand, $Ly6C^{-}CX3CR1^{+}$ (M2-like) macrophages, characterised by secretion of anti-inflammatory cytokines, such as transforming growth factor-β (TGF-β) and IL-10, may represent anti-inflammatory macrophages [66]. M2-like macrophages develop in response to IL-4, IL-13 or glucocorticoids and promote angiogenesis [434]. $Ly6C^{+}CX3CR1^{+}$ (M3) macrophages are proposed to be an intermediate of $Ly6C^{+}CX3CR1^{-}$ (M1-like macrophages) and $Ly6C^{-}CX3CR1^{+}$ (M2-like macrophages) and retain some of their anti-tumour properties, as they respond to anti-inflammatory cytokines by increased production of pro-inflammatory cytokines [436].

No changes in BM M0 macrophages were observed with healthy ageing or in the presence of mesothelioma relative to their age-matched counterparts (Figure 3.5C). No age-related or tumour-induced changes were observed in BM M1-like macrophages and M2-like macrophages (Figure 3.5 D and E). No effect of healthy ageing was observed in M3 BM macrophages. However, an inverse correlation was observed in M3 macrophages in BM with mesothelioma in young and old mice compared to their healthy counterparts, i.e. M3 macrophage proportions decreased in young mice with mesothelioma relative to their healthy controls whilst M3 cells increased in old young mice with mesothelioma relative to their healthy controls (Figure 3.5 F).

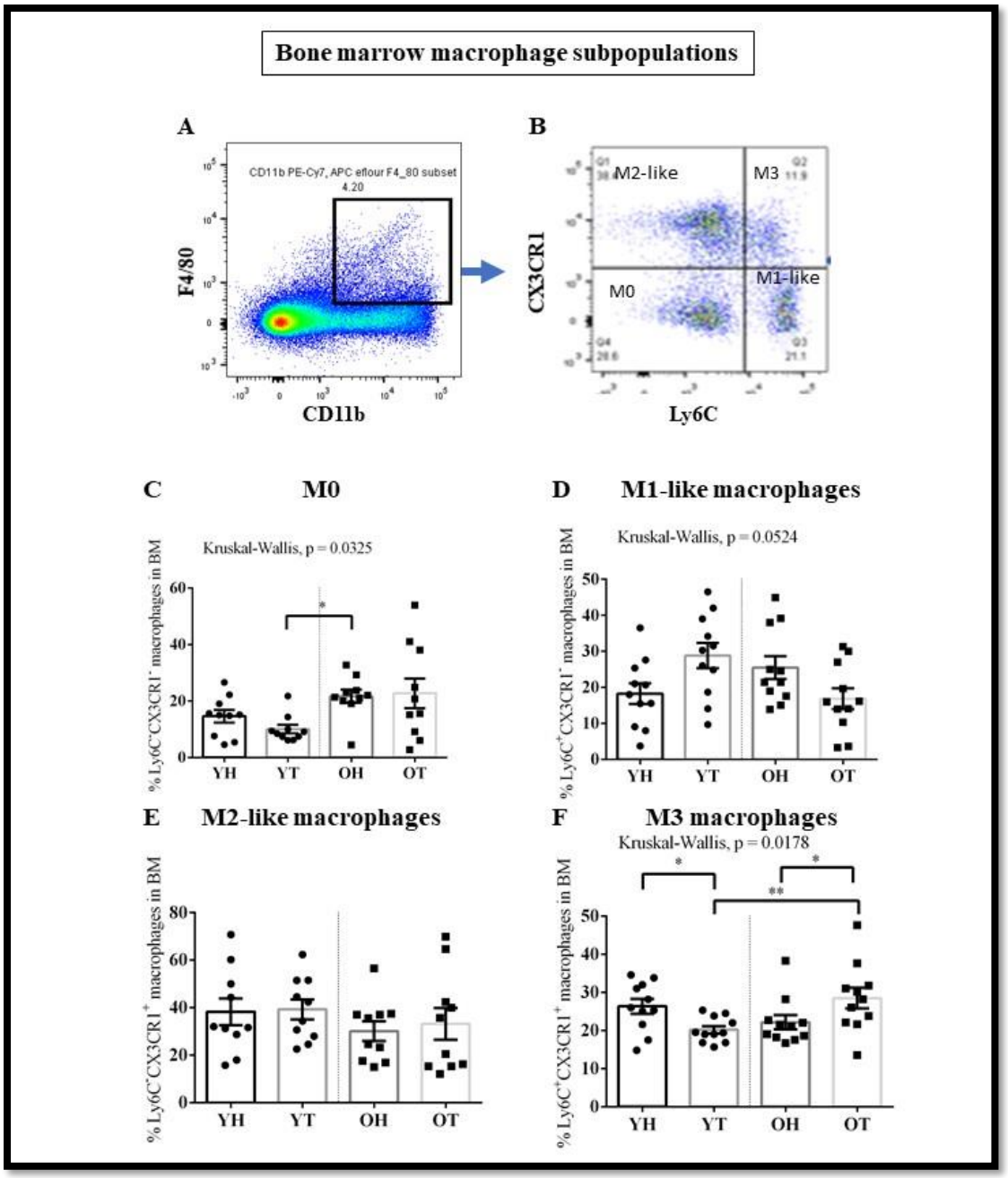

Figure 3.5: Macrophage subpopulation proportions in bone marrow change with age and tumour

BM from YH, YT, OH and OT were stained and $CD11b^+F4/80^+$ macrophages (**A**) selected, as described in Figure 3.3. Macrophage subsets were identified based on $Ly6C^+$ and CX3CR1 expression (**B**). $Ly6C^-CX3CR1^-$ (M0) macrophages **(C)**, $Ly6C^+CX3CR1^-$ (M1-like) macrophages (**D)**, $Ly6C^-CX3CR1^+$ (M2-like) macrophages **(E)**, and $Ly6C^+CX3CR1^+$ (M3) macrophages **(F).** Data shown as mean ± SEM, n = 10-11 mice per group. * = $p<0.05$, ** = $p<0.005$. Statistical significance assessed by Kruskal-Wallis test followed by post hoc Dunn's Test.

3.2.5 M2-like macrophages dominate BM, M1-like macrophages dominate spleen, while M3 macrophages dominate TAMs

An analysis of the different macrophage subpopulations showed that M2-like and M1-like macrophages constitute the dominant group in BM (Figure 3.6A) and spleen respectively (Figure 3.6B), while M3 macrophages are the dominant macrophage population in tumours (Figure 3.6C). This change in tumours, with intermediate M3 macrophages becoming the dominant population is consistent with previous findings of our group showing that mesothelioma leads to incomplete polarisation of macrophage populations indicated by the presence of double positive Ly6C and CX3CR1 cells [437].

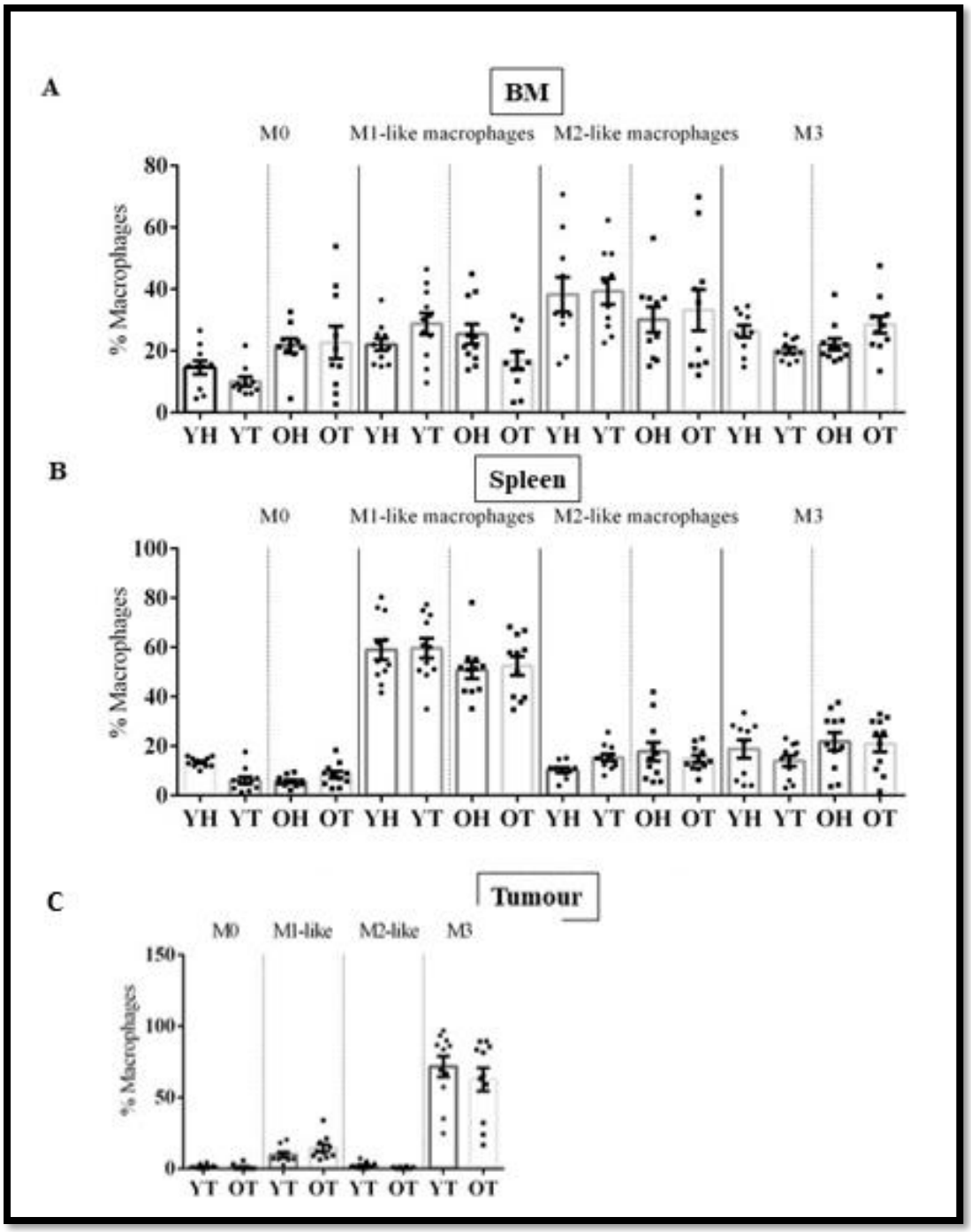

Figure 3.6: M1-like macrophages are the dominant subpopulation in BM and spleen; M3 are dominant in tumours

Macrophages were gated according to Figures 3.3. Proportions of $Ly6C^{-}CX3CR1^{-}$ (M0) macrophages, $Ly6C^{+}CX3CR1^{-}$ (M1-like) macrophages, $Ly6C^{-}$ $CX3CR1^{+}$ (M2-like) macrophages, $Ly6C^{+}CX3CR1^{+}$ (M3) macrophages in BM **(A)**, spleens **(B)**, LN **(C)** and tumours **(D)** shown as mean ± SEM, n = 10-11 mice/group.

3.2.6 Mesothelioma increases lipid content in elderly BM macrophages

Recent studies have shown that lipid metabolism involving lipid uptake, synthesis or transportation play an important role in carcinogenesis via induction of abnormal expression of various proteins and genes, as well as dysregulation of cytokines and signalling pathways [438]. No change in lipid levels was observed with healthy ageing in BM or splenic macrophages. Similarly, no change in lipid levels was noticed with the presence of mesothelioma in young mice compared to their healthy counterparts in BM and splenic macrophages (Figures 3.7 and 3.8). A significant increase was seen in lipid content in old tumour-bearing mice in BM M0 macrophages, BM and splenic M1-like macrophages (Figures 3.7 A, B and 3.8B), and M1-like and M3 TAMs relative to their age-matched controls (Figures 3.9 D and F). These data prompted a study of the molecules that are involved with lipid uptake.

3.2.7 CD36 remains unaffected with age and tumour in BM, spleen, and tumour

CD36, a membrane glycoprotein, present on the surface of many cells including macrophages [439] governs the uptake of cellular fatty acid from endosomes to the plasma membrane, thus participating in lipid utilisation and fat absorption and may contribute to metabolic disorders [440, 441]. No effect on CD36 was observed in BM, spleens, and tumour (Supplementary Figure 3.1, 3.2 and 3.3.).

3.2.8 CD147 increases in BM and splenic M2-like macrophages with healthy ageing

CD147, also known as basigin or extracellular matrix metalloproteinase inducer (EMMPRIN) is a transmembrane protein [343, 442]. CD147 upregulates SREBP1c and represses PPARα and p53 [443, 444], resulting in increased lipogenesis, decreased fatty acid oxidation (FAO) and increased glycolysis [445]. No change in CD147 was observed in M0, M1-like and M3 macrophages (Figure 3.10 A, B and D) with healthy ageing. In contrast, CD147 significantly increased with healthy ageing in M2-like macrophages in BM (Figure 3.10 C) as well as in splenic M0 and M2-like macrophages (Figures 3.10 E and G). No change was observed with healthy ageing in M3 splenic macrophages (Figure 3.10 H).

Lipids – Bone Marrow

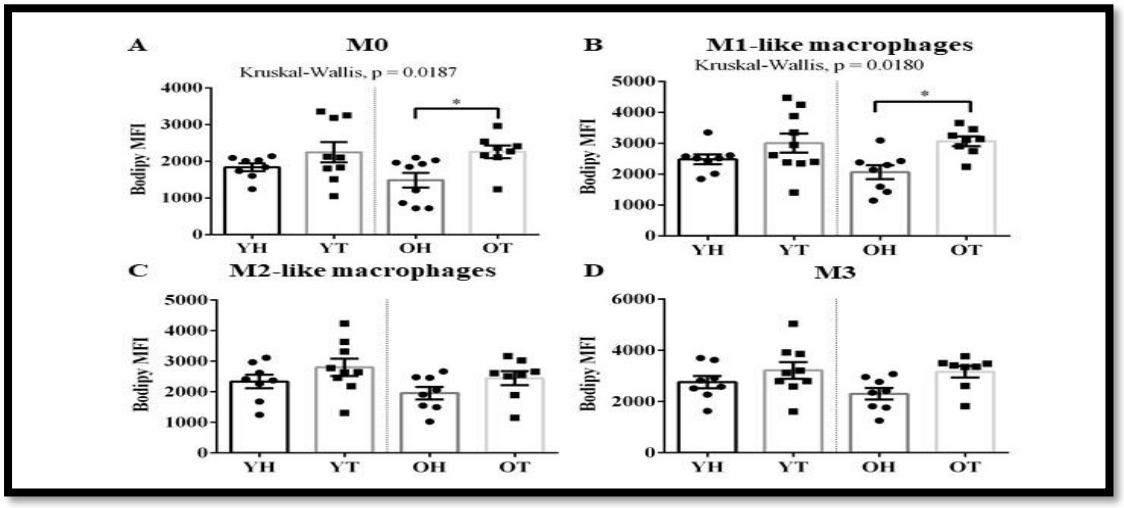

Figure 3.7: Lipid levels increase in BM MO and M1-like macrophages in tumour bearing old mice

BM macrophages from YH, YT, OH and OT were stained with Bodipy to measure neutral lipids and analysed by flow cytometry and expression levels of Bodipy (MFI) in Ly6C$^-$CX3CR1$^-$ (M0) macrophages **(A)**, Ly6C$^+$CX3CR1$^-$ (M1-like) macrophages (**B)**, Ly6C$^-$CX3CR1$^+$ (M2-like) macrophages **(C)**, and Ly6C$^+$CX3CR1$^+$ (M3) macrophages **(D)**. Data shown as mean ± SEM, n = 10-11 mice per group. * = p<0.05, ** = p<0.005. Statistical significance assessed by Kruskal-Wallis test followed by post hoc Dunn's Test.

Lipids – Spleen

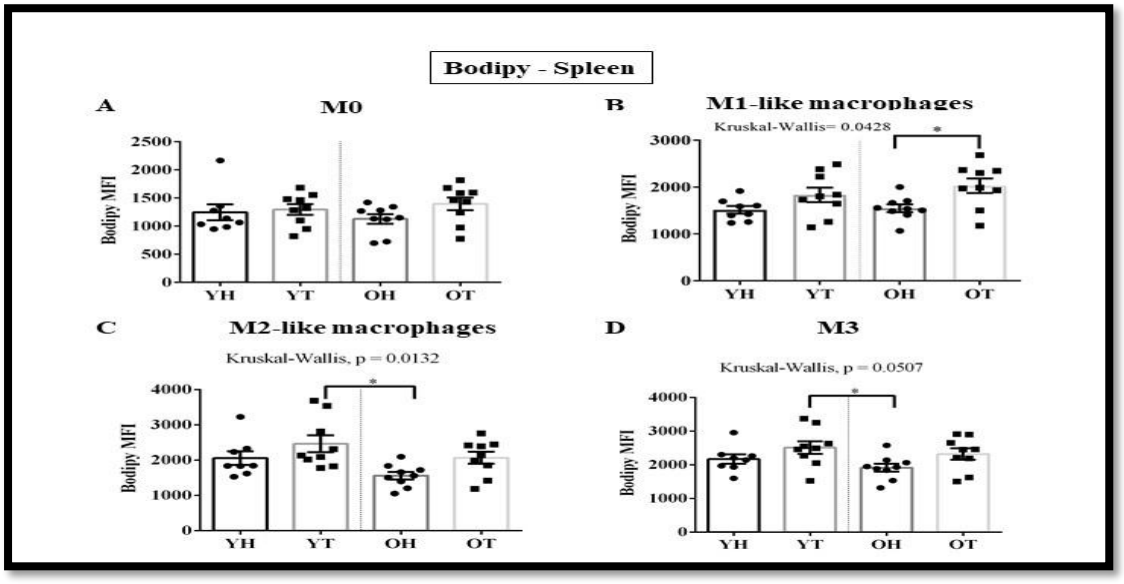

Figure 3.8: Lipid levels increase in splenic M1-like macrophages in tumour-bearing old mice

Splenic macrophages from YH, YT, OH and OT were stained with Bodipy to measure neutral lipids and analysed by flow cytometry. Expression levels of Bodipy (MFI) in Ly6C$^-$CX3CR1$^-$ (M0) macrophages **(A)**, Ly6C$^+$CX3CR1$^-$ (M1-like) macrophages (**B)**, Ly6C$^-$CX3CR1$^+$ (M2-like) macrophages **(C)**, and Ly6C$^+$CX3CR1$^+$ (M3) macrophages **(D)** are shown as mean ± SEM, n = 10-11 mice per group. * = p<0.05, ** = p<0.005. Statistical significance assessed by Kruskal-Wallis test followed by post hoc Dunn's test.

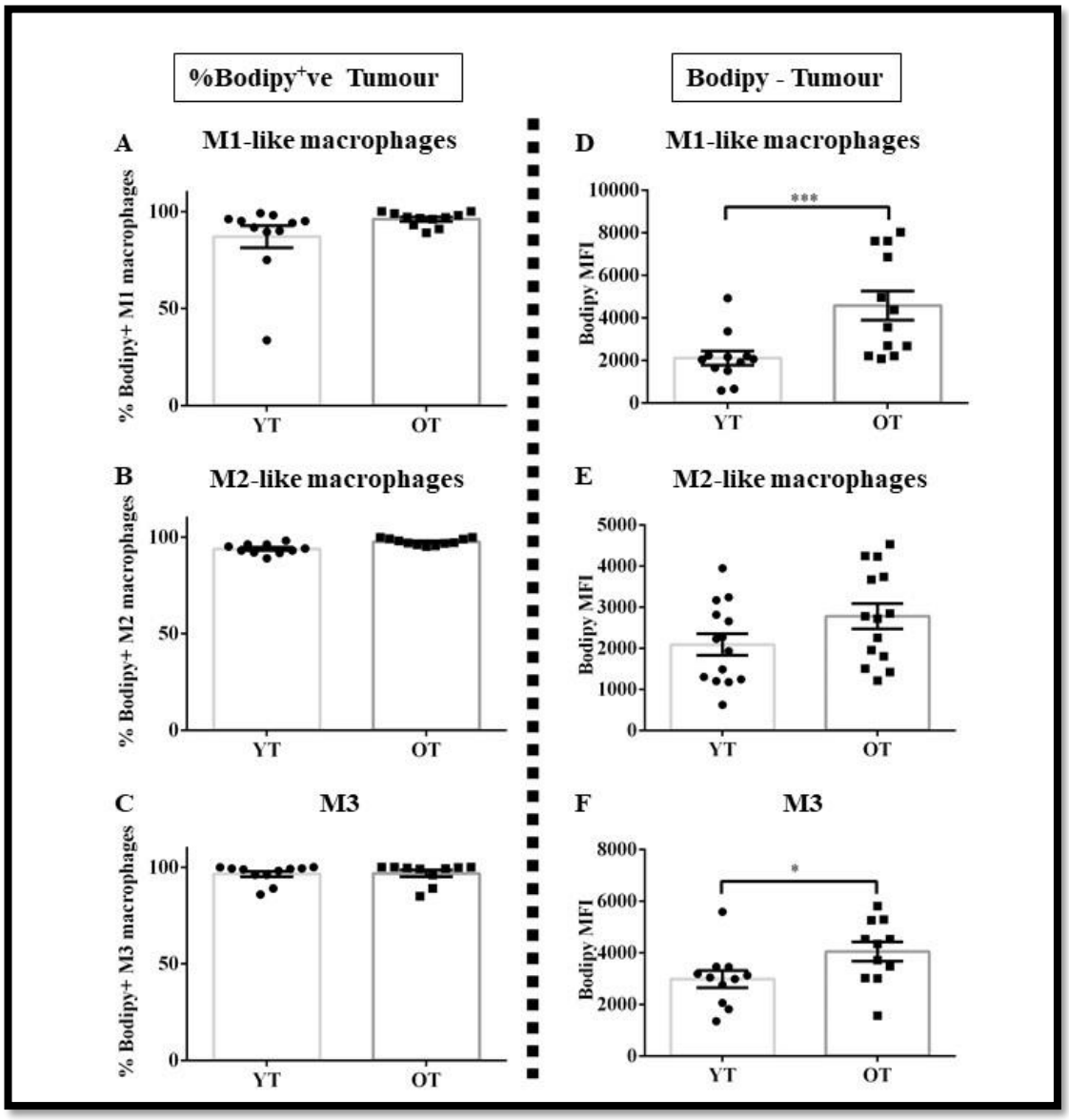

Figure 3.9: Lipid levels significantly increase in M1-like and M3 macrophage subsets in old tumour-bearing mice

TAMs from young tumour bearing (YT) and old tumour bearing mice (OT) were stained with Bodipy to measure neutral lipids and analysed by flow cytometry. Percentage of Bodipy$^+$ cells in Ly6C$^+$CX3CR1$^-$ (M1-like) macrophages (**A)**, Ly6C$^-$CX3CR1$^+$ (M2-like) macrophages **(B)**, and Ly6C$^+$CX3CR1$^+$ (M3) macrophages **(C)** and expression levels of Bodipy (MFI) in Ly6C$^+$CX3CR1$^-$ (M1-like) macrophages **(D)**, Ly6C$^-$CX3CR1$^+$ (M2-like) macrophages **(E)**, and Ly6C$^+$CX3CR1$^+$ (M3) macrophages **(F)** were measured. Data are shown as mean ± SEM, n=10-11, young tumour bearing mice (YT) and n =10-11; old tumour bearing mice (OT). * = $p<0.05$, *** = $p<0.0005$. Statistical significance comparing two groups was assessed by Mann Whitney U test.

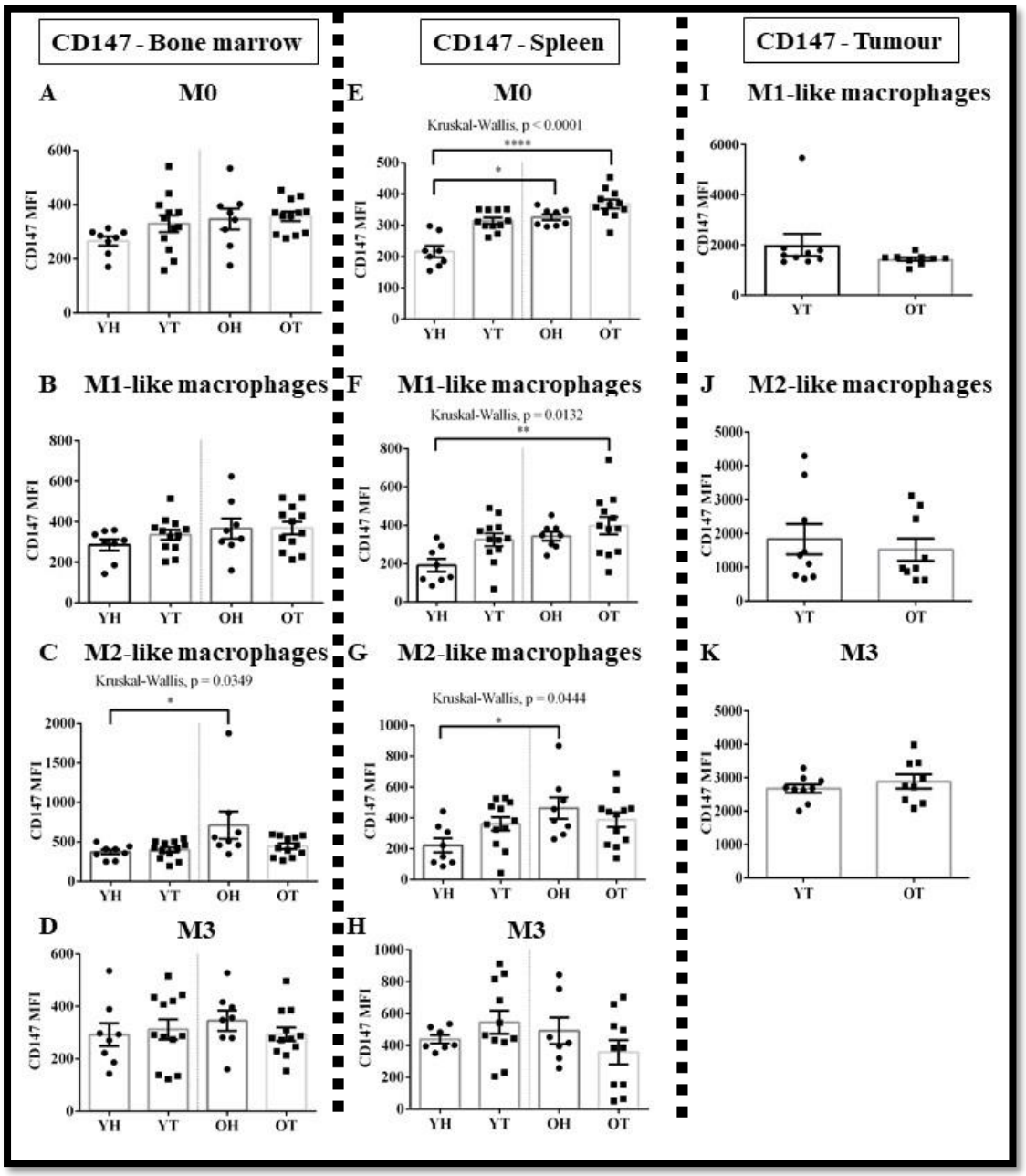

Figure 3.10: CD147 increases with healthy ageing in M2 BM and splenic macrophages

BM, splenic macrophages from YH, YT, OH and OT and TAMs were stained for CD147 expression. Expression levels of CD147 (MFI) in Ly6C$^-$CX3CR1$^-$ (M0) macrophages **(A,E)**, Ly6C$^+$CX3CR1$^-$ (M1-like) macrophages (**B,F,I)**, Ly6C$^-$CX3CR1$^+$ macrophages (M2-like) **(C,G,J)**, and Ly6C$^+$CX3CR1$^+$ (M3) macrophages **(D,H,K)** are shown as mean ± SEM, n = 6 YH mice, n=10-12; YT mice, n =6 OH, n =10-12; OT mice (OT * = $p<0.05$, ** = $p<0.005$, *** = $p<0.0005$. Statistical significance for three or more than three groups was assessed by Kruskal-Wallis test followed by post hoc Dunn's test while Mann Whitney U test is used to compare two groups.

3.2.9 Mesothelioma plus ageing further increase CD147 in M0 and M1-like splenic macrophages

CD147 expression increased in M0 and M1-like splenic macrophages in old tumour bearing mice compared to young healthy mice (Figures 3.10 E and F); no change was observed in BM and TAMs (3.10 A-D, I-K).

3.2.10 Ageing leads to increased MHC-I expression in bone marrow macrophages

Macrophages internalise antigens for processing and presentation on MHC molecules [446]. The number and stability of MHC-peptide complexes are crucial for effective antigen presentation and induction of an immune response [447]. Others have shown that as tumours progress, the tumour microenvironment is increasingly dominated by MHC-II^{low} TAMs [448] and genes involved in MHC-II dependent antigen presentation are downregulated [99]. Here, surface molecules associated with antigen presentation (such as MHC-I and MHC-II) and T cell co-stimulatory molecules (such as CD80, CD40) were examined in lymphoid organs and tumours.

This study found that the proportion of BM MHC-I^{+} M0 macrophages increases with age and mesothelioma in OT mice compared to YH (Figure 3.11A), more importantly their MHC-I expression levels significantly elevated in OT relative to YT mice. Similarly, increased MHC-I expression was seen in M1-like BM macrophages in OT mice compared to YT mice (Figure 3.11 E and F) suggesting maintenance of macrophage antigen presenting function with ageing. No effect of age or tumour was seen on splenic macrophages (Supplementary Figure 3.4).

3.2.11 Mesothelioma decreases the proportion of MHC-I^{+} M2-like and M3 TAMs

The proportion of MHC-I^{+} M2-like and M3 TAMs in elderly mice was significantly reduced in tumour tissue compared to young mice (Figures 3.12 B and C), with significantly decreased expression levels of MHC-I on M3 TAMs (Figure 3.12F), suggesting a reduced capacity to activate CD8^{+} T cells in elderly mesothelioma tumours.

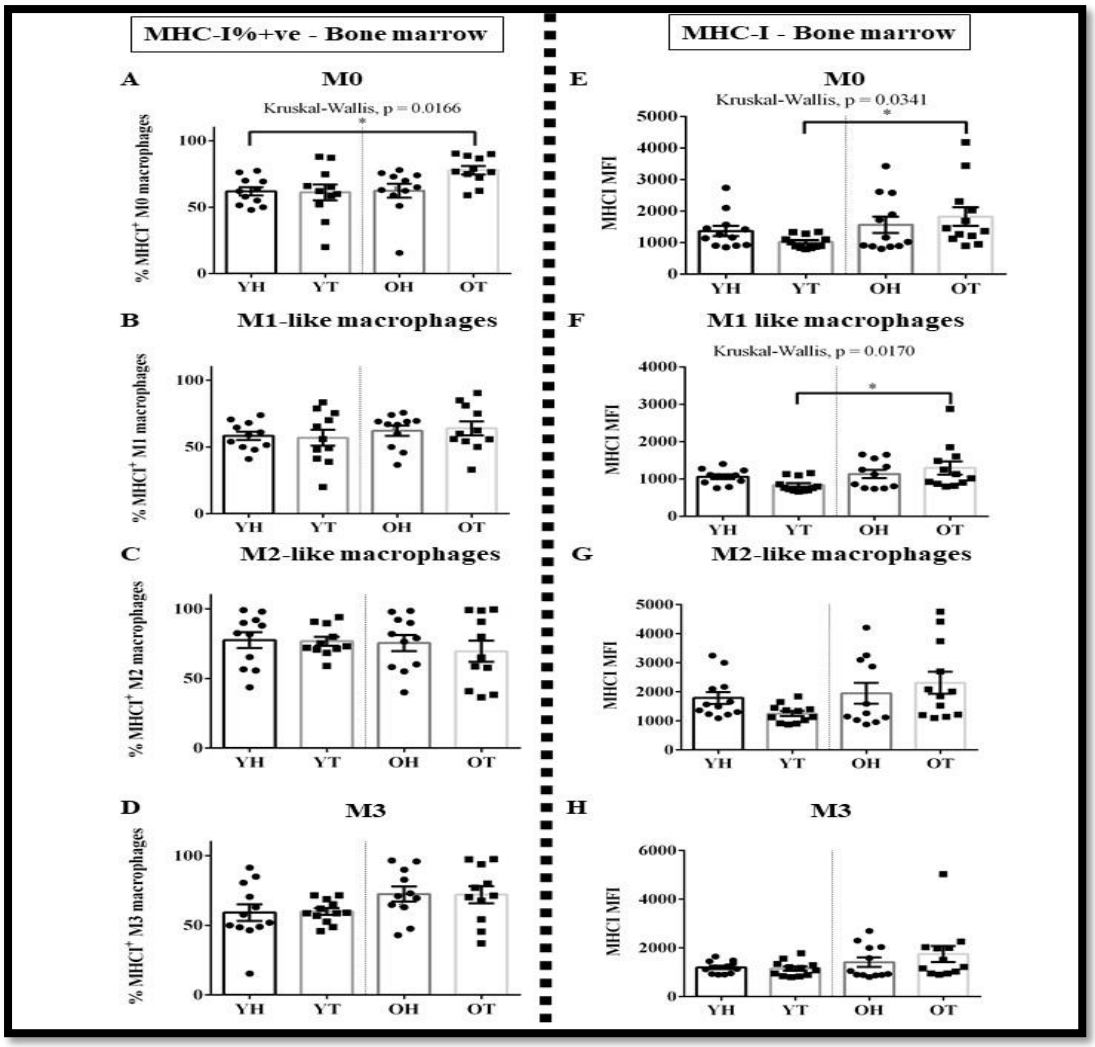

Figure 3.11: MHC-I increases with age in MO and M1-like BM macrophages in tumour-bearing mice

BM macrophages from YH, YT, OH and OT mice were stained for MHC-I expression and analysed by flow cytometry. Percentages of MHC-I$^+$ cells in Ly6C$^-$CX3CR1$^-$ (M0) macrophages **(A)**, Ly6C$^+$CX3CR1$^-$ (M1-like) macrophages (**B)**, Ly6C$^-$CX3CR1$^+$ (M2-like) macrophages **(C)**, and Ly6C$^+$CX3CR1$^+$ (M3) macrophages **(D)** plus expression levels of MHCI I (MFI) in the same macrophage subpopulations were measured. Data shown as mean ± SEM, n = 10-11 mice/group. * = $p<0.05$, ** = $p<0.005$. Statistical significance assessed by Kruskal-Wallis test followed by post hoc Dunn's test.

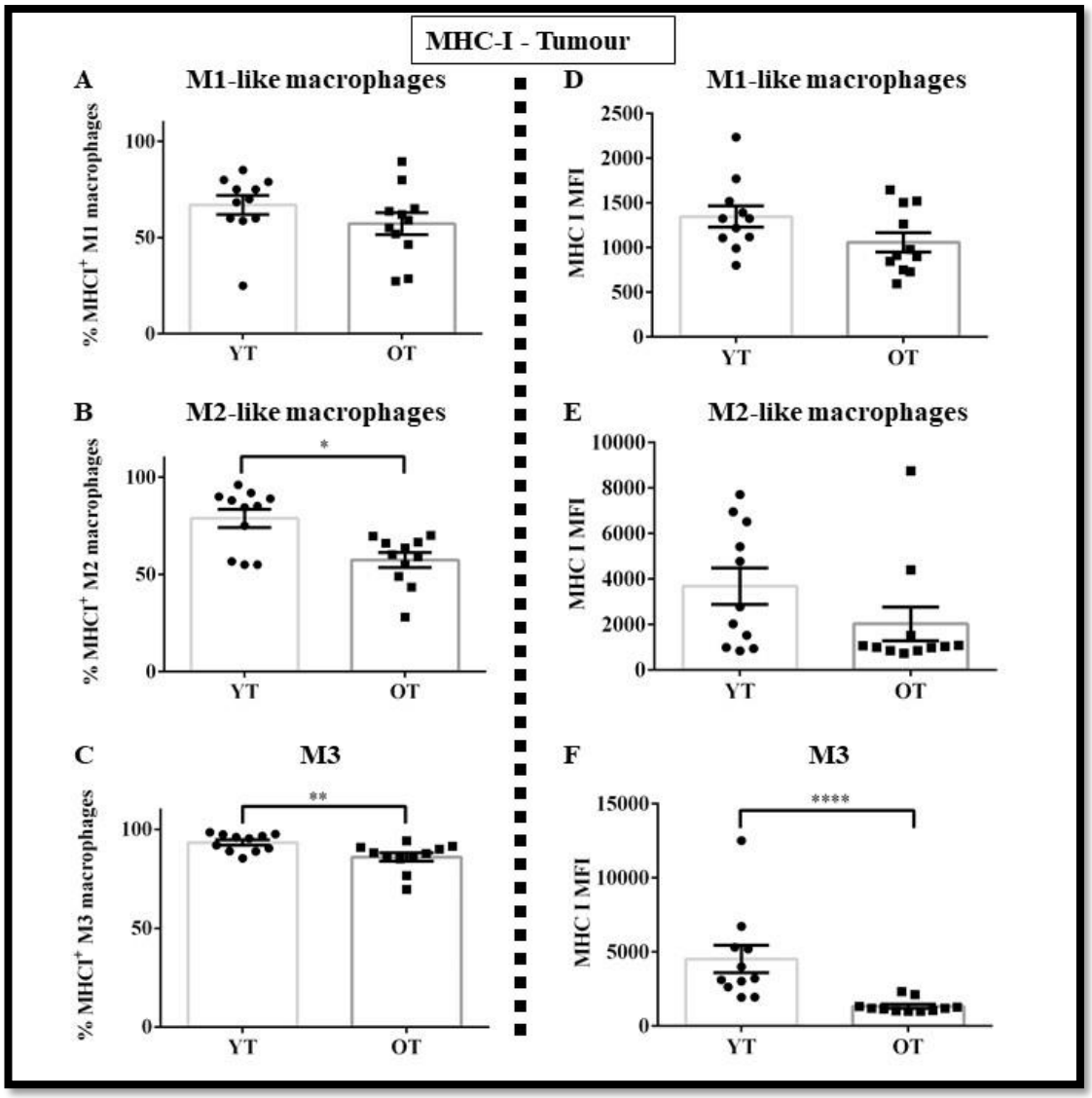

Figure 3.12: MHC-I decreases with age in M2-like and M3 TAMs

TAMs from young tumour-bearing (YT) and old tumour-bearing mice (OT) were stained for MHC-I and analysed by flow cytometry. Percentages of MHC I^+ cells in $Ly6C^+CX3CR1^-$ (M1-like)macrophages (**A)**, $Ly6C^-CX3CR1^+$ (M2-like) macrophages **(B)**, and $Ly6C^+CX3CR1^+$ (M3) macrophages **(C)** and expression levels of Bodipy (MFI) in $Ly6C^+CX3CR1^-$ (M1-like) macrophages **(D)**, $Ly6C^-CX3CR1^+$ (M2-like) macrophages **(E)**, and $Ly6C^+CX3CR1^+$ (M3) macrophages **(F)** were measured. Data are shown as mean ± SEM, n=10-11, young tumour bearing mice (YT) and n =10-11; old tumour bearing mice (OT). * = $p<0.05$, *** = $p<0.0005$. Statistical significance comparing two groups was assessed by Mann Whitney U test.

3.2.12 MHC-II in BM macrophages increase with healthy ageing

The proportion of MHC-II$^+$ BM M2-like macrophages decreases in OH and OT mice compared to YT (Figure 3.13 C). In contrast, MHC-II expression levels significantly increased with healthy ageing in BM M1-like macrophages (Figure 3.13 F), and further increased in BM M1-like macrophages in old mice with mesothelioma (Figure 3.13F). A similar increase in MHC-II expression was observed in splenic M2-like macrophages in spleen (Figure 3.14C).

3.2.13 MHC-II decreases in M1-like TAM subsets

MHC-II expression levels appeared to decrease in all TAM subsets with age however, a statistically significant difference was only seen for M1-like macrophages (Figures 3.14 E–G).

3.2.14 CD80\ expression increases with age in splenic M0 and M1-like macrophages

CD80 (B7-1) is a co-stimulatory molecule shown to contribute to T lymphocyte activation and expansion [449]. Different macrophage populations were gated according to Figure 3.2. No changes in CD80 expression levels or in the proportion of CD80 positive cells were observed in BM macrophage subsets. In contrast, the proportion of CD80$^+$ cells in spleens increased with age which was further elevated by the presence of mesothelioma in M0 macrophages and M1-like macrophages compared to their younger counterparts (Figures 3.15A and B). CD80 expression levels increased with healthy ageing in splenic M1-like macrophages and M3 macrophages (Figures 3.15 F and H) suggesting that elderly macrophages in spleen retain their ability to co-stimulate and activate T cells. M1-like macrophages in OT mice further increased CD80 expression suggesting they are more activated than their younger counterparts (Figure 3.15 F).

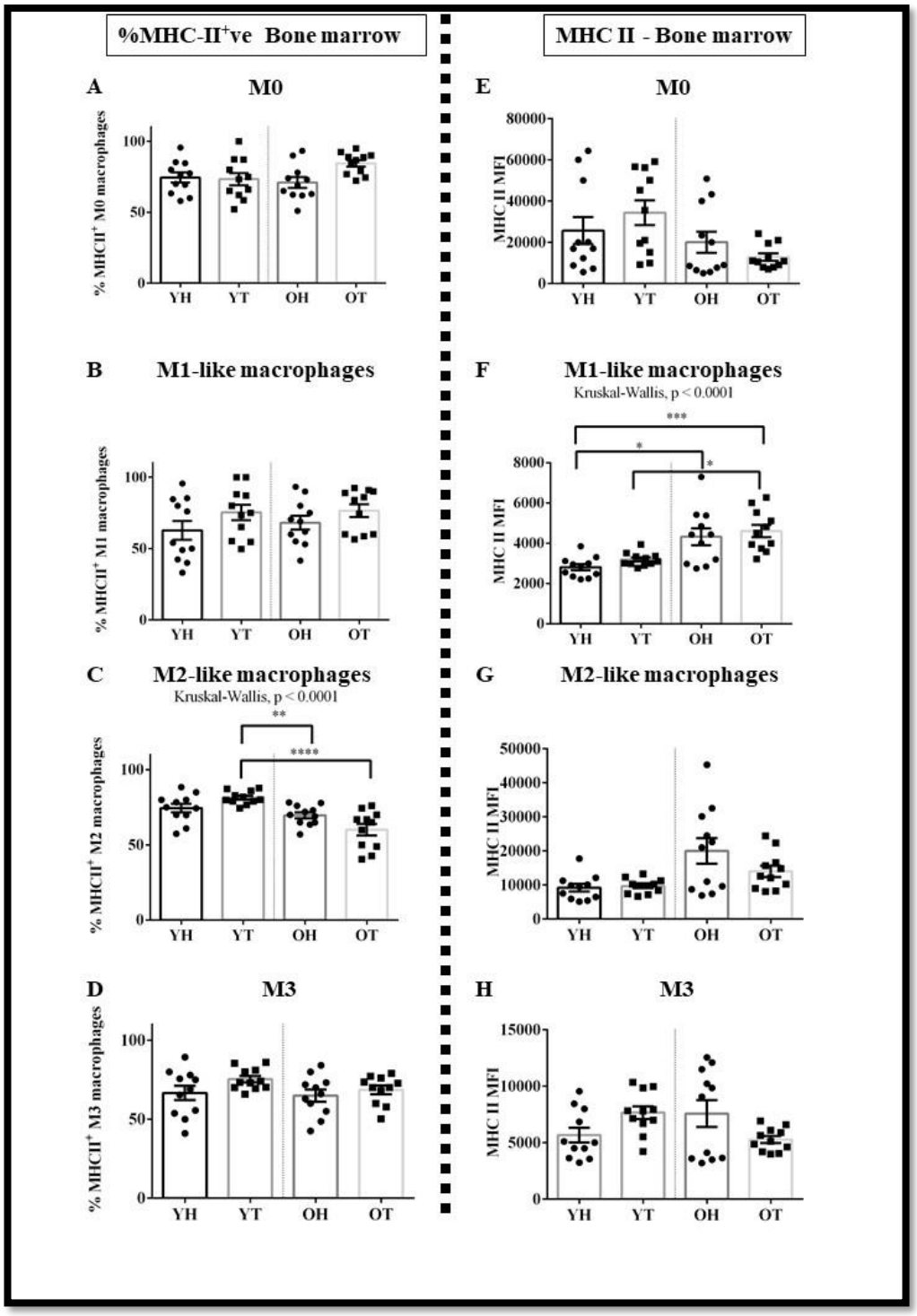

Figure 3.13: MHC-II increases with age in M1-like BM macrophages

BM macrophages from YH, YT, OH and OT mice were stained for MHC-II expression and analysed by flow cytometry. Percentages of MHC-II$^+$ cells in Ly6C$^-$CX3CR1$^-$ (M0) macrophages **(A)**, Ly6C$^+$CX3CR1$^-$ (M1-like) macrophages, and **(B)** MHC-II expression levels in the same subpopulations were measured; data shown as mean ± SEM, n = 10-11 mice/group. * = p<0.05, ** = p<0.005, *** = p<0.0005, **** =p<0.0001. Statistical significance assessed by Kruskal-Wallis test followed by post hoc Dunn's test.

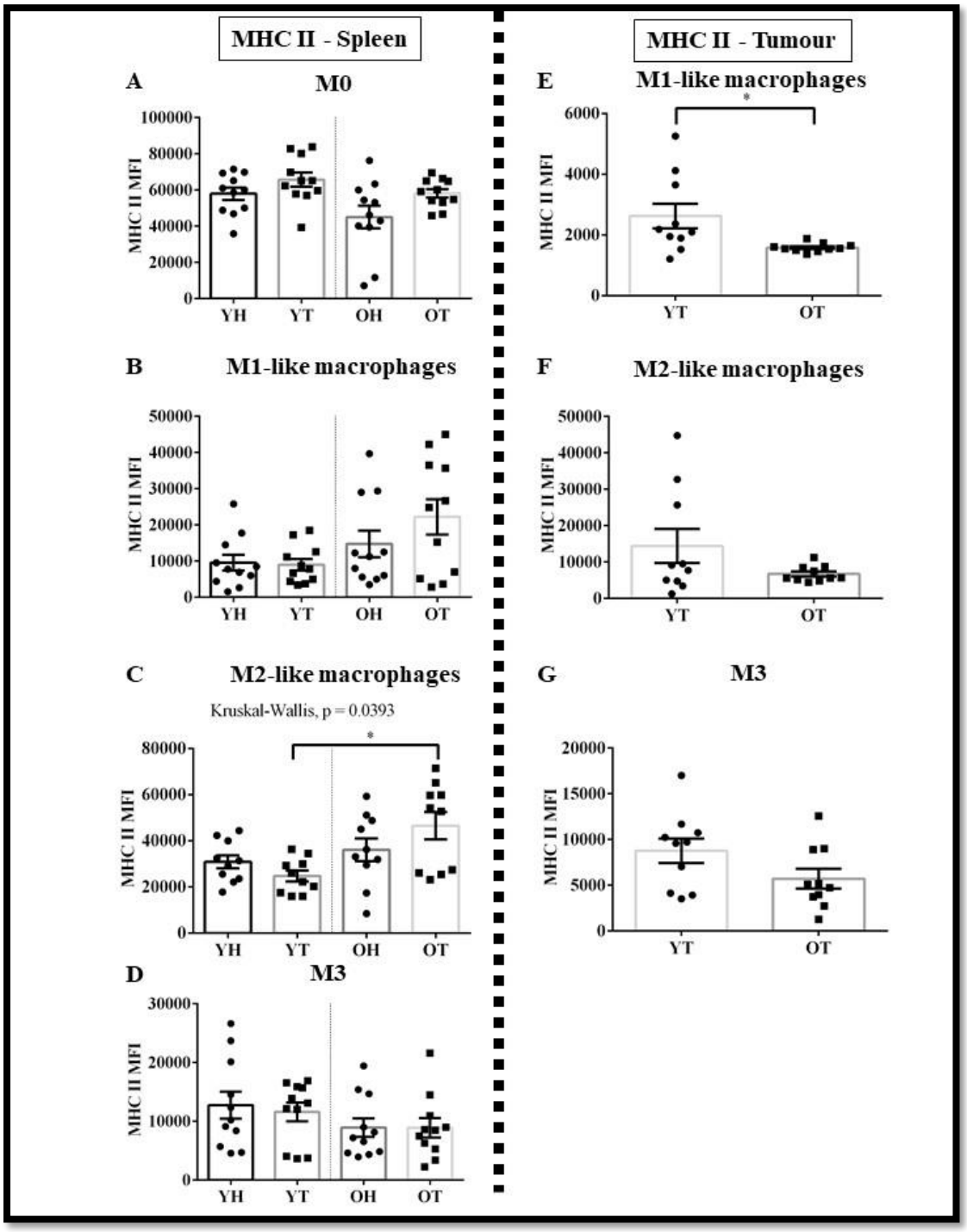

Figure 3.14: MHC-II increases with age and tumours in splenic M2 macrophages while decreases in old tumours

Splenic macrophages from YH, YT, OH and OT and TAMs for young mice (YT) and old mice (OT) were stained for MHC-II expression and expression levels of MHC-II (MFI) $Ly6C^{-}CX3CR1^{-}$ (M0) macrophages **(A)**, $Ly6C^{+}CX3CR1^{-}$ (M1-like) macrophages (**B,F)**, $Ly6C^{-}CX3CR1^{+}$ (M2-like) macrophages **(C,G)**, and $Ly6C^{+}CX3CR1^{+}$ (M3) macrophages **(D)**are shown as mean ± SEM, n = 10-11 mice/group. * = $p<0.05$. Statistical significance for three or more than three groups was assessed by Kruskal-Wallis test followed by post hoc Dunn's test while Mann Whitney U test is used to compare two groups.

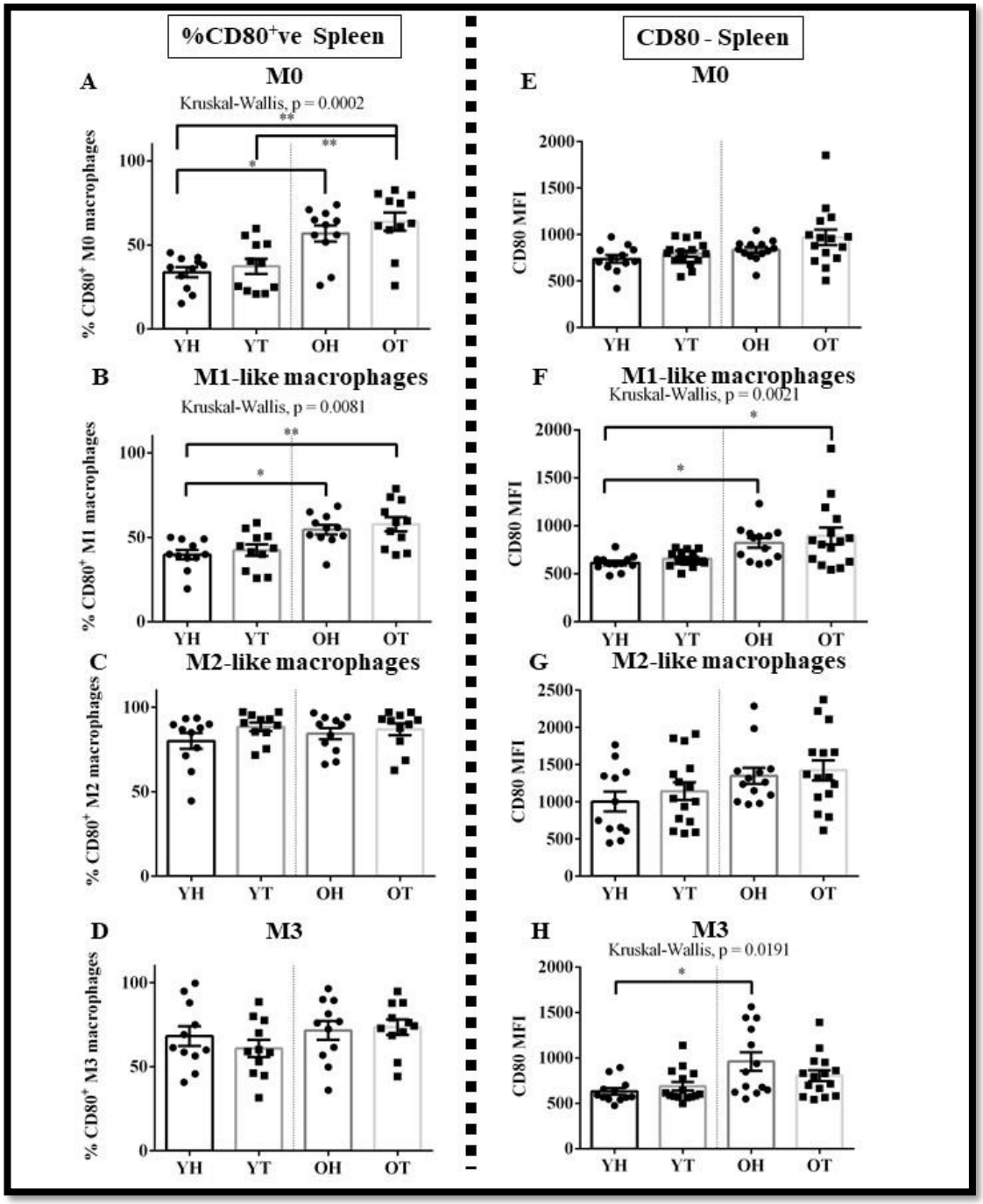

Figure 3.15: CD80 increases with age in M0 and M1 macrophages with ageing

Splenic macrophages from YH, YT, OH and OT mice were stained with CD80 and analysed by flow cytometry. Percentages of $CD80^+$ cells in $Ly6C^-CX3CR1^-$ (M0) macrophages **(A)**, $Ly6C^+CX3CR1^-$ (M1-like) macrophages (**B)**, $Ly6C^-CX3CR1^+$ (M2-like) macrophages **(C)**, and $Ly6C^+CX3CR1^+$ (M3) macrophages **(D)** and expression levels of CD80 (MFI) in M0 macrophages **(E)**, M1-like macrophages (**F)**, M2-like macrophages **(G)**, and M3 macrophages **(H)** were measured. Data shown as mean ± SEM, n = 10-11 mice/group. * = $p<0.05$, ** = $p<0.005$. Statistical significance assessed by Kruskal-Wallis test followed by post hoc Dunn's test.

3.2.15 CD80 expression increases in M1-like TAMs in old tumour-bearing mice

The proportion of $CD80^+$ cells appeared to increase with age in all TAM subsets, although a statistically significant difference was only reached in M1-like TAMs in the tumour tissue of elderly mice compared to young mice (Figure 3.16 A).

3.2.16 No changes in CD40 expression were observed in different lymphoid organs

The proportion of $CD40^+$ cells and CD40 expression levels, a co-stimulatory molecule for antigen presentation [450], remained unchanged in all macrophage subsets in BM, spleen and tumour (supplementary figure 3.5, 3.6 and 3.7).

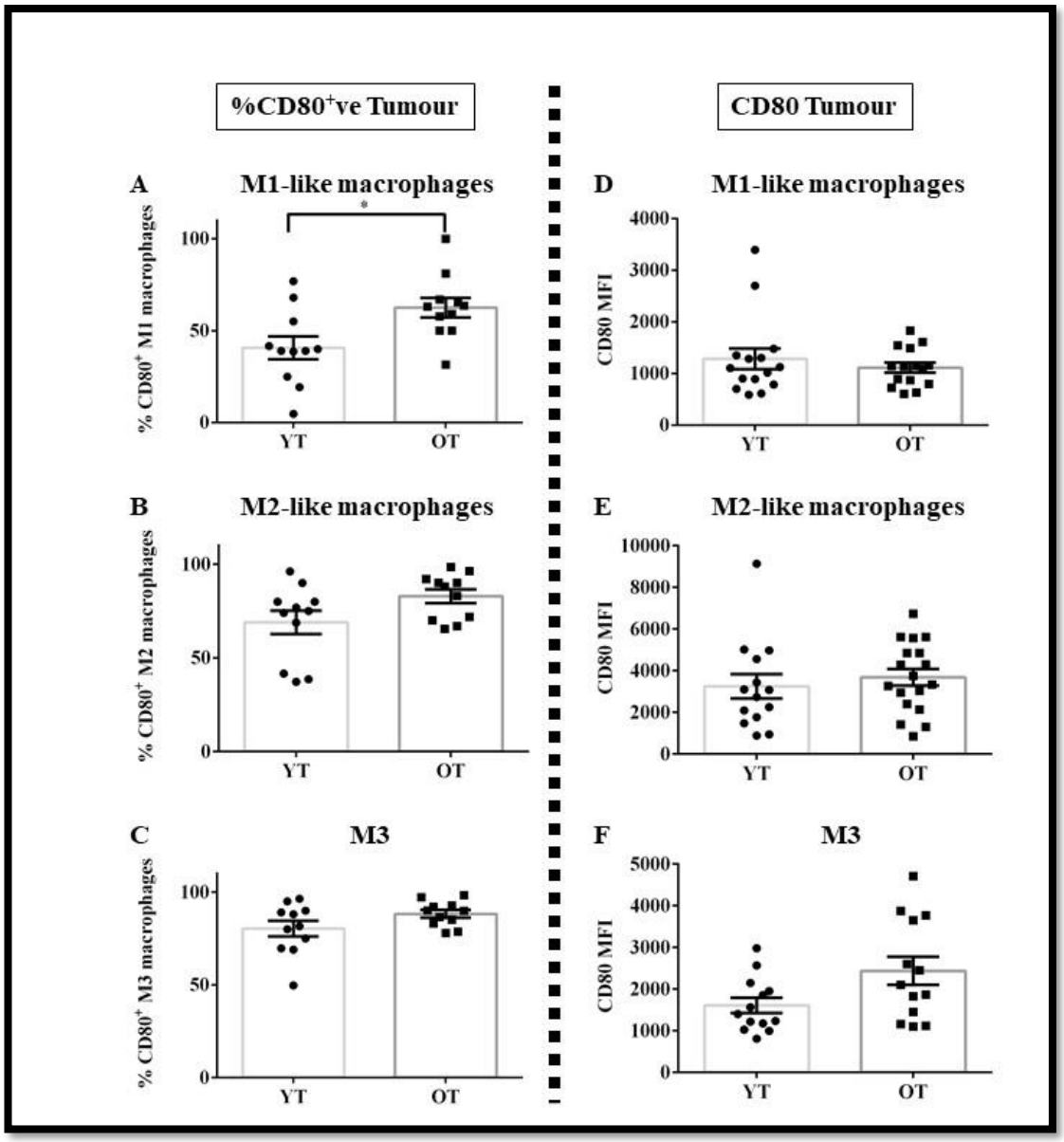

Figure 3.16: CD80$^+$ M1 TAMs increase with age

TAMs from young tumour-bearing mice (YT) and old tumour-bearing mice (OT) were stained with CD80 and analysed by flow cytometry. Percentages of CD80$^+$ cells in Ly6C$^+$CX3CR1$^-$ (M1-like) macrophages (**A**), Ly6C$^-$CX3CR1$^+$ (M2-like) macrophages **(B)**, and Ly6C$^+$CX3CR1$^+$ (M3) macrophages **(C)**, and expression levels of CD80 (MFI) in Ly6C$^+$CX3CR1$^-$ (M1-like) macrophages (**D**), Ly6C$^-$CX3CR1$^+$ (M2-like) macrophages **(E)**, and Ly6C$^+$CX3CR1$^+$ (M3) macrophages **(F)** were measured. Data are shown as mean ± SEM, n=10-11 mice/group. * = $p<0.05$. Statistical significance comparing two groups was assessed by Mann Whitney U test.

3.3 Splenic red pulp and white pulp macrophages

This study also looked at splenic red pulp macrophages (RPM) and white pulp macrophages (WPM). RPM are localised in splenic red pulp [451]. They are generated during embryogenesis and maintained through adult life. RPM play a key role in the clearance of damaged red blood cells and iron recycling [452, 453]. Around 75% of the spleen is composed of red pulp [454]. RPM can be characterised as $F4/80^{+}$ and $CD11b^{low}$ macrophages [455]. The remaining part of the spleen is composed of white pulp which is separated from the red pulp by an interface called the marginal zone [456]. WPM lack F4/80 [457]. Newly produced macrophages from spleen can migrate to tumours and contribute to new tumour associated macrophages [458, 459]. Splenic $CD11b^{+}F4/80^{+}$ macrophages have been shown to acquire higher lipid levels in tumour bearing mice compared to healthy controls [460]. The effect of ageing and mesothelioma on RPM and WPM had not been examined therefore splenic RPM and WPM were identified based on expression of CD11b and F4/80, as shown in Figure 3.17.

3.3.1 Lipid levels do not change in splenic red pulp and white pulp macrophages with healthy ageing or mesothelioma

No changes were seen in the proportion or expression levels of $Bodipy^{+}$ splenic RPM and WPM with healthy ageing or with mesothelioma (Figure 3.18).

3.3.2 MHC-I expression decreases with mesothelioma and ageing in splenic white pulp macrophages

No effect of healthy ageing on MHC-I expression was observed in splenic RPM and WPM. However, MHC-I was significantly reduced in old mice with tumours compared to healthy elderly mice (Figure 3.19 D).

3.3.3 MHC-II expression increases with healthy ageing in splenic white pulp macrophages

MHC-II expression was found to be increased with healthy ageing in splenic WPM compared to young healthy mice (Figure 3.20 D).

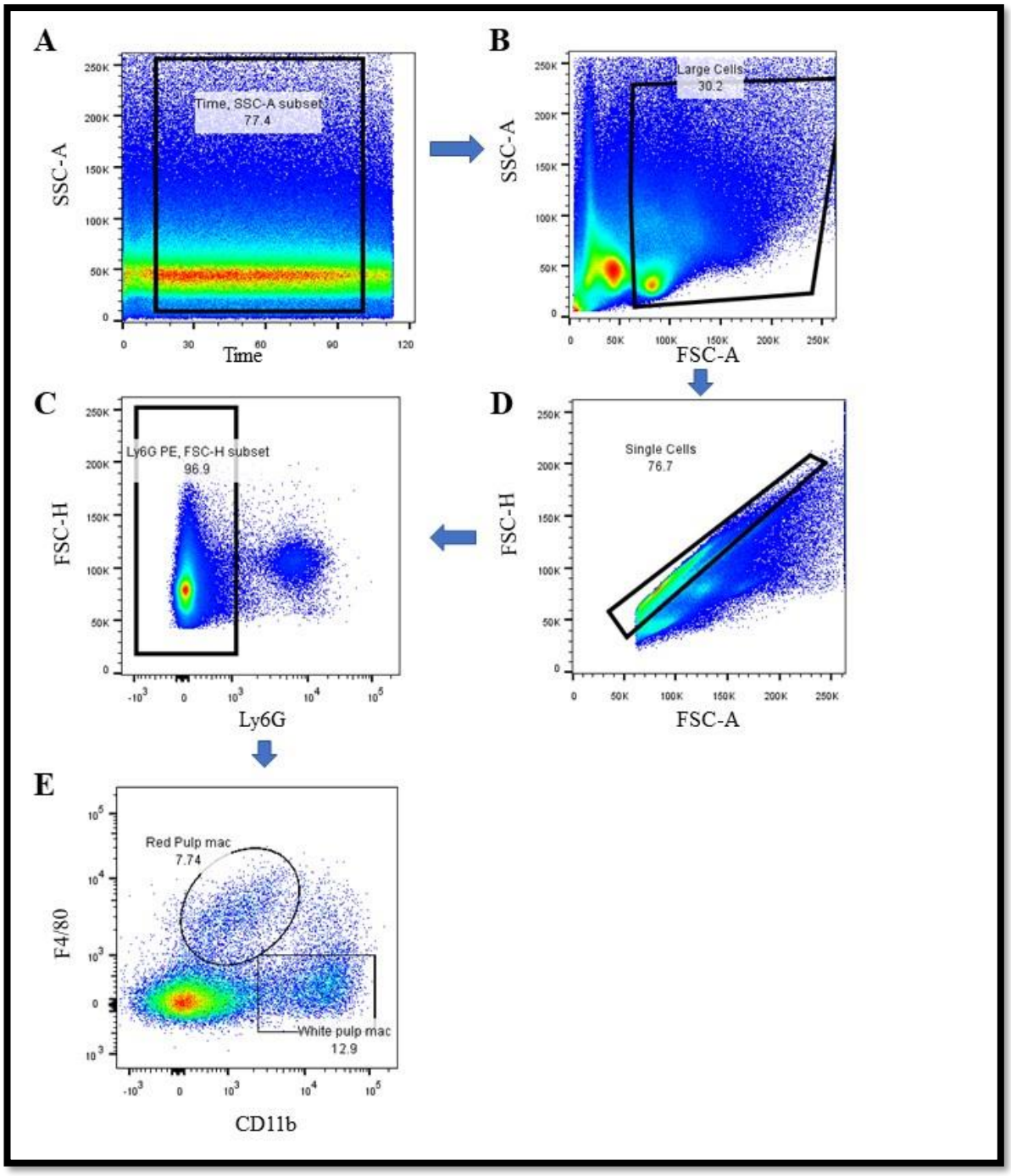

Figure 3.17: Gating Strategy for red pulp and white pulp macrophages
Splenic macrophages from young healthy C57BL/6J mice (YH; aged 2-5 months; equivalent to 16-26 human years), young tumour bearing mice (YT), old healthy C57BL/6J mice (OH; aged 20-27 months; equivalent to 60-80 human years) and old tumour bearing mice (OT) were stained for $CD11b^{+}$ and $F4/80^{+}$. (**A)** Time-gating was used to ensure there were no clogging or other instrumental issues during acquisition (**B).** This was followed by gating on large cells, and (**C)** single cells to avoid doublets. (**D)** Neutrophils were excluded using Ly6G staining, before (**E)** $F4/80^{+}$ and $CD11b^{low}$ (red pulp macrophages), and $CD11b^{+}F4/80^{-}$ (white pulp macrophages) were gated.

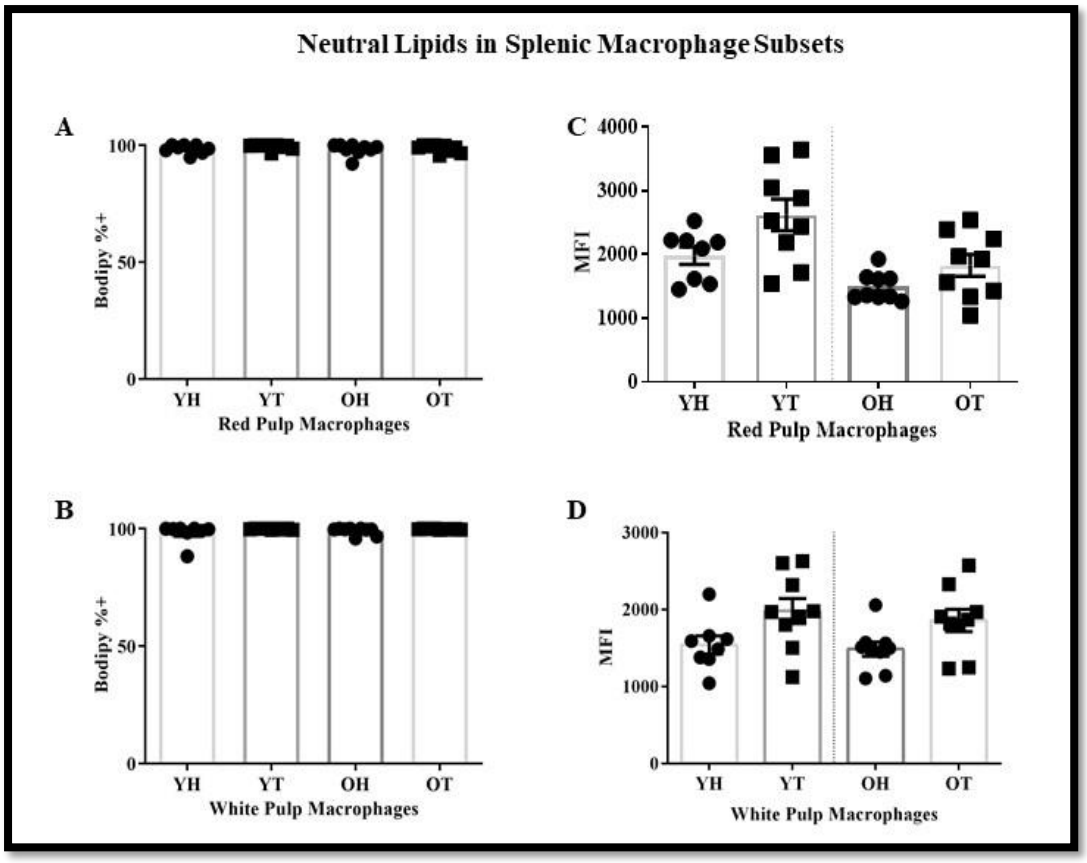

Figure 3.18: No change in lipid levels observed in splenic red and white pulp macrophages
Splenic macrophages from YH, YT, OH and OT were stained with Bodipy to measure neutral lipids and analysed by flow cytometry. Percentage of Bodipy^{+} cells in macrophages of **(A)** Red pulp **(B)** White pulp , and expression levels of Bodipy (measured as geometric mean fluorescence intensity; MFI in different subpopulations of macrophages **(C)** Red pulp macrophages, **(D)** White pulp macrophages were measured. Data are shown as mean ± SEM, n = 10-11; YH, n=10-11; YT, n =10-11; OH, n =10-11; OT. ** = $p<0.005$. Statistical significance assessed by Kruskal Wallis followed by ad hoc Dunn's Test.

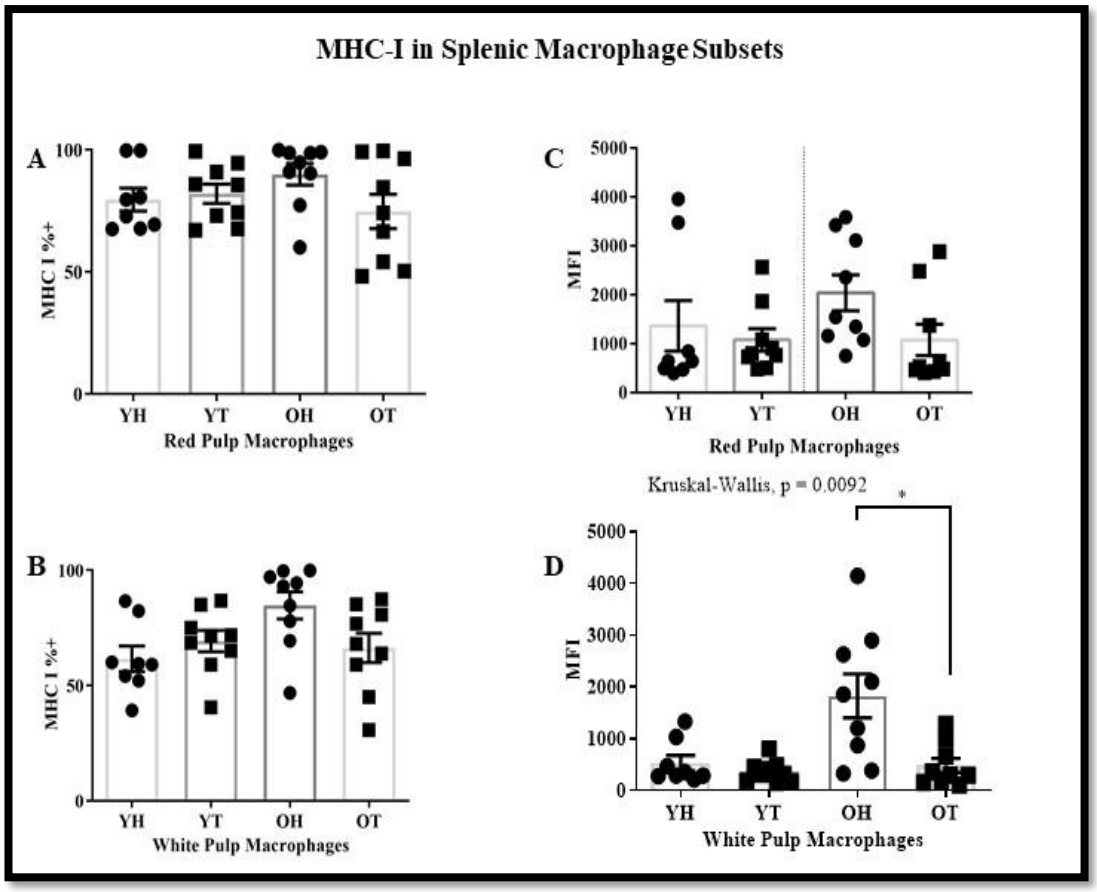

Figure 3.19: MHC-I decreases in tumour bearing old mice compared to old healthy mice in white pulp macrophages

Splenic macrophages from YH, YT, OH and OT were stained with MHC-I which is an antigen presenting molecule that present peptides to $CD8^+$ T cells and analysed by flow cytometry. Percentages of MHC I^+ cells in **(A)** Red pulp, **(B)** White pulp, expression levels of MHC-I (measured as geometric mean fluorescence intensity; MFI in different subpopulations of macrophages **(C)** Red pulp macrophages, **(D)** White pulp macrophages were measured. Data are shown as mean ± SEM, n = 10-11; YH, n=10-11; YT, n =10-11; OH, n =10-11; OT. * = $p<0.05$. Statistical significance assessed by Kruskal Wallis followed by ad hoc Dunn's Test.

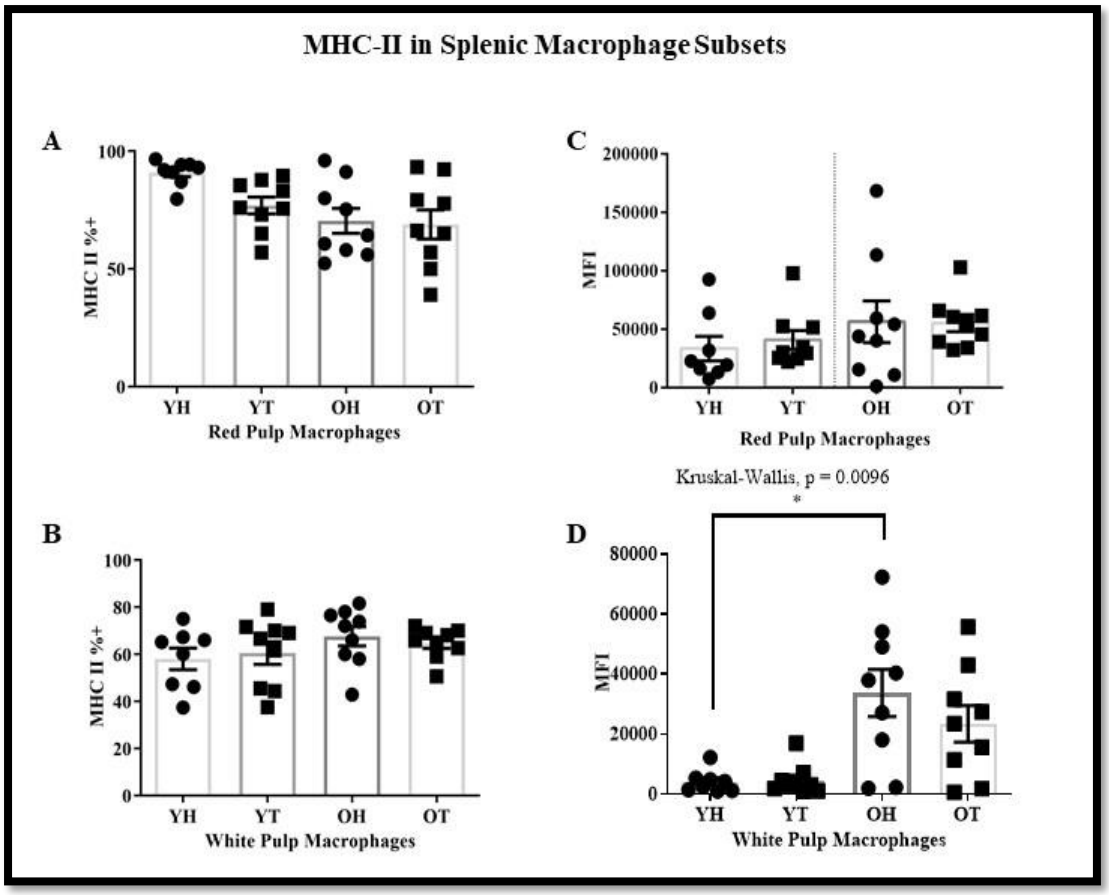

Figure 3.20: Increased MHC-II was observed with healthy ageing in white pulp macrophages
Splenic macrophages from YH, YT, OH and OT were stained with MHC-II which is an antigen presenting molecule that present peptides to $CD4^+$ T cells and analysed by flow cytometry. Percentages of MHC II^+ cells in **(A)** Red pulp, **(B)** White pulp, expression levels of MHC-II (measured as geometric mean fluorescence intensity; MFI in different subpopulations of macrophages **(C)** Red pulp macrophages, **(D)** White pulp macrophages were measured. Data are shown as mean ± SEM, n = 10-11; YH, n=10-11; YT, n =10-11; OH, n =10-11; OT. * = $p<0.05$. Statistical significance assessed by Kruskal Wallis followed by ad hoc Dunn's Test.

3.3.4 No changes in lipid uptake or co-stimulatory molecules were seen in splenic red/white pulp macrophages

No changes in the lipid uptake CD36 or CD147 molecules were seen in splenic RPM and WPM with ageing and mesothelioma (Supplementary Figure 3.8). Similarly, no changes were observed in expression of CD80 in either splenic population (Supplementary Figure 3.8).

Table 3.1: Summarising the effect of ageing and/or mesothelioma on tumour-associated macrophage subsets

Organ	Macrophage Subpopulation	Effect of healthy ageing	Combined effect of age + mesothelioma	Mesothelioma Effect
BM	M0	NO	YES	NO
BM	M1-LIKE	NO	NO	NO
BM	M2-like	NO	NO	NO
BM	M3	YES	NO	YES
SPLEEN	M0	NO	NO	NO
SPLEEN	M1-LIKE	NO	NO	NO
SPLEEN	M2-like	NO	NO	NO
SPLEEN	M3	NO	NO	NO
LN	M0	NO	NO	NO
LN	M1-LIKE	NO	NO	NO
LN	M2-like	NO	NO	NO
LN	M3	NO	NO	NO
LIPIDS Expression Levels (MFI – Bodipy)				
BM	M0	NO	NO	YES
BM	M1-LIKE	NO	NO	YES
BM	M2-like	NO	NO	NO
BM	M3	NO	NO	NO
SPLEEN	M0	NO	NO	NO
SPLEEN	M1-LIKE	NO	NO	YES
SPLEEN	M2-like	NO	YES	NO
SPLEEN	M3	NO	YES	NO
TUMOUR	M0	N/A	N/A	N/A
TUMOUR	M1-LIKE	NO	NO	YES
TUMOUR	M2-like	NO	NO	NO
TUMOUR	M3	NO	NO	YES
CD147 Expression Levels				
BM	M0	NO	NO	NO
BM	M1-LIKE	NO	NO	NO
BM	M2-like	YES	NO	NO

BM	M3	NO	NO	NO
SPLEEN	M0	YES	YES	NO
SPLEEN	M1-LIKE	NO	YES	NO
SPLEEN	M2-like	YES	NO	NO
SPLEEN	M3	NO	NO	NO
TUMOUR	M0	N/A	NA	N/A
TUMOUR	M1-LIKE	YES	NO	NO
TUMOUR	M2-like	NO	NO	NO
TUMOUR	M3	NO	NO	NO
MHC-I Expression Levels				
BM	M0	NO	NO	NO
BM	M1-LIKE	NO	NO	NO
BM	M2-like	NO	NO	NO
BM	M3	NO	NO	NO
SPLEEN	M0	NO	NO	NO
SPLEEN	M1-LIKE	NO	NO	NO
SPLEEN	M2-like	NO	NO	NO
SPLEEN	M3	NO	NO	NO
TUMOUR	M0	N/A	N/A	N/A
TUMOUR	M1-LIKE	NO	NO	NO
TUMOUR	M2-like	NO	NO	NO
TUMOUR	M3	YES	NO	NO
MHC-I Percentage Of Cells Positive				
BM	M0	NO	NO	YES
BM	M1-LIKE	NO	NO	NO
BM	M2-like	NO	NO	NO
BM	M3	NO	NO	NO
SPLEEN	M0	NO	NO	NO
SPLEEN	M1-LIKE	NO	NO	NO
SPLEEN	M2-like	NO	NO	NO
SPLEEN	M3	NO	NO	NO
TUMOUR	M0	NO	NO	NO
TUMOUR	M1-LIKE	NO	NO	NO

TUMOUR	M2-like	YES	NO	NO
TUMOUR	M3	YES	NO	NO
MHC-II Expression Levels				
BM	M0	NO	NO	NO
BM	M1-LIKE	YES	YES	NO
BM	M2-like	NO	NO	NO
BM	M3	NO	NO	NO
SPLEEN	M0	NO	NO	NO
SPLEEN	M1-LIKE	NO	NO	NO
SPLEEN	M2-like	YES	NO	NO
SPLEEN	M3	NO	NO	NO
TUMOUR	M0	N/A	N/A	N/A
TUMOUR	M1-LIKE	NO	NO	YES
TUMOUR	M2-like	NO	NO	NO
TUMOUR	M3	NO	NO	NO
MHC-II Percentage Of Cells Positive				
BM	M0	NO	NO	NO
BM	M1-LIKE	NO	NO	NO
BM	M2-like	YES	YES	NO
BM	M3	NO	NO	NO
SPLEEN	M0	NO	NO	NO
SPLEEN	M1-LIKE	NO	NO	NO
SPLEEN	M2-like	NO	NO	NO
SPLEEN	M3	NO	NO	NO
TUMOUR	M0	N/A	N/A	N/A
TUMOUR	M1-LIKE	NO	NO	NO
TUMOUR	M2-like	NO	NO	NO
TUMOUR	M3	NO	NO	NO
CD80 Expression Levels				
BM	M0	NO	NO	NO
BM	M1-LIKE	NO	NO	NO
BM	M2-like	NO	NO	NO
BM	M3	NO	NO	NO

SPLEEN	M0	NO	NO	NO
SPLEEN	M1-LIKE	YES	YES	NO
SPLEEN	M2-like	NO	NO	NO
SPLEEN	M3	YES	NO	NO
TUMOUR	M0	N/A	N/A	N/A
TUMOUR	M1-LIKE	NO	NO	NO
TUMOUR	M2-like	NO	NO	NO
TUMOUR	M3	NO	NO	NO
CD80 Percentage Of Cells Positive				
BM	M0	NO	NO	NO
BM	M1-LIKE	NO	NO	NO
BM	M2-like	NO	NO	NO
BM	M3	NO	NO	NO
SPLEEN	M0	YES	YES	NO
SPLEEN	M1-LIKE	YES	YES	NO
SPLEEN	M2-like	NO	NO	NO
SPLEEN	M3	NO	NO	NO
TUMOUR	M0	N/A	N/A	N/A
TUMOUR	M1-LIKE	YES	NO	NO
TUMOUR	M2-like	NO	NO	NO
TUMOUR	M3	NO	NO	NO

3.4 Discussion

The influence of ageing in combination with mesothelioma on macrophages has yet to be fully characterised. With advancing age, there are many alterations in innate and adaptive immunity, which have been described as deleterious, hence the term immunosenescence. Decreasing immunity with age could contribute to the increased cancer incidence in the elderly [461]. The studies in this chapter examined the influence of ageing and cancer on macrophages, as these cells are key regulators of the complex interplay between the immune system and cancer [462].

TAMs originating from the embryonic yolk sac start out as tissue resident macrophages that take on tissue-specific roles during development, or as BM monocytes that circulate in blood until they are recruited to tissues. Tumours secrete CCL2 and CSF-1 that attract tissue-resident macrophages and monocytes and convert these cells to tumour-supporting TAMs [463]. TAMs secrete IL-10 that likely prevent DCs from activating anti-tumour T cell responses by suppressing IL-12 expression in intra-tumoural DCs [192]. DCs have been shown to accumulate lipids in response to tumour-derived factors, causing DC dysfunction [101, 230, 464]. The lipid accumulation shown by some macrophage subsets here may also be in response to cues present in the tumour microenvironment that reprogram their metabolic processes. This is supported by the in vitro study showing that BM macrophages elevate their lipid content in response to mesothelioma-derived factors. Moreover, studies examining the lung tumour microenvironment showed increased expression of multiple genes involved in lipid metabolism and lipid signalling in macrophages [465]. In particular, increased cyclooxygenase-2 (COX2) expression and increased prostaglandin E2 (PGE2) production was found in macrophages infiltrating tumour-bearing lungs suggesting that cancer cells and immune cells increase prostaglandin (a group of physiologically active lipid compounds) synthesis resulting in lipid accumulation in cells in lung tumours [465, 466] promoting tumour growth and suppressing tumour immunity. However, the functional consequences of lipid accumulation by macrophages are unclear, as some studies have shown that lipid-loaded macrophages are inflammatory and tumoricidal [467, 468]. For example, Schlager et al. [467] showed that increased lipid content, especially those enriched with polyunsaturated fatty acids, in murine peritoneal macrophages was associated with increased cytotoxic activity against tumours. Therefore, a consensus has yet to be reached.

Here, *in-vitro* studies examined the effect of mesothelioma-derived factors on young BM-derived macrophages. The study demonstrated that tumour exposed macrophages had increased lipid accumulation compared to unexposed macrophages. Similar data was seen in the *in-vivo* studies, i.e., increased lipid accumulation was observed in all macrophage subsets in old mice with mesothelioma in BM, spleen, and tumours.

Possible mechanisms of lipid uptake were also examined in *in-vivo* study. CD36 plays a key role in fatty acid transport and FAO [469, 470]. This study found no change in CD36 expression in different macrophage subsets. CD147, a multifunctional transmembrane protein [343, 471] found to play a role in anti-tumour therapy [445], increased in BM and spleen macrophages with healthy ageing and in tumour bearing old mice compared to young tumour bearing mice in M0 splenic macrophages. CD147 has shown to be upregulated in *in-vitro* studies when tumour cells are co-cultured with other cells such as endothelial cells [472, 473], or fibroblasts [474]. One study examined monocytes and macrophages co-cultured with tumour cells; CD147 was expressed at very low levels in both cells types however co-culturing tumour cells with macrophages and monocytes resulted in elevated CD147 on both cell types [475]. That study concluded that tumour cells were responsible for increased expression of CD147 on macrophages and monocytes. CD147 mediates tumour cell-macrophage interactions and has been shown to induce matrix metalloproteinase and vascular endothelial growth factor (VEGF) [476]. In this study, CD147 was mostly increased in BM and splenic macrophages in elderly mice with tumours, and could contribute to increased lipid accumulation in ageing hosts with mesothelioma. Therefore, CD147 could be a useful target for treatment for elderly people with mesothelioma.

The increase in lipid accumulation was associated with decreased MHC-I and MHC-II expression in *in-vitro* studies in young mice with mesothelioma compared to healthy mice which could lead to reduced capacity to activate tumour-infiltrating $CD8^+$ and $CD4^+$ T cells. Similar data was seen in the *in-vivo* studies, i.e., increased lipid accumulation was associated with decreased MHC-I and MHC-II expression in TAMs in old tumour-bearing mice compared to young tumour-bearing mice. However, no changes were observed with healthy ageing by itself. These data suggest tumours could be solely responsible for reduced MHC function rather than combined effect of age and tumour. Lipid accumulation in the BM and spleen could be due to the distal effects of tumour. This is supported by Han et al who showed that tumours can induce immunosuppressive or inflammatory changes in distant organs [477]. Moreover, spleens are often enlarged in tumour bearing hosts [478], again suggesting the influence of tumour-derived factors that might elevate CD147 expression by macrophages leading to elevated lipid levels in spleen and bone marrow. It is likely that the situation is more complex, as Wang et al. looked at changes in MHC-II levels

in TAMs during tumour development, where tumours were harvested on days 7, 14, 21 and 28. The study found two distinct TAMs subsets in a murine hepatocellular carcinoma Hepa1-6 model; MHC class II^{hi} TAM associated with tumour suppression appeared in early the stages of tumour development whilst MHC class II^{low} TAM formed the dominant population as tumours progressed [479].

Increased lipid accumulation has been observed in macrophages in atherosclerosis [247] and different cancers such as breast cancer [480], colorectal cancer [396, 481], liver cancer [482] and prostate cancer [483]. Studies conducted in tumours have shown that increased lipid synthesis promotes cancer cell proliferation as it helps in the generation of membranes and provides energy to dividing cancer cells [484]. However, there is little knowledge about lipid metabolism and its role in shaping the functional phenotypes of tumour TAMs. Future studies in our group will look at the metabolic effect of mesothelioma on TAMs.

Several studies in humans and mice have shown that lipid accumulation leads to downregulated MHC in different antigen presenting cells such as DCs. Shaikh et al looked at the effects of lipid overload on human APCs and found that APCs treated with saturated palmitic acid and oleic acid led to decreased MHC-I antigen presentation [485]. In the cancer setting, Herber et al demonstrated a reduced capacity of lipid laden DCs to present tumour associated antigens [486]. Earlier studies by our group showed partial activation of tumour-associated DCs and DCs from elderly mice tissues such as plasmacytoid and $CD8^{+}CD4^{-}$ cDCs, possibly as a result of lipid accumulation [246]. Another study showed that lipid bodies containing electrophilic oxidatively truncated (ox-tr) lipids accumulate in DCs in tumour-bearing hosts. These ox-tr lipids can bind to chaperone heat shock protein 70. This binding can interfere with peptide-MHC complex translocation to the cell surface thus affecting stimulation of $CD8^{+}$ T cell responses [487]. Katrin et al, using an in-vitro human coculture model to generate tumour-induced macrophages, reported upregulation of lipid biosynthesis pathways in tumour-exposed macrophages. That study also noticed increased lipid content and intracellular lipids in tumour exposed macrophages *in-vitro* [488]. The effect of mesothelioma and ageing on DCs is addressed in the next chapter.

Looking at the effect ageing and mesothelioma on co-stimulatory molecules, this study noticed increased CD80 expression in macrophages in spleens with healthy ageing,

this is supported by publications reporting increased CD80 and HLA-DR by monocytes with ageing, as a result of immunosenescence [489, 490]. The proportion of $CD80^+$ TAMs increased with ageing, although CD80 expression levels remained unchanged. One possibility is that CD80 on macrophages inhibit T cell responses with ageing as increased CTLA-4 expression on elderly T cells has been reported [491, 492] and T cell activation is negatively regulated by ligation of CTLA-4 and CD80 [493].

Only a few studies have examined the combined effects of ageing and cancer on macrophages. There is evidence that macrophages from aged mice do not lose their functional plasticity/adaptivity [494, 495]. Our group looked at responses to treatment with intra-tumoral IL-2/anti-CD40 antibody immunotherapy in young and elderly mesothelioma-bearing mice [30]. Responses to IL-2/anti-CD40 were less effective in elderly (38% tumour regression) compared to young mice (90% tumour regression) [30]. The study also found increased *in-vivo* anti-tumour T cell activity with macrophage depletion in elderly but not young mice [30] suggesting age-related changes in macrophages could sabotage elderly anti-tumour responses. Mahbub et al. [496] showed that aged murine BM macrophages cultured *ex vivo* have similar mRNA expression/cytokine production of M1/M2 markers to younger BM macrophages. This demonstrates that macrophages from aged mice do not lose their functional plasticity/adaptivity and reveals that altered responses by macrophages from aged mice are likely due to microenvironmental effects.

To summarise, data presented in this chapter suggests that mesothelioma may upregulate CD147 expression leading to increased lipid accumulation in BM and splenic M1-like macrophages. This was not associated with changes to CD80 and CD40 expression but was associated with decreased MHC-I and MHC-II suggesting a reduced capacity to activate $CD8^+$ and $CD4^+$ T cells, particularly those infiltrating tumours, thereby providing an advantage for mesothelioma tumours. Healthy ageing had no effect on lipid levels and costimulatory molecule expression levels, however ageing further reduced MHC-I and MHC-II on TAMs suggesting age additionally compromises anti-tumour immunity. Nonetheless, macrophages retain plasticity, as shown in other studies [497-499] and treatments that repolarise macrophages might be

useful for elderly people with mesothelioma. The next chapter examines DCs in young and elderly mice with mesothelioma.

Chapter 4: Examining the effects of mesothelioma and ageing on murine DCs

4.1 Introduction

The studies in chapter 3 examining murine macrophages showed that increased age plus the presence of mesothelioma lead to increased intracellular lipid levels. This was associated with decreased expression of surface MHC-I and MHC-II, suggesting reduced numbers of peptide/MHC complexes on macrophages likely impairing the ability of macrophages to present antigens to $CD8^+$ and $CD4^+$ T cells. The studies were extended to look at the effect of ageing and mesothelioma on DCs, which are highly potent antigen presenting cells (APCs).

The three main tissue resident cDC subsets in murine lymphoid tissue were examined. $CD8^+CD11b^-$ cDCs ($CD8^+$ cDCs) are derived from a BM precursor distinct from monocytes that continuously seed lymphoid organs [110]. $CD8^+$ cDCs are potent cross-presenting cells that present exogenous antigens on MHC-I molecules to $CD8^+$ T cells. Upon activation, $CD8^+$ cDCs produce IL-12 and stimulate pro-inflammatory responses [500]. $CD8^+$ cDCs play a crucial role in activating $CD8^+$ cytotoxic T lymphocytes (CTLs) [131, 501, 502] and Th1 responses [503]. The other main lymphoid tissue resident cDC subset is $CD11b^+CD8\alpha^-$ cDCs ($CD8^-$ cDCs) which is further sub-divided into $CD11b^+CD8\alpha^-CD4^+$ cDCs ($CD4^+$ cDCs) and $CD11b^+CD8^-CD4^-$ cDCs ($CD4^-$ cDCs) [106, 246, 504, 505]. These DC subsets represent 55% and 20% of total splenic DCs respectively [505] and share similar gene expression profiles [180, 506] and functions [105]. In contrast to $CD8^+$ cDCs, $CD8^-$ cDCs are poor cross-presenters and mainly present extracellular antigens to $CD4^+$ T cells to promote Th2 responses [131, 500, 503]. Murine $CD11c^+B220^+GR1^+$ pDCs (pDCs) mostly play a role in immune tolerance and mediate antiviral immunity [112, 246, 507-510] and are also found in lymphoid tissues [511].

The reason for this study is that there have been contradictory reports regarding changes to DC subpopulation numbers in tissues with healthy ageing. For example, splenic and LN $CD8^+$ cDCs have been shown to decrease [512-515] or remain unchanged with increasing age [246, 516, 517]. $CD8^-$ cDCs on the other hand have been reported to increase [515, 518], decrease [246] or remain steady [518, 519], whilst pDCs have been reported to remain consistent [516-518] or reduce with age [246, 513, 514]. Similarly, with regards to age-related changes to DC function, there

have been inconsistent reports on expression of different co-stimulatory molecules (such as CD40, CD80 and CD86) and antigen presentation capacity. One study suggested there was increased expression of CD40, CD80, MHC-II and CD86 in murine splenic DCs [513] while another study suggested reduced expression of MHC-II and no change in CD40, CD80 and CD86 expression [246]. These inconsistencies could be due to use of different mouse strains, tissues and/or different markers to identify DC subsets. Therefore, a consensus has not yet been reached regarding the effects of healthy ageing on DC subsets, even less is known regarding the combined effect of aging and cancer in DCs.

DCs can activate tumour specific cytotoxic $CD8^+$ T cells that lyse tumour cells leading to tumour regression [520, 521]. However, tumours can alter DC precursor differentiation, suppress DC maturation and activation [522, 523] and induce development of Treg with immunosuppressive functions [524, 525]. An earlier study in our group demonstrated that circulating DCs in humans with mesothelioma have defects in DC numbers and antigen processing function indicated by reduced MHC molecules and reduced expression of co-stimulatory molecules [197]. It should be noted that majority of mesothelioma cases emerge in people aged more than 60 years [526]. Another study in our group by Gardner et al. demonstrated reduced MHC-I, MHC-II and CD80 on $CD11c^+$ cells in elderly mesothelioma-bearing mice and decreased expression of IFNγ $CD4^+$ and $CD8^+$ T cells compared to younger counterparts, suggesting age-related loss of immune function [527].

Herber et al. showed that the presence of a tumour can lead to increased lipid accumulation in DCs which is associated with DC dysfunction and impaired anti-tumour immunity [486]. A few studies using different cancer models have shown that tumours impair antigen cross presentation by elevating intracellular lipid levels [486, 528-530]. Similarly, Gardner et al. showed that mesothelioma driven DC dysfunction was associated with lipid accumulation in young tumour-bearing mice and in DCs from young healthy donors that were exposed to mesothelioma-derived soluble factors [198]. The gap in knowledge that is addressed in these studies is the dual effect of mesothelioma and ageing on DCs, as this scenario better represents the human situation. Therefore, this study looked at the effects of mesothelioma and ageing on murine DCs, focussing on changes to lipid content, molecules associated with lipid uptake and molecules associated with antigen-presentation.

4.2 Results

4.2.1 Mesothelioma factors elevate lipid levels in murine bone marrow-derived DCs from young mice

The first series of experiments investigated the effects of AE17 mesothelioma-derived TCM on lipid levels and MHC expression in BM-derived DCs (BMDCs). BM cells from young C57BL/6J healthy mice (2-5 months old) were cultured *in-vitro* as shown in chapter 2 (section 2.3.5). DCs were exposed to TCM on Day 7 for 24 hours and stained with Bodipy (to detect neutral lipids) and anti-MHC-I and MHC-II antibodies for analysis by flow cytometry. The gating strategy is shown in Figures 4.1 A- C. Whilst the proportions of $Bodipy^{+}$ cells between unexposed and TCM-exposed BMDCs remained consistent (Figure 4.1 D), lipid levels, shown as MFI, significantly increased in tumour-exposed BMDCs (Figures 4.1 E). This increase in lipid content in mesothelioma-exposed DCs was visualised and confirmed through staining with Bodipy and confocal microscopy (Figures 4.1 F, G). No changes in MHC- I expression levels were observed between the two groups (Figure 4.1 H). In contrast, a significant reduction in MHC-II expression levels was noticed in TCM-exposed BMDCs (Figure 4.1 I), as observed earlier in macrophages (chapter 3 - Figure 3.1). These data confirm findings from others that mesothelioma elevates lipid levels in DCs from young hosts [198, 486{Gardner, 2015 #583].

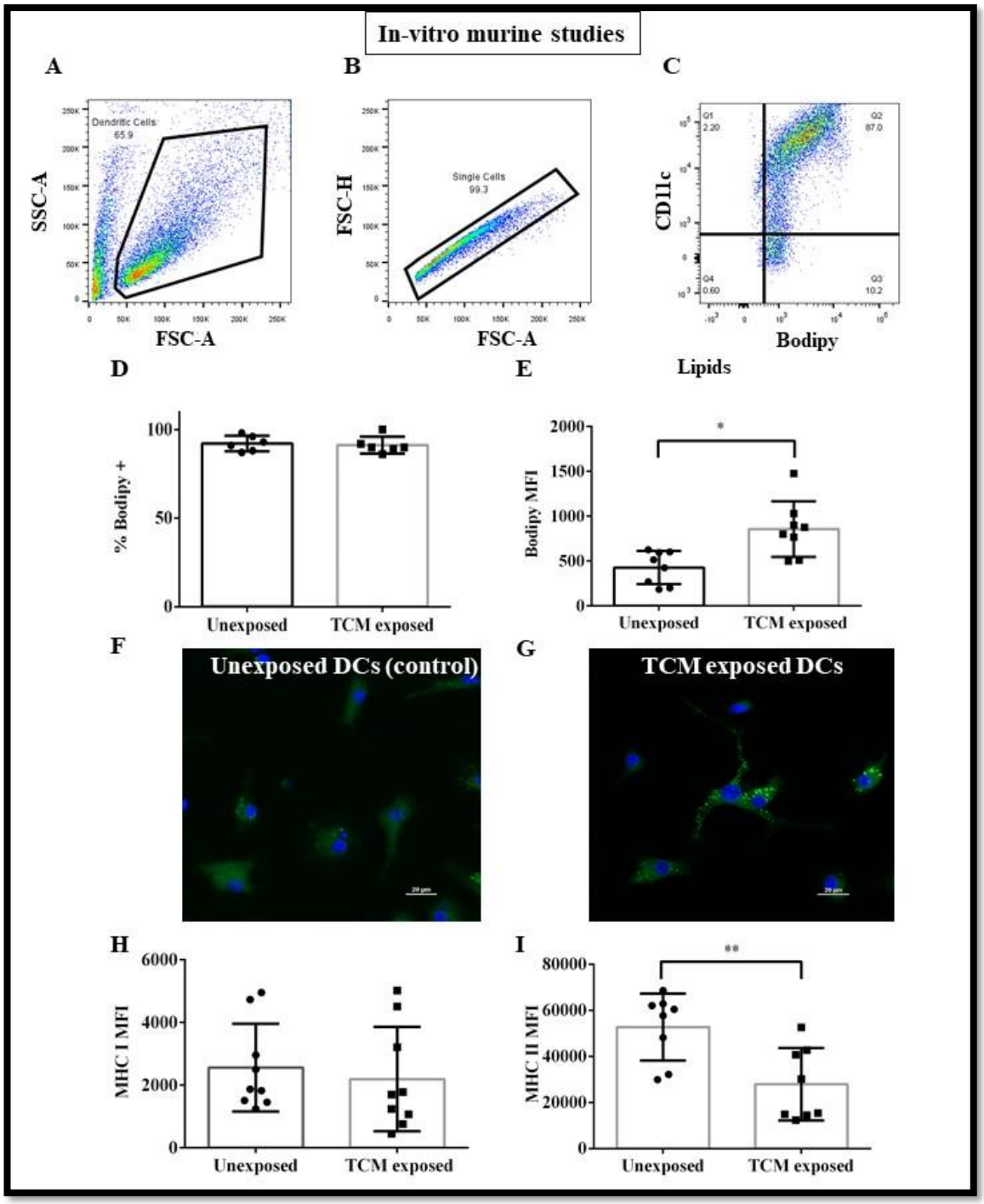

Figure 4.1: Mesothelioma increases lipid content and decreases MHC-II in DCs
DCs generated from BM from healthy mice aged 2-5 months were either left untreated or exposed to AE17 mesothelioma-derived tumour conditioned media (TCM) before being stained with Bodipy to measure neutral lipids as well as with antibodies directed against MHC-I and MHC-II. Large cells **(A)**, single cells **(B)**, then $CD11c^{+}Bodipy^{+}$ **(C)** were gated. **D** shows the percentage of cells positive for Bodipy and (**E)** shows Bodipy MFI. (**F)** and (**G)** show DCs cultured on glass bottom plates and stained with Bodipy (green) and DAPI (nucleus, blue). After fixation, the cells were visualised using a Nikon confocal microscope. **(H)** and **(I)** show the MFI of MHC-I and MHC-II. Data shown as mean ± SEM, n = 6-9 experiments. ** = $p<0.005$. Statistical significance assessed by Wilcoxon Signed Ranked Test.

4.2.2 Examining the *in-vivo* effects of mesothelioma on murine CD11c$^+$ cells

The next series of experiments investigated the simultaneous *in-vivo* effects of ageing and mesothelioma on DCs in different lymphoid compartments using young mice (6 to 8 weeks old) and elderly mice (18 months old) inoculated with AE17 mesothelioma cells. The BM was examined to determine distal effects on the central lymphoid compartment that might be mediated by mesothelioma-derived factors in the aged setting. Spleens and draining lymph nodes (dLNs) were examined to identify changes to the key secondary lymphoid organs that mediate adaptive immune responses.

4.2.2.1 CD11c$^+$ cells increase with ageing and mesothelioma in dLNs while splenic pDCs decrease

CD11c$^+$ cells were gated according to Figure 4.2; this was based on the group's previous work [246]. These CD11c$^+$ cells contain DCs as well as other APCs, such as macrophages and B cells. The total proportion of CD11c$^+$ cells remained unchanged in BM, spleens and dLNs with healthy ageing (Figures 4.3 A,C,E). In contrast, pDCs decreased with healthy ageing in spleens (Figure 4.3 D) while no age-related changes were observed in BM and dLNs (Figures 4.3B, F). However, the presence of mesothelioma led to an increase in the proportion of CD11c$^+$ cells in elderly dLNs (Figure 4.3 E).

4.2.2.1 Neither age nor mesothelioma modulate lipid content in CD11c$^+$ cells in lymphoid organs

No significant changes were seen in lipid levels in CD11c$^+$ cells in the different lymphoid compartments regardless of age or the presence of a mesothelioma (Supplementary figure 4.1, 4.2). Similarly, no significant changes were observed in lipid levels in tumour-associated DC subsets, although greater variation in lipid levels were seen in elderly mice (Figure 4.4). Expression levels of the lipid uptake molecules, CD36 and CD147, also did not change in response to an ageing environment or mesothelioma (Supplementary figure 4.2, 4.3).

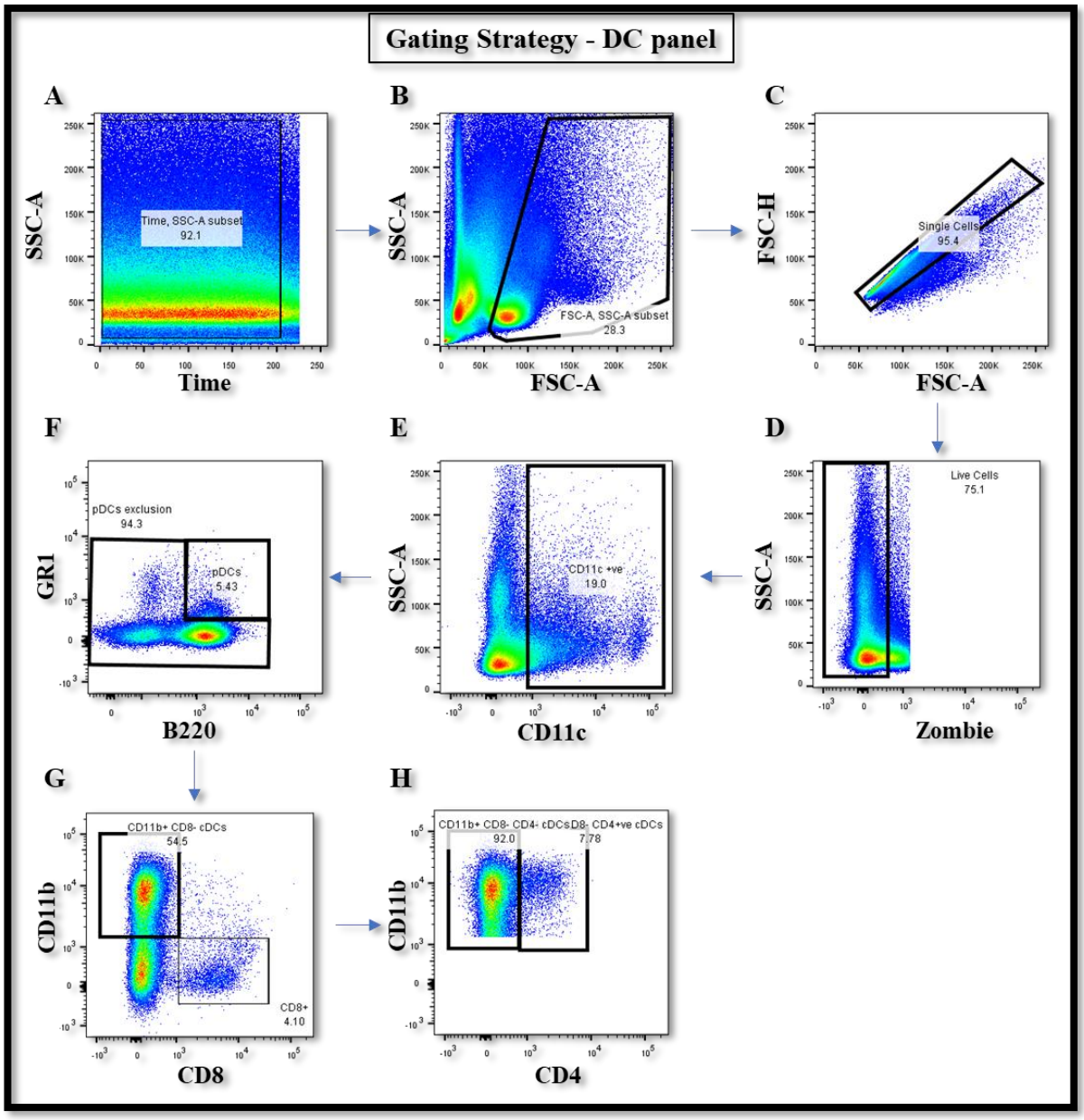

Figure 4.2: Experimental approach and flow cytometry gating strategy

Young and old C57BL/6J mice were inoculated with $5x10^5$ AE17 cells in 100µl of PBS on day 0 and monitored daily until tumours reached $120mm^2$ when bone marrow, tumours, dLN and spleens were collected and stained with fluorescently-labelled antibodies to detect DCs subpopulations using flow cytometry (Chapter 3; figure 3.2). Lymphoid organs were stained for markers of DC subsets (CD11c, B220, GR-1, CD11b, CD8α and CD4) and analysed by flow cytometry. Within the $CD11c^+$ cells gate **(E)**, plasmacytoid cells were gated as $B220^+GR1^+$ cells **(F)**. Within the pDC exclusion gate (i.e., cells that are not B220 and GR-1 double positive **(F)**; $CD8^+CD11b^-$ conventional DCs (cDCs) and $CD11b^+CD8^-$ cDCs were gated **(G)**, and $CD11b^+CD8^-$ cDCs were further distinguished into $CD4^+$ and $CD4^-$ subsets **(H)**.

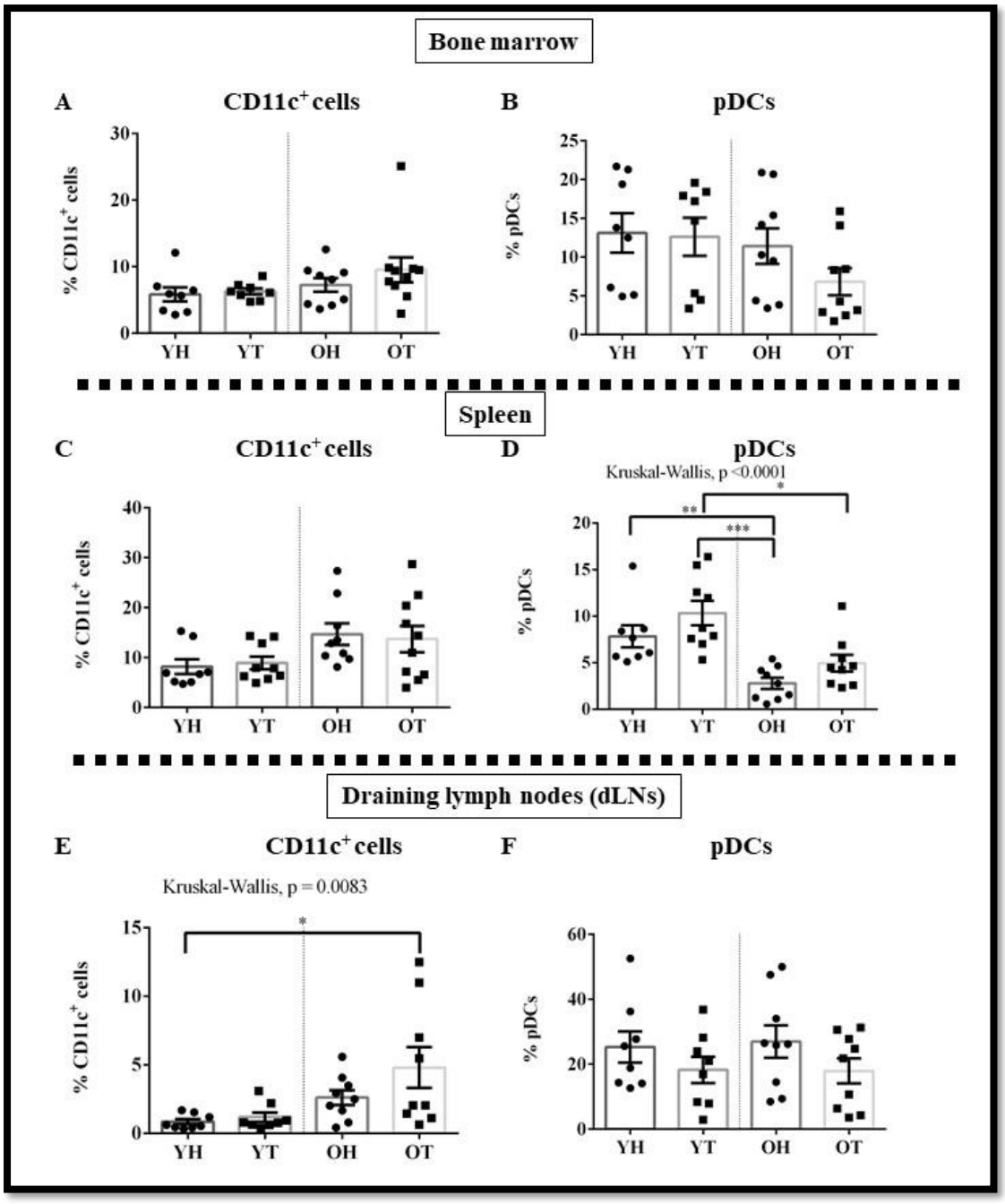

Figure 4.3: CD11c$^+$ cells increase in dLNs with ageing and cancer

Bone marrow (BM), spleens and draining lymph nodes (dLNs) from young healthy (YH), young tumour-bearing (YT), old healthy (OH) and old tumour-bearing mice (OT) were stained with markers to isolate APCs and CD11c$^+$ cells were selected as described in Figure 4.2. The proportion of CD11c$^+$ cells and pDCs in BM **(A, B)**, spleens **(C, D)** and lymph nodes **(E, F)** are shown as mean ± SEM, n = 10-11 mice in each group. * = p<0.05, ** = p<0.005, *** = p<0.0005. Statistical significance between all groups was assessed by a Kruskal-Wallis test, followed by a post-hoc Dunn's test to measure differences between two groups.

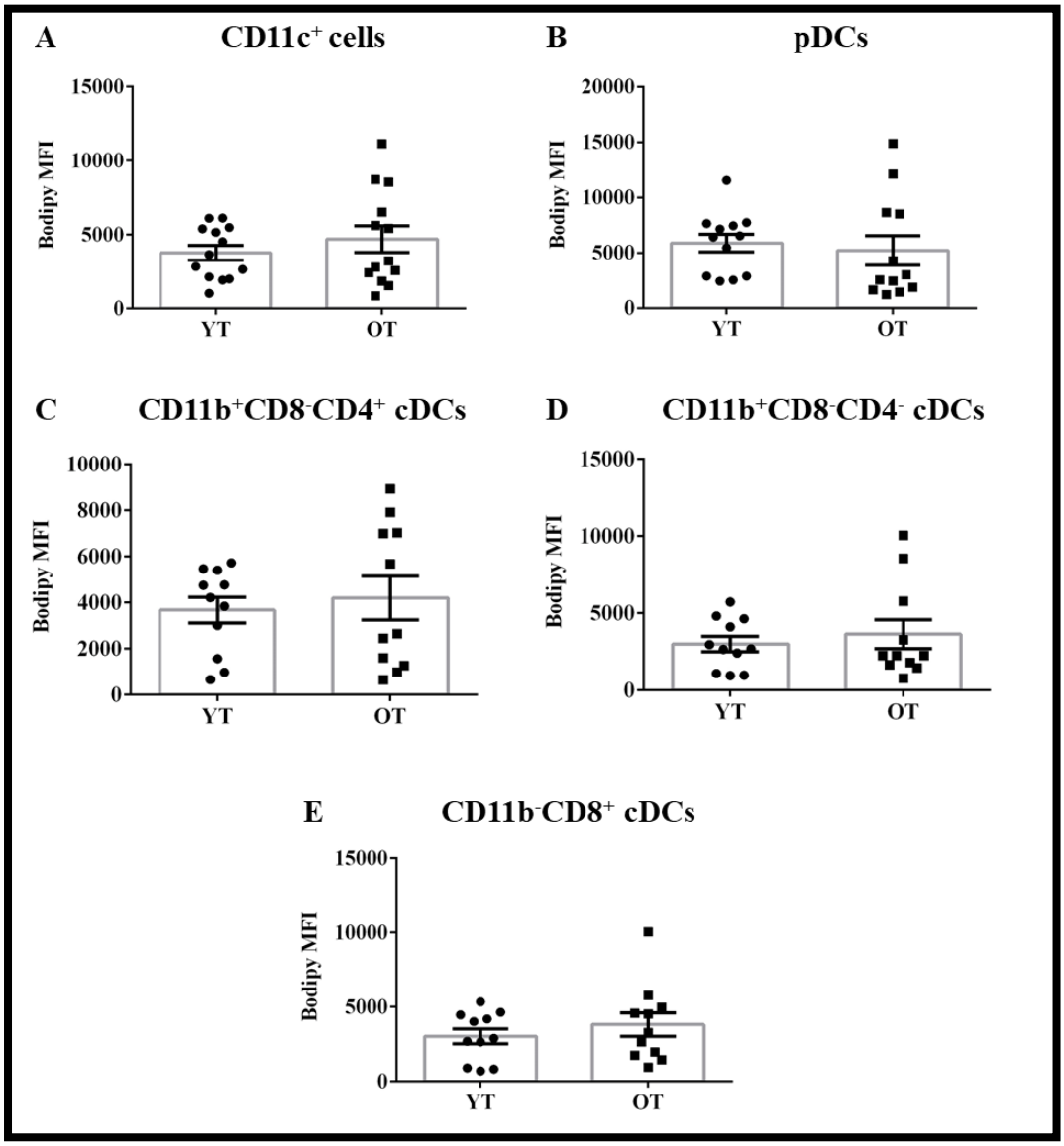

Figure 4.4: Variable lipid levels are seen in elderly tumour-associated dendritic cell subsets

Tumour-associated DCs from young tumour-bearing (YT) and old tumour-bearing mice (OT) were stained with Bodipy to measure neutral lipids and analysed by flow cytometry. Expression levels of Bodipy (measured as MFI) in $CD11c^+$ cells **(A)**, pDCs **(B)**, $CD11b^+CD8^-CD4^+$ cDCs **(C)**, $CD11b^+CD8^-CD4^-$ cDCs **(D)**, $CD11b^-CD8^+$ cDCs **(E)**. Data are shown as mean ± SEM, n = 10-11 mice/group. Statistical significance assessed by Mann Whitney U Test.

4.2.2.3. MHC-I decreases with healthy ageing in splenic CD11c$^+$ cells, yet increases in LN CD11c$^+$ cells

No changes in MHC-I expression were observed in different DC subsets in BM with healthy ageing (Supplementary figure 4.4). However, MHC-I expression levels decreased with healthy ageing on splenic CD11c$^+$ cells, pDCs and CD11b$^+$CD8$^-$CD4$^+$ cDCs (Figures 4.5A-C). This was accompanied by a reduced percentage of splenic MHC-I$^+$CD11c cells, MHC-I$^+$pDCs, MHC-I$^+$CD11b$^+$CD8$^-$CD4$^+$ cDCs and MHC-I$^+$CD11b$^+$CD8$^-$CD4$^-$ cDCs (Figures 4.5E-H). The data suggest that healthy ageing modulates the splenic microenvironment resulting in downregulation of MHC-I on DCs. In contrast, there appeared to be an increased percentage of dLN MHC-I$^+$CD11c$^+$ cells, MHC-I$^+$CD11b$^+$CD8$^-$CD4$^-$ cDCs and MHC-I$^+$CD8$^+$ cDCs (Figures 4.7A, C, D) in healthy old mice, with a statistically significance difference reached in CD11b$^+$CD8$^-$CD4$^-$ cDCs and CD8$^+$ cDCs relative to young mice.

4.2.2.4 Mesothelioma reduces MHC-I in BM, splenic and LN CD11c$^+$ cells in old mice

An age-related effect was seen with mesothelioma, as MHC-I expression levels decreased in splenic CD11c$^+$ cells, pDCs and CD8$^-$CD4$^+$ cDCs (Figures 4.5 A-C) along with reduced percentage of BM MHC-I$^+$ pDCs in old tumour-bearing mice relative to young tumour-bearing mice (Figures 4.6). These data show that tumour-derived factors affect the aged splenic and BM microenvironments by downregulating MHC-I on CD11c$^+$ cells and their DC subsets likely impairing their ability to present tumour antigen to CD8$^+$ T cells.

A different age-related effect was seen in LNs. CD11b$^+$CD8$^-$CD4$^-$ cDCs and CD11b$^-$CD8$^+$ cDCs, but not pDCs, demonstrated elevated MHC-1 with healthy ageing (Figure 4.7 C, D). The presence of mesothelioma decreased MHC-I$^+$ in the elderly CD11b$^-$CD8$^+$ LN DC subset (Figure 4.7 D). In contrast, MHC-I$^+$ in young CD11b$^-$CD8$^+$ LN DCs was elevated by mesothelioma (Figure 4.7 D). These data suggest an increased capacity to present antigen to CD8$^+$ T cells in old LNs could be compromised by mesothelioma.

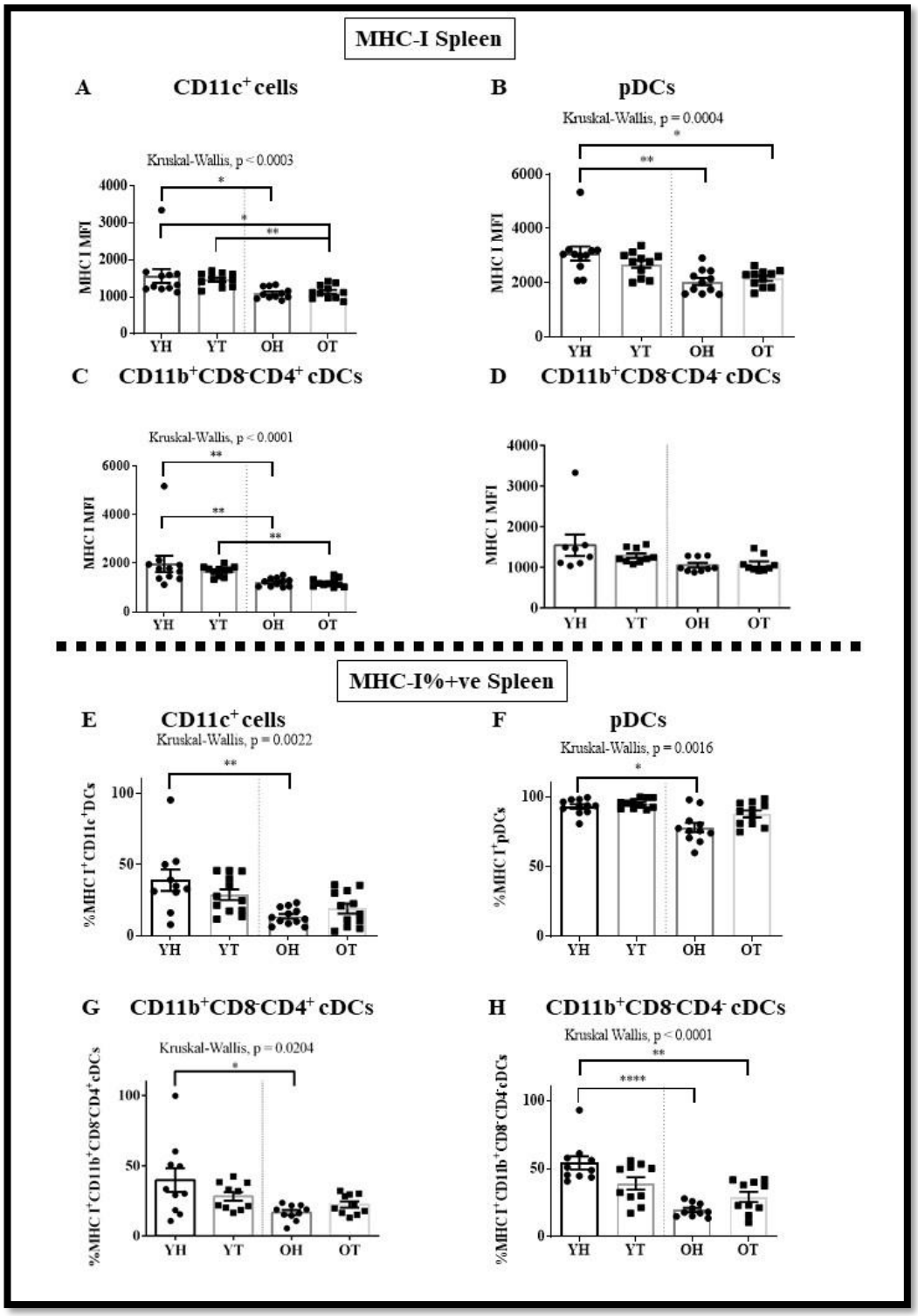

Figure 4.5: MHC-I decreases in old healthy compared to young healthy mice

Splenic DCs from YH, YT, OH and OT were stained for CD11c, CD11b, CD8, CD4, MHC-I and MHC-II, and analysed by flow cytometry to identify specific DC subsets, as shown in Fig 4.2. Expression levels (MFI) of MHC-I in $CD11c^+$ cells **(A)**, pDCs **(B)**, $CD11b^+CD8^-CD4^+$ cDCs **(C)**, $CD11b^+CD8^-CD4^-$ cDCs **(D)**, % $MHC\text{-}I^+$ CD11c **(E)**, as well as the percentage of $MHC\text{-}I^+$ pDCs **(F),** $MHC\text{-}I^+CD11b^+CD8^-CD4^+$ cDCs **(G)** and $MHC\text{-}I^+$ $CD11b^+CD8^-CD4^-$ cDCs **(H)** were measured. Data shown as mean ± SEM, n = 10-11 mice/group. * = $p<0.05$, ** = $p<0.005$,**** =$p<0.0001$. Statistical significance between all groups was assessed by a Kruskal-Wallis test, followed by a post-hoc Dunn's test to measure differences between two groups.

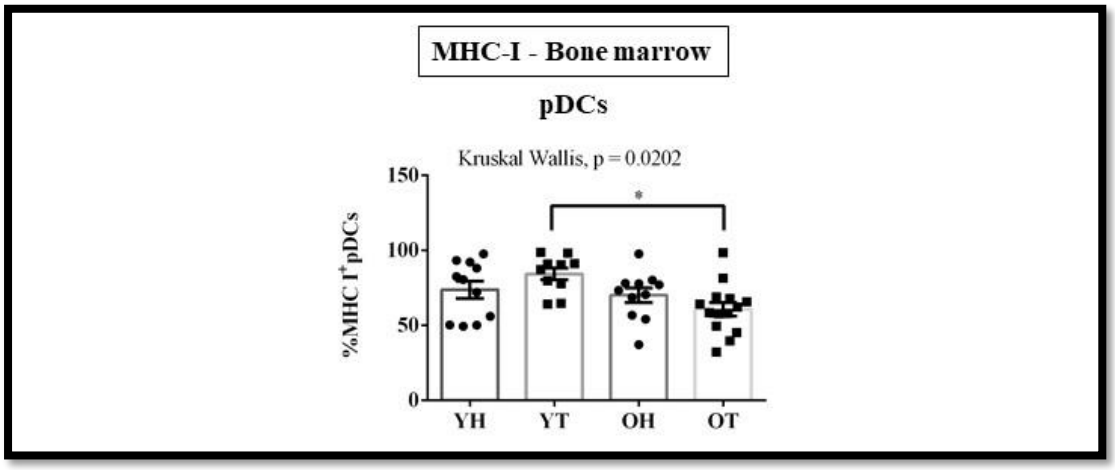

Figure 4.6: MHC-I decreases in old compared to young tumour bearing mice in BM pDCs

BM DCs from YH, YT, OH and OT were stained for CD11c, CD11b, CD8, CD4, MHC-I and MHC-II, and analysed by flow cytometry to identify specific DC subsets, as shown in Fig 4.2. The percentage of MHC-I$^+$ pDCs were recorded. Data are shown as mean ± SEM, n = 10-11 mice/group. * = p<0.05. Statistical significance between all groups was assessed by a Kruskal-Wallis test, followed by a post-hoc Dunn's test to measure differences between two groups.

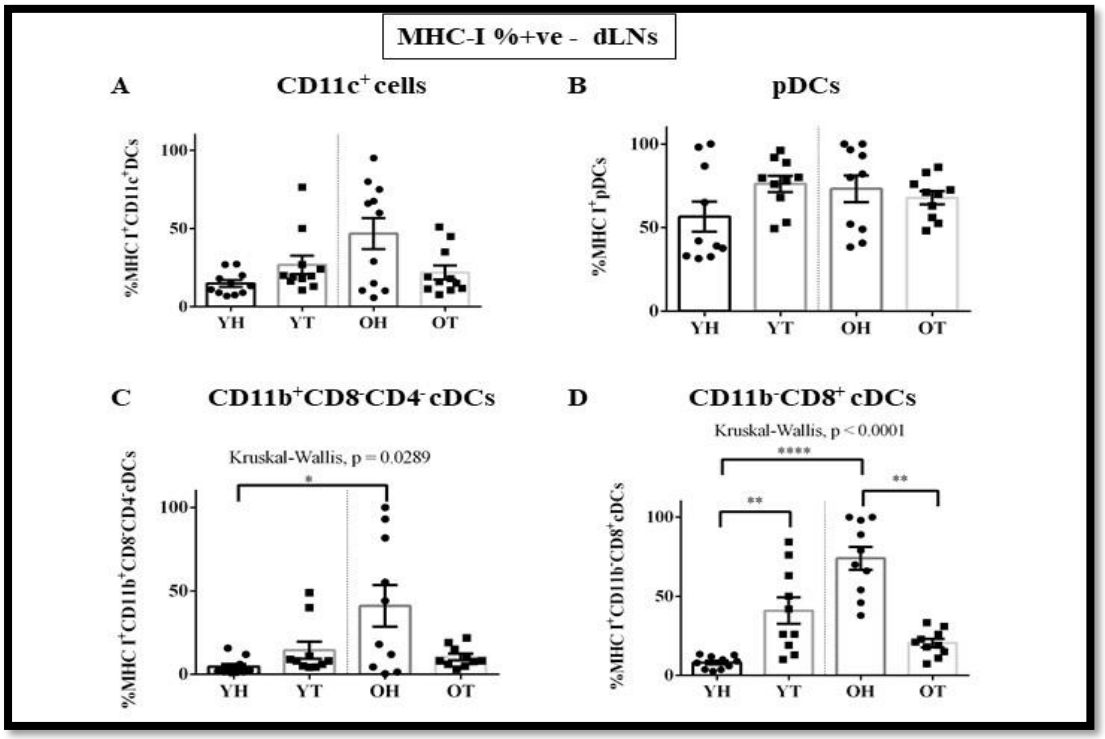

Figure 4.7: MHC-I expression increases with healthy ageing in different LN DC subsets

DLN DCs from YH, YT, OH and OT were stained for CD11c, CD11b, CD8, CD4, MHC-I and MHC-II, and analysed by flow cytometry to identify specific DC subsets as shown in Fig 4.2. The percentage of MHC-I$^+$ cells in CD11c$^+$ DCs **(A)**, pDCs **(B)**, CD11b$^+$CD8$^-$CD4$^-$ cDCs **(C)**, CD11b$^-$CD8$^+$ cDCs **(D)** were measured. Data shown as mean ± SEM, n = 10-11 mice/group. * = p<0.05, ** = p<0.005, **** =p<0.0001. Statistical significance between all groups was assessed by a Kruskal-Wallis test, followed by a post-hoc Dunn's test to measure differences between two groups.

4.2.2.5 Healthy ageing is associated with increased MHC-II in BM, splenic and CD4$^-$ dLN DCs

Increased MHC-II expression levels in BM pDCs with healthy ageing (Figure 4.8 B) were accompanied by an increased percentage of BM MHC-II$^+$CD11b$^+$CD8$^-$CD4$^-$ cDCs with healthy ageing (Figure 4.8 E). Increased MHC-II expression levels were also observed in splenic CD11c$^+$ cells, pDCs and CD11b$^+$CD8$^-$CD4$^-$ cDCs with healthy ageing (Figure 4.9 A-C). In contrast, MHC-II decreased in splenic CD8$^+$ cDCs (Figure 4.9 D). An increase in MHC-II expression with healthy ageing in LN CD11b$^+$CD8$^-$CD4$^-$ cDCs accompanied by an increased percentage of MHC-II$^+$CD4$^-$ LN cDCs was also observed (Figure 4.9E, F).

4.2.2.6 Mesothelioma modulates age-related MHC-II changes in specific splenic DC subsets

Mesothelioma elevated MHC-II expression in aged splenic CD11c$^+$ cDCs, CD11b$^+$CD8$^-$CD4$^-$ cDCs and CD11b$^-$CD8$^+$ cDCs (Figure 4.9A, C, D), yet reduced MHC-II expression in aged dLNs (Figure 4.9 E).

4.2.2.7 CD80 increases with healthy ageing in dLN DCs

CD80 expression significantly increased with ageing in CD11c$^+$ cells in dLN along with an increased percentage of CD8$^-$CD4$^-$ healthy cDCs and CD8$^+$ cDCs (Figure 4.10 A-D).

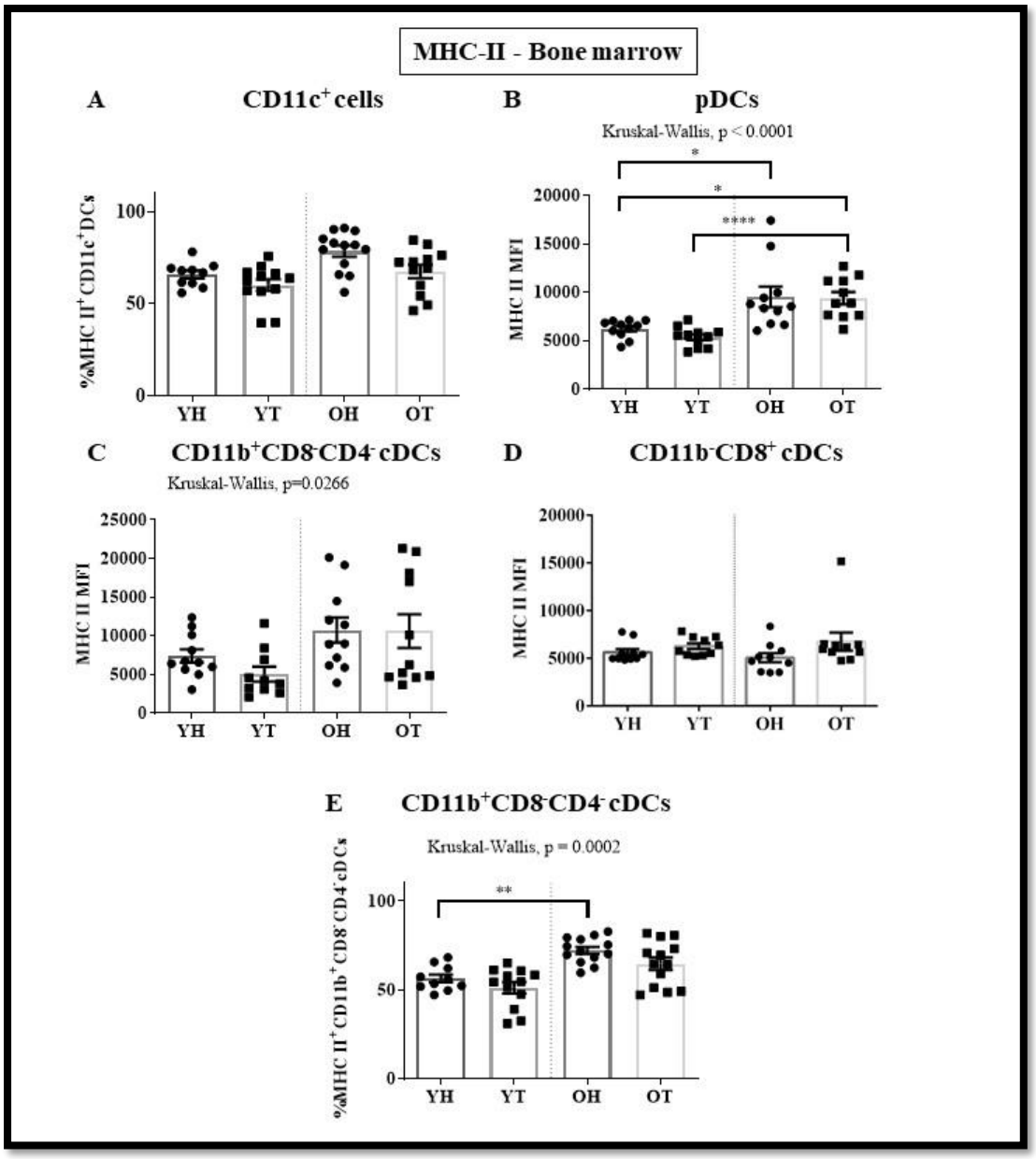

Figure 4.8: MHC-II increases with healthy ageing in BM pDCs and CD11b$^+$CD8$^-$ CD4$^-$ DCs

BM DCs from YH, YT, OH and OT were stained for CD11c, CD11b, CD8, CD4, MHC-I and MHC-II, and analysed by flow cytometry to identify specific DC subsets as shown in Fig 4.2 Expression levels of MHC-II (MFI) in pDCs **(B)**, CD11b$^+$CD8$^-$CD4$^-$ DCs **(C)**, CD11b$^+$ CD8$^+$ cDCs **(D)**, plus percent cell MHC-II positive of CD11b$^+$CD8$^-$CD4$^-$ cDCs **(E)**, and percentage of MHC-II$^+$ CD11c$^+$ cells **(A)** were measured. Data shown as mean ± SEM, n = 10-11 mice/group. * = p<0.05, ** = p<0.005, *** = p<0.0005, **** =p<0.0001. Statistical significance assessed by Kruskal-Wallis test followed by post hoc Dunn's Test.

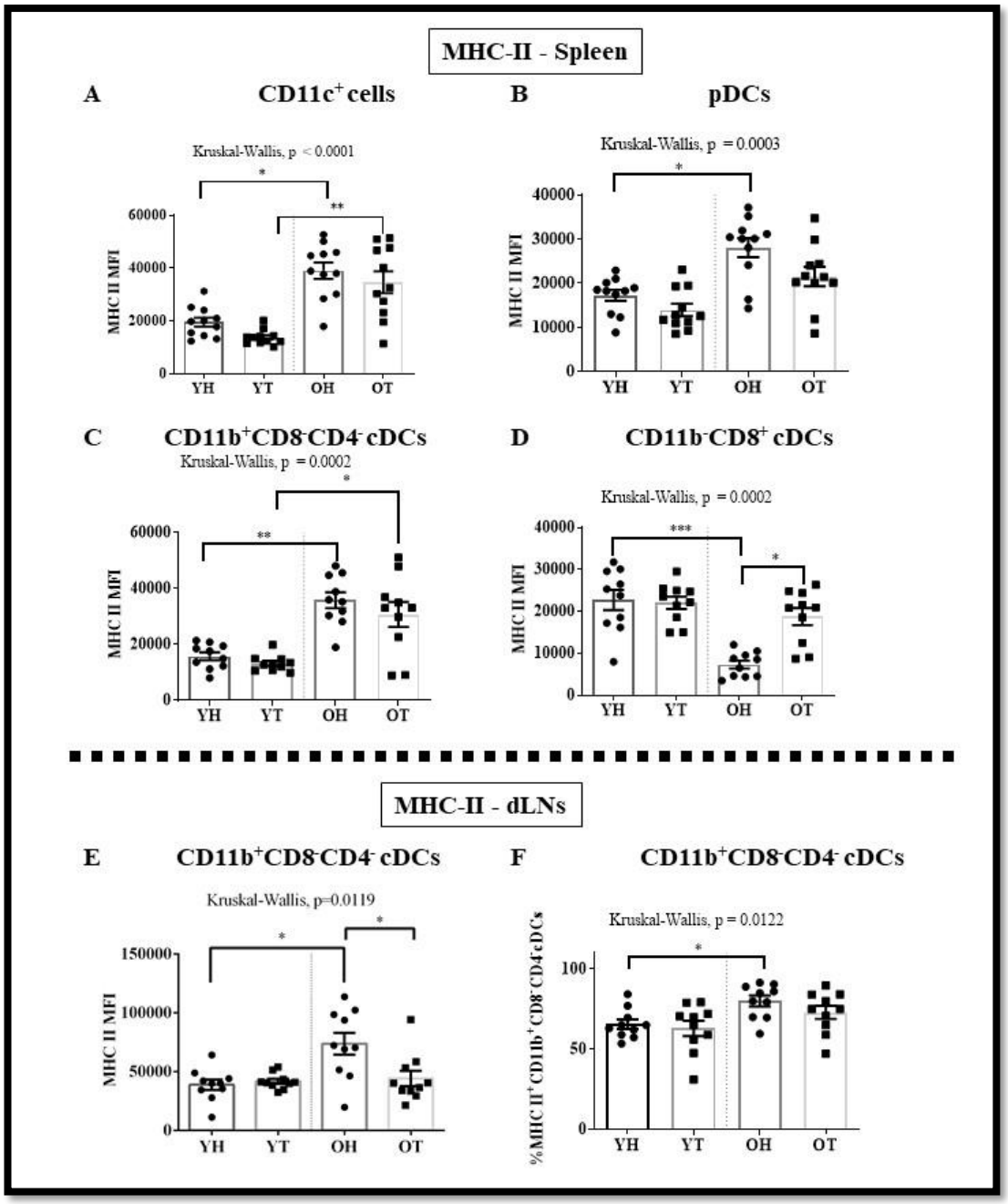

Figure 4.9: Ageing is associated with increased MHC-II expression in all splenic and LN DCs except CD11b$^-$CD8$^+$ cDCs in spleen

Splenic and dLN DCs from YH, YT, OH and OT were stained for CD11c, CD11b, CD8, CD4, MHC-I and MHC-II, and analysed by flow cytometry to identify specific DC subsets as shown in Fig 4.2. Expression levels of MHC-II (MFI) in CD11c$^+$ DCs **(A)**, pDCs **(B)**, CD11b$^-$CD8$^-$CD4$^-$ cDCs **(C, E)**, CD11b$^+$ CD8$^+$ DCs **(D),** CD11b$^+$CD8$^-$CD4$^-$ cDCs **(E)** and MHC-II%$^+$ cells in dLN CD11b$^-$CD8$^-$CD4$^-$ cDCs **(F)** were measured. Data shown as mean ± SEM, n = 10-11 mice/group. * = p<0.05, ** = p<0.005, *** = p<0.0005, ****= p <0.0001. Statistical significance assessed by Kruskal-Wallis test followed by post hoc Dunn's Test.

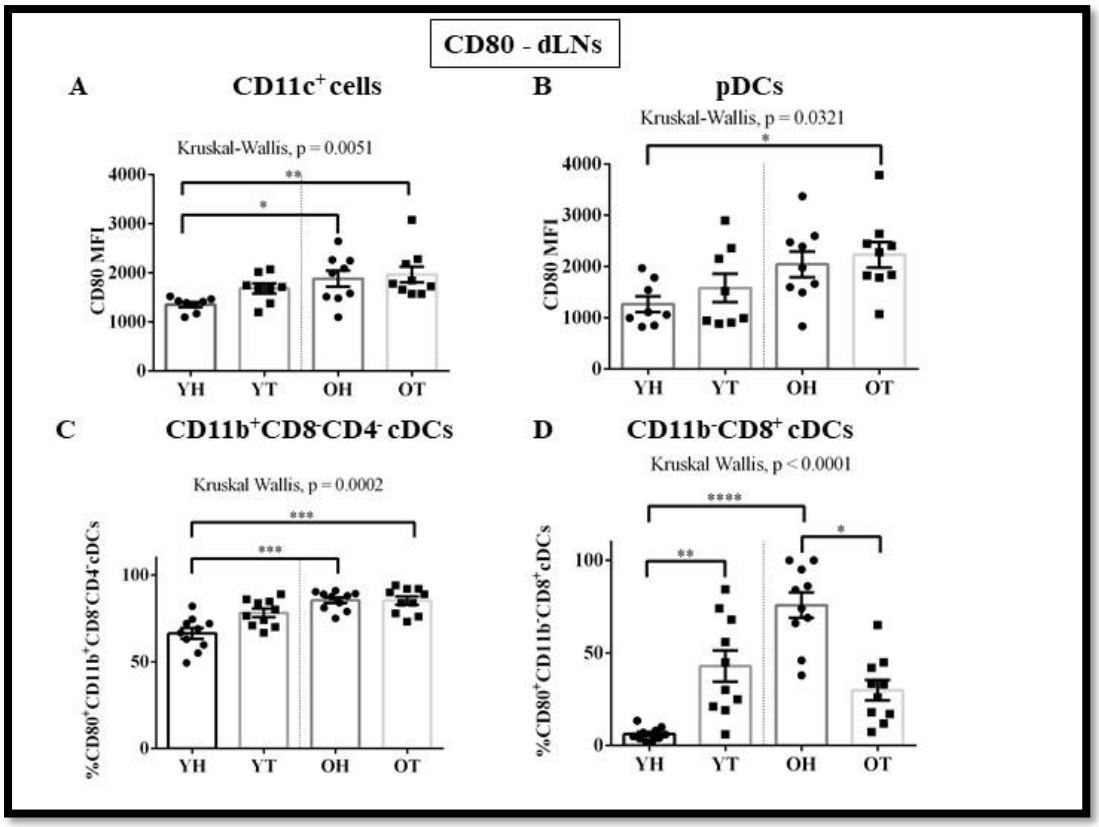

Figure 4.10: The proportion of CD80$^+$ cells increase with healthy ageing in DC subsets

LN DC from YH, YT, OH and OT stained for CD11c, CD11b, CD8, CD4, CD80, CD40, MHC-I, MHC-II, and CD80 and analysed by flow cytometry to identify specific DC subsets as shown in Fig 4.2. CD80 MFI in CD11c$^+$ cells **(A),** pDCs **(B),** percentage of CD80$^+$ CD11b$^+$CD8$^-$CD4$^-$ cDCs **(C)** and percentage of CD80$^+$ CD11b$^-$CD8$^+$ cDCs **(D)** were measured. Data shown as mean ± SEM, n = 10-11 mice/group. * = p<0.05, ** = p<0.005, *** = p<0.0005, **** =p<0.0001. Statistical significance assessed by Kruskal-Wallis test followed by post hoc Dunn's Test.

4.2.2.8 Mesothelioma reduces CD80 on $CD8^+$ LN DCs in old but not young mice

Mesothelioma reduced the proportion of $CD80^+$ cells in old dLN $CD8^+$ LN DCs (Figure 4.10 D). In contrast, the proportion of $CD80^+$ cells were elevated in young $CD8^+$ dLN cDCs with mesothelioma (Figure 4.10 D). No other changes in CD80 were observed in BM, spleens, and tumours (Supplementary figure 4.5, 4.6, 4.7).

4.2.2.9 $CD40^+$ DCs increase in dLNs with ageing and mesothelioma

In dLN, the proportion of $CD40^+CD8^-CD4^-$ cDCs increased with healthy ageing and further increased in the presence of mesothelioma (Figure 4.11). No other age or mesothelioma-related changes were seen in BM DCs, other splenic or dLN DC subsets, or in tumour-associated DCs (Supplementary figure 4.8, 4.9, 4.10).

4.2.2.10 Mesothelioma increases all tumour associated DC subsets except $CD8^+$ cDCs and pDCs in old mice

An age-related increase in tumour-associated proportions was observed in all $CD11c^+$ subpopulations, except for pDCs and $CD8^+$ DCs in tumours (Figure 4.12 A-D).

4.2.2.10 Mesothelioma reduces MHC-II in tumour-associated DCs

All DC subsets (pDCs, $CD11b^+CD8^-CD4^-$ cDCs, $CD11b^+CD8^-CD4^+$ cDCs) showed a significant reduction in MHC-II expression levels in tumour-associated DCs (Figure 4.13 A-D). This was accompanied by a reduced percentage of $MHC\text{-}II^+CD11b^+CD8^-CD4^-$ cDCs (Figure 4.13 G).

4.2.2.11 Tumour-associated DCs demonstrate loss of MHC-I expression

The percentage of $MHC\text{-}I^+$ pDCs and $MHC\text{-}I^+$ $CD8^-CD4^-$ cDCs significantly reduced in elderly tumours relative to young tumours (Figure 4.14 B,C). A similar trend was seen in all other DC subsets in terms of proportions (Figure 4.14 A, D) and expression levels (MFI; data in Supplementary figure 4.13), however the differences did not reach statistical significance.

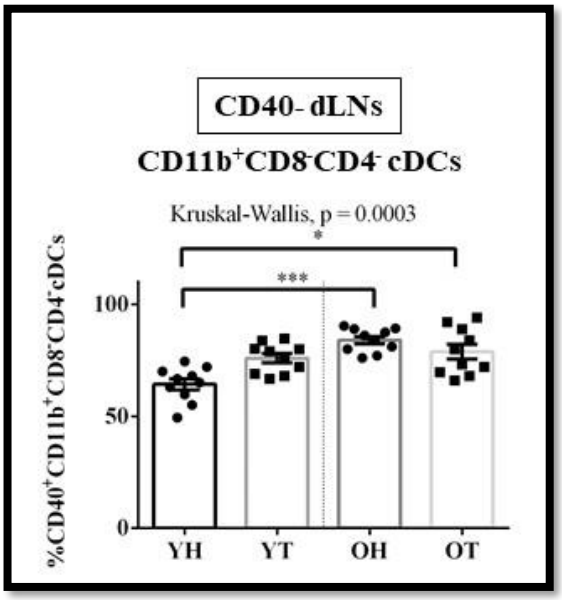

Figure 4.11: Healthy ageing is associated with increased CD40 expression in $CD8^-CD4^-$ cDCs

DLN DCs from YH, YT, OH and OT were stained for CD11c, CD11b, CD8, CD4, CD40, CD80, MHC-I and MHC-II, and analysed by flow cytometry to identify specific DC subsets as shown in Fig 4.2. Percentages of $CD40^+$ cells in pDCs in $CD11b^+CD8^-CD4^-$ cDCs in dLNs were measured. Data shown as mean ± SEM, n = 10-11 mice/group. * = $p<0.05$, *** = $p<0.0005$. Statistical significance assessed by Kruskal-Wallis test followed by post hoc Dunn's Test.

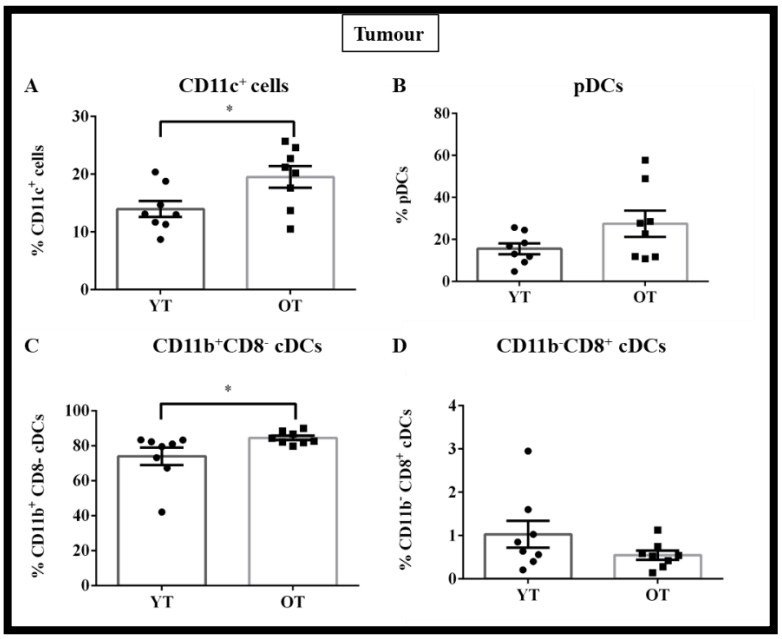

Figure 4.12: $CD11c^+$ and $CD8^-$ tumour-associated DCs increase with ageing

Tumour associated DCs from young tumour-bearing (YT) and old tumour-bearing mice (OT) were stained with CD11c as per Figure 5.2. The proportion of $CD11c^+$ DCs **(A),** pDCs **(B),** $CD11b^+CD8^-$ cDCs **(C)** and $CD11b^-CD8^+$ cDCs **(D)** are shown as mean ± SEM, n = 10-11 mice in each group. * = $p<0.05$. Statistical significance assessed by Mann Whitney U Test.

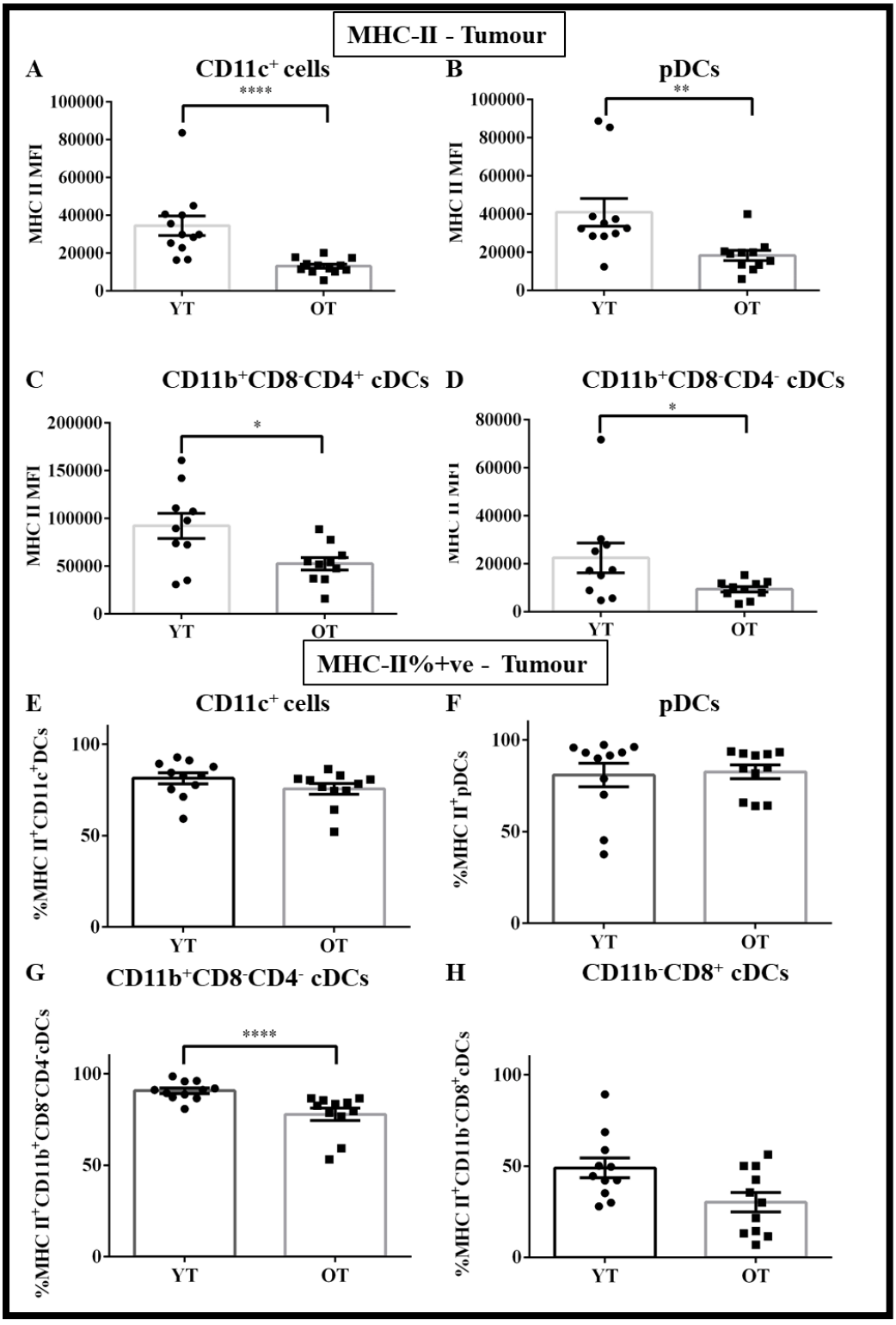

Figure 4.13: Mesothelioma leads to decreased MHC-II expression in tumour-associated DCs

Tumour-associated DCs from young tumour-bearing (YT) and old tumour-bearing mice (OT) were stained for MHC-II and analysed by flow cytometry. Expression levels of MHC-II (MFI) and percent MHC-II$^+$ in CD11c$^+$ DCs **(A, E),** pDCs **(B, F),** CD11b$^+$CD8$^-$CD4$^-$ cDCs **(D, G),** CD11b$^+$CD8$^-$CD4$^+$ cDCs **(C) and** %+ MHC-II$^+$ CD8$^+$ cDCs **(H)** were measured. Data are shown as mean ± SEM, n = 10-11 mice/group. Statistical significance assessed by Mann Whitney U Test. * = $p<0.05$, ** = $p<0.005$, **** =$p<0.0001$.

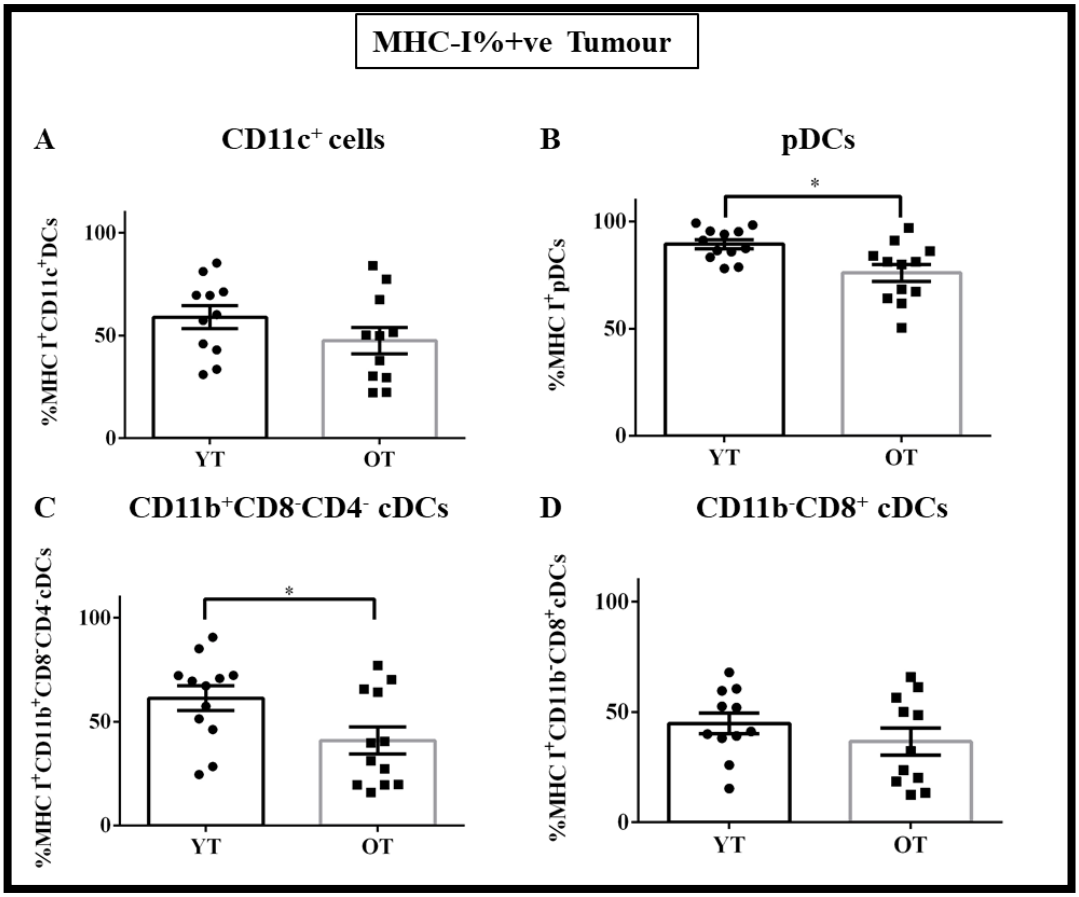

Figure 4.14 MHC-I decreases in tumour-associated CD8$^-$ cDCs and pDCs in old mice

Tumour-associated DCs from young tumour-bearing (YT) and old tumour-bearing mice (OT) were stained for MHC-I and analysed by flow cytometry. Percentage of MHC-I$^+$ cells in CD11c$^+$ DCs **(A)**, pDCs **(B)**, CD11b$^+$CD8$^-$CD4$^-$ cDCs **(C),** CD11b$^-$CD8$^+$ cDCs **(D)** were measured. Data are shown as mean ± SEM, n = 10-11 mice/group. Statistical significance assessed by Mann Whitney U Test. * = $p<0.05$.

4.3 Applying alternative gating strategy to isolate DCs

The above *in-vivo* data was re-analysed using an alternative gating stratey as $CD11c^+$ cells contain macrophages and B cells, as well as DCs. The new gating strategy focussed on isolating $CD11c^{high}MHC\text{-}II^{high}$ cells and has been used in other studies to classify potent APCs that are more representative of DCs (Figure 4.15) [531-533]. The results are shown below.

4.3.1 Lipid levels increase with healthy ageing in specific subsets of BM DCs and LN DCs

No changes in lipid levels in healthy splenic DCs were observed (Supplementary figure 4.15). However, increased lipid levels were seen in BM pDCs, BM $CD8^+$ cDCs (Figure 4.16) and LN pDCs (Figure 4.17) with healthy ageing. The latter is different to the CD11c gating strategy (but consistent with our group's previous work showing increased lipid content in healthy elderly LN pDCs [534]. These data show that there were differences between the staining and gating strategies that have been published by other members of this group and this study.

This study extended our group's previous work by looking at the combined effect of ageing and mesothelioma, and found increased lipid uptake in all aged BM DC subsets (Figure 4.16). Lipid levels also increased in elderly tumour-associated $CD8^+$ DCs (Figure 4.18). All cells were Bodipy positive (supplementary figure 4.16).

4.3.2 MHC-II decreases with healthy ageing in specific splenic and BM DCs, and is further reduced with mesothelioma

An age-related decrease in MHC-II expression was observed in healthy splenic $CD11c^+MHC\text{-}II^+$ cells and $CD8^-$ cDCs (Figure 4.19) and BM pDCs (Figure 4.20). No age-related changes in MHC-II were found in LN DCs (Supplementary figure 4.17). The data suggest that healthy ageing modulates the splenic microenvironment resulting in downregulation of MHC-II on DCs. This is consistent with our group's previous work [246] where the data showed decreased MHC-II with healthy ageing in superficial cervical LN.

The presence of mesothelioma further reduced MHC-II in all elderly splenic DCs (except pDCs) (Figure 4.19), BM pDCs (Figure 4.20) as well as in elderly tumour associated $CD8^+$ cDCs (Figure 4.21). This is consistent with the $CD11c^+$ gating

strategy, apart from BM pDCs where the data showed increased expression of MHC-II.

4.3.3 MHC-I decreases with healthy ageing and further reduces with mesothelioma in specific splenic pDCs

An age-related decrease in MHC-I was observed in splenic pDCs (Figure 4.22). No changes in MHC-I were seen in LN DCs (supplementary figure 4.18).

The presence of mesothelioma reduced MHC-I in elderly splenic pDCs (Figure 4.22) as well as in tumour associated elderly $CD11c^{+}MHC\text{-}II^{+}$ cells and pDCs (Figure 4.23). This data was consistent with the $CD11c^{+}$ gating strategy which showed a similar decrease in $CD11c^{+}$ splenic cells along with decreased MHC-I in splenic pDCs and splenic $CD8^{-}CD4^{+}$ cDCs.

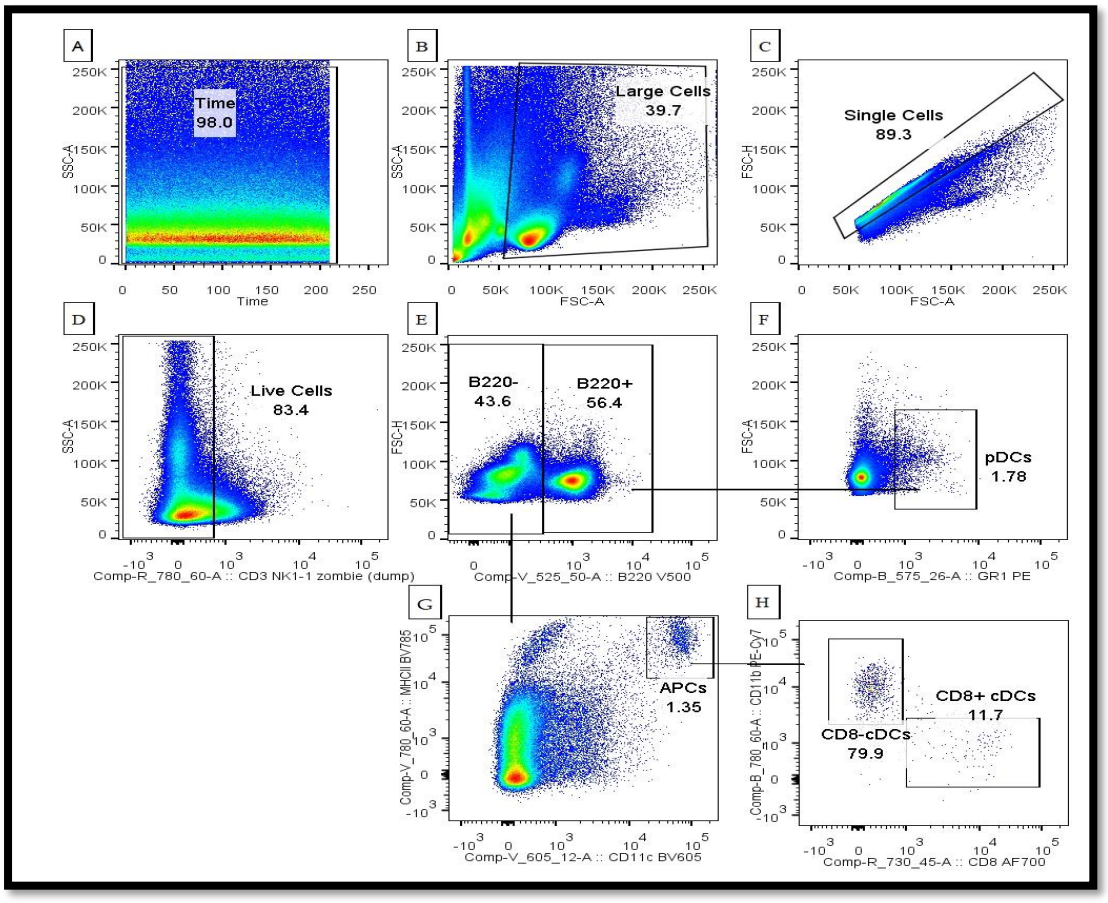

Figure 4.15: Flow cytometry gating strategy to identify $CD11c^{high}MHC\text{-}II^{high}$ putative DCs and their subsets

Lymphoid organs were stained for DC subset markers (CD11c, B220, GR-1, CD11b, CD8α) and analysed by flow cytometry [531, 535]. A **Time gate (A) was used to select areas with a stable flow stream**, followed by gating on large cells **(B)** and singlets **(C).** A dump channel was used to exclude dead cells, NK, and T cells **(D).** GR-1^{+} cells were selected from the $B220^{+}$ population to identify pDCs **(F).** $CD11c^{+}$MHC-II bright cells were selected from the $B220^{-}$ population to exclude B cells **(G).** These $B220^{-}CD11c^{+}MHCII^{+}$ were subdivided into $CD8^{+}CD11b^{-}$ cDC and $CD11b^{+}CD8^{-}$ cDC **(H).**

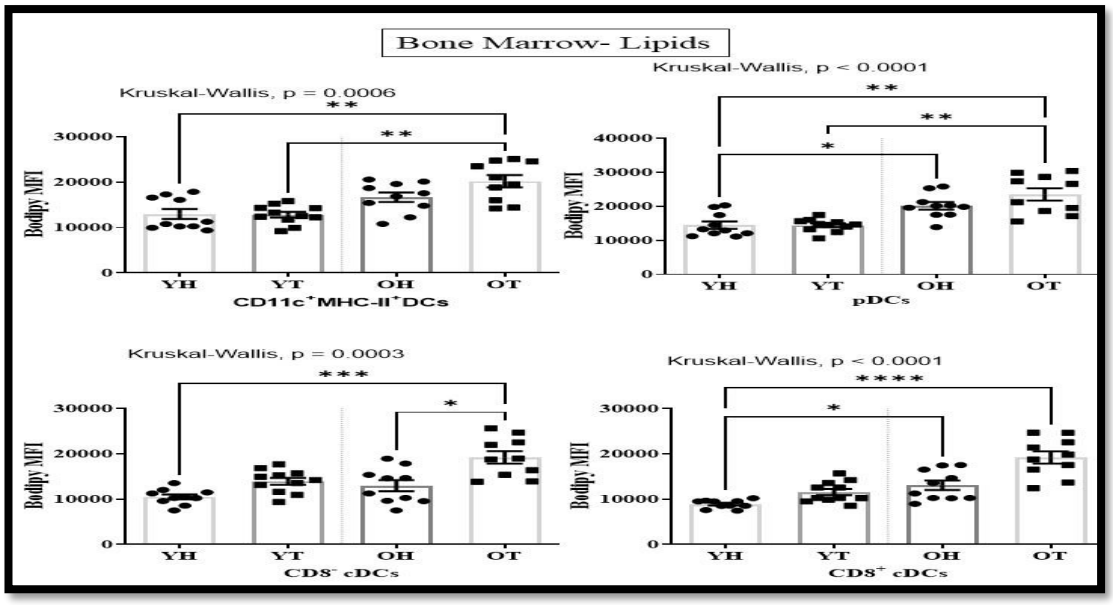

Figure 4.16: Lipid levels increase in specific BM DC subsets with healthy ageing and mesothelioma

BM DCs from YH, YT, OH and OT were stained for neutral lipid content using the Bodipy dye and analysed by flow cytometry. Expression levels of Bodipy (measured as MFI) in $CD11c^+$ $MHC\text{-}II^+$ cells **(A)**, pDCs **(B)**, $CD11b^+CD8^-$cDCs **(C)**, $CD11b^-CD8^+$cDCs **(D)** were measured. Statistical significance between all groups was assessed by a Kruskal-Wallis test, followed by a post-hoc Dunn's test to measure differences between two groups. Data shown as mean ± SEM, n = 10-11 mice/group. * = $p<0.05$, ** = $p<0.005$, *** = $p<0.0005$.

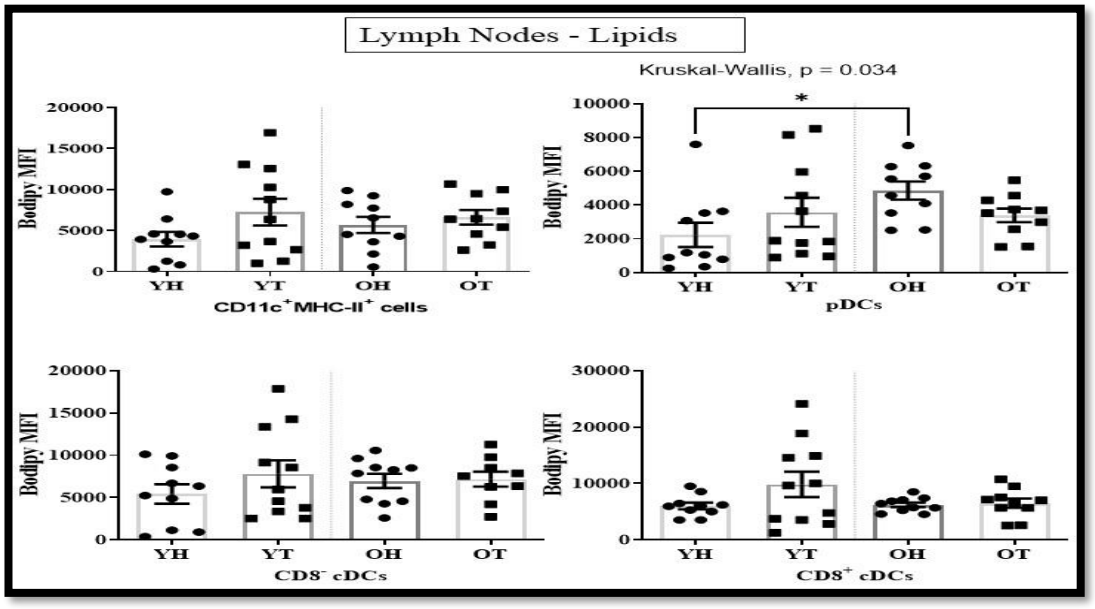

Figure 4.17: Lipid levels increase in LN pDCs with healthy ageing

LN DCs from YH, YT, OH and OT were stained for DC subset markers as shown in Fig 4.15. Neutral lipid content measured using the Bodipy dye and analysed by flow cytometry. Expression levels of Bodipy (measured as MFI) in $CD11c^+$ $MHC\text{-}II^+$ cells **(A)**, pDCs **(B)**, $CD11b^+CD8^-$cDCs **(C)**, $CD11b^-CD8^+$cDCs **(D)** were measured. Statistical significance between all groups was assessed by a Kruskal-Wallis test, followed by a post-hoc Dunn's test to measure differences between two groups. Data shown as mean ± SEM, n = 10-11 mice/group. * = $p<0.05$.

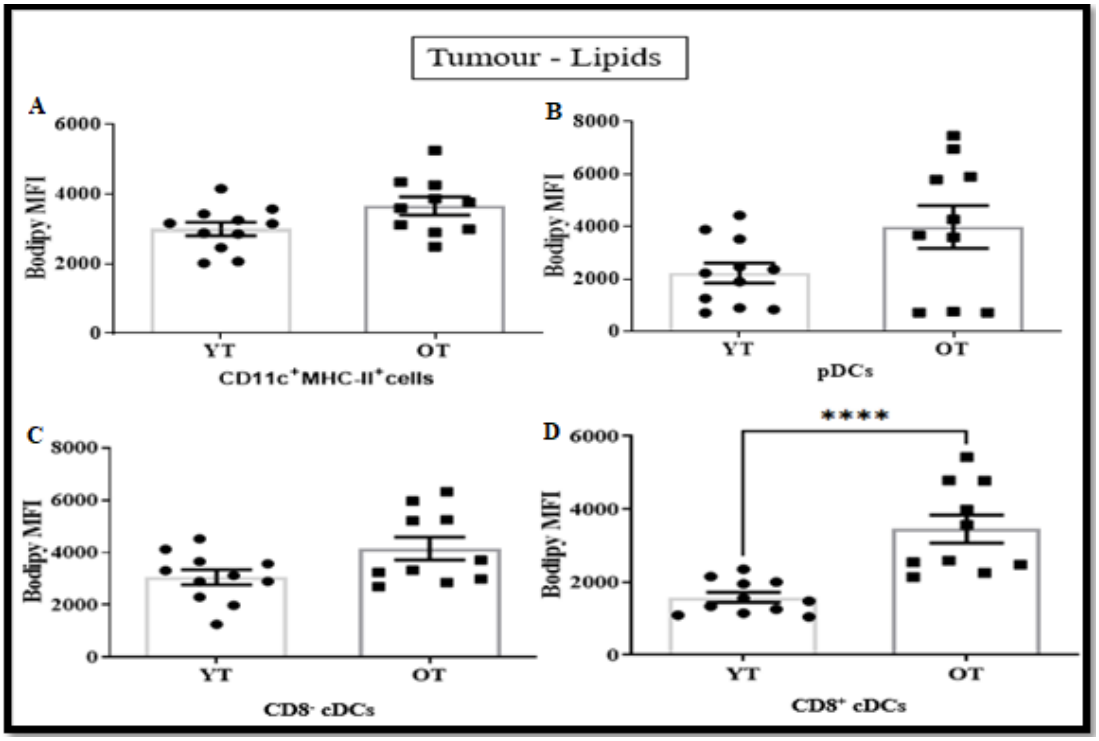

Figure 4.18: Lipid levels increase in tumour-associated CD8$^+$ cDCs with ageing

Tumour DCs from YT and OT were stained as shown in Fig 4.15. Neutral lipid content was measured using the Bodipy dye and analysed by flow cytometry. Expression levels of Bodipy (MFI) in CD11c$^+$ MHC-II$^+$ cells **(A)**, pDCs **(B)**, CD11b$^+$CD8$^-$cDCs **(C)**, CD11b$^-$CD8$^+$cDCs **(D)** were measured. Statistical significance assessed by Mann Whitney U Test. Data shown as mean ± SEM, n = 10-11 mice/group. **** = p<0.0001.

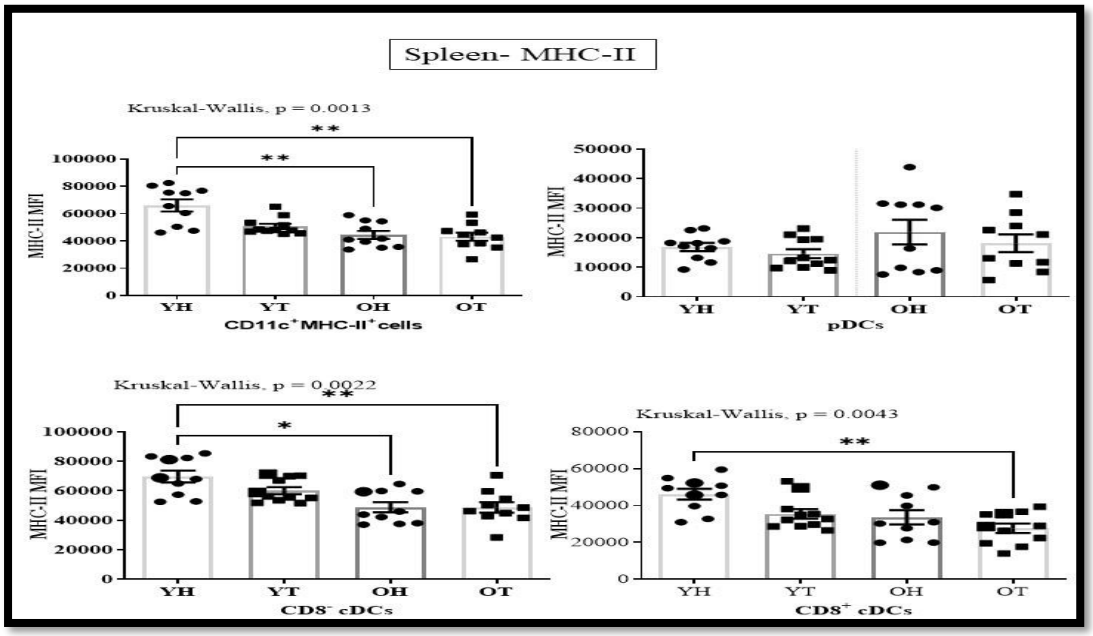

Figure 4.19: MHC-II decreases in splenic DCs with ageing

Splenic DCs were stained as shown in Fig 4.15. Expression levels of MHC-II (MFI) in CD11c$^+$ MHC-II$^+$ cells **(A)**, pDCs **(B)**, CD11b$^+$CD8$^-$cDCs **(C)**, CD11b$^-$CD8$^+$cDCs **(D)** were measured. Statistical significance between all groups assessed by a Kruskal-Wallis test, followed by a post-hoc Dunn's test to measure differences between two groups. Data shown as mean ± SEM, n = 10-11 mice/group. * = p<0.05, ** = p<0.005.

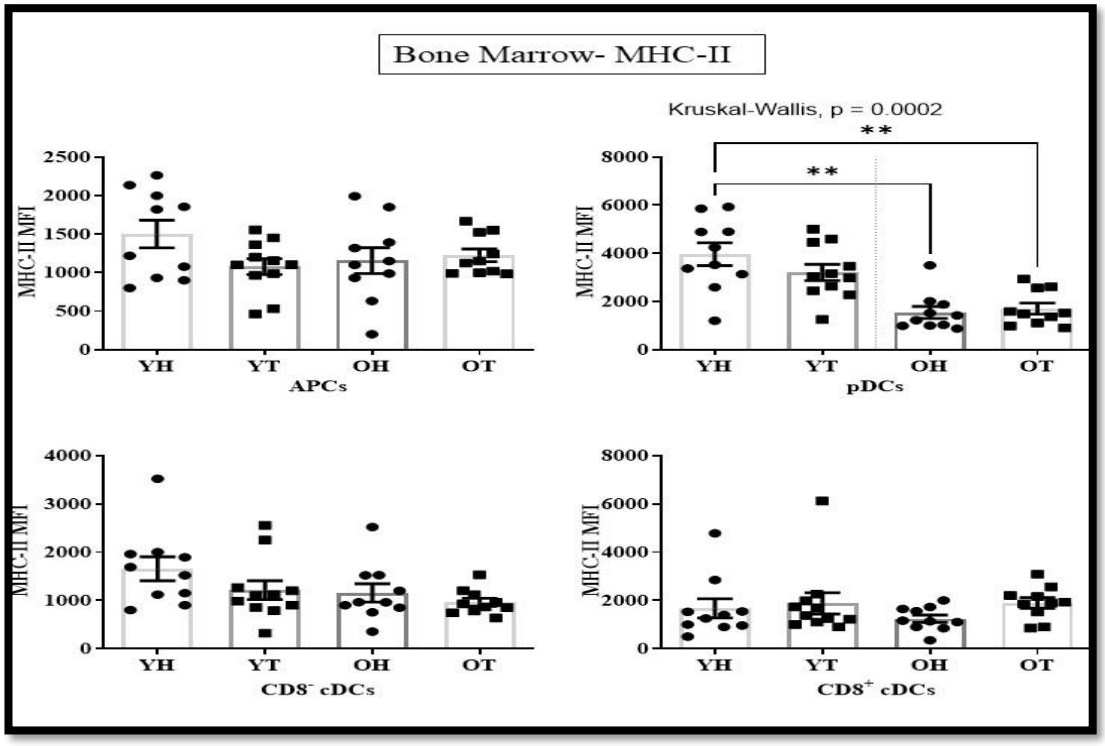

Figure 4.20: MHC-II decreases in BM pDCs with ageing

BM DCs from YH, YT, OH and OT were stained for DC subset markers as shown in Fig 4.15. Expression levels of MHC-II (measured as MFI) in $CD11c^+$ $MHC\text{-}II^+$ cells **(A)**, pDCs **(B)**, $CD11b^+CD8^-$ cDCs **(C)**, $CD11b^-CD8^+$cDCs **(D)** were measured. Statistical significance between all groups was assessed by a Kruskal-Wallis test, followed by a post-hoc Dunn's test to measure differences between two groups. Data shown as mean ± SEM, n = 10-11 mice/group. ** = $p<0.005$.

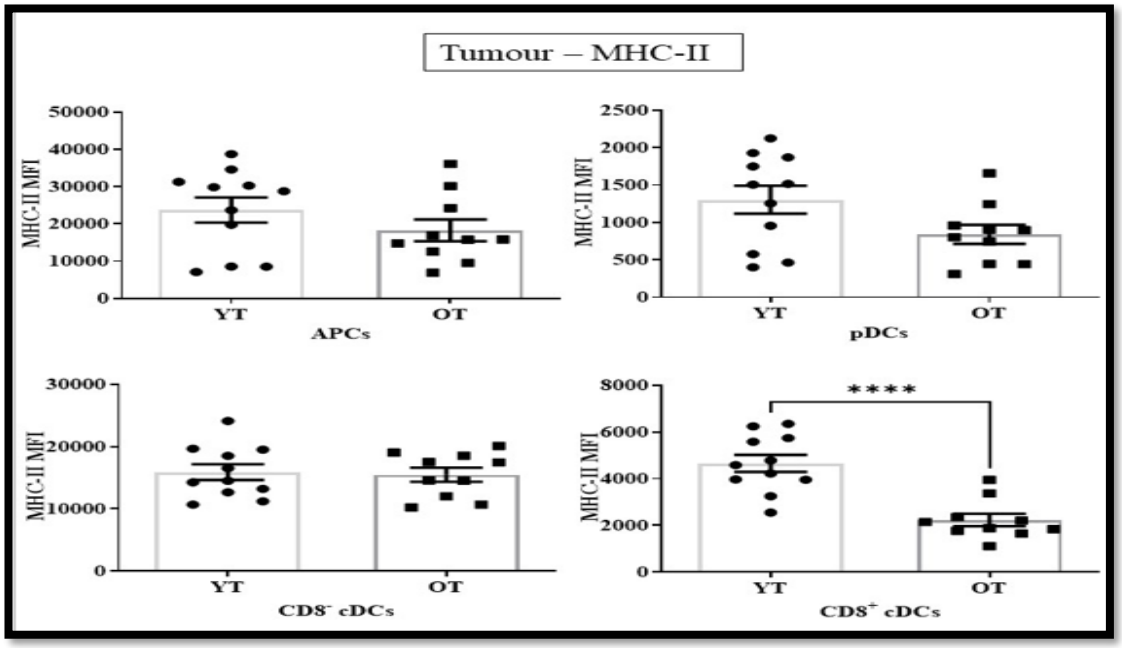

Figure 4.21: MHC-II decreases in tumour-associated $CD8^+$ cDCs with ageing

Tumour associated DCs from YT and OT were stained for DC subset markers as shown in Fig 4.15. Expression levels of MHC-II (measured as MFI) in APCs ($CD11c^+$ $MHC\text{-}II^+$ cells) **(A)**, pDCs **(B)**, $CD11b^-CD8^-$cDCs **(C)**, $CD11b^+CD8^+$cDCs **(D)** were measured. Statistical significance assessed by Mann Whitney U Test. Data shown as mean ± SEM, n = 10-11 mice/group. **** = $p<0.0001$.

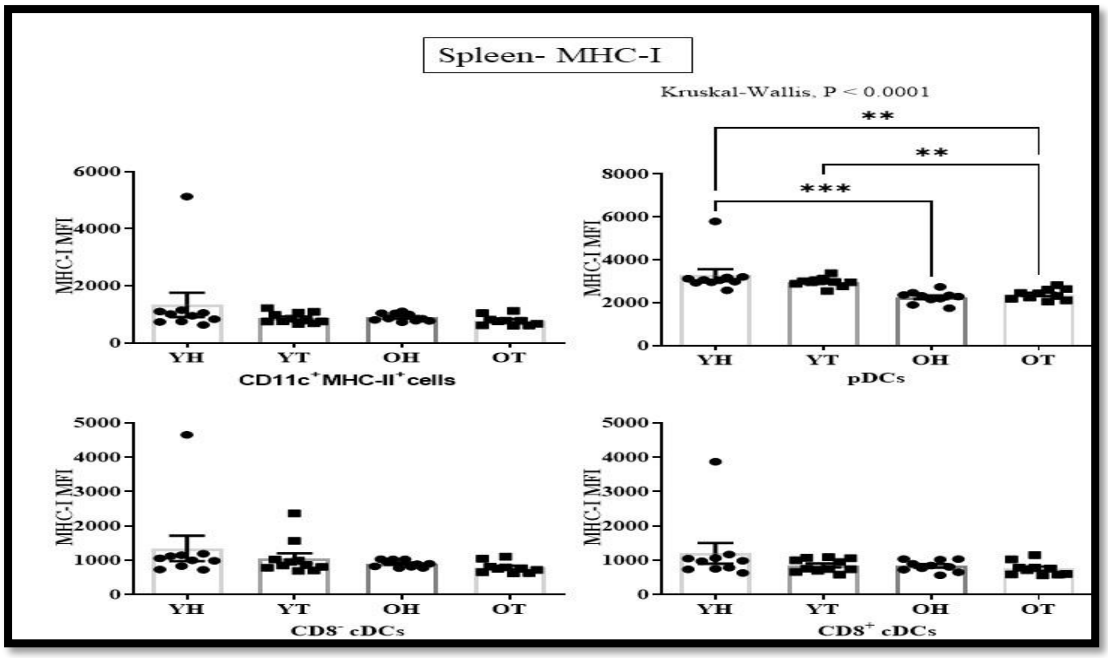

Figure 4.22: MHC-I decreases with ageing in splenic pDCs

Splenic DCs from YH, YT, OH and OT were stained for DC subset markers as shown in Fig 4.15. Expression levels of MHC-I (measured as MFI) in APCs ($CD11c^+$ $MHC\text{-}II^+$) **(A)**, pDCs **(B)**, $CD11b^+CD8^-$cDCs **(C)**, $CD11b^-CD8^+$cDCs **(D)** were measured. Statistical significance between all groups was assessed by a Kruskal-Wallis test, followed by a post-hoc Dunn's test to measure differences between two groups. Data shown as mean ± SEM, n = 10-11 mice/group. * = $p<0.05$, ** = $p<0.005$, *** = $p<0.0005$.

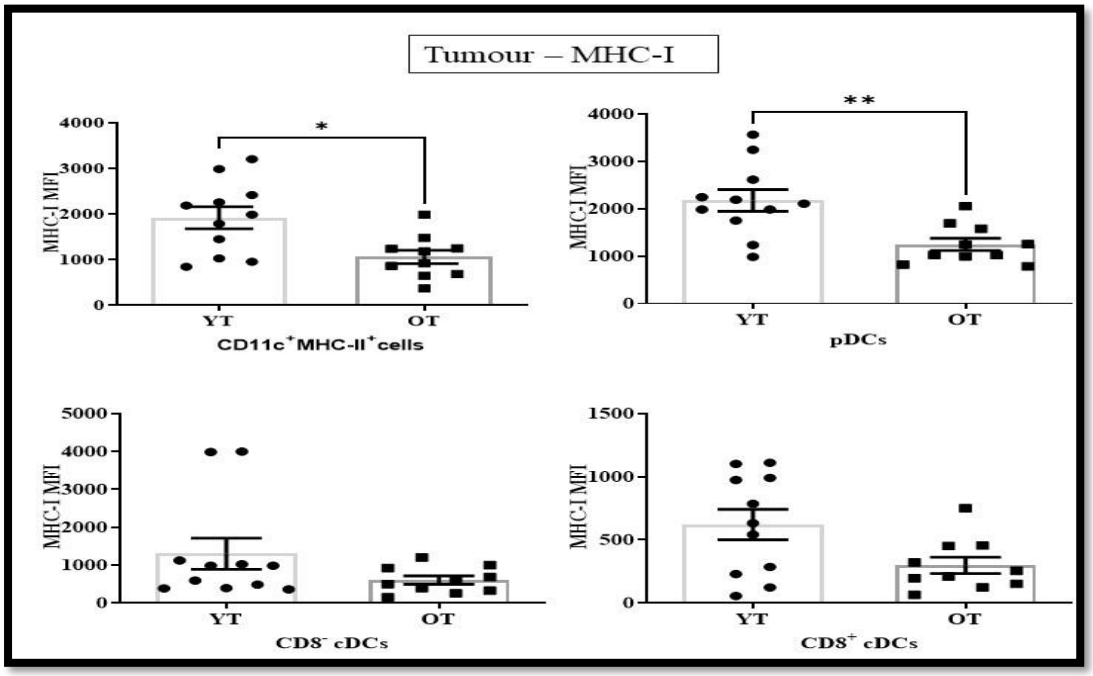

Figure 4.23: MHC-I decreases in tumour-associated $CD11c^+$ $MHC\text{-}II^+$ cells and pDCs with ageing

Tumour associated DCs from YT and OT were stained for DC subset markers as shown in Fig 4.15. Expression levels of MHC-I (measured as MFI) in APCs ($CD11c^+$ $MHC\text{-}II^+$) **(A)**, pDCs **(B)**, $CD11b^+CD8^-$cDCs **(C)**, $CD11b^-CD8^+$cDCs **(D)** were measured. Statistical significance assessed by Mann Whitney U test. Data shown as mean ± SEM, n = 10-11 mice/group. * = $p<0.05$, ** = $p<0.005$.

4.3.5 CD80 expressesion increases with healthy ageing in BM APCs

CD80 expression increased in BM $CD11c^{+}MHC\text{-}II^{+}$ cells with healthy ageing (Figure 4.24); no changes were observed in splenic populations (supplementary figure 4.19). In contrast, tumour-associated $CD8^{-}$ cDCs showed an age-related decrease in CD80 expression (Figure 4.25). This is contrasts with the $CD11c^{+}$ DC subsets in LN where the data showed increased expression of CD80 (Figure 4.10).

4.3.6 The lipid uptake molecules, CD147 and CD36, increase with ageing and mesothelioma in distinct DC populations

CD147 expression increased with healthy ageing in BM $CD11c^{+}MHC\text{-}II^{+}$ cells and was further increased in the presence of mesothelioma (Figure 4.26). Mesothelioma was also associated with increased CD147 in BM $CD8^{-}$ cDCs regardless of age (Figure 4.26). CD36 expression increased with ageing and mesothelioma in BM $CD11c^{+}MHC\text{-}II^{+}$ cells and $CD8^{-}$cDCs (Figure 4.27) but remained unchanged in splenic, LN and tumour-associated DCs (supplementary figure 4.20, 4.21). This is in contrast to the data obtained by gating $CD11c^{+}$ cells, as none of the $CD11c^{+}$ cells showed significant changes in CD36 or CD147.

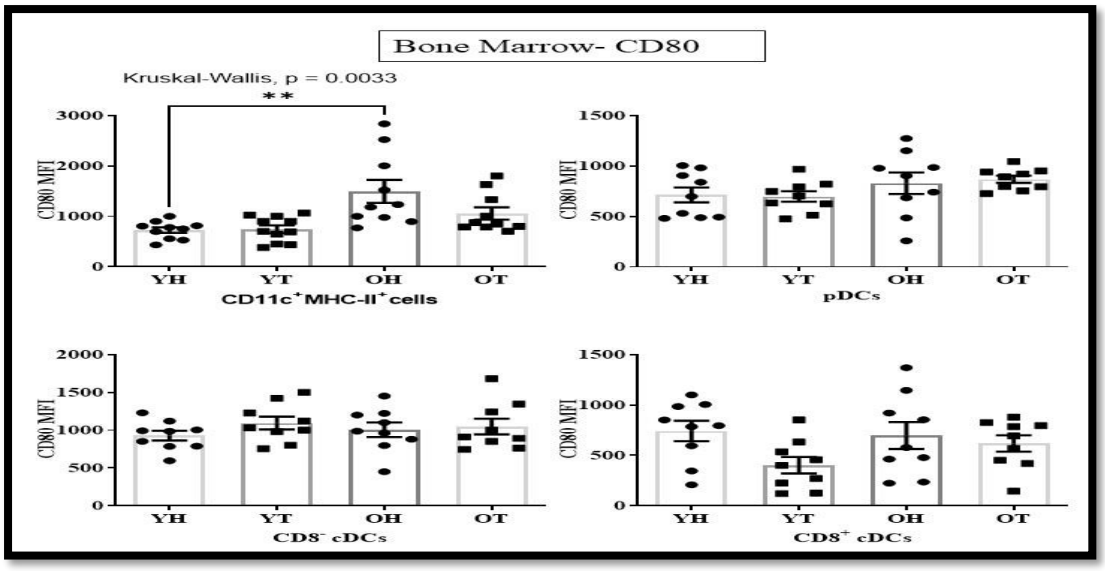

Figure 4.24: CD80 increases with healthy ageing in BM APCs

BM DCs from YH, YT, OH and OT were stained for DC subset markers as shown in Fig 4.15. Expression levels of CD80 (measured as MFI) in APCs ($CD11c^+$ $MHC\text{-}II^+$) **(A)**, pDCs **(B)**, $CD11b^+CD8^-$cDCs **(C)**, $CD11b^-CD8^+$cDCs **(D)** were measured. Statistical significance between all groups was assessed by a Kruskal-Wallis test, followed by a post-hoc Dunn's test to measure differences between two groups. Data shown as mean ± SEM, n = 10-11 mice/group. ** = $p<0.005$.

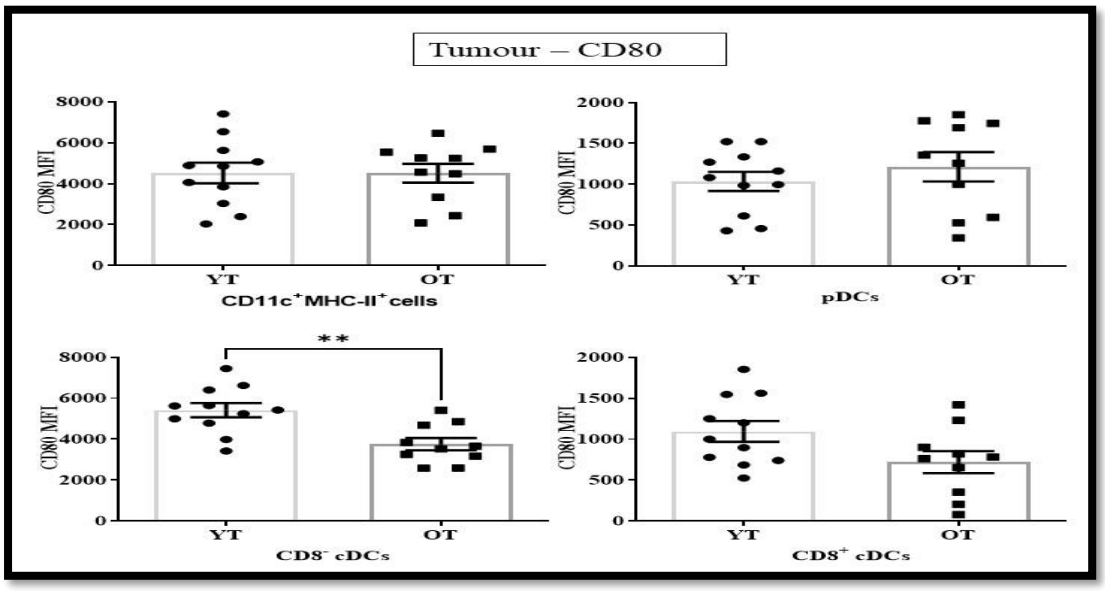

Figure 4.25: CD80 expression decreases in tumour-associated $CD8^-$ cDCs with ageing

Tumour associated DCs from YT and OT were stained for DC subset markers as shown in Fig 4.15. Expression levels of CD80 (measured as MFI) in APCs ($CD11c^+$ $MHC\text{-}II^+$) **(A)**, pDCs **(B)**, $CD11b^+CD8^-$cDCs **(C)**, $CD11b^-CD8^+$cDCs **(D)** were measured. Statistical significance assessed by Mann Whitney U Test. Data shown as mean ± SEM, n = 10-11 mice/group. ** = $p<0.005$.

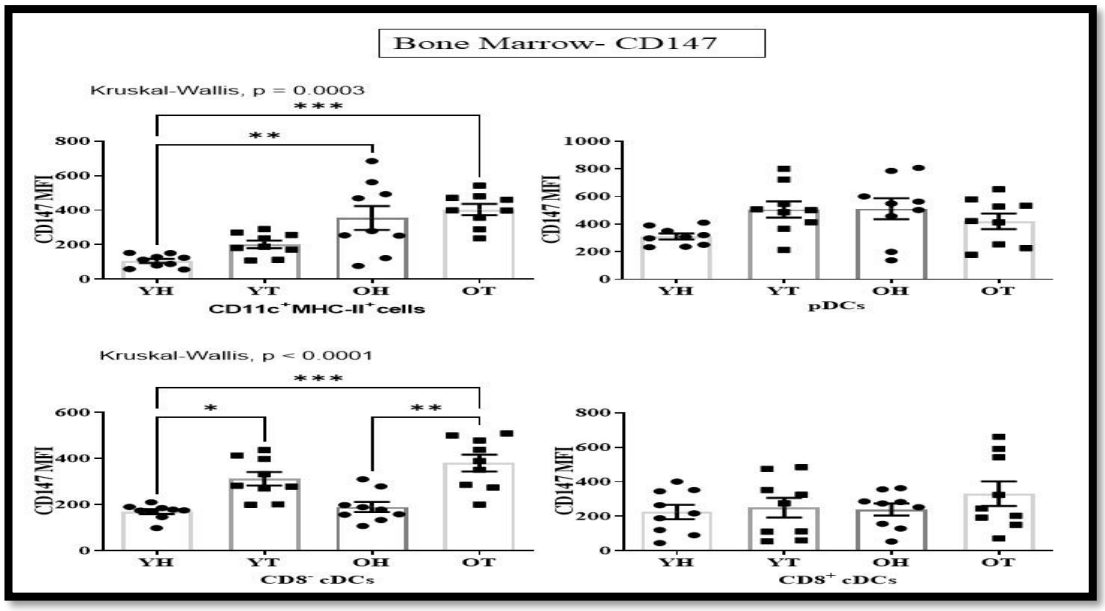

Figure 4.26: CD147 expression increases with mesothelioma in BM CD8$^-$ DCs

BM DCs from YH, YT, OH and OT were stained for DC subset markers as shown in Fig 4.15. Expression levels of CD147 (measured as MFI) in APCs (CD11c$^+$ MHC-II$^+$) **(A)**, pDCs **(B)**, CD11b$^+$CD8$^-$cDCs **(C)**, CD11b$^-$CD8$^+$cDCs **(D)** were measured. Statistical significance between all groups was assessed by a Kruskal-Wallis test, followed by a post-hoc Dunn's test to measure differences between two groups. Data shown as mean ± SEM, n = 10-11 mice/group. * = p<0.05, ** = p<0.005, *** = p<0.0005.

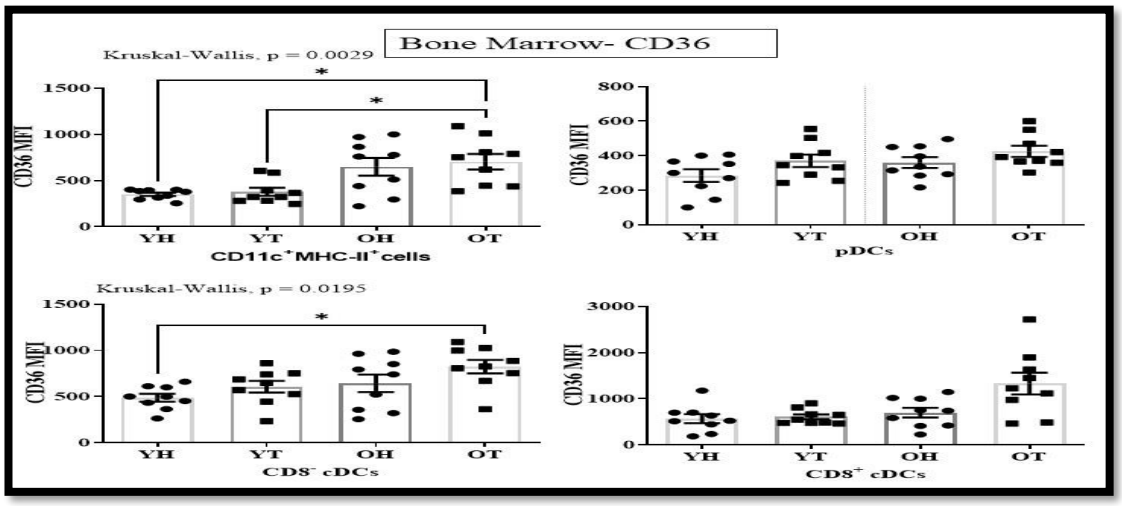

Figure 4.27: CD36 expression increases with mesothelioma and ageing in BM APCs

BM DCs from YH, YT, OH and OT were stained for DC subset markers as shown in Fig 4.15. Expression levels of CD36 (measured as MFI) in APCs (CD11c$^+$ MHC-II$^+$) **(A)**, pDCs **(B)**, CD11b$^+$CD8$^-$cDCs **(C)**, CD11b$^-$CD8$^+$cDCs **(D)** were measured. Statistical significance between all groups was assessed by a Kruskal-Wallis test, followed by a post-hoc Dunn's test to measure differences between two groups. Data shown as mean ± SEM, n = 10-11 mice/group. * = p<0.05.

Summarising the changes in CD11c^{high}MHC-II^{high} (APC) cell populations

4.4 Changes associated with healthy ageing in BM, Spleens and dLNs

To summarise, two different gating strategies were used. One collected all $CD11c^{+}$ cells based on the premise they are likely to be APC with DC-like features, although this approach also included other APCs, in particular B cells and macrophages. The other gating strategy focussed upon $CD11c^{high}MHC\text{-}II^{high}$ cells and exlcuded B cells and low $CD11c^{+}MHC\text{-}II^{+}$ marophages, meaning a more concentrated population of potent APCs and DCs.

This study found increased lipid content in BM $CD11c^{high}MHC\text{-}II^{high}$ pDCs, BM $CD8^{+}$ cDCs and LN pDCs with healthy ageing. In contrast, no age-related changes to lipid content were seen in these DC subsets with the original gating strategy consisting of $CD11c^{+}$ cells (Figure 4.28). Increased CD147 was observed only in BM $CD11c^{high}MHC\text{-}II^{high}$ cells suggesting that CD147 could be responsible for increased lipid uptake (Figure 4.28). A decrease in MHC-I and MHC-II was observed in variable splenic/BM subsets using the $CD11c^{high}MHC\text{-}II^{high}$ gating strategy, while gating using CD11c showed increased MHC-II in different splenic and BM DC subsets, consistent with the group's previous work [240] (Figure 4.38 and 4.29). No changes in CD40 and CD80 expression were observed in $CD11c^{high}MHC\text{-}II^{high}$ subsets while gating on CD11c showed increased expression of both CD80 and CD40 in LN DC subsets (Figure 4.29).

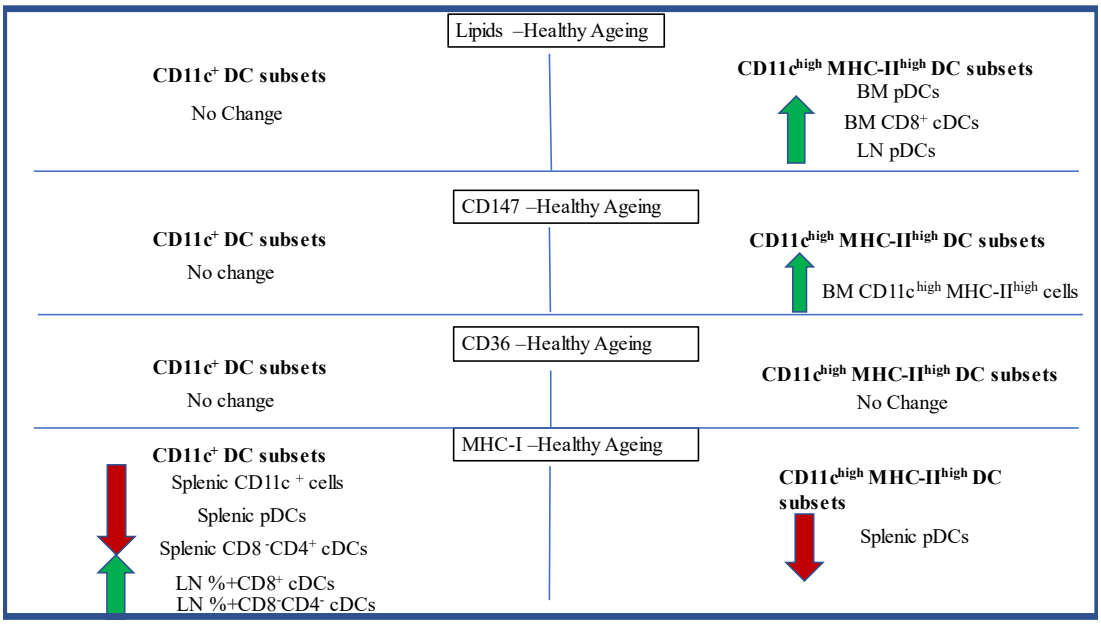

Figure 4.28: Changes to different markers in healthy elderly mice relative to healthy young mice comparing gating on $CD11c^{+}$ cells versus gating on $CD11c^{high}MHC\text{-}II^{high}$

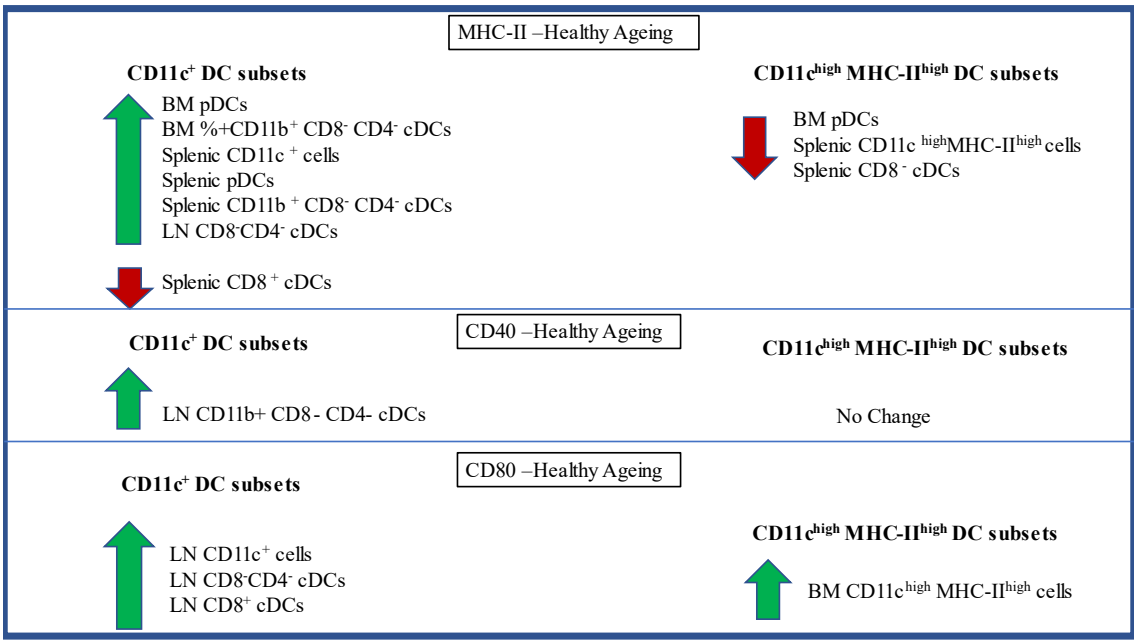

Figure 4.29: Changes to different markers in healthy elderly mice relative to healthy young mice comparing gating on CD11c^{+} cells versus gating on CD11c^{high}MHC-II^{high}

4.4 Changes associated with ageing and mesothelioma in BM, Spleens , dLNs and tumour

Upon gating CD11c^{high}MHC-II^{high} cells, the data showed that elderly mesothelioma-associated CD8^{+} cDCs and all BM DC subsets had increased lipid levels relative to their younger counterparts. This was associated with increased expression of the lipid uptake molecule, CD147. Gating on the broader CD11c^{+} population showed no change in lipid uptake or lipid uptake markers with cancer and ageing (Figure 4.30).

Decreased levels of MHC-I and MHC-II was observed with ageing and mesothelioma in CD11c^{high}MHC-II^{high} cell populations in different lymphoid organs. This was similar to CD11c gated populations, apart from BM pDCs which showed increased expression of MHC-II (Figure 4.30, 31). Finally, tumour associated CD8^{-} cDCs showed decreased CD80 when gating on CD11c^{high}MHC-II^{high} ; this contrasts to increased CD80 and CD40 expression LN DCs in CD11c gated populations. (Figure 4.31)

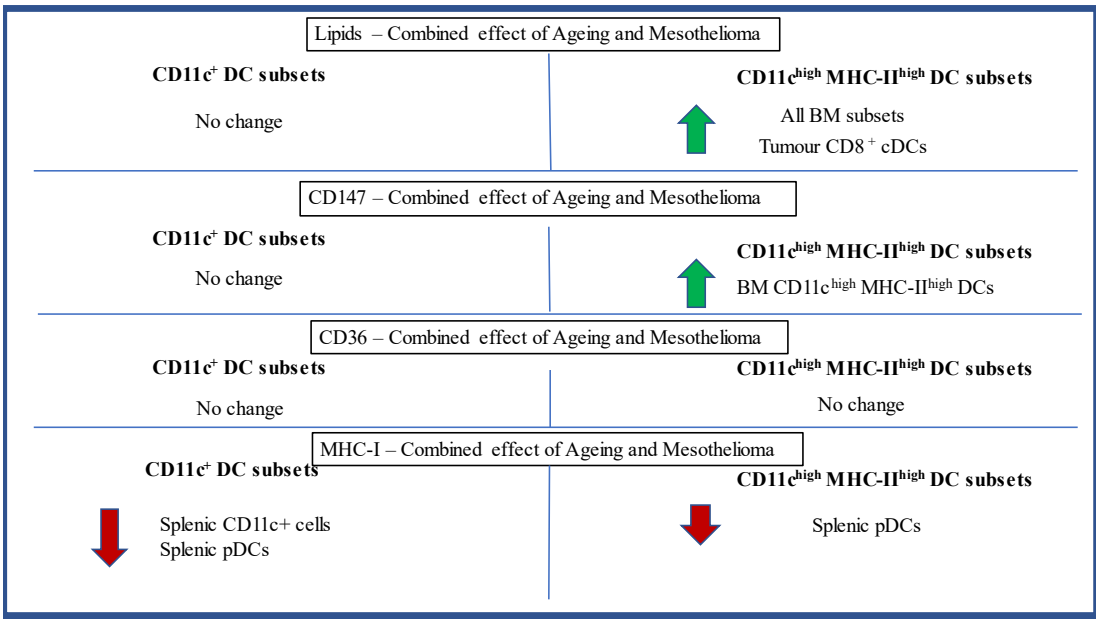

Figure 4.30: Comparison of lipid accumulation based upon CD11c and CD11c^{high}MHC-II^{high} gating strategies in tumour-bearing elderly versus young tumour-bearing mice

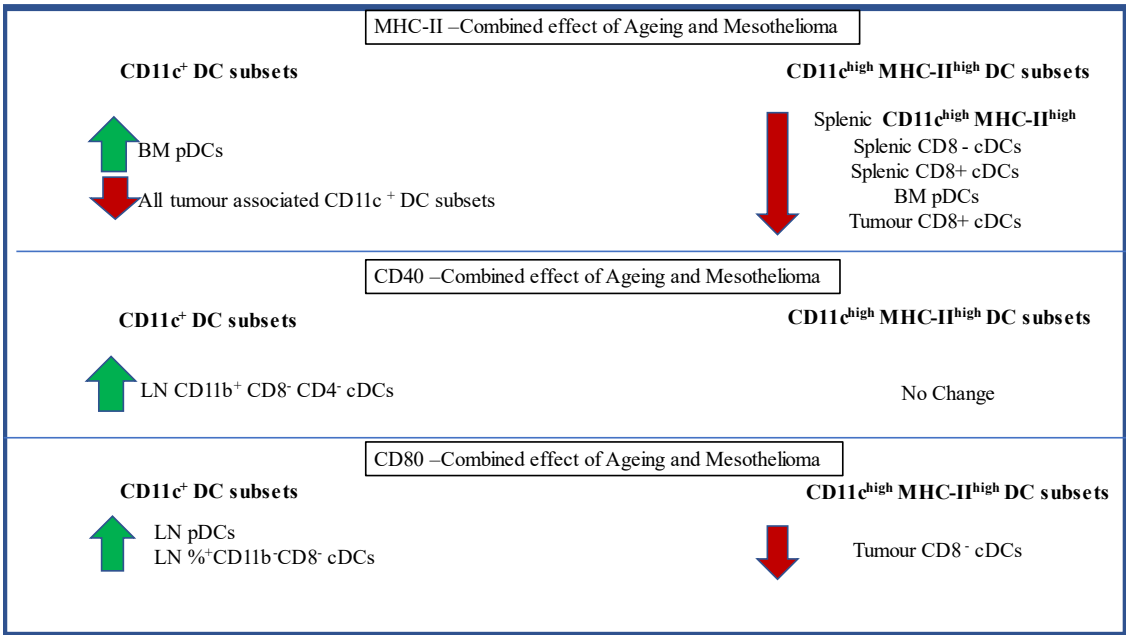

Figure 4.31: Comparison of different markers based upon CD11c and CD11c^{high}MHC-II^{high} gating strategies in elderly relative to young tumour-bearing mice

4.5 Discussion

This chapter examined changes in murine DCs during healthy ageing and asked whether mesothelioma further modulated DCs in elderly hosts.

The effect of healthy ageing on bone marrow dendritic cells

This study looked at BM derived DCs (Figure 4.32). BM is considered as the source of DC precursors [536] however, this study found that mature DC subsets also resided in the BM. Whilst, the role of these BM DCs is uncertain, the data here shows that with healthy ageing there is an increase in lipid accumulation in BM CD11c^{high}MHC-II^{high} pDCs and CD8^{+} cDCs (Figure 4.16) along with increased expression of the lipid uptake markers such as CD147 in CD11c^{high}MHC-II^{high} cells in elderly mice compared to young healthy mice (Figure 4.26). DC precursors usually migrate from BM through the blood stream to other organs [536]. It is unclear whether lipid accumulation in BM DCs has an effect on their migration capacity. Future studies could look at chemokines such as CCR7 that regulate DC migration from peripheral tissues to draining LNs or spleens [537, 538]. It is possible that these lipid laden DCs migrate from BM to spleens where they downregulate MHC-I and MHC-II (Figure 4.32). It would be interesting to track the migration of DCs in future studies which could be performed by using *in-vivo* optical imaging [539].

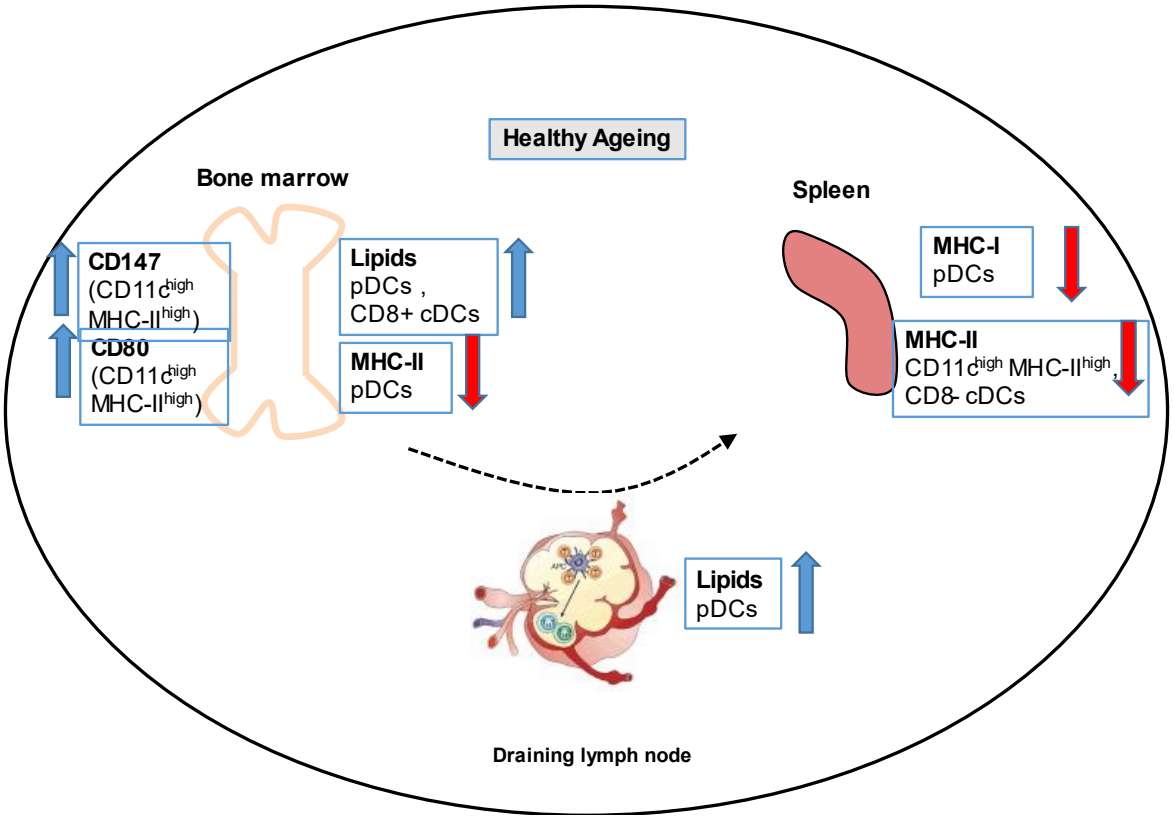

Figure 4.32: Summarising the effects of healthy ageing on CD11c^{high}MHC-II^{high} putative dendritic cells

The effect of healthy ageing on splenic dendritic cells

In regards to healthy ageing and DC dysfunction, Komatsubara et al. found that aged splenic DCs (from healthy mice aged 2 months, 10 months and 23 months) retained their ability to prime T cells *in vitro* [540]. This was consistent with another study showing that the ability of cDCs in mice to prime antigen-specific T cells was retained with age [541]. Moreover, aged BM-derived cDCs and splenic cDCs demonstrated similar priming of allogeneic T cells to their young cDCs counterparts *in vitro* and *in vivo* [542]. This agrees with another study that showed aged splenic cDCs prime T cell receptor transgenic CD4$^+$ T cells to a similar degree to that of young mice *in vitro* [515]. The studies in this chapter showed increased MHC-II in splenic CD11c$^+$ cells, CD11c$^+$pDCs and CD11c$^+$CD8$^-$CD4$^-$cDCs compared to young healthy mice (Figure 4.9), suggesting maintenance or even improved ability of CD11c$^+$ cells to prime T cells with ageing. However, gating on MHC-II^{high}CD11c^{high} cells, showed reduced

MHC-II in splenic $CD11c^+MHC\text{-}II^+$cells, splenic $CD8^-$ cDCs and BM pDCs (Figure 4.19), along with decreased MHC-I in splenic pDCs (Figure 4.22). The broad CD11c gate showed enhanced MHC levels in the absence of lipid accumulation, while the much more focused $CD11c^+MHC\text{-}II^+$ gating revealed DC subsets with reduced MHC levels and high lipid accumulation. The latter suggests that lipids play a role in reducing surface MHC molecules. These contrasting results could be because of the diluting influence of a large number of cells expressing CD11c, such as macrophages and B cells when gated using CD11c staining.

The effect of healthy ageing on lymph node dendritic cells

A key site for T cell priming is the LN however, no changes in $CD11c^+MHC\text{-}II^+$ dLN DCs were observed with healthy ageing, apart from increased lipids in pDCs (Figure 4.17) which could be lipid laden pDCs that migrated from BM to dLNs. However, gating on $CD11c^+$ LN cells showed an increase in the proportion of $MHC\text{-}I^+CD8^-CD4^-$ cDCs and $CD8^+$ cDCs (Figure 4.7) along with increased expression of MHC-II in elderly $CD8^-CD4^-$ cDCs compared to those from young healthy mice (Figure 4.9). These data suggest better capacity of LN DCs to present tumour antigens to T cells. Contamination by $CD11c^+$ macrophages or B cells could account for the contradictory results. The study further looked at CD40 and CD80 as increased expression of MHC along with increased expression of CD80 can lead to better immune responses. On the other hand, increased MHC coupled with reduced CD80 can lead to tumour evasion [543]. Generation of CTL responses requires priming of naïve $CD8^+$ T cells by mature, activated DCs that express high levels of MHC and the co-stimulatory molecules. This process mostly occurs in LNs. Mature DCs deliver three signals that determine the fate of naïve T cells. The first signal is TCR-peptide-MHC-interactions. This is followed by T cell stimulation through co-stimulatory molecules. Signal 3 is provided by polarizing cytokines secreted by DCs [544]. The sum of positive and negative signals determines the outcome of T cell responses [545]. This study found increased CD80 expression with healthy ageing in LN $CD11c^+$ cells and pDCs, plus an increased proportion of $CD80^+$ LN $CD8^-CD4^-$ cDCs (Figure 4.10) as well as increased expression of MHC-II in LN $CD8^-CD4^-$ cDCs (Figure 4.9) suggesting antigen presentation to T cells may be maintained or even improved with age in the LN. This is interesting, as other studies have demonstrated that expression of the CD80 ligand, CD28, is reduced with age on T cells [546-549] suggesting reduced T cell activation

potential in the elderly. CD80 is considered as a co-stimulatory molecule, but if it binds to CTLA-4, it can lead to reduced T cell activation in the elderly [491-493]. CTLA-4 outcompetes CD28 in binding CD80. CD28 can be highly expressed on T cells but has low affinity for CD80 while CTLA-4 has higher affinity for CD80 but is in low abundance in resting cells [550]. However, healthy elderly $CD4^+$ T cells have been shown to express higher levels of CTLA-4 than their younger councterparts [527]. These data suggest that with ageing CTLA-4 can dampen the immune response either through increased expression on elderly T cells or by outcompeting CD28 in binding CD80.

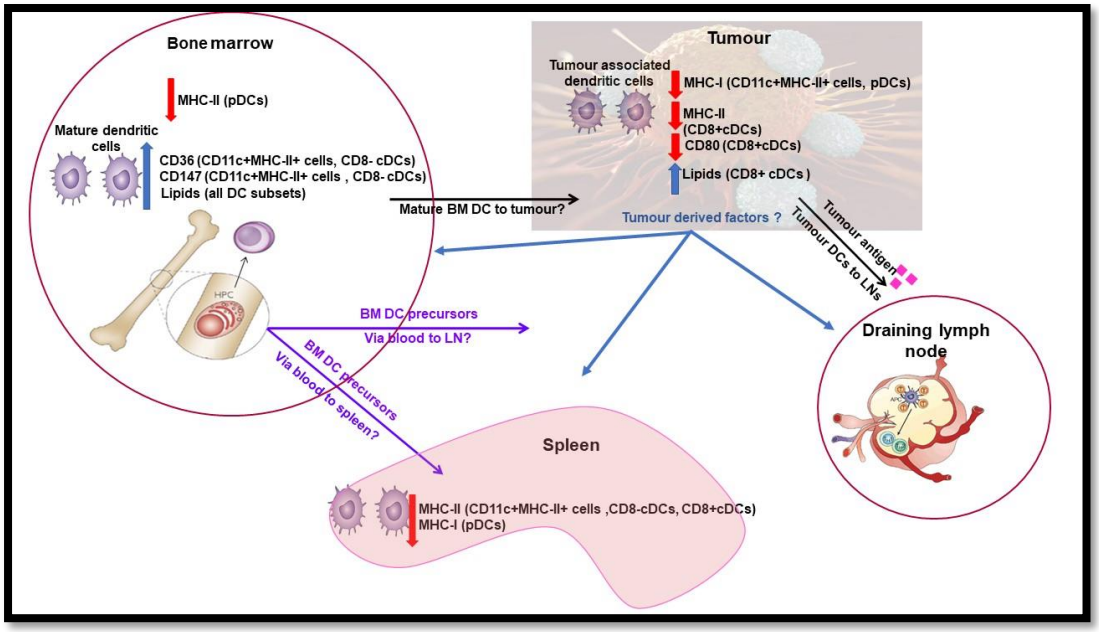

Figure 4.33 Summarising the effect of ageing and cancer on $CD11c^{high}MHC\text{-}II^{high}$ putative DCs

Tumour derived antigens/factors may reach the BM leading to increased lipid levels in all aged relative to young BM DC subsets and lipid uptake molecules in specific DC subsets. Tumour derived soluble factors may also drain into the spleen and affect resident aged splenic APC by reducing MHC-I/II. Lipid laden BM DCs may migrate to spleen and LNs. Aged tumour associated DCs acquire lipids and downregulate MHC and co-stimulatory molecules; these tolerogenic DCs may migrate to draining LNs

The effect of mesothelioma and ageing on bone marrow dendritic cells

This study looked at the effect of mesothelioma and ageing on DCs. Preliminary *in-vitro* studies showed a significant increase in lipids alongside a significant decrease in MHC-II in young murine BMDCs exposed to mesothelioma-derived factors. These data are similar to other studies showing that a range of solid tumours induce lipid accumulation in DCs leading to significant dysfunction [101, 198]. Lipid accumulation was not seen in the *in-vivo* studies involving young and elderly mice

with mesothelioma when using a broad gating strategy that included all $CD11c^+$ cells. However, when the gating strategy was changed to focus only on $CD11c^{high}MHC\text{-}II^{high}$ cells, increased lipid levels were seen in BM pDCs and BM $CD8^+$ cDCs with healthy ageing (Figure 4.32) along with increased expression of the lipid uptake marker, CD147. This apparent increase could be due to the fact that other APCs had been excluded, specifically $B220^+$ B cells and $CD11c^{negative}$ or $CD11c^{low}$ macrophages meaning that BM DCs are more likely to be affected. It is recognised that $CD11c^{high}$ macrophages could still be present [533]. This study also found decreased expression of MHC-II, thus suggesting reduced capacity of BM DCs to present tumour antigens to T cells.

The effect of mesothelioma and ageing on splenic dendritic cells

Until now, only one study had examined lipid accumulation in ageing DCs using different tissues [246]. That study did not see an age-related increase in lipid levels in most DC subsets in spleens and lungs, yet increased lipid levels were seen in elderly pDCs regardless of anatomical location [246]. Several studies have shown that lipid accumulation causes DC dysfunction [551, 552]. This study found no changes in lipid levels in elderly splenic DCs compared to young splenic DCs. However, different splenic $CD11c^+MHC\text{-}II^+$ DC subsets showed reduced MHC-I and MHC-II with mesothelioma and ageing (Figure 4.19, 4.22). No changes in co-stimulatory molecules were observed in splenic DCs with mesothelioma and ageing. Thus, the data suggest that tumour derived soluble factors may lead to a reduced capacity of aged splenic DCs to present tumour antigens to T cells. As mentioned earlier, these contradictory results could be because gating on $CD11^{high}MHC\text{-}II^{high}$ cells reduces the influence of larger number of $CD11c^+$ cells.

The effect of mesothelioma and ageing on LN dendritic cells

No change in lipid levels was observed in LN $CD11c^+$ DCs with tumour and ageing. Also, $CD11c^+$ LN DCs showed no change in MHC expression, however increased expression of co-stimulatory molecules such as CD40 and CD80 was seen in elderly compared to young mice in $CD11c^+CD8^-CD4^-$cDCs and pDCs respectively. Similarly, when gated based on $CD11c^{high}MHC\text{-}II^{high}$ no changes in lipids or MHC expression in LN DCs were seen in elderly mice compared to young mice. This could be because elderly lipid laden DCs with reduced surface MHC molecules failed to emigrate from the tumour site to draining lymph nodes, which has been demonstrated in other studies

[553, 554], thus compromising the anti-tumour immune response. Several tumours, including mesothelioma [555] produce transforming growth factor β (TGF-β) that prevents the migration of DCs from tumour to draining lymph nodes [556]. In contrast, Hirao et al. showed that co-culture with tumour cells induces CCR7 expression on DC leading to their migration from tumours to draining lymph nodes [557]. Also, it has been shown that tumours can lead to migration of non-activated DCs to LNs, thus driving a tolerogenic response to enable immune escape [558]. Ageing has been shown to impair DC migration in both *in-vitro* and *in-vivo* studies [559]. For example, Linton et al demonstrated impaired DC migration to dLNs in aged mice [560]. This was attributable to age related changes such as increased expression of phosphatase and tensin homolog (PTEN) with ageing. The increased expression of PTEN negatively regulated PI3 kinase activity and thus contributing to impaired DC migration [561]. Future studies could look at tracking DC migration which can be performed by a variety of techniques such as optical imaging methods (fluorescence (FLI) or bioluminescence imaging (BLI) [562]. This will also allow us to track the migration of DCs from BM to LN or tumour sites and to understand whether tumour or ageing changes their physiology or function.

The effect of mesothelioma and ageing on tumour associated DCs

This study found increased lipid accumulation in all elderly $CD11c^+$ tumour associated cells and putative DC subsets compared to young mice with mesothelioma tumours (Figure 4.12), yet gating on $CD11c^+MHC\text{-}II^+$ cells showed increased lipid accumulation in only tumour associated $CD8^+$ DCs (Figure 4.18) in elderly mice with mesothelioma. Mesothelioma tumours have been shown to induce defects in human and murine DCs [197, 198]. As discussed in multiple review articles, tumour-infiltrating cDCs have been shown to present antigens to T cells while still in tumours suggesting DCs in the tumour microenvironment influence the function of local anti-tumour T cells [563-565]. Tumour-infiltrating $CD8^+$ cDCs may be able to capture and cross-present tumour antigens to $CD8^+$ T cells, expanding tumour specific CTLs in tumour [566, 567], [130, 191, 192, 567-569]. However, this study found decreased expression of MHC-II in tumour-associated $CD11c^{high}MHC\text{-}II^{high}$ $CD11b^-CD8^+$ cDCs (Figure 4.21) in elderly relative to young mesothelioma-bearing mice implying a reduced number of peptide/MHC complexes on elderly DCs which might impair the

ability of these DCs to present tumour antigen to $CD8^+$ and $CD4^+$ T cells in the tumour microenvironment. These data suggest cross-presentation could be compromised in elderly tumours. This is supported by studies showing that tumour-specific $CD8^+$ T cells in elderly mice can be primed by DCs yet lose their lytic function [199].

This can be measured in future studies by using antigen presentation assays such as an MLR (mixed lymphocyte reaction) or the "SIAT antigen presentation assay" developed by creative biolabs using mass spectrometry that measures antigen processing and presentation. MLR assays measure the ability of DCs to stimulate T cell proliferation [570]. Previous studies in our group performed MLR assays to measure the functional maturation of immature human MoDCs (iMoDCs) exposed to mesothelioma derived factors [570]. The study found decreased CD1a on $CD11c^+$ iMoDCs upon exposure to Ju77 mesothelioma cells. CD1a is associated with the presentation of lipid antigens to T cells thus suggesting decreased capacity of lipid laden DCs to present lipid antigens to T cells. [570].

Another way to look at antigen presentation is by splitting the process into multiple steps as discussed by Roper [571]. Antigen presentation can be split into various steps starting from acquisition of antigen, antigen processing leading to peptide loading onto MHC molecules, antigen transport, T cell binding to MHC molecules, co-stimulatory molecules involvement, cell signalling and proliferation of T cells. Rooper developed assays to measure immune response in multiple steps that are involved in antigen presentation. Using the supernatants, nitric oxide (NO) can be measured to assess the response of APC to the antigen presentation [571-573].

This study also showed an age-related increase in the proportion of $CD11c^+$ cells in tumours likely comprising of DCs, macrophages and B cells. An increase in these tumour-associated $CD11c^+$ cells could favour tumour progression as tumours have the capacity to alter their immunostimulatory role into an immunosuppressive one [574]. For example, Liu et al. demonstrated large quantities of PGE2 and TGF-B released by murine lung tumour cells leading to the conversion of immune activating DCs into immune-suppressive DC [574].

Other DC subsets, such as pDCs, are a small population of DCs expressing low amounts of CD11c with variable levels of CD8α and CD4 [575]. pDCs express MHC-II molecules and can mature in similar fashion to cDCs [575]. pDCs can internalise,

process and present antigens to $CD4^+$ T cells and cross-present antigens to $CD8^+$ T cells [576, 577] suggesting pDCs function as APCs. However, studies in this chapter showed reduced MHC-I and MHC-II in elderly tumour-associated pDCs compared to young tumour-associated pDCs suggesting reduced APC function by pDCs in mesothelioma tumours, the consequences of this remain to be clarified. This decreased expression of MHC molecules may lead to tumour escape from the immune response [578]. DCs have been shown to play a central role in tumour specific immunity [579]. This has been demonstrated in mice deficient for $CD8^+$ cDCs as $CD8^+$ cDCs deficient mice did not respond to immunotherapy with anti-PD1 and anti PDL1 [580, 581]. Tumours modulate tumour infiltrating DCs that can lead to their dysfunction. Lipid accumulation, as shown in this chapter, could be one of the factors involved in tumour associated DC dysfunction by downregulation of MHC molecules that leads to T cell tolerance rather immunity.

Future studies may look at DC-T cell interactions in mesothelioma. DCs prime $CD4^+$ and $CD8^+$ naïve T cells by physically interacting with T cells [582]. Optimal priming depends on the quality and the magnitude of these signals which depends upon the nature of antigen and anatomical site [582]. These DC-T cell interactions can be studied using intravital imaging techniques such as using intravital multiphoton laser scanning. This allows the cells to be scanned at real time inside intact LN of live mice [583-585] as LN play an important role in priming effective tumour T cell responses.

4.6 Summary

To summarise, data presented in this chapter showed that healthy ageing had no effect on lipid levels in the broad $CD11c^+$ cell population however, when focussing on $CD11c^{high}MHC^{high}$ cells the data showed increased lipid accumulation in different BM subsets and LN pDCs. Ageing was associated with elevated MHC-II expression in $CD11c^+$ cells in BM ($CD11c^+$ cells, pDCs and $CD11b^+CD8^-CD4^-$ cDCs), splenic ($CD11c^+$ cells, pDCs and $CD11b^+CD8^-CD4^-$ cDCs) and LN DCs ($CD11c^+$ cells and pDCs) suggesting that ageing does not impair their antigen presentation capacity. These DCs also demonstrated increased expression of co-stimulatory CD80 in LN

$CD11c^+$ cells, pDCs and $CD11b^+CD8^-CD4^-$ cDCs implying that effector T cells could be generated by elderly DCs. However, gating on $CD11c^{high}MHC\text{-}II^{high}$ cells revealed reduced MHC-I and MHC-II in splenic and BM DC subsets with no changes in CD40 expression, but increased CD80 in BM $CD11c^{high}MHC\text{-}II^{high}$ cells. The increase in co-stimulatory molecules such as CD80 could help compensate for the reduced number of peptide/MHC complexes on DCs.

Mesothelioma-derived factors clearly increased lipid accumulation in BMDCs from young mice, as shown in the *in-vitro* studies. Moreover, $CD11c^+$ cells and $CD11c^{high}MHC\text{-}II^{high}$ cells from elderly mice with mesothelioma were also associated with elevated lipid levels in all BM DC subsets, along with increased lipid levels in tumour associated DCs. This was associated with an increase in the lipid uptake molecule, CD147, in BM $CD11c^{high}MHC\text{-}II^{high}$ cells along with decreased CD80 expression in tumour associated $CD8^+$ cDCs. However, no changes were observed in CD40 expression. Different splenic and BM DC subsets showed reduced expression of MHC-I and MHC-II with ageing and cancer, suggesting a reduced capacity to activate tumour infiltrating $CD8^+$ and $CD4^+$ T cells thereby providing an advantage for mesothelioma tumours in elderly hosts. The decrease in MHC and co-stimulatory molecules has been attributed to tolerogenic induction in DCs and studies have shown that MHC expression is sensitive to modulation of metabolic pathways, such as glycolysis [586, 587]. This is investigated in the next chapter that assesses whether mesothelioma alters metabolic pathways that may contribute towards DC tolerogenecity.

Chapter 5: Investigating the effects of mesothelioma on human and murine DC metabolism

5.1 Introduction

DCs have a uniquely efficient ability to activate naïve T cells, a process that mostly occurs in LN [228]. DCs express CD11c (also known as integrin alpha X that promotes antigen uptake and binds complement iC3b to mediate phagocytosis [588] and MHC class I and II molecules (for antigen presentation to $CD8^+$ and $CD4^+$ T cells respectively). After DC activation expression levels of surface MHC I/II and other co-stimulatory molecules such as CD80 and CD40 increases enabling them to present antigen and activate T cells [228]. Different stages of immune cell activation coincide with different types of cellular metabolism to meet their biosynthetic and bioenergetic needs. This has been extensively shown in lymphocytes and macrophages [205, 589, 590], however less work has been undertaken in DCs, and there are no publications to-date addressing the effect of mesothelioma on DC metabolism. Studies have shown that altering the metabolic state of DCs can impact their inflammatory responses which can be used for therapeutic effects [591, 592]. Rehman et al showed that fatty acid synthesis (FAS) plays an important role in the differentiation of monocytes into DCs *in-vitro*. In their *in-vivo* experiments development of DCs in lymphoid organs was also found to be dependent on FAS [229]. This shows that metabolic pathways affect the DC differentiation process. Pearce et al have shown that upon PAMP stimulation via TLR, immature DCs transition into activated DCs. This process is accompanied by a transition from OXPHOS and mitochondrial beta oxidation into aerobic glycolysis [593]. Activated DCs rely highly on glucose for survival, and upon glucose limitation become more vulnerable to death [593]. Thus, glycolysis is critical for full DC activation. Moreover, substrates generated during glycolysis may help DC activation. For example, GAPDH helps with the regulation of protein translation critical for DC activation [594].

Quiescent DCs have a different metabolic requirement compared to an activated DCs. These changes play a crucial role for the successful activation of DCs. This is made more complex as metabolic requirements are different in quiescent or immature DCs compared to activated or mature DCs. Mesothelioma may affect immature DCs that migrate into tumours, or mesothelioma-derived soluble factors that

reach lymph nodes may modulate mature LN DCs. As noticed earlier in chapter 4, mesothelioma-exposed DCs accumulated lipids, which could be responsible for DCs dysfunction and could also affect DCs metabolism as much of the functionality of tolerogenic DCs is intertwined with metabolic activity, such as lipid accumulation or catabolism of amino acids. This chapter focusses on changes to immature and mature human and murine DC metabolism when exposed to soluble factors derived from mesothelioma tumour cells compared to non-tumour exposed.

5.2 Results

5.2.1 Determining if mesothelioma induces metabolic changes to human monocyte derived DCs (MoDCs)

5.2.1.1 Establishing metabolic studies model for DCs culture

Previous studies have shown that bacterial lipopolysaccharide (LPS), a Toll-Like Receptor (TLR)-4 agonist induces DC activation when used at concentrations between 10 ng to 1 μg/ml [595] alongside a rapid metabolic switch to glycolysis [593, 596, 597]. Therefore, to establish a useful biological control, the effect of LPS on human MoDCs after LPS exposure was examined. To do this, immature human MoDCs were generated as shown in chapter 2 (section 2.2.4). On day 7, DCs were either left untreated in medium alone or activated with LPS for 3 h and 24 h when loosely adherent cells (shown to consist of 80-90% $CD11c^+$ cells [598]) were harvested and seeded in a seahorse XFe96 cell culture plate with 7×10^4 cells per well. Protocol to generate DCs has been adopted from the previous work published in our group [570]. Glycolytic stress test was conducted (Figure 5.1 A). The data show a statistically significant increase in glycolysis measured after glucose injection in DCs treated with LPS for 24 h (Figure 5.1 C) which has also been shown in other studies reasoning that the longer time point likely allowed enough time for an immune response to occur before attenuation [596, 599] but in contrast to other studies, no change was observed in 3 h LPS-exposed DCs which could be because of the low glucose concentration (2.5 mM) used in the study (Figure 5.1 B). Glucose concentration was changed to 11 mM in seahorse basal media to match the concentration of the culture media. They were also rested for one hour prior to loading onto the Seahorse XFe96 Analyser. A final concentration of 1 μg/ml of LPS was injected. Extracellular acidification rate (ECAR) was then measured in real time for 180 minutes after LPS exposure. In agreement with the literature, glycolysis rapidly increased upon LPS exposure confirming the reproducibility of these experiments [599, 600] (Figure 5.2 A). This is more clearly seen when the data is shown as fold change (Figure 5.2 B).

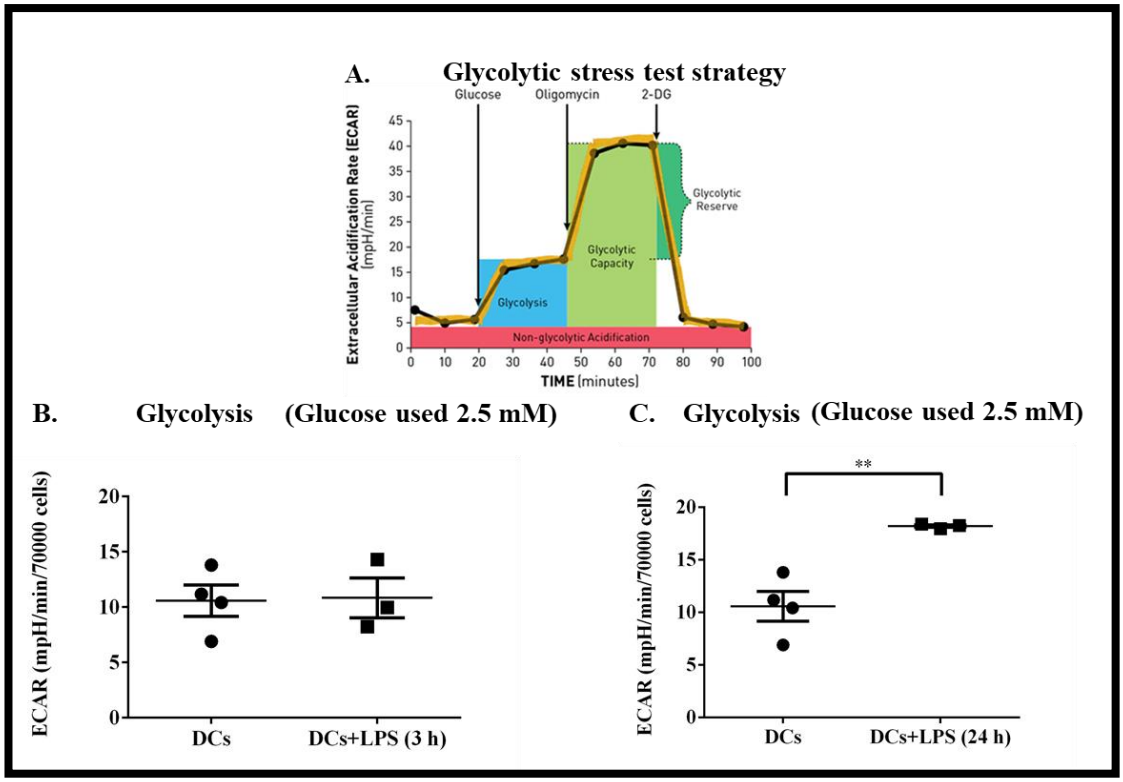

Figure 5.1: Long-term LPS activation increases glycolysis in DCs

Immature human MoDCs were generated using GM-CSF and IL-4, as (shown in chapter 2, section 2.2.4). On day 6, DCs were left untreated in medium alone or pre-activated with 1μg/ml LPS for 3 hours and 24 hours after which loosely adherent cells were harvested and seeded in a seahorse XF-96 cell culture plate at 7 x 10^4 cells/well and real-time rates of ECAR, as a readout for lactate production, were determined. **A.** ECAR measurements obtained upon injections of glucose (2.5mM), oligomycin (Oligo) and 2-deoxglucose (2-DG) were used to calculate glycolysis. The first injection is a saturating concentration of glucose which was 2.5mM in the preliminary experiments. Cells utilise this glucose via the glycolytic pathway to catabolise it to pyruvate, producing NADH, ATP, water and protons. Oligomycin, the second injection, is an ATP synthase inhibitor. Oligomycin inhibits mitochondrial ATP production and shifts energy production towards glycolysis. 2DG is the final injection in the glycolytic stress test. It is a glucose analog, that offers competitive binding to glucose hexokinase thereby inhibiting glycolysis. Figure A sourced from Tan et al [601]. **B, C**. There is a significant increase in glycolysis in 24 h LPS-exposed DCs but none in 3 h LPS exposed DCs. Data is shown as mean ± SEM from 3-4 independent experiments with 4-6 replicates in each experiment. Statistical significance was assessed Mann Whitney U Test and $**p < 0.01$.

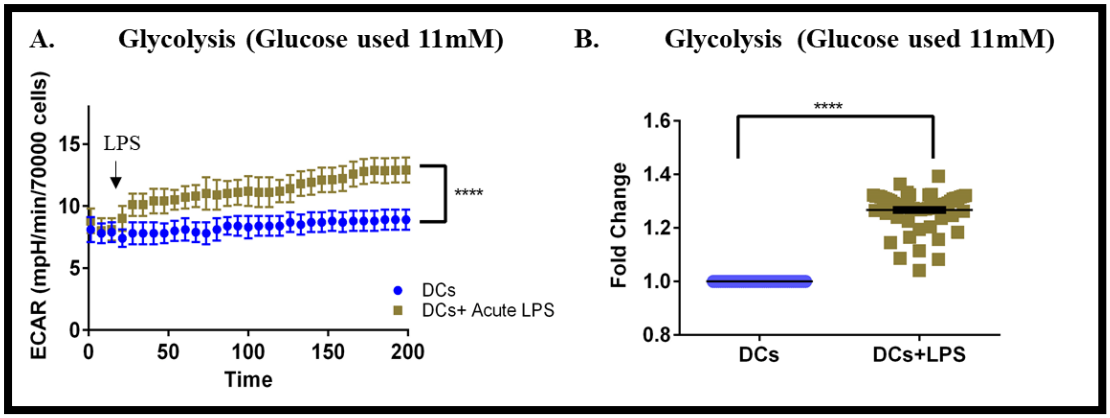

Figure 5.2: Acute LPS increases glycolysis in monocyte-derived dendritic cells

A. Immature human MoDCs were generated using GM-CSF and IL-4, as (shown in chapter 2, section 2.2.4). At day 7 MoDCs were pooled, counted and seeded into seahorse XF-96 analyser plates at 7 x 10^4 cells/well with 8 replicates per condition; 20 mins later control wells were injected with media and a further 8 wells injected with 1µg/ml LPS. Seahorse media in this experiment contained 11mM glucose to match the concentration of glucose in the culture media. **A.** Real-time rates of ECAR, as a readout for lactate production, were determined every 6 minutes over 200 minutes. Data from one representative experiment with 8 replicates/condition is shown as mean ± SEM. **B.** Pooled data showing fold change of LPS-treated relative to controls from 3 independent experiments with 4-6 replicates in each experiment is shown as mean ± SEM. Statistical significance was assessed by Mann Whitney U Test, ****p <0.0001.

5.2.1.2 Mesothelioma-derived soluble factors also increase glycolysis in human MoDCs

The overall aim of this study was to determine the effect of mesothelioma-derived factors on human MoDCs. Before the study could begin, mesothelioma derived tumour-conditioned media (TCM) had to be generated. To do this, human Ju77 mesothelioma tumour cells were weaned onto and cultured in serum-free media (SFM) to avoid any confounding effects mediated by foetal calf serum (FCS) (as shown in chapter 2, Figure 2.1). Immature human MoDCs were generated and on day 7 were either left untreated in medium alone (resting DCs) or exposed to 50% TCM for 3 h (short term) and 24 h (long term) when loosely adherent cells were collected (Figure 5.3 A), counted and seeded in a seahorse XF-96 cell culture plate at 7 x 10^4 cells per well, and a glycolysis stress test conducted.

Immature human MoDCs demonstrated significantly elevated glycolysis following 24 h, but not 3 h of TCM exposure (Figure 5.3 B). These data suggest that mesothelioma tumours induce metabolically active DCs reminiscent of the activated DCs.

5.2.1.3 Basal respiration in human MoDCs

Oxidative phosphorylation (OXPHOS) combines electron transport with cell respiration and ATP synthesis and is a key functional unit in mitochondria that produces energy in the form of ATP. This process is driven by the cellular energy demands of a cell. Therefore, this study also investigated changes in OXPHOS in human MoDCs exposed to TCM and LPS was used as a control.

5.2.1.4 LPS exposure results in decreased basal respiration in human MoDCs

Several studies have shown that activated DCs exhibit increased glycolysis and decreased OXPHOS [212, 602-604]. This study also found that when immature human DCs are exposed to acute LPS injection and when activated with LPS for 3 h and 24 h, OXPHOS as measured by basal respiration rapidly decreases (Figure 5.4 B, Figure 5.5 A) suggesting altered mitochondrial function and is consistent with other publication [599]. Shows

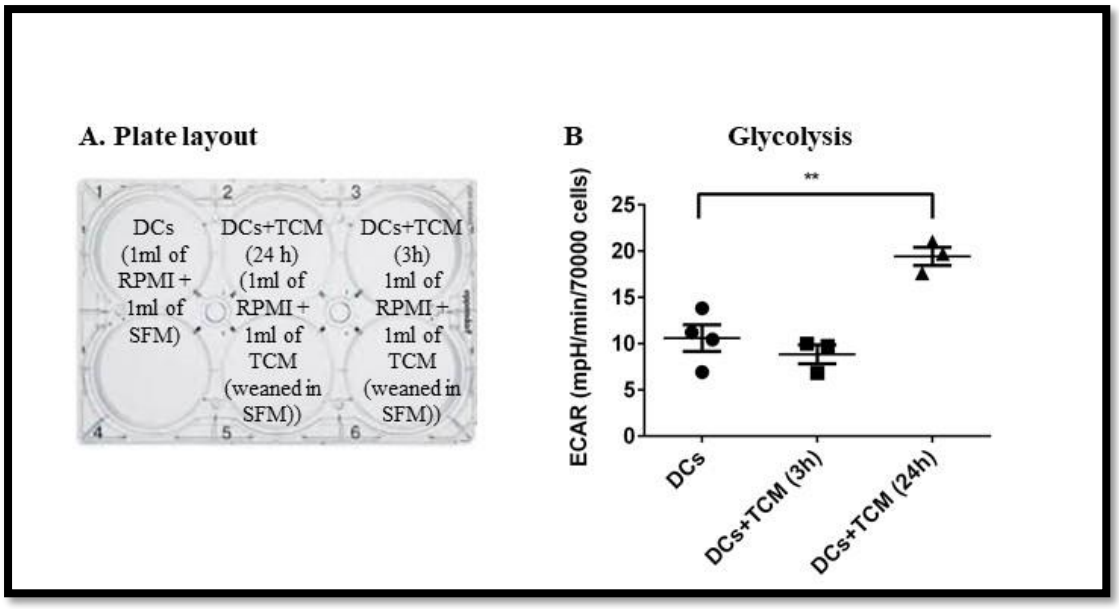

Figure 5.3: Mesothelioma-derived factors increase glycolysis in immature MoDCs

TCM media was generated as shown in Figure 2.1. **A**. MoDCs left untreated as controls or pre-exposed with 50% Ju77 TCM for 3 hours and 24 hours were seeded into a Seahorse XF-96 Analyzer plate at 7 x 10^4 cells per well and real-time rates of ECAR determined. **B**. TCM exposed MoDCs show significant increases in glycolysis after 24 hours TCM exposure. Data represented as mean ± SEM of 3-4 independent experiments each with 4-6 replicates. Statistical significance assessed by Mann Whitney U Test, $^{**}p < 0.01$.

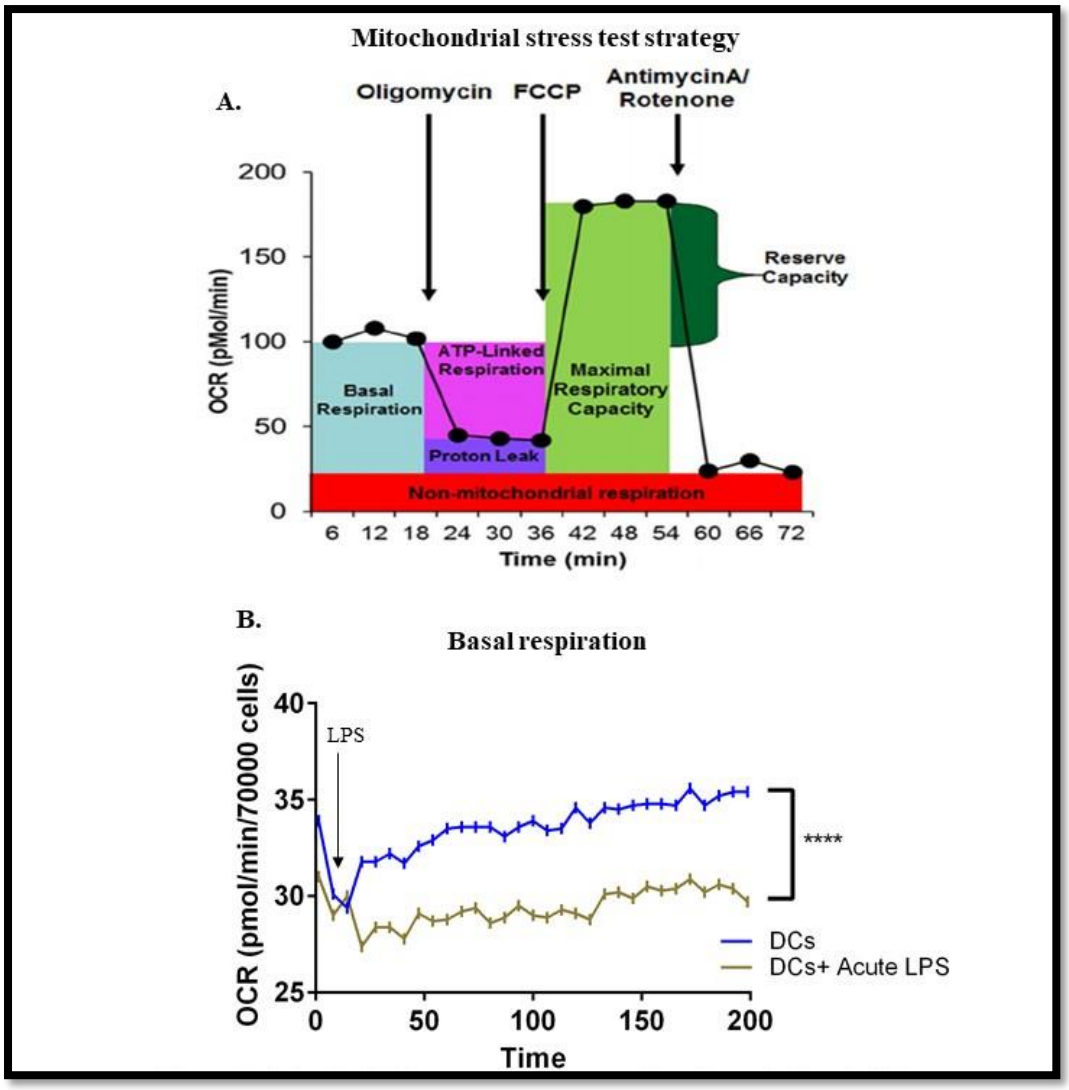

Figure 5.4: Acute LPS exposure decreases basal respiration in DCs

MoDCs were generated as per Figure 2.2. **A**. Outlines the mitochondrial (mito) stress test injection strategy. Oligomycin is injected to block ATP synthase activity. Then FCCP is injected to act as an uncoupling agent and disrupt mitochondrial membrane potential. A mixture of rotenone and antimycin is injected to completely block mitochondrial respiration. Figure A sourced from Rose et al.[605]. **B**. Real time oxygen consumption rates (OCR) which measure basal mitochondrial respiration were determined every 6 minutes over 200 minutes. Data from one representative experiment with 8 replicates for each condition is shown as mean ± SEM. Statistical significance assessed by Mann Whitney U Test, ****p <0.0001. Basal respiration shows a significant decrease in LPS-activated DCs meaning mitochondrial respiration is reduced.

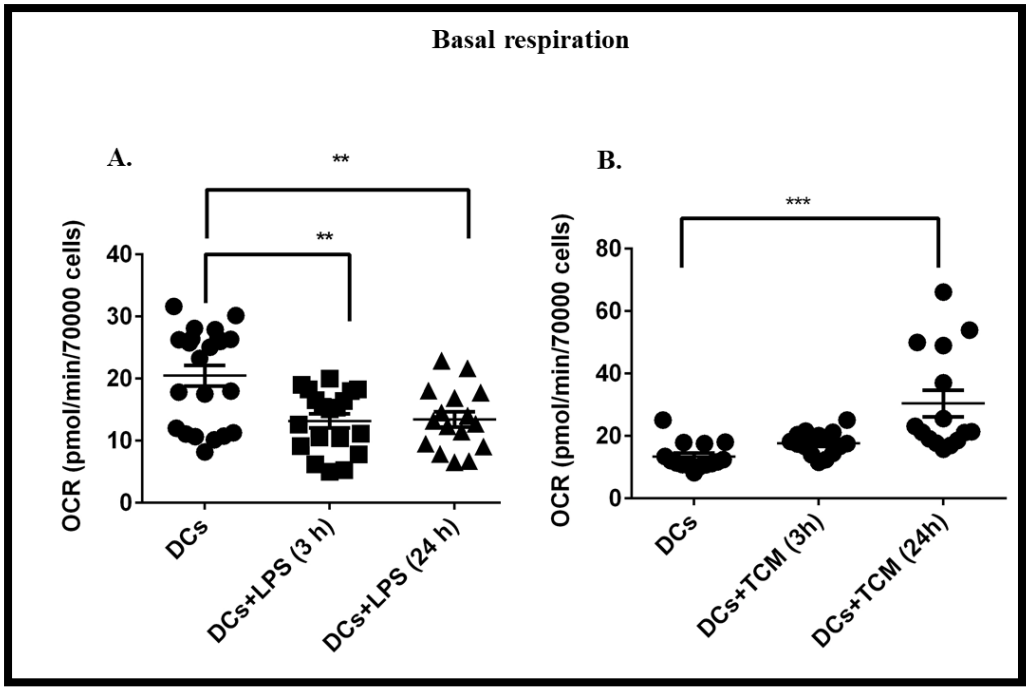

Figure 5.5: Basal respiration decreases in LPS-exposed DCs and increases in tumour-exposed DCs

A. MoDCs were either left untreated as controls or pre-activated with 1µg/ml LPS for 3 h and 24 h or pre-exposed to TCM for 3 h and 24 h. MoDCs were collected and seeded in a Seahorse XF-96 Analyzer with 7 x10^4 cells per well and real-time rates of OCR (to measure basal mitochondrial respiration), were determined. Pooled data of LPS-activated MoDCs from 3 independent experiments with 4-8 replicates in each experiment is shown as mean ± SEM. **B**. Ju77-derived tumour conditioned media (TCM) significantly increases OXPHOS in MoDCs, measured by real time OCR rates. Pooled data of TCM-exposed DCs from 3 independent experiments with 4-8 replicates in each experiment is shown as mean ± SEM. Statistical significance assessed by Mann Whitney U Test , $^{**}p<0.01$, $^{***}p<0.001$. Two groups are compared at a time.

5.2.1.5 Mesothelioma-derived soluble factors increase OXPHOS in human MoDCs

The effect of TCM on OXPHOS was examined. Immature human DCs showed a significant increase in OXPHOS measured in terms of basal respiration after continuous exposure to TCM for 24 h but not for 3 h (Figure 5.5 B). Taken together, these data suggest that mesothelioma tumours may induce tolerogenic DCs as increased glycolysis and OXPHOS represents a characteristic metabolic profile of tolerogenic DCs [606, 607]. Tolerogenic DCs are also characterised by increased glycolytic capacity and glycolytic reserve [606] which was examined in the next part of the study.

5.2.1.6 Mesothelioma-derived soluble factors increase glycolytic capacity and glycolytic reserve in human MoDCs

Immune cells usually operate at a metabolic rate lower than the highest rate achievable allowing them to respond to changing energetic demands [608]. The maximum rate by which cells can operate glycolysis is called maximum glycolytic capacity [609]. On the other hand, glycolytic reserve is the difference between maximum glycolytic capacity and basal glycolysis. The effect of LPS and Ju77 TCM on human MoDCs over 3 h versus 24 h was examined. This timeframe may allow DCs to reach their maximum glycolytic capacity and reserve. The data show that both maximum glycolytic capacity (Figure 5.6 A) and glycolytic reserve (Figure 5.6 B) significantly increased in DCs after 24 h exposure to TCM further suggesting that mesothelioma induces tolerogenic DCs as others have shown that glycolytic capacity, glycolytic reserve are more pronounced in tolerogenic DCs as mentioned earlier [606]. Tolerogenic DCs are mostly characterised by low expression of immunogenic co-stimulatory molecules along with the higher expression of inhibitory molecules [586]. Further evidence of a tolerogenic phenotype in this study is supported by the data showing decreased MHC-I and MHC-II (gating strategy shown in Fig 5.7), and a trend to an increase in the inhibitory molecule A2A ($P<0.09$, Figure 5.8 G) although no change was observed in TCM-exposed DCs in the expression of co-stimulatory molecules CD40 and CD86 or other inhibitory molecules such as CD39, CD73 (Figure 5.8). Earlier studies in our group by Gardner et al. found up-regulated expression of inhibitory molecules such as CD73, CD39, A_{2A} and A_{2B} receptors and programmed cell death ligand-1 (PD-L1) ([527]). Taken together, the group's previous work and

the metabolic changes showed in this study, the data suggests tumour-exposed DCs adopt a tolerogenic profile. More experiments are required to confirm if tumour-exposed DCs are truly tolerogenic.

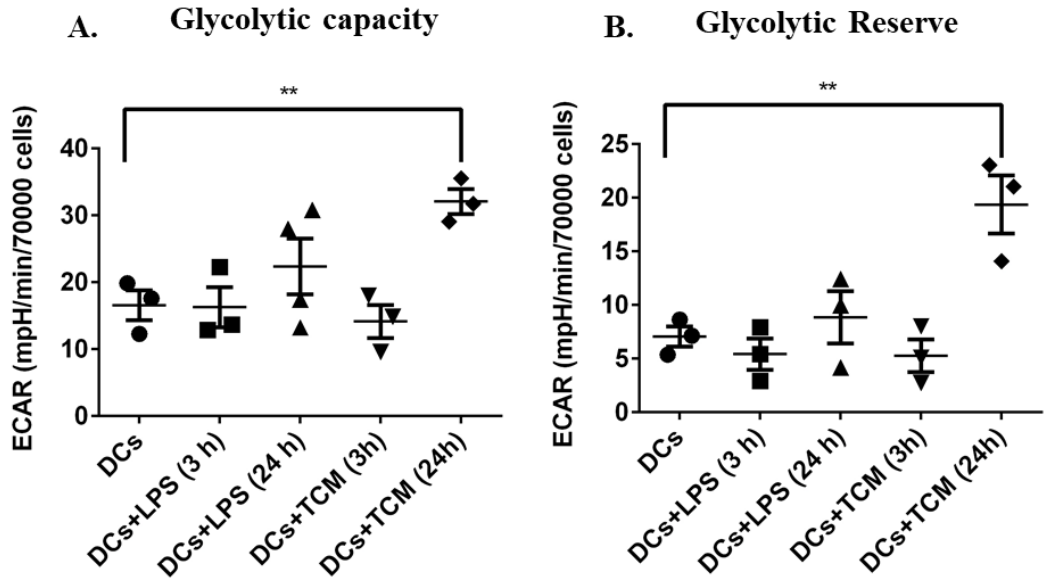

Figure 5.6: Mesothelioma TCM-exposed MoDCs demonstrate increased glycolytic capacity and glycolytic reserve

Human MoDCs were left untreated, exposed to 50% Ju77-derived TCM for 3 hours and 24 hours, or activated with 1ug/ml LPS for 3 hours or 24 hours. MoDCs were collected and seeded in a Seahorse XF-96 Analyzer at 7 x 10^4 cells/well after which real-time rates of ECAR were determined. **A.** Shows the maximum glycolytic capacity achieved after oligomycin injection as per Figure 5.1A. Data shows significant increase in glycolytic capacity in TCM-exposed MoDCs. Data shown as mean ± SEM of n = 3 independent experiments, each with 6-8 replicates for each condition. Statistical significance assessed by *t*-test and **p<0.01 **B.** Shows the glycolytic reserve measured after 2DG injection as per Figure 5.1A. Data shows significant increase in glycolytic reserve in TCM-exposed DCs. Data shown as mean ± SEM of n = 3 independent experiments, each with 6-8 replicates for each condition. Statistical significance assessed by Mann Whitney U Test and **p<0.01. Two groups are compared at a time.

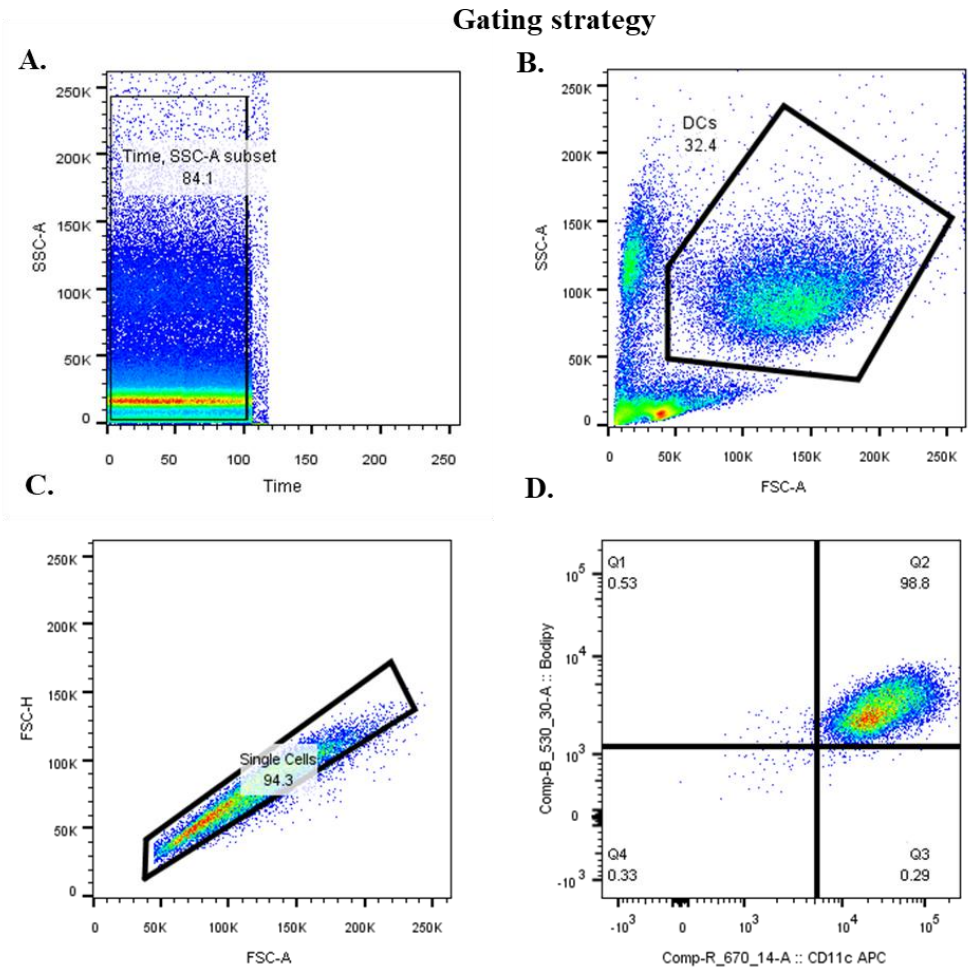

Figure 5.7: Gating strategy

Human MoDCs were generated as discussed in chapter 2 (section 2.2.4). Time gate was used as an internal control to exclude the poorly collected populations **(A)**, large cells **(B)**, single cells **(C)**, $CD11c^{+}Bodipy^{+}$ **(D)** were gated.

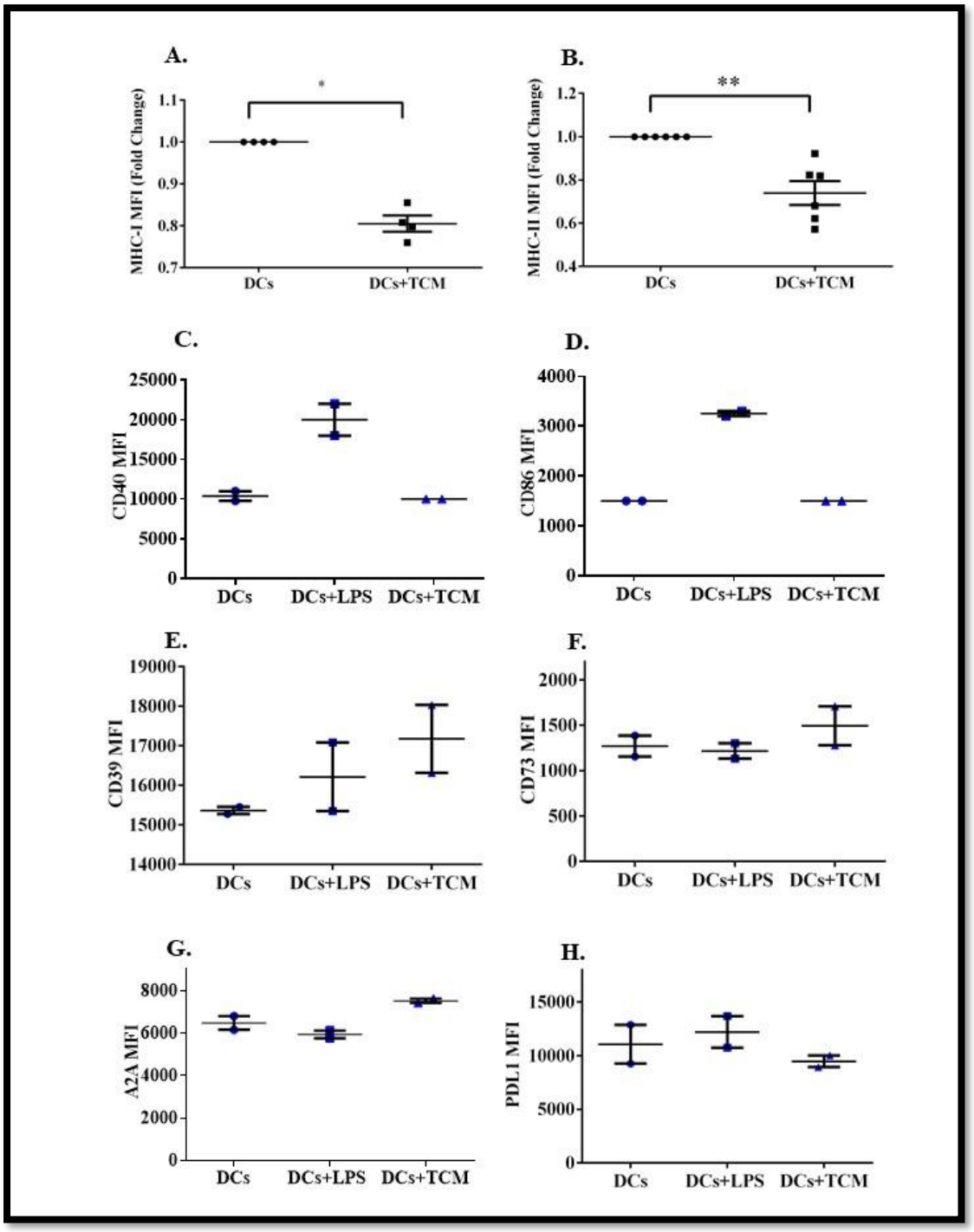

Figure 5.8: Mesothelioma leads to a decrease in MHC in human DCs

Data shows MFI of antigen presenting molecules MHC-I (A), MHC-II (B), co-stimulatory molecules; CD40 (C), CD86 (D), inhibitory molecules; CD39 (E) CD73 (F), A2A (G) and PD-L1 (H). Data shown as mean ± SEM, n = 2 experiments. Statistical significance assessed by Mann Whitney U Test, **p*<0.05, **p<0.01. Two groups are compared at a time.

5.2.1.7 Hexokinase II and GAPDH increase in TCM-exposed MoDCs

Different glycolytic enzymes (as shown in Figure 5.9) that may be responsible for the increased glycolysis seen in MoDCs exposed to LPS and TCM were examined using western blotting (Figure 5.10).Hexokinase II (HK-II) was increased in both LPS-activated DCs and DCs exposed to TCM., which may account for increased glycolysis for both (Figure 5.10). However, an isolated incident showing decreased HK-II was observed in TCM-exposed DCs, more studies may be required for the data to reach significance. Glyceraldehyde 3-phosphate dehydrogenase (GAPDH), an enzyme that catalyses the 6^{th} step in the glycolysis cycle increased in LPS and TCM-exposed MoDCs (Figure 5.10). Increased GAPDH gene expression is associated with increased cell proliferation [211] and a study demonstrated that inhibition of GAPDH down regulates glycolysis in myeloid and lymphoid cells suggesting its role in increased expression of glycolysis [610] . β-actin was used as a loading control as its expression level remained consistent in all groups regardless of the different treatments. No changes were observed in other glycolytic enzymes.

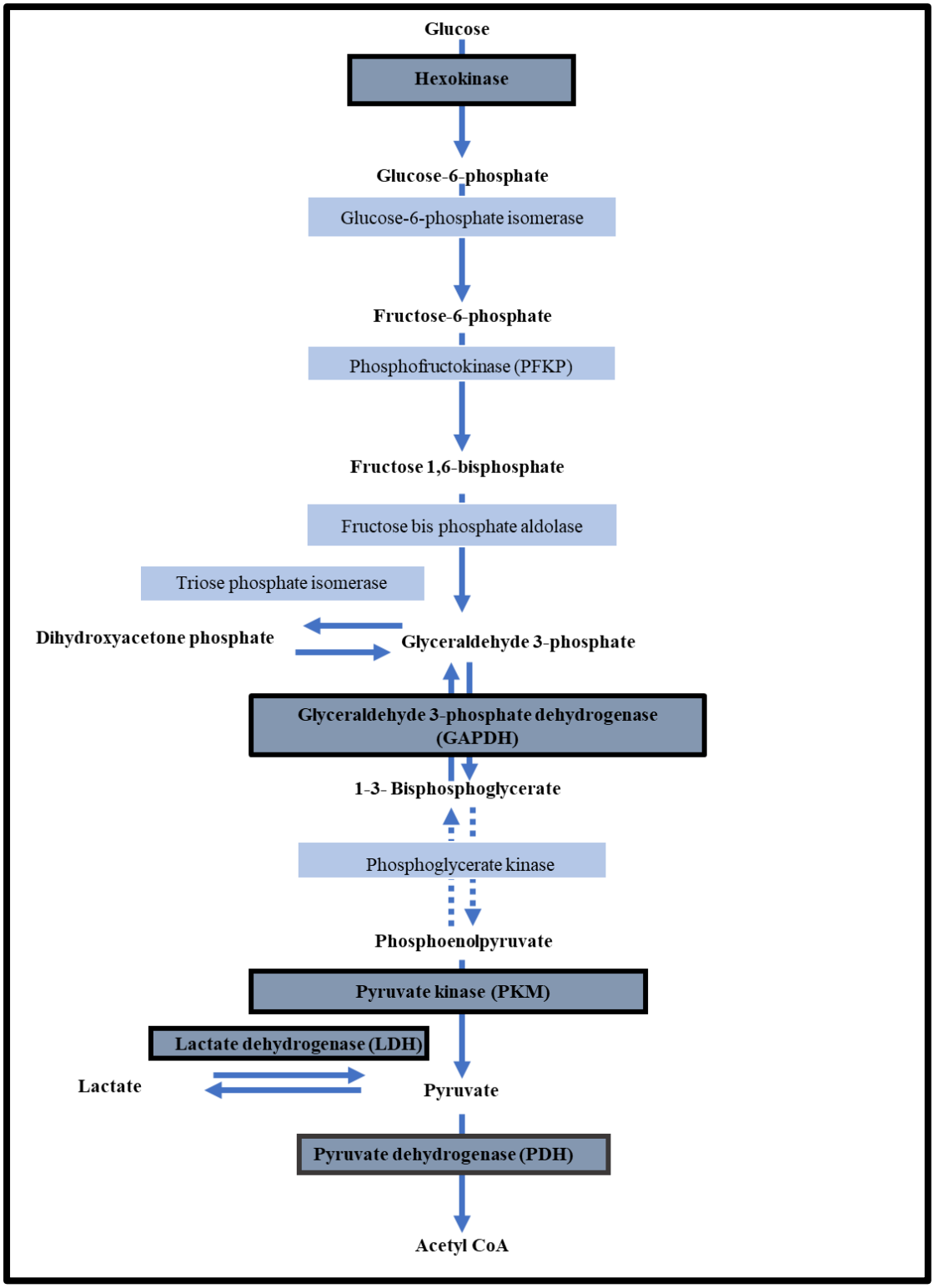

Figure 5.9: Enzymes involved in the glycolytic pathway

Key enzymes involved in the glycolytic pathway are shown. **Those examined using western blotting are bolded and highlighted**

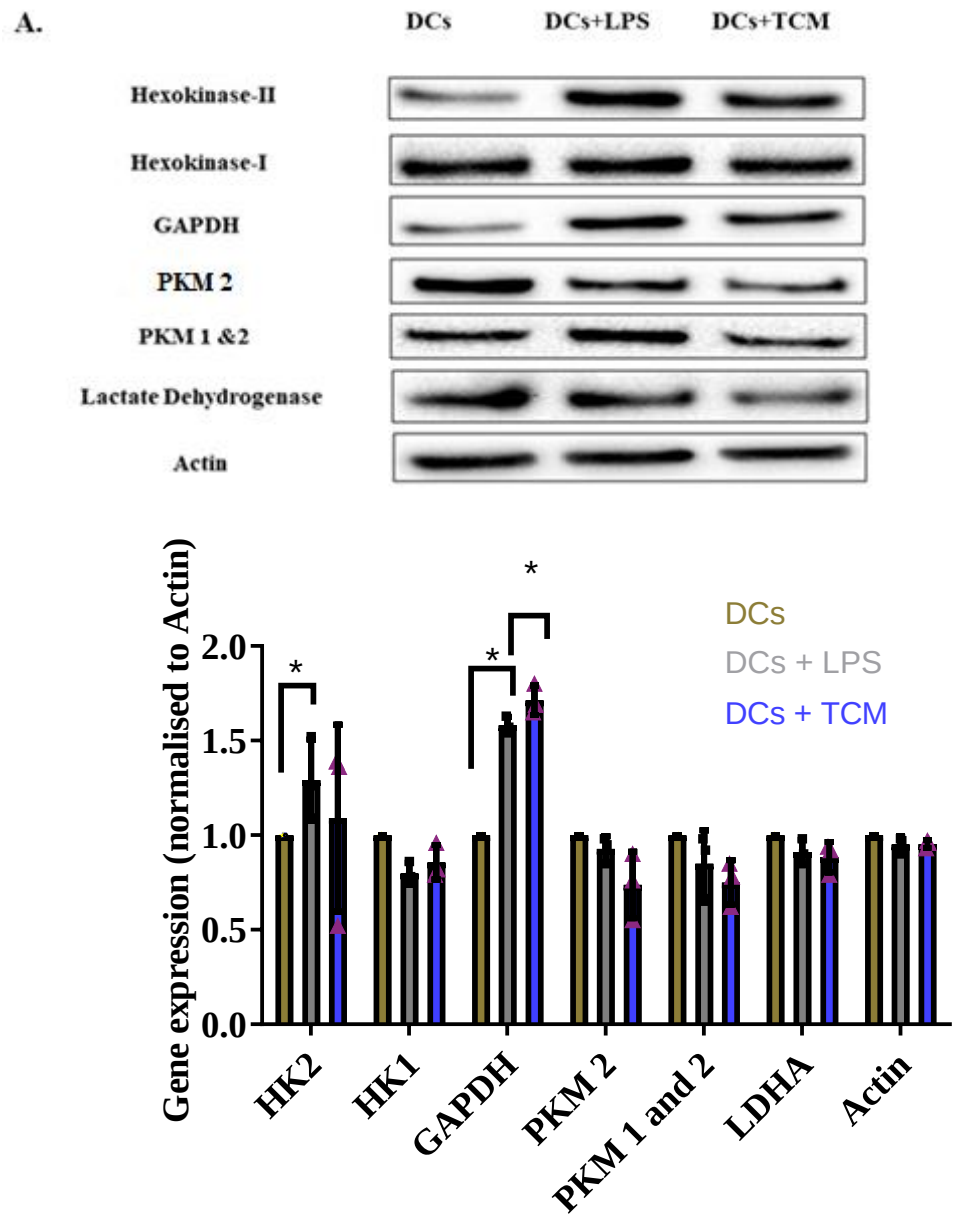

Figure 5.10: Hexokinase II and GAPDH increase in DCs in response to LPS and mesothelioma-derived soluble factors

DCs collected according to Figure 5.3A at 2 x 10^6 cells were (i) left untouched as control DCs, (ii) LPS-exposed (24 hours) or (iii) TCM-exposed (24 hours). **A.** Western blotting (WB) and **(B)** Semi quantitative analysis, showing enzymes associated with the glycolytic pathway as per Figure 5.9. Actin was used as a loading control. Supernatants run on SDS-PAGE gels were transferred onto 0.45µm nitrocellulose which was sequentially incubated with primary rabbit antibodies directed against the glycolytic enzymes, followed by a secondary polyclonal goat anti-rabbit antibody conjugated with HRP before blotted bands were read in a BIO-RAD western blot imaging system using Image Lab. Statistical significance assessed Mann Whitney U Test, *p<0.05.

5.2.1.8 MitoTracker™ Green and MitoTracker Deep Red increase TCM-exposed MoDCs

TCM-exposed MoDC increased basal respiration; to explore if other mitochondrial characteristics were also affected, MitoTracker™ Green FM and MitoTracker™ Deep Red were used to determine mitochondrial mass and membrane potential respectively. Study by Malinarich et al. found that proteins involved in OXPHOS pathways were increased in tolerogenic MoDCs, thus suggesting a potential for increased mitochondrial activity [606]. MitoTracker™ Green FM shows increased fluorescence upon accumulation in the mitochondrial lipid environment, regardless of membrane potential. [611]. After staining and flow cytometric analysis using the gating strategy (shown in Figure 5.11 A), LPS-exposed MoDCs and TCM exposed DCs demonstrated a significant increase in MitoTracker™ Green expression (Figure 5.11 B) which could be because of increased mitochondrial biogenesis via activation of nuclear respiratory factor-1 [612]. MitoTracker Deep Red, a measure of membrane potential [613], was also significantly increased in LPS and TCM exposed DCs (Figure 5.11 C) suggesting functionally active mitochondria and also could be due to the tolerogenic nature of TCM exposed DCs which is shown by Malinarich [606]. These data show that both the increase in Mito-Tracker Green (indicative of membrane mass) and Mito-Tracker Red (indicative of membrane potential), are in line with the increase in basal respiration in TCM-exposed DCs. Along with increased MitoTracker™ Green, data for TCM-exposed MoDCs suggested there may be increased spare respiratory capacity however the range in spare respiratory capacity levels shows that more mice are be needed to reach conclusion (Supplementary figure 5.1) However, LPS also lead to increase in MitoTracker™ Green and MitoTracker Deep Red, but a reduction in respiration as shown earlier. One possible explanation for this could be that mitochondria are not only there for OXPHOS, they also have very important biosynthetic roles like anaplerosis through the Krebs cycle [614].

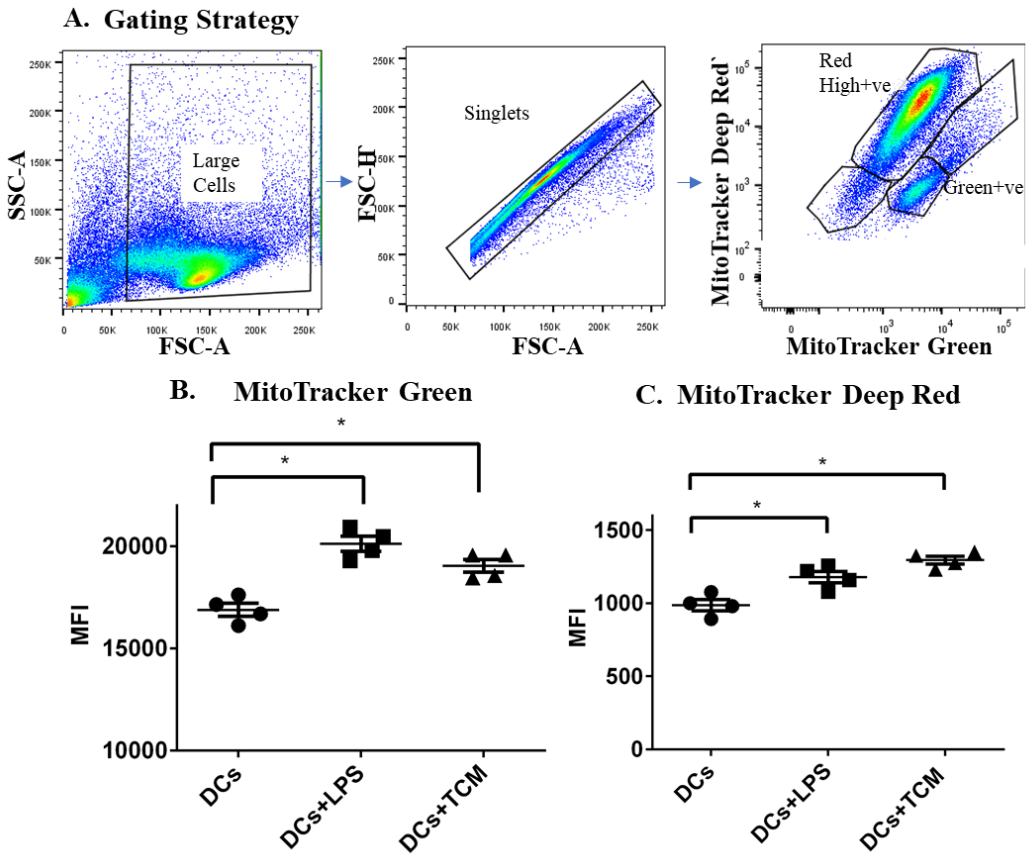

Figure 5.11: Increased MitoTracker Deep-Red expression in TCM exposed DCs

A. Gating strategy of MoDCs. MoDCs were collected as described in Figure 2.2 and stained with MitoTracker Deep Red and MitoTracker Green to measure functionally active mitochondria and total mitochondrial mass respectively. MitoTracker expression was measured using flow cytometric analysis. Firstly, large cells were gated using forward and side scatter plots. Single cells were selected using forward scatter area and height then high MitoTracker Red and high MitoTracker Green +ve cells were selected **B**. MitoTracker Green is significantly increased in LPS-exposed MoDCs as well as mesothelioma TCM-exposed DCs **C**. Mito-Tracker Deep Red is significantly increased in mesothelioma TCM-exposed DCs. Pooled data shown as mean ± SEM from 4 independent experiments. Statistical significance assessed by Mann Whitney U Test, *p<0.05.

5.3 Investigating the effects of TCM on murine DC metabolism

5.3.1 Determining if TCM induces metabolic changes to BM-derived murine DCs

A parallel series of experiments were conducted using BM-derived monocytes differentiated into immature BMDCs in the continuous presence of murine GM-CSF and IL-4 for 7 days (as shown in chapter 2, section 2.3.5) when they were transferred to Seahorse plates and allowed to rest for 20 minutes before LPS exposure. ECAR was then measured in real time for 200 minutes after LPS exposure (figure 5.12 A). In contrast with the literature, glycolysis did not rapidly increase upon LPS exposure [228] (Figure 5.12 B). Similarly, longer LPS exposure did not induce a significant change in glycolysis (Figure 5.12 C).

5.3.2 Mesothelioma increases glycolysis and glycolytic capacity in murine DCs

Murine BM-derived DCs were generated as shown in chapter 2 (section 2.3.5) and on day 7 were left untreated in media alone (resting DCs) or exposed to 50% murine AE17 TCM for 3 h and 24 h when loosely adherent cells were collected, counted and seeded in a seahorse XF-96 cell culture plate at 7 x 10^4 cells per well. Similar to human MoDCs, murine DCs demonstrated an increasing trend in glycolysis and glycolytic capacity after TCM exposure, although statistical significance was not reached, again suggesting that mesothelioma tumours may activate DCs (Figure 5.13 A, B).

5.3.3 Basal respiration remains unchanged with LPS and TCM exposure in murine DCs

The effect of LPS and TCM on OXPHOS was also examined in murine BMDCs. Murine BMDCs showed no change in OXPHOS measured in terms of basal respiration after continuous exposure to AE17 TCM for 3 h and 24 h (Figure 5.14).

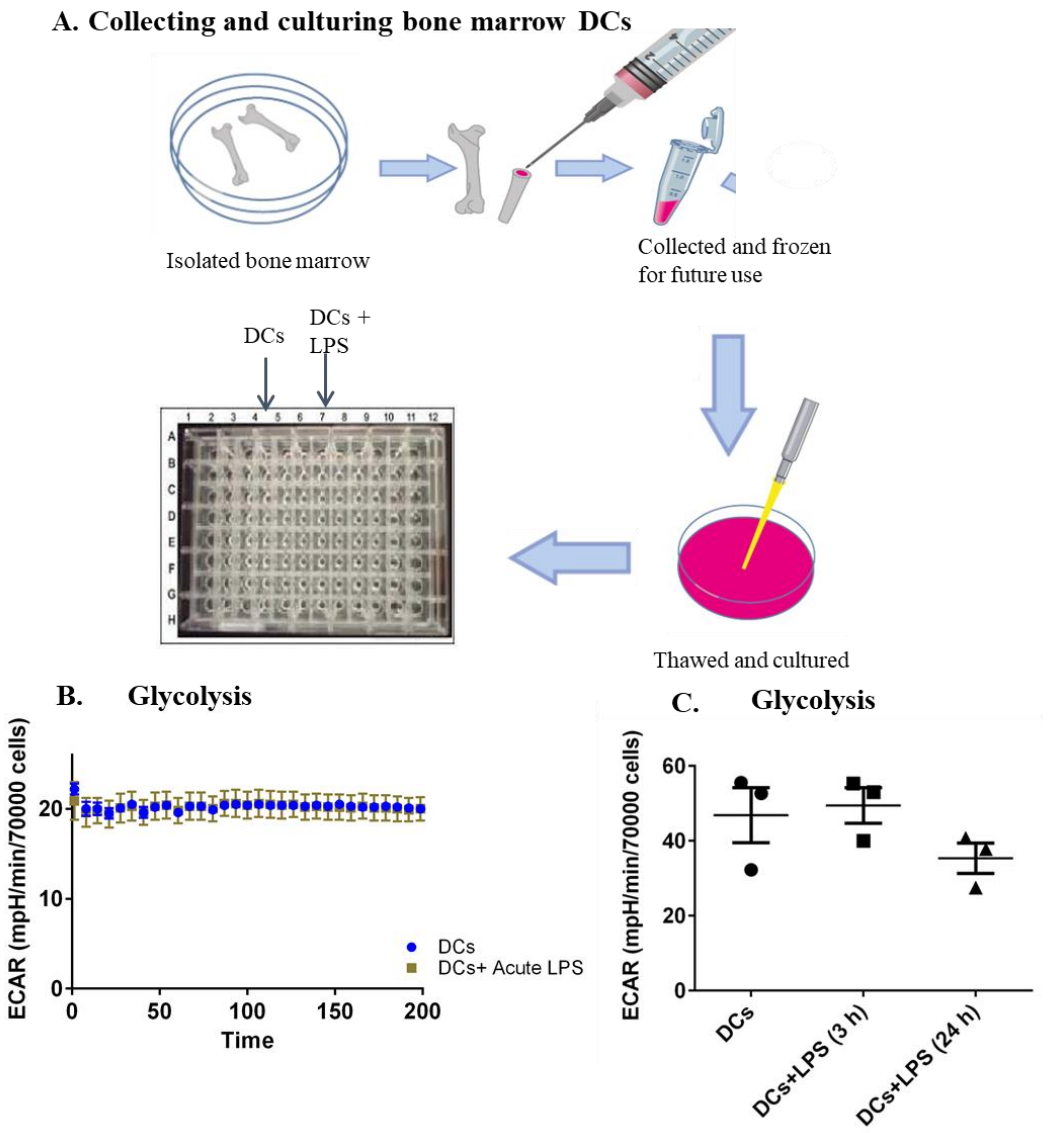

Figure 5.12: Acute LPS does not change glycolysis in murine DCs

A. Bone marrow from young mice (6-8 weeks old) was frozen at -80ºC for future experiments when cells were thawed and cultured in 6 well plates at 5 x 10^6 cells/well in GM-CSF and IL-4 to generate bone marrow-derived (BM)DCs. At day 7, BMDCs were pooled, counted and seeded into seahorse XF-96 analyser plates at 7 x 10^4 cells/well with 8 replicates per condition; 20 mins later controls were injected with media and a further 8 wells injected with 1µg/ml LPS. **B**. Real-time rates of ECAR were determined every 6 minutes over 200 minutes. Data from one representative experiment with 8 replicates for each condition is shown as mean ± SEM. **C**. ECAR measurements obtained upon injections of glucose (10 mM), oligomycin (Oligo) and 2-deoxglucose (2-DG) were used to calculate glycolysis. Data is shown as mean ± SEM from 3 independent experiments with 4-6 replicates in each experiment.

A.

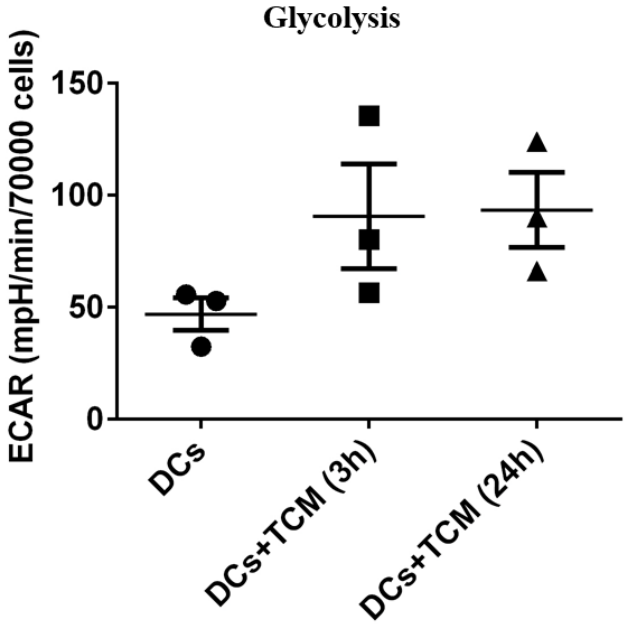

B.

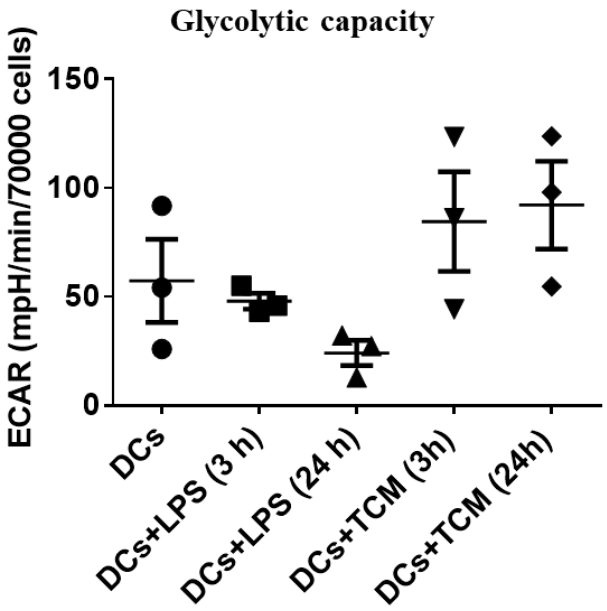

Figure 5.13: No change in glycolysis and glycolytic capacity observed in murine bone marrow-derived dendritic cells

A. AE17 murine mesothelioma tumour conditioned media (TCM) was generated according to Figure 2.1. Murine DCs left untreated as controls or pre-exposed with 50% AE17 TCM for 3 hours and 24 hours (as per Figure 5.3A) were seeded into a Seahorse XF-96 Analyzer plate at 7 x 10^4 cells per well and real-time rates of ECAR determined. Data represents mean ± SEM of 3 independent experiment each with 4-6 replicates. B. Glycolytic capacity measured after injecting oligomycin as shown in Figure 4.2A shown as mean ± SEM of 3 independent experiment each with 4-6 replicates.

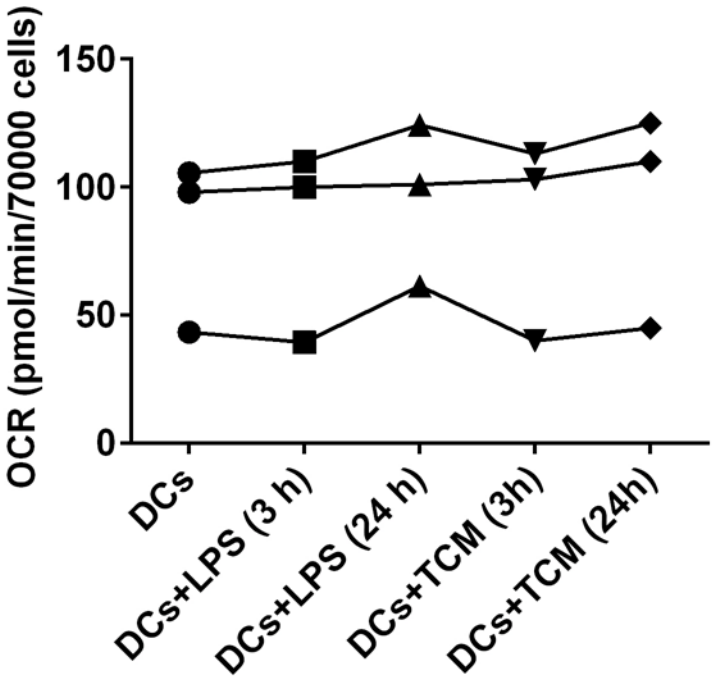

Figure 5.14: Basal respiration remains unchanged in LPS and tumour-exposed murine DCs

A. Murine BMDCs were either left untreated as controls or activated with 1ug/ml LPS for 3 h and 24 h. Cells were collected and seeded in a Seahorse XF-96 Analyzer with 7 x10^4 cells per well after which real-time rates of OCR were determined. Data lines represents three different experiments.

5.4 Discussion

Until now, no studies had examined the effect of mesothelioma on DC metabolism. We therefore examined metabolic changes in human MoDCs and murine BMDCs in response to mesothelioma-derived soluble factors. LPS was chosen as a control on the basis of previous descriptions of its effects on glycolysis and OXPHOS in DCs. Indeed, in this study human MoDCs exposed to LPS showed increased glycolysis and a decrease in respiration in line with other published studies [593, 599] . However, no change was seen in glycolysis and OXPHOS in murine BMDCs. The studies on murine BMDCs were less informative than the human MoDCs, likely due to a freezing effect as frozen murine BM samples were used. Liu et al showed that fresh cells processed and used immediately had a higher metabolic activity than cryopreserved cells [615]. Similarly, Lauterboeck et al showed that the metabolic activity of monkey derived cells is impaired 48-hour post thawing and only partially recovered after 72 hours [616]. As only fresh human MoDCs were used and the data was more reliable, this discussion focuses on MoDCs results which account for the majority of experiments.

Mice and humans are considered useful examples showing metabolic homogeneity as they have the same organs and show similar systemic physiology [617]. However, they may behave metabolically differently as Vijayan [618] showed that upon LPS stimulation human monocyte derived macrophages showed no shift towards glycolysis and kept relying on OXPHOS while mouse BM derived macrophages showed an increase in glycolysis and decrease in OXPHOS; this difference which could be due to evolutionary divergence [619]. Metabolic differences between species such as human and mice needs to be explored further. Therefore, the emphasis in the discussion is on MoDCs and which account for the vast majority of experiments.

The overall aim of this study was to determine the effect of mesothelioma-derived factors on human MoDCs. Current study showed that mesothelioma-derived soluble factors increased glycolysis, glycolytic capacity and basal respiration in MoDCs suggesting, mesothelioma may render DCs tolerogenic [606, 607]. This was consistent with the study by Malinarich et al. where they generated tolerogenic DCs using 100nM vitamin D3 and dexamethasone in combination [606]. This is currently considered as

an accepted model to generate tolerogenic DCs with a therapeutic utility [620]. The study found tolerogenic DCs have enhanced mitochondrial oxidase activity with increased spare respiratory capacity and increased OXPHOS along with increased glycolysis, glycolytic capacity and reserve [606]. The changes observed in DCs in response to mesothelioma derived TCM compared to LPS could be due to many soluble factors present in TCM that can reprogram DCs metabolism. One of the study where TCM was generated in breast cancer cell line found varied concentrations of many different soluble factors in TCM [621]. Although another study by Zhao et al. shown that Wnt5a derived from melanoma can induce metabolic reprogramming in DCs that drives tolerization [622]. The exact composition of mesothelioma derived TCM still needs to be studied.

During normal functioning, cells rely primarily on mitochondrial OXPHOS to generate ATP for energy. However, many studies suggest that upon activation, immune cells undergo metabolic reprogramming and switch from OXPHOS to aerobic glycolysis [594, 623]. Similar changes are seen in cancer cells and is known as the Warburg effect. Otto Warburg investigated the metabolic profile of tumours and described the condition in tumours where glycolysis predominates even in the presence of oxygen. And pyruvate that was produced by the glycolytic pathway is metabolised to lactate rather than going to TCA cycle [212]. To understand metabolic changes in innate immune cells upon activation, the Warburg effect is an important concept [624]. In 1950s, Sbarra et al. found in neutrophils that activation by LPS exhibit increased glycolysis [625]. In 1969, another study on activated macrophages showed increased glycolysis and decreased oxygen consumption [626]. And in 1987, Newsholme et al. studied metabolism in macrophages and found that activated macrophages demonstrated increased HK-II, suggesting an increase in glycolytic activity in macrophages [627]. Similarly in DCs, like macrophages, activation through a range of stimuli (such as LPS [593], type 1 IFN [628], TLR3 ligand poly (I:C)[628] induces a phenomenon in these cells just like Warburg effect characterised by increased glycolysis and decreased OXPHOS. These changes in metabolic pathways are considered to be essential to providing bio-energetic resources to program new gene expression and protein synthesis during robust cellular proliferation [629, 630]. A recent study has shown that pathogen associated molecular pattern (PAMP) stimulation via TLRs induces metabolic transition in resting immature DCs, is

characterised by transition from OXPHOS and mitochondrial β-oxidation of lipids to glycolysis [593]. On the other hand, some have argued the Warburg effect in DCs is different relative to cancer cells and effector T cells, as it enables DC activation and survival upon TLR stimulation rather than just fuelling cell division. Everts et al. found that NO production that occurs following DC activation inhibits OXPHOS and the switch to glycolysis is to ensure sufficient ATP can be produced [599]. Increased glycolysis is also dependent on PI3K/AKT pathway (latter can activate HK-II) [631]. Elsewhere, AKT is also involved, via influences on SREBP1, in upregulation of fatty acid and cholesterol synthesis and LDLR expression [632]. Along with increased glycolysis and OXPHOS, this study also observed increased mitochondrial mass (measured using MitoTracker™ Green) and membrane potential (measured using MitoTracker Red) in TCM-exposed DCs, that Malinarich also found that tolerogenic treatment of DCs with dexamethasone/vitamin D3 also resulted in increased membrane potential [606]. Interestingly the study also found an increase in mitochondrial mass in LPS treated cells which could be due to increased mitochondrial biogenesis as an effect of LPS via expression of factors responsive to reactive oxygen species, *i.e.* nuclear respiratory factor-1 (NRF-1) and mitochondrial transcription factor-A [612], and increase in Mito-Tracker Red suggesting an increased membrane potential. Exact effects of LPS on the ETC and mitochondrial transcription factors in immune cells is unknown but one of the studies in murine BM derived macrophages has shown that exposure to LPS for 6 h leads to increased expression of cytochrome c oxidase (COX, complex IV of ETC) through phosphorylation of PI3Kinase/AKT pathway leading to recovery of mitochondrial mass and function [633].

Different glycolytic enzymes involved in the glycolytic pathway were examined to determine the underlying mechanisms of increased glycolysis in TCM-exposed DCs. Increased expression of GAPDH and a possible increase in HK-II was seen. HK-II is a key glycolytic enzyme that catalyses the conversion of glucose to glucose-6-phosphate which is the first step in the glycolytic pathway while GAPDH is the sixth enzyme in the glycolytic cycle. Increase in HK-II in response to LPS is consistent with another study showing glycolytic burst in human MoDCs as a result of enhanced expression of HK-II as an effect of LPS [596]. HK-II appeared to be increased in TCM-exposed DCs, but an isolated event showed decreased HK-II, so more

experiments may be needed. The increase in glycolysis observed could be a result of increased expression of these glycolytic enzymes. This result corresponds to other studies in macrophages and lymphoid cells, with similar outcomes [212, 634] Another study has shown that inhibition of HK-II by 2-DG inhibits the activation of DCs [635]. While another study showing inhibition of GAPDH also downregulates glycolysis. [634] This shows the importance of these enzymes (HK-II and GAPDH) in enhanced glycolysis as observed in TCM-exposed DCs in this study.

It will be interesting to look at the effects of mesothelioma on different DC subsets in the future as other studies have shown changes in metabolism in response to TLRs in different subsets of DCs such as conventional (c)DCs (also called myeloid (m)DC1 and (m)DC2) and plasmacytoid (p)DCs. Metabolic profile changes in TLR activated cDCs included increased glycolysis, increased fatty acid synthesis and decreased OXPHOS, while pDCs showed increased OXPHOS and increased fatty acid oxidation (FAO). Similarly, TLR activated GM-CSF BMDCs showed increased rapid glycolysis and increased fatty acid synthesis in association with decreased OXPHOS [636, 637]. However, our understanding of metabolic programming of different DCs subsets especially in TCM-exposed DCs remains limited, future studies will test metabolic reprogramming in human and murine different DC subsets.

To summarise, data presented in this chapter suggests that mesothelioma may render DCs tolerogenic as evidenced by the simultaneous increase of OXPHOS and glycolysis and enhanced membrane potential. This process appeared to be mediated by increased GAPDH and a possible increase in HK-II. An increase in both pathways may be to generate more energy to meet the biosynthetic demands of mesothelioma-activated DCs. Moreover, as discussed in previous chapter, TCM-exposed DCs were found to have higher lipid levels which could be because of changes in lipid metabolism. This lipid loading of DCs could be responsible for decreased anti-tumour responses.

Chapter 6: Final Discussion

This thesis examined changes in murine macrophages and DCs during healthy ageing and cancer (mesothelioma) and looked at metabolic changes in response to mesothelioma-derived factors in DCs in human and mice.

The effect of healthy ageing on macrophages

Healthy ageing is associated with a significant increase in circulating lipid concentration [638]. Thus, tissue macrophages and DCs in healthy elderly hosts may be exposed to elevated lipid levels leading to intracellular lipid accumulation by macrophages and DCs, and several studies have shown that immune cells, including macrophages and DCs, can accumulate lipids [101, 230, 231, 639]. Those studies reported that lipid accumulation is a contributing factor to DC and macrophage dysfunction. Earlier studies by our group examined lipid accumulation by tissue DC subsets with healthy ageing and demonstrated organ specific changes in DC subsets and DC activation status with ageing. Plasmacytoid(p)DCs and $CD8^+$ cDCs contained the highest lipid levels of all DC subsets in young 6-8 week old mice and those levels further increased with healthy ageing up to 22-24 months old [246]. There has been a clear gap in knowledge regarding lipid uptake/levels in different subsets of macrophages and DCs during healthy ageing and when elderly hosts have cancer.

This study examined the effect of healthy ageing on macrophages and DCs as there are publications showing that ageing can compromise antigen presentation, cytokine production, phagocytosis, and ROS production in macrophages [640, 641]. However, a consensus has yet to be reached, as Makinodan et al. and Sondell et al. did not see changes in phagocytic capacity of murine macrophages with age [642, 643] whilst others describe impaired phagocytosis [644, 645]. Murine healthy elderly-derived macrophages have been shown to be less responsive to pro-inflammatory stimuli (LPS and IFN-γ) compared to young-derived macrophages *in-vitro* [646, 647]. Moreover, MHC-II expression has been shown to be downregulated in elderly IFN-γ stimulated BM macrophages compared to young mice [648]. Some studies have demonstrated that ageing can lead to macrophage activation, likely due to elevated cytokines, oxidised low density lipoproteins and immunoglobulins, this has been termed inflammageing [649, 650].

This study looked at different macrophage subsets identified on the basis of Ly6C and CX3CR1 expression, similar to other studies [70, 399, 427, 651, 652]. This thesis looked at 4 different macrophage subsets. Double negative Ly6C and CX3CR1 macrophages are termed M0 cells; M1-like cells are $Ly6C^{+}CX3CR1^{-}$; M2-like cells are $Ly6C^{-}CX3CR1^{+}$; and M3 cells are $Ly6C^{+}CX3CR1^{+}$. M1 or classically activated macrophages constitute the first line of defence. While M2 or alternatively activated macrophages play a role in angiogenesis and fungal, helminthic, and parasitic infections [652, 653]. Several groups [499, 654, 655], including our own [70, 427], have called intermediate M1-M2 macrophages, M3 macrophages. This study found increased MHC-II in BM M1-like macrophages in elderly healthy mice compared to young mice. This was associated with increased expression of the co-stimulatory molecule, CD80, in splenic M1-like and splenic M3 macrophages, although no change in CD80 was observed in BM macrophages. These conflicting results could be due to macrophages isolated from different sites. The data suggests that factors associated with ageing drive more mature pro-inflammatory M1-like macrophages in the BM (a primary lymphoid organ). The BM can supply monocytes and macrophages to the spleen, a secondary lymphoid organ [656, 657]. The increased pro-inflammatory state in elderly BM macrophages could be due to inflammageing. Inflammageing is characterised by increased circulation of pro-inflammatory cytokines [658]. Healthy ageing is associated with tissue microenvironmental changes characterized by marked upregulation of interferon-response pathways and pro-inflammatory cytokines, including TNF and IL-6, that may be caused by increased circulating microbial products due to increased intestinal permeability, leading to release of damage associated molecular pattern molecules (DAMPs), cytosolic DNA and mitochondrial DNA stress [659]. The increase in pro-inflammatory cytokines is due to a number of signalling pathways being involved in inflammaging, such as NF-kB, TOR, RIG-1, Notch, Sirtuins, TGF-B and Ras [660].

CD147 has been shown to correlate with high lipid levels in lipid-loaded macrophages, also called foam cells [661]. CD147 is also involved in de novo lipogenesis which again can contribute to increased lipid accumulation [662]. These data suggest CD147 plays a key role in lipid uptake by cells. CD147 expression increased in BM M2-like and splenic M0 and M2-like) macrophages with healthy ageing, however there was no concomitant increase in lipid levels with healthy ageing. Future studies could

determine the role of CD147 with healthy ageing. One possibility is that CD147 could be saturated as the biological effects it promotes depend on receptor saturation [663]. Blocking CD147 using specific monoclonal antibodies could be a way to look at its role in lipid uptake by macrophages [664]. Another way could be to use CD147 knockout mice [665]. Lipid accumulation by macrophages has been shown in several studies [233, 666] and they can accumulate lipids through other pathways including macropinocytosis, phagocytosis and scavenger receptor-mediated pathways [667]. Macrophages can also take up lipoproteins from dying cells and eliminate cholesterol by reverse cholesterol transport, a key step in macrophage cholesterol efflux [668]. However, an inability to eliminate excess cholesterol may lead to the generation of foam cells [247], as seen in disease settings such as atherosclerosis. To conclude, the first part of the studies indicated that healthy ageing does not lead to increased lipid accumulation in macrophages yet is characterized by a shift towards pro-inflammatory M1 macrophages.

The effect of healthy ageing on DCs

Under normal healthy conditions, DCs are continuously exposed to self-antigens generated as a result of normal cell death. In this case DCs take up antigens but are not activated due to the absence of pathogen-associated molecular pattern molecules (PAMPS) and DAMPS. This leads to T cell tolerance as presentation of self-antigens to T cells is in the absence of costimulatory molecules or other activation signals. However, ageing has been shown to activate DCs likely due to an age-related secretion of higher basal levels of pro-inflammatory cytokines relative to younger hosts [669, 670]. Indeed, Agrawal et al. found increased reactivity of DCs to self-DNA in aged subjects along with reduced uptake of apoptotic cells [671]. This was associated with an increased immune response instead of tolerance to self-antigens, further contributing to inflammageing.

This study examined different DC subsets based upon two different gating strategies. The first strategy looked at broad $CD11c^+$ cells while the other gating strategy targeted $CD11c^+$MHC-II^+ cells and has been used in other studies to classify potent APCs that are more representative of DCs [531-533]. In viral infection and cancer settings the most important DC subset is $CD8^+$ cDCs as they are potent cross-presenting cells that

present cytoplasmic antigens (e.g., viral, self or cancer-derived antigens) on MHC-I molecules to $CD8^+$ T cells. Upon activation they stimulate immune responses and are major producers of IL-12 [110]. Under normal conditions, in the absence of danger signals they help maintain tolerance towards self-antigens [110]. In contrast, pDCs mainly accumulate in lymphoid tissue via circulation, express low levels of MHC-II, the integrin CD11c and co-stimulatory molecules [119] and respond to viral pathogens by secreting large amounts of type 1 IFN [672]. $CD8^-$ cDCs are poor cross-presenters and present extracellular antigens to $CD4^+$ T cells to promote Th2 responses [131]. $CD8^-$ cDCs are further divided into two subsets, $CD8^-CD4^-$ cDCs and $CD8^-CD4^+$ cDCs that are equivalent in their capacity to prime and direct $CD4^+$ and $CD8^+$ T cell differentiation [673].

In-vitro studies have shown that with healthy ageing DCs retain their ability to prime T cells [540, 541]. However, this study found decreased MHC-I expression levels along with a decreased proportion of MHC-I^+ splenic DCs and decreased MHC-II in BM pDCs when gated using the $CD11c^+$MHC-II^+ gate suggesting healthy ageing modulates different tissue microenvironments differently, which could impair the ability of some DCs to stimulate T cells. A key difference is that this was an *in-vivo* study, and no antigen presentation assays were used to confirm the hypothesis that reduced MHC-1 and/or MHC-II compromises the ability of elderly DCs to present antigen to T cells. The literature in this field has not yet reached a consensus and the antigen presenting abilities of aged DCs remain poorly characterised. For example, Grolleau et al have shown that BMDCs in elderly mice retain MHC-I expression [674]. Others have shown that accumulation of oxidised proteins within endosomes may lead to decreased exogenous antigen processing in splenic DCs in elderly mice [675]; this may result in reduced expression of MHC complexes on the cell surface, possibly impairing antigen presentation in elderly [676].

This study also found evidence supporting the studies suggesting T cell priming capability is retained with health ageing. While no changes were observed in MHC-I expression levels in BM DCs using either gating strategy, the proportion of LN $CD11c^+$MHC-$I^+CD8^-CD4^-$ cDCs increased, suggesting maintenance or even an improved ability of DCs to prime $CD8^+$ and $CD4^+$ T cells in LNs with ageing. CD80 increased with ageing in LNs in both $CD11c^+$ cells and pDCs which could be

responsible for activating T cells via CD28 interactions, or for inhibiting T cell responses, as others have demonstrated increased CTLA-4 on T cells with age [677]. Interactions between CTLA-4 and CD80 negatively regulate T cell activation [491-493]. CD80 can bind to both CD28 (to provide co-stimulatory signals required for T cell activation) and CTLA-4 which has a higher affinity for CD80 [678]. The higher affinity binding of CTLA-4 is due to a periodic arrangement in which bivalent homodimers bridge bivalent CD80 molecules [679, 680].

To summarise, there was no effect on lipid levels when gated using the broad $CD11c^+$ cells with healthy ageing in DCs, however increased MHC-II expression was seen in elderly BM DCs ($CD11c^+$ cells, pDCs and $CD11b^+CD8^-CD4^-$ cDCs), splenic ($CD11c^+$ cells and pDCs) and LN DCs ($CD11c^+$ cells and pDCs) compared to young mice suggesting that ageing does not reduce the number of peptide/MHC-II complexes on DCs and therefore may not account for changes to $CD4^+$ T cells with age. In contrast, gating on $CD11c^{high}MHC\text{-}II^{high}$ cell populations found increased lipid content in BM $CD11c^{high}MHC\text{-}II^{high}$ pDCs, BM $CD8^+$ cDCs and LN pDCs with healthy ageing. Increased CD147 was observed only in BM $CD11c^{high}MHC\text{-}II^{high}$ cells suggesting that CD147 could be responsible for increased lipid uptake in this population. Indeed, others have shown that $CD8^+$ and $CD4^+$ T cells show remarkable changes with ageing. Ageing leads to a reduction in the size of the thymus and thymic tissue replacement with fat [681-684], which can lead to reduced thymic output of naïve $CD8^+$ and $CD4^+$ T cells in elderly mice [683, 685-687] and humans [688-691]. Changes to T cells with ageing are well documented. Studies have shown that ageing can result in a reduced T cell repertoire and reduced IL-2 production [692-695]. Li et al showed that as the T cell pool decreases with age, it is accompanied by increases in the CD4 to CD8 ratio in the circulation [696]. For future studies, using an MLR to measure young versus aged $CD4^+$ and $CD8^+$ T cell responses to aged DCs from healthy mice would be one way to test T cell responses. Moreover, increased expression of co-stimulatory CD80 in LN $CD11c^+$ cells and pDCs implies that helper or regulatory $CD4^+$ T cells could be generated by elderly DCs which may induce or impair effector $CD8^+$ T cells.

The combined effect of mesothelioma and ageing on macrophages

The study also looked at the combined effect of mesothelioma with age in macrophages and DCs and confirmed lipid accumulation in murine macrophages, and in human and murine DCs (discussed later) with age and cancer, the latter reported by others [233, 235, 486, 552]. This appears to be the first study looking at lipid accumulation in macrophages in aged hosts with mesothelioma.

The first set of studies showed that mesothelioma-derived factors lead to lipid accumulation in murine macrophages *in-vitro* as well as decreased MHC-I and MHC-II expression in young adult mice. These data suggest reduced numbers of peptide/MHC complexes on young macrophages which might impair their ability to present tumour antigen to $CD8^+$ and $CD4^+$ T cells. MHC downregulation or loss is a mechanism used by tumours to escape from T lymphocytes [697-700] and tumour-derived factors may influence macrophages to downregulate MHC on their cell surface. A similar pattern was observed *in-vivo* in murine macrophages with ageing and mesothelioma. This study found increased lipid accumulation in BM M0, BM M1-like macrophage, splenic M1-like macrophages and tumour associated M1-like and M3 macrophages implying that tumour-derived factors reach and modulate immune cells in the BM and spleen. Ageing and cancer are considered to be highly correlated [701] and senescent cells that accumulate as a result of ageing can be pro-tumorigenic (as shown in Figure 6.1) [701].

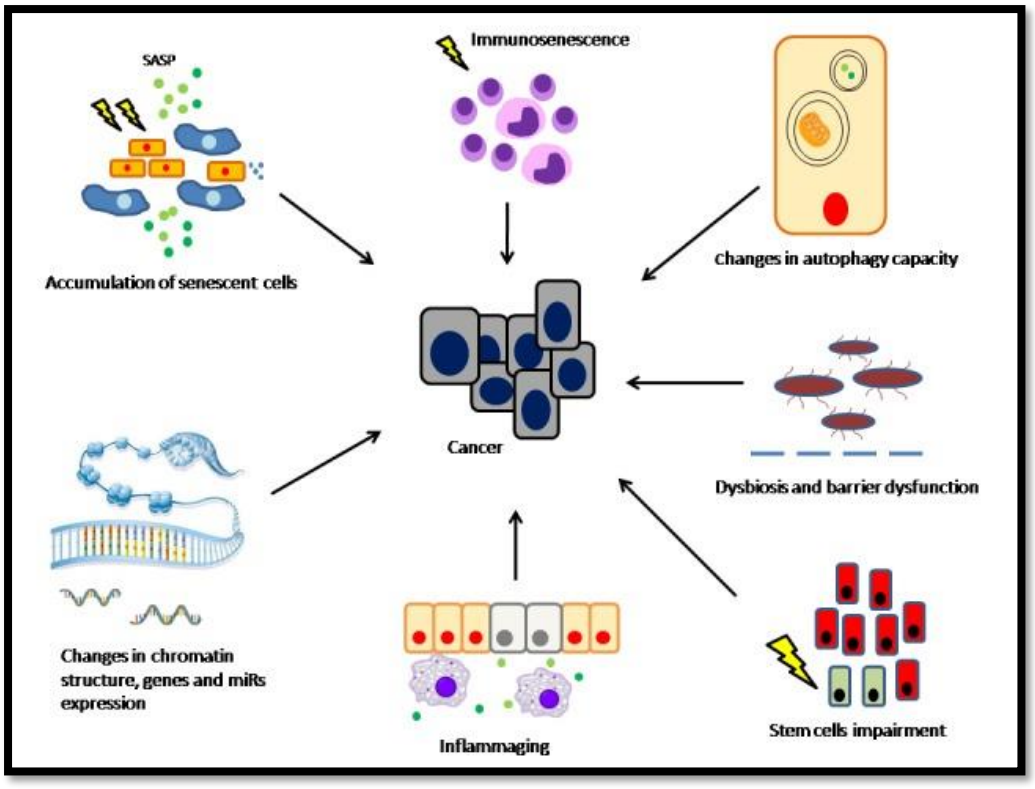

Figure 6.1 Cancer and ageing involve a unique inflammatory network which joins multiple processes. Ageing can lead to changes in chromatin function, autophagy (reduction), the microbiome and intestinal barrier function, thus creating a pro-tumorigenic environment [701]. **Image from:** Cancer and Aging - the Inflammatory Connection.

There is evidence that tumours can directly alter the host hematopoietic system and induce biased differentiation of myeloid cells to favour tumour growth [702]. Different haematopoietic cytokines such as placental growth factor (PlGF) [703, 704], granulocyte/macrophage colony-stimulating factor (GM-CSF) [705], macrophage colony-stimulating factor (M-CSF) [706], vascular endothelial growth factor A (VEGF-A) [703, 707], transforming growth factor-β (TGF-β) [707], osteopontin [708, 709] and tumour necrosis factor-α (TNF-α) [707, 710] are secreted by a variety of tumours that affect the BM. This is supported by Han et al who showed that tumours can induce immunosuppressive, inflammatory changes in distant organs [477], and spleens are often found to be enlarged in tumour bearing hosts [478]. Different studies have shown that tumours secrete VEGF [711], prostaglandins [712], GM-CSF [713], gangliosides [714], IL-10 [715], IL-6 [716], and TGF-B [717] leading to abnormal DC

differentiation. Mesothelioma has been shown to secrete VEGF, angiogenin, and TGF-B that can lead to immune suppression [718]

This study observed increased lipid accumulation in BM M0 and M1-like macrophages and splenic M1-like macrophages in mesothelioma bearing elderly mice relative to healthy elderly mice. This was associated with increased CD147 in splenic M0 and M1-like macrophages that might account for elevated lipids in these elderly mice with mesothelioma.

Increased expression of MHC-II was seen in M1-like BM macrophage subsets with age and mesothelioma, whilst no change was observed in MHC-II expression in splenic macrophages. Increased proportions of MHC-I BM M0 macrophages were observed in tumour bearing old mice compared to young healthy mice, while increased expression of MHC-I was observed in BM M0 and M1-like macrophages in tumour bearing old mice compared to tumour bearing young mice. These data suggest mesothelioma may not impair antigen presentation in central and secondary lymphoid organs.

The combined effect of mesothelioma and ageing on tumour associated macrophages

This study demonstrated significantly increased lipid levels in elderly tumour associated macrophages compared to young tumour-associated macrophages (shown by bodipy staining) and reduced MHC-I and MHC-II suggesting mesothelioma along with ageing could be responsible for intratumoural macrophage dysfunction. The increase in lipid content observed in tumour-associated macrophages could also be because of lipid biosynthesis as seen in the cancer setting in TAMs [488], further contributing to their pro-tumoural functional characteristics by increasing ROS production leading to tumour cell growth. This was supported by a recent study using transcriptome and metabolome analyses [719] and showed enhanced lipid content in macrophages in a human co-culture model using thyroid carcinoma cell line and monocytes isolated from PBMCs [488].

The effect of mesothelioma and ageing on BM, splenic and LN DCs

Mesothelioma led to increased lipid levels in all subsets of BM $CD11c^{high}MHC\text{-}II^{high}$ DCs in elderly mice, which was accompanied by reduced MHC-I and MHC-II compared to healthy elderly mice. Mesothelioma induced distal effects in BM, dLN and splenic DCs with ageing, as MHC-I downregulated in splenic $CD11c^{+}$ cells and

splenic pDCs in elderly tumour bearing mice compared to young tumour bearing mice. MHC-II expression was also decreased in splenic $CD11c^{+}MHC\text{-}II^{+}$ DCs, splenic $CD8^{+}$ cDCs, BM pDCs and tumour associated $CD8^{+}$ cDCs in elderly mice with mesothelioma compared to young mice with mesothelioma. This is likely to impair the ability of DCs in elderly mice with mesothelioma to present tumour antigen to $CD8^{+}$ T and $CD4^{+}$ T cells .

Age-related distal effects were seen in elderly mice with mesothelioma in which elderly BM $CD8^{+}$ cDCs showed reduced MHC-I expression compared to healthy elderly mice. A decreased percentage of BM $MHC\text{-}I^{+}$ pDCs in old relative to young tumour-bearing mice was also observed. These data suggest that whilst healthy ageing does not affect the BM microenvironment in terms of MHC-I expression, mesothelioma-derived factors downregulate MHC-I on BM pDCs and $CD8^{+}$ cDCs.

In spleens, MHC-I expression decreased in $CD11c^{+}$ DCs, pDCs, $CD4^{-}$ cDCs and $CD4^{+}$ cDCs with age and tumour, suggesting mesothelioma-derived factors further affect the splenic microenvironment and downregulate MHC-I on DCs.

In dLN, the presence of mesothelioma decreased $MHC\text{-}I^{+}CD8^{+}$ dLN cDCs with ageing suggesting decreased capacity to present antigen to $CD8^{+}$ T cells with mesothelioma and ageing.

The combined effect of mesothelioma and ageing on tumour associated DCs

Mesothelioma led to increased lipid levels in tumour associated $CD8^{+}$ cDCs and reduced MHC-II expression in all DC subsets in elderly tumour bearing mice compared to young mice with mesothelioma. The proportion of $MHC\text{-}I^{+}$ pDCs significantly reduced in elderly tumours relative to young tumours. All other elderly DC subsets followed a similar trend in terms of MHC-I expression levels compared to young tumour bearing mice and in the proportions of DCs positive for MHC-I, but the data did not reach statistical significance. This slight decrease in $MHC\text{-}I^{+}$ tumour-associated DCs may represent a strategy used by tumours to escape CTL recognition, especially if these DC migrate to LNs. However, the data also shows that MHC-II expression levels in $CD8^{+}$ cDCs in tumour draining LNs in young mice increased compared to young healthy mice suggesting that CTL responses can still be generated in young mice with mesothelioma. Nonetheless, even if tumour-specific T cells are activated and expanded in the dLNs, tumours can still escape CTL killing through

antigenic loss, mutation or failure to process and present tumour antigen on MHC molecules [720] [721]. With ageing tumour-associated $CD8^-$ cDCs showed reduced MHC-II expression levels compared to young tumour associated DCs along with a reduced proportion of $CD8^-$ cDCs in elderly tumour associated DCs. The tumour microenvironment contains a variety of cytokines and soluble factors that can dampen DC differentiation, activation, proliferation, and migration, as well impairing the effector function of T cells. Such factors include IL-10, IL-6, M-CSF, VEGF and TGF-β [722]. As discussed above, mesothelioma secretes VEGF, angiogenin and TGF-β that can suppress DC function [718]. Cancer cells can also acquire resistance to apoptosis to escape CTL killing [723] and human mesothelioma cells lines such as HuT 28, LRK1A and REN have been shown to be resistant to apoptosis [724]. Failure of normal apoptosis can lead to cancer progression and enhance resistance to therapy. Finally, death receptor ligands (such as Fas ligand) may be expressed by tumours to eliminate tumour specific T cells [725]. This has been reported in mesothelioma through use of a human mesothelioma cell line (H2373) xenograft in nude mice that showed increased Fas expression *in-vivo* [726] which can lead to killing of tumour-specific CTLs [727].

The effect of mesothelioma on metabolic OXPHOS and glycolysis in DCs

This study also looked at changes in the metabolic status of DCs in response to mesothelioma derived factors. Dysregulated metabolic programs have been shown to cause lipid accumulation in cancer cells to enable survival and meet bioenergetic demands, the same is likely true for immune cells [728]. In various cancer types, such as lymphoma, melanoma, colon, mammary adenocarcinoma, ovarian cancer and mesothelioma, there is evidence that mouse and human tumour infiltrating myeloid cells accumulate intracellular lipids, leading to dysfunction in anti-tumour immunity [198, 528, 729-733]. The scavenger receptor MSR1 can import and accumulate lipids in the intracellular spaces of tumour resident cDCs [486]. In various tumour types, abnormal lipid accumulation via MSR1 diminished the antigen presentation capacity of cDCs [486]. This study found that mesothelioma derived factors led to a simultaneous increase in OXPHOS and glycolysis in human DCs which has been associated with the metabolic profile of tolerogenic DCs [606]. Thus, suggesting that mesothelioma may render DCs tolerogenic. This could be because of changes

observed in the glycolytic enzymes Hexokinase-II and GAPDH. A switch to glycolytic metabolism is generally consistent with fatty acid metabolism and immune cell activation, whilst lipogenesis is thought to promote quiescence [734, 735]. However, lipids play a complex biological/physiological role and determining the role of lipid accumulation in DC function in the context of mesothelioma requires further investigation. Upon DC maturation and especially after LPS exposure, DCs take on a lacy appearance consisting of fat and glycogen containing lipid bodies [736]. These high lipid DCs accumulate lipids via high levels of scavenger receptors including macrophage receptor with collagenase structure/macrophage scavenger receptor 1 (MARCO/MSR1) [736]. Lipids not only serve as building blocks for many facets of DC biology but also play an important role in the ability of DC to process and present antigens. MHC-I cross presentation, critical for the generation of tumour-specific $CD8^+$ T cells, is highly dependent upon lipid body assembly, as diacylglycerol acyl-transferase inhibitors that prevent triacylglycerol accumulation disrupt MHC-I cross presenting ability [737]. Bourgneres et al. showed that DCs with an elevated lipid content had a reduced capacity to cross present antigens [738]. Lipid levels normalised using a pharmacological inhibitor of acetyl-CoA carboxylase-1 (ACC-1), an enzyme that plays a key role in lipogenesis, restored the functional activity of lipid laden DCs [738]. In the context of cancer, Herber and colleagues, demonstrated increased lipid levels, especially triacylglycerol, in DCs during progression of lymphoma, breast and colon cancer in patients and in preclinical mouse models [486]. Increased lipid accumulation was a consequence of lipid uptake via upregulated scavenger receptor A (SRA, MSR1/CD204). The effect of different types of lipids (such as short chain versus long chain fatty acids) remains to be explored on DC subsets in mesothelioma. Fatty acids can also be transported into the mitochondria, aside from just being stored in lipid droplets and oxidised into acetyl-CoA by fatty acid oxidation (FAO). Carnitine palmitoyltransferase I (Cpt1) mediate this transport of fatty acids into the mitochondria [739].

Mitochondrial metabolism may influence T cell priming by DCs, as suppression of FAO can limit expression of the co-stimulatory molecule, CD86 [740], suggesting that for DC function, it is important to have coordinated actions of mitochondrial and fatty acid metabolism. FAO can also produce increased levels of citrate from the TCA cycle for de novo fatty acid synthesis and lipid droplet formation [741]. FAO has shown to

be higher in tolerogenic DCs [606] and inhibiting FAO could restore DC function that can be useful for clinical treatment of mesothelioma.

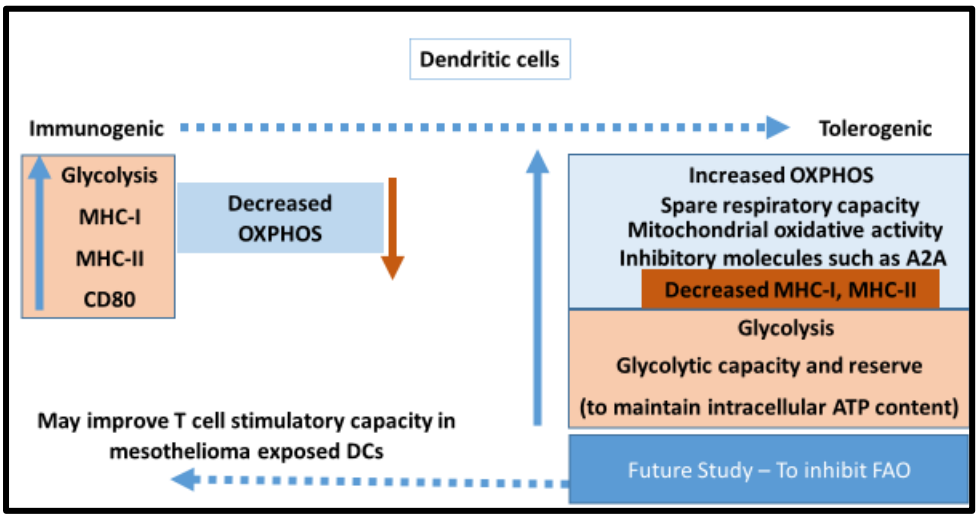

Figure 6.2: Graphical summary representing metabolic changes in DCs

To summarise, this study found that mesothelioma upregulates CD147 expression, which is associated with lipid accumulation in macrophages, but not in DCs. Other lipid uptake markers would be interesting to examine, as increased lipid uptake was observed in *in-vitro* murine studies and the *in-vivo* murine studies suggested tumour-associated DCs may acquire increased lipid with age. Lipid uptake was not associated with changes to CD80 and CD40 expression in macrophages or DCs. However, lipid uptake was associated with decreased MHC-I and MHC-II in all TAMs and tumour-associated DC subsets, suggesting a reduced capacity to activate tumour infiltrating $CD8^+$ and $CD4^+$ T cells, thereby providing an advantage for mesothelioma tumours in elderly hosts. DCs exposed to mesothelioma-derived factors simultaneously upregulated glycolysis and OXPHOS, this fits the metabolic profile of tolerogenic DCs, as previously described [606, 741]. Tolerogenic DCs can also be defined as those with increased expression of inhibitory molecules. Earlier *in-vivo* studies in our group found up-regulated expression of inhibitory molecules, such as CD73, CD39, A2A and A2B receptors, as well as programmed cell death ligand-1 (PD-L1) on DCs in mesothelioma-bearing young and elderly mice confirming the skewing of DCs towards a tolerogenic profile in mesothelioma exposed DCs [527].

References:

1. Carbone, M. and H. Yang, *Mesothelioma: recent highlights.* Annals of translational medicine, 2017. **5**(11): p. 238-238.
2. Ahmed, I., S. Ahmed Tipu, and S. Ishtiaq, *Malignant mesothelioma.* Pakistan journal of medical sciences, 2013. **29**(6): p. 1433-1438.
3. Bibby, A.C., et al., *Malignant pleural mesothelioma: an update on investigation, diagnosis and treatment.* European Respiratory Review, 2016. **25**(142): p. 472.
4. Rossini, M., et al., *New Perspectives on Diagnosis and Therapy of Malignant Pleural Mesothelioma.* Frontiers in oncology, 2018. **8**: p. 91-91.
5. Sekido, Y., *Molecular pathogenesis of malignant mesothelioma.* Carcinogenesis, 2013. **34**(7): p. 1413-9.
6. Treasure, T., et al., *Extra-pleural pneumonectomy versus no extra-pleural pneumonectomy for patients with malignant pleural mesothelioma: clinical outcomes of the Mesothelioma and Radical Surgery (MARS) randomised feasibility study.* The Lancet. Oncology, 2011. **12**(8): p. 763-772.
7. Patel, S.C. and J.E. Dowell, *Modern management of malignant pleural mesothelioma.* Lung Cancer (Auckland, N.Z.), 2016. **7**: p. 63-72.
8. Hasegawa, S., *Extrapleural pneumonectomy or pleurectomy/decortication for malignant pleural mesothelioma.* General thoracic and cardiovascular surgery, 2014. **62**(9): p. 516-521.
9. Dixit, R., et al., *Diagnosis and management options in malignant pleural effusions.* Lung India : official organ of Indian Chest Society, 2017. **34**(2): p. 160-166.
10. Clive, A.O., et al., *Prophylactic radiotherapy for the prevention of procedure-tract metastases after surgical and large-bore pleural procedures in malignant pleural mesothelioma (SMART): a multicentre, open-label, phase 3, randomised controlled trial.* The Lancet. Oncology, 2016. **17**(8): p. 1094-1104.
11. Vogelzang, N.J., et al., *Phase III study of pemetrexed in combination with cisplatin versus cisplatin alone in patients with malignant pleural mesothelioma.* J Clin Oncol, 2003. **21**(14): p. 2636-44.
12. Chee, S.J., et al., *Evaluating the effect of immune cells on the outcome of patients with mesothelioma.* British journal of cancer, 2017. **117**(9): p. 1341-1348.
13. Nelson, D., S. Fisher, and B. Robinson, *The "Trojan Horse" approach to tumor immunotherapy: targeting the tumor microenvironment.* J Immunol Res, 2014. **2014**: p. 789069.
14. Jackaman, C., D.E. Dye, and D.J. Nelson, *IL-2/CD40-activated macrophages rescue age and tumor-induced T cell dysfunction in elderly mice.* Age (Dordr), 2014. **36**(3): p. 9655.
15. Dozier, J., H. Zheng, and P.S. Adusumilli, *Immunotherapy for malignant pleural mesothelioma: current status and future directions.* Translational lung cancer research, 2017. **6**(3): p. 315-324.
16. Bakker, E., et al., *Immunotherapy advances for mesothelioma treatment.* Expert Rev Anticancer Ther, 2017. **17**(9): p. 799-814.
17. Bograd, A.J., et al., *Immune responses and immunotherapeutic interventions in malignant pleural mesothelioma.* Cancer Immunol Immunother, 2011. **60**(11): p. 1509-27.
18. Anraku, M., et al., *Impact of tumor-infiltrating T cells on survival in patients with malignant pleural mesothelioma.* J Thorac Cardiovasc Surg, 2008. **135**(4): p. 823-9.
19. Yamada, N., et al., *CD8+ tumor-infiltrating lymphocytes predict favorable prognosis in malignant pleural mesothelioma after resection.* Cancer Immunol Immunother, 2010. **59**(10): p. 1543-9.

20. Ujiie, H., et al., *The tumoral and stromal immune microenvironment in malignant pleural mesothelioma: A comprehensive analysis reveals prognostic immune markers.* Oncoimmunology, 2015. **4**(6): p. e1009285.
21. Kalinski, P., R. Muthuswamy, and J. Urban, *Dendritic cells in cancer immunotherapy: vaccines and combination immunotherapies.* Expert review of vaccines, 2013. **12**(3): p. 285-295.
22. Banchereau, J., et al., *Dendritic cells: controllers of the immune system and a new promise for immunotherapy.* Ann N Y Acad Sci, 2003. **987**: p. 180-7.
23. Sabado, R.L., S. Balan, and N. Bhardwaj, *Dendritic cell-based immunotherapy.* Cell Research, 2017. **27**(1): p. 74-95.
24. Hegmans, J.P., et al., *Immunotherapy of murine malignant mesothelioma using tumor lysate-pulsed dendritic cells.* Am J Respir Crit Care Med, 2005. **171**(10): p. 1168-77.
25. Tan, Z., et al., *Antimesothelioma Immunotherapy by CTLA-4 Blockade Depends on Active PD1-Based TWIST1 Vaccination.* Molecular therapy oncolytics, 2020. **16**: p. 302-317.
26. Guazzelli, A., et al., *Anti-CTLA-4 therapy for malignant mesothelioma.* Immunotherapy, 2017. **9**(3): p. 273-280.
27. Jackaman, C., et al., *Deliberately provoking local inflammation drives tumors to become their own protective vaccine site.* Int Immunol, 2008. **20**(11): p. 1467-79.
28. Jackaman, C., et al., *Murine mesothelioma induces locally-proliferating IL-10(+)TNF-α(+)CD206(-)CX3CR1(+) M3 macrophages that can be selectively depleted by chemotherapy or immunotherapy.* Oncoimmunology, 2016. **5**(6): p. e1173299.
29. Malignant mesothelioma: Number of deaths by sex, race, age group, and median age at death, U.S. residents age 15 and over, 2001–2010 2014; Available from: https://wwwn.cdc.gov/eWorld/Data/Malignant_mesothelioma_Number_of_deaths_by_sex_race_age_group_and_median_age_at_death_US_residents_age_15_and_over_20052014/799.
30. Duong, L., et al., *Macrophage Depletion in Elderly Mice Improves Response to Tumor Immunotherapy, Increases Anti-tumor T Cell Activity and Reduces Treatment-Induced Cachexia.* Frontiers in genetics, 2018. **9**: p. 526-526.
31. Marshall, J.S., et al., *An introduction to immunology and immunopathology.* Allergy, asthma, and clinical immunology : official journal of the Canadian Society of Allergy and Clinical Immunology, 2018. **14**(Suppl 2): p. 49-49.
32. Padbury, J.F., *Skin—the first line of defense.* The Journal of Pediatrics, 2008. **152**(6): p. A2.
33. Turvey, S.E. and D.H. Broide, *Innate immunity.* The Journal of allergy and clinical immunology, 2010. **125**(2 Suppl 2): p. S24-S32.
34. Ito, T., et al., *The linkage of innate and adaptive immune response during granulomatous development.* Frontiers in immunology, 2013. **4**: p. 10-10.
35. Ginhoux, F., M. Guilliams, and S.H. Naik, *Editorial: Dendritic Cell and Macrophage Nomenclature and Classification.* Frontiers in immunology, 2016. **7**: p. 168-168.
36. Epelman, S., K.J. Lavine, and G.J. Randolph, *Origin and functions of tissue macrophages.* Immunity, 2014. **41**(1): p. 21-35.
37. Moberg, C.L., *An appreciation of Ralph Marvin Steinman (1943–2011).* Journal of Experimental Medicine, 2011. **208**(12): p. 2337-2342.
38. Steinman, R.M. and Z.A. Cohn, *Identification of a novel cell type in peripheral lymphoid organs of mice. I. Morphology, quantitation, tissue distribution.* The Journal of experimental medicine, 1973. **137**(5): p. 1142-1162.
39. Naik, S.H., *Demystifying the development of dendritic cell subtypes, a little.* Immunol Cell Biol, 2008. **86**(5): p. 439-52.

40. Perie, L. and S.H. Naik, *Toward defining a 'lineage'--The case for dendritic cells.* Semin Cell Dev Biol, 2015. **41**: p. 3-8.
41. Elhelu, M.A., *The role of macrophages in immunology.* Journal of the National Medical Association, 1983. **75**(3): p. 314-317.
42. Beutler, B., *The Toll-like receptors: analysis by forward genetic methods.* Immunogenetics, 2005. **57**(6): p. 385-92.
43. Glass, C.K. and G. Natoli, *Molecular control of activation and priming in macrophages.* Nature immunology, 2015. **17**(1): p. 26-33.
44. Mantovani, A., et al., *The chemokine system in diverse forms of macrophage activation and polarization.* Trends Immunol, 2004. **25**(12): p. 677-86.
45. Baccarini, M., et al., *IFN-gamma/lipopolysaccharide activation of macrophages is associated with protein kinase C-dependent down-modulation of the colony-stimulating factor-1 receptor.* The Journal of Immunology, 1992. **149**(8): p. 2656.
46. Zhang, M.-Z., et al., *IL-4/IL-13-mediated polarization of renal macrophages/dendritic cells to an M2a phenotype is essential for recovery from acute kidney injury.* Kidney international, 2017. **91**(2): p. 375-386.
47. *Macrophages: Origin, Functions and Biointervention*. 2017.
48. Mosser, D.M. and J.P. Edwards, *Exploring the full spectrum of macrophage activation.* Nature reviews. Immunology, 2008. **8**(12): p. 958-969.
49. Martinez, F.O., et al., *Macrophage activation and polarization.* Front Biosci, 2008. **13**: p. 453-61.
50. Sironi, M., et al., *Differential regulation of chemokine production by Fcgamma receptor engagement in human monocytes: association of CCL1 with a distinct form of M2 monocyte activation (M2b, Type 2).* J Leukoc Biol, 2006. **80**(2): p. 342-9.
51. Martinez, F.O. and S. Gordon, *The M1 and M2 paradigm of macrophage activation: time for reassessment.* F1000prime reports, 2014. **6**: p. 13-13.
52. Leopold Wager, C.M. and F.L. Wormley, *Classical versus alternative macrophage activation: the Ying and the Yang in host defense against pulmonary fungal infections.* Mucosal Immunology, 2014. **7**(5): p. 1023-1035.
53. Gordon, S., *Alternative activation of macrophages.* Nature Reviews Immunology, 2003. **3**(1): p. 23-35.
54. Palma, A., et al., *Gene Regulatory Network Modeling of Macrophage Differentiation Corroborates the Continuum Hypothesis of Polarization States.* Front Physiol, 2018. **9**: p. 1659.
55. Chan, G., M.T. Nogalski, and A.D. Yurochko, *Human Cytomegalovirus Stimulates Monocyte-to-Macrophage Differentiation via the Temporal Regulation of Caspase 3.* Journal of Virology, 2012. **86**(19): p. 10714.
56. Bi, Y., et al., *M2 Macrophages as a Potential Target for Antiatherosclerosis Treatment.* Neural plasticity, 2019. **2019**: p. 6724903-6724903.
57. Jackaman, C., et al., *Targeting macrophages rescues age-related immune deficiencies in C57BL/6J geriatric mice.* Aging Cell, 2013. **12**(3): p. 345-357.
58. Wynn, T.A., A. Chawla, and J.W. Pollard, *Macrophage biology in development, homeostasis and disease.* Nature, 2013. **496**(7446): p. 445-455.
59. Dai, X.M., et al., *Targeted disruption of the mouse colony-stimulating factor 1 receptor gene results in osteopetrosis, mononuclear phagocyte deficiency, increased primitive progenitor cell frequencies, and reproductive defects.* Blood, 2002. **99**(1): p. 111-20.
60. Tushinski, R.J., et al., *Survival of mononuclear phagocytes depends on a lineage-specific growth factor that the differentiated cells selectively destroy.* Cell, 1982. **28**(1): p. 71-81.

61. Gordon, S., *Alternative activation of macrophages.* Nat Rev Immunol, 2003. **3**(1): p. 23-35.
62. Cicchese, J.M., et al., *Dynamic balance of pro- and anti-inflammatory signals controls disease and limits pathology.* Immunological reviews, 2018. **285**(1): p. 147-167.
63. Krausgruber, T., et al., *IRF5 promotes inflammatory macrophage polarization and TH1-TH17 responses.* Nature Immunology, 2011. **12**: p. 231.
64. Kayagaki, N., et al., *Noncanonical inflammasome activation by intracellular LPS independent of TLR4.* Science, 2013. **341**(6151): p. 1246-9.
65. McNally, A.K., K.M. DeFife, and J.M. Anderson, *Interleukin-4-induced macrophage fusion is prevented by inhibitors of mannose receptor activity.* The American journal of pathology, 1996. **149**(3): p. 975-985.
66. Chéné, A.-L., et al., *Pleural Effusions from Patients with Mesothelioma Induce Recruitment of Monocytes and Their Differentiation into M2 Macrophages.* Journal of Thoracic Oncology, 2016. **11**(10): p. 1765-1773.
67. Sheikhpour, E., et al., *A Survey on the Role of Interleukin-10 in Breast Cancer: A Narrative.* Reports of biochemistry & molecular biology, 2018. **7**(1): p. 30-37.
68. Acuner-Ozbabacan, E.S., et al., *The structural network of Interleukin-10 and its implications in inflammation and cancer.* BMC Genomics, 2014. **15 Suppl 4**: p. S2.
69. Hashimoto, S., et al., *Serial analysis of gene expression in human monocytes and macrophages.* Blood, 1999. **94**(3): p. 837-44.
70. Jackaman, C., et al., *Murine mesothelioma induces locally-proliferating IL-10(+)TNF-alpha(+)CD206(-)CX3CR1(+) M3 macrophages that can be selectively depleted by chemotherapy or immunotherapy.* Oncoimmunology, 2016. **5**(6): p. e1173299.
71. Kalish, S.V., et al., *[Reprogrammed M1 macrophages with inhibited STAT3, STAT6 and/or SMAD3 extends lifespan of mice with experimental carcinoma].* Patol Fiziol Eksp Ter, 2017. **61**(2): p. 4-9.
72. Pathria, P., T.L. Louis, and J.A. Varner, *Targeting Tumor-Associated Macrophages in Cancer.* Trends Immunol, 2019. **40**(4): p. 310-327.
73. Atanasov, G., et al., *TIE2-expressing monocytes and M2-polarized macrophages impact survival and correlate with angiogenesis in adenocarcinoma of the pancreas.* Oncotarget, 2018. **9**(51): p. 29715-29726.
74. Gartrell, R.D., et al., *Quantitative Analysis of Immune Infiltrates in Primary Melanoma.* Cancer Immunol Res, 2018. **6**(4): p. 481-493.
75. Zhang, W.-j., et al., *Tumor-associated macrophages correlate with phenomenon of epithelial-mesenchymal transition and contribute to poor prognosis in triple-negative breast cancer patients.* Journal of Surgical Research, 2018. **222**: p. 93-101.
76. Sørensen, M.D., et al., *Tumour-associated microglia/macrophages predict poor prognosis in high-grade gliomas and correlate with an aggressive tumour subtype.* Neuropathology and Applied Neurobiology, 2018. **44**(2): p. 185-206.
77. Hu, Y., et al., *Seasonal dynamics and microgeographical spatial heterogeneity of malaria along the China–Myanmar border.* Acta Tropica, 2016. **157**: p. 12-19.
78. Wang, H., et al., *High numbers of CD68+ tumor-associated macrophages correlate with poor prognosis in extranodal NK/T-cell lymphoma, nasal type.* Ann Hematol, 2015. **94**(9): p. 1535-44.
79. Kaneda, M.M., et al., *PI3Kγ is a molecular switch that controls immune suppression.* Nature, 2016. **539**: p. 437.
80. Klemperer, P. and B.R. Coleman, *Primary neoplasms of the pleura. A report of five cases.* Am J Ind Med, 1992. **22**(1): p. 1-31.
81. Eisenstadt, H.B. and F.W. Wilson, *Primary malignant mesothelioma of the pleura.* J Lancet, 1960. **80**: p. 511-4.

82. Davis, J.M., *The histopathology and ultrastructure of pleural mesotheliomas produced in the rat by injections of crocidolite asbestos.* British journal of experimental pathology, 1979. **60**(6): p. 642-652.
83. Moalli, P.A., et al., *Acute injury and regeneration of the mesothelium in response to asbestos fibers.* Am J Pathol, 1987. **128**(3): p. 426-45.
84. Shin, M.L. and H.I. Firminger, *Acute and chronic effects of intraperitoneal injection of two types of asbestos in rats with a study of the histopathogenesis and ultrastructure of resulting mesotheliomas.* The American journal of pathology, 1973. **70**(3): p. 291-313.
85. Wagner, J.C. and G. Berry, *Mesotheliomas in rats following inoculation with asbestos.* British journal of cancer, 1969. **23**(3): p. 567-581.
86. Mossman, B.T. and A. Churg, *Mechanisms in the pathogenesis of asbestosis and silicosis.* Am J Respir Crit Care Med, 1998. **157**(5 Pt 1): p. 1666-80.
87. Hansen, K. and B.T. Mossman, *Generation of superoxide (O2-.) from alveolar macrophages exposed to asbestiform and nonfibrous particles.* Cancer Res, 1987. **47**(6): p. 1681-6.
88. Dostert, C., et al., *Innate immune activation through Nalp3 inflammasome sensing of asbestos and silica.* Science, 2008. **320**(5876): p. 674-7.
89. Tanaka, S., et al., *Asbestos inhalation induces reactive nitrogen species and nitrotyrosine formation in the lungs and pleura of the rat.* J Clin Invest, 1998. **102**(2): p. 445-54.
90. Choe, N., et al., *Pleural macrophage recruitment and activation in asbestos-induced pleural injury.* Environ Health Perspect, 1997. **105 Suppl 5**: p. 1257-60.
91. Bograd, A.J., et al., *Immune responses and immunotherapeutic interventions in malignant pleural mesothelioma.* Cancer immunology, immunotherapy : CII, 2011. **60**(11): p. 1509-1527.
92. Izzi, V., et al., *Immunity and malignant mesothelioma: from mesothelial cell damage to tumor development and immune response-based therapies.* Cancer Lett, 2012. **322**(1): p. 18-34.
93. Heusinkveld, M. and S.H. van der Burg, *Identification and manipulation of tumor associated macrophages in human cancers.* J Transl Med, 2011. **9**: p. 216.
94. Demetri, G.D., et al., *Expression of colony-stimulating factor genes by normal human mesothelial cells and human malignant mesothelioma cells lines in vitro.* Blood, 1989. **74**(3): p. 940-6.
95. Schmitter, D., et al., *Hematopoietic growth factors secreted by seven human pleural mesothelioma cell lines: interleukin-6 production as a common feature.* Int J Cancer, 1992. **51**(2): p. 296-301.
96. Schmid, M.C. and J.A. Varner, *Myeloid cells in the tumor microenvironment: modulation of tumor angiogenesis and tumor inflammation.* J Oncol, 2010. **2010**: p. 201026.
97. Bremnes, R.M., et al., *The role of tumor-infiltrating immune cells and chronic inflammation at the tumor site on cancer development, progression, and prognosis: emphasis on non-small cell lung cancer.* J Thorac Oncol, 2011. **6**(4): p. 824-33.
98. Ujiie, H., et al., *The tumoral and stromal immune microenvironment in malignant pleural mesothelioma: A comprehensive analysis reveals prognostic immune markers.* Oncoimmunology, 2015. **4**(6): p. e1009285-e1009285.
99. Chang, Y.C., et al., *Epigenetic control of MHC class II expression in tumor-associated macrophages by decoy receptor 3.* Blood, 2008. **111**(10): p. 5054-63.
100. Georgoudaki, A.-M., et al., *Reprogramming Tumor-Associated Macrophages by Antibody Targeting Inhibits Cancer Progression and Metastasis.* Cell Reports, 2016. **15**(9): p. 2000-2011.

101. Herber, D.L., et al., *Lipid accumulation and dendritic cell dysfunction in cancer.* Nature medicine, 2010. **16**(8): p. 880-886.
102. Katsnelson, A., *Kicking off adaptive immunity: the discovery of dendritic cells.* The Journal of experimental medicine, 2006. **203**(7): p. 1622-1622.
103. Howard, C.J., et al., *The role of dendritic cells in shaping the immune response.* Anim Health Res Rev, 2004. **5**(2): p. 191-5.
104. Banchereau, J., et al., *Immunobiology of dendritic cells.* Annu Rev Immunol, 2000. **18**: p. 767-811.
105. Merad, M., et al., *The dendritic cell lineage: ontogeny and function of dendritic cells and their subsets in the steady state and the inflamed setting.* Annu Rev Immunol, 2013. **31**: p. 563-604.
106. Shortman, K. and Y.J. Liu, *Mouse and human dendritic cell subtypes.* Nat Rev Immunol, 2002. **2**(3): p. 151-61.
107. Fogg, D.K., et al., *A clonogenic bone marrow progenitor specific for macrophages and dendritic cells.* Science, 2006. **311**(5757): p. 83-7.
108. Puhr, S., et al., *Dendritic cell development-History, advances, and open questions.* Semin Immunol, 2015. **27**(6): p. 388-96.
109. Onai, N., et al., *Flt3 in regulation of type I interferon-producing cell and dendritic cell development.* Ann N Y Acad Sci, 2007. **1106**: p. 253-61.
110. Shortman, K. and W.R. Heath, *The CD8+ dendritic cell subset.* Immunol Rev, 2010. **234**(1): p. 18-31.
111. Helft, J., et al., *Origin and functional heterogeneity of non-lymphoid tissue dendritic cells in mice.* Immunol Rev, 2010. **234**(1): p. 55-75.
112. Colonna, M., G. Trinchieri, and Y.J. Liu, *Plasmacytoid dendritic cells in immunity.* Nat Immunol, 2004. **5**(12): p. 1219-26.
113. Reizis, B., et al., *Plasmacytoid dendritic cells: recent progress and open questions.* Annu Rev Immunol, 2011. **29**: p. 163-83.
114. Villadangos, J.A. and L. Young, *Antigen-presentation properties of plasmacytoid dendritic cells.* Immunity, 2008. **29**(3): p. 352-61.
115. Reizis, B., *Regulation of plasmacytoid dendritic cell development.* Current opinion in immunology, 2010. **22**(2): p. 206-211.
116. Gilliet, M., et al., *The development of murine plasmacytoid dendritic cell precursors is differentially regulated by FLT3-ligand and granulocyte/macrophage colony-stimulating factor.* J Exp Med, 2002. **195**(7): p. 953-8.
117. Naik, S.H., et al., *Development of plasmacytoid and conventional dendritic cell subtypes from single precursor cells derived in vitro and in vivo.* Nat Immunol, 2007. **8**(11): p. 1217-26.
118. Asselin-Paturel, C., et al., *Mouse type I IFN-producing cells are immature APCs with plasmacytoid morphology.* Nat Immunol, 2001. **2**(12): p. 1144-50.
119. Hochrein, H., M. O'Keeffe, and H. Wagner, *Human and mouse plasmacytoid dendritic cells.* Hum Immunol, 2002. **63**(12): p. 1103-10.
120. Heil, F., et al., *Species-specific recognition of single-stranded RNA via toll-like receptor 7 and 8.* Science, 2004. **303**(5663): p. 1526-9.
121. Hochrein, H. and H. Wagner, *Of men, mice and pigs: looking at their plasmacytoid dendritic cells [corrected].* Immunology, 2004. **112**(1): p. 26-27.
122. Villadangos, J.A. and P. Schnorrer, *Intrinsic and cooperative antigen-presenting functions of dendritic-cell subsets in vivo.* Nat Rev Immunol, 2007. **7**(7): p. 543-55.
123. Mildner, A. and S. Jung, *Development and function of dendritic cell subsets.* Immunity, 2014. **40**(5): p. 642-56.
124. Banchereau, J. and R.M. Steinman, *Dendritic cells and the control of immunity.* Nature, 1998. **392**(6673): p. 245-52.

125. Bevan, M.J., *Cross-priming for a secondary cytotoxic response to minor H antigens with H-2 congenic cells which do not cross-react in the cytotoxic assay.* The Journal of experimental medicine, 1976. **143**(5): p. 1283-1288.
126. Rock, K.L., *The ins and outs of cross-presentation.* Nat Immunol, 2003. **4**(10): p. 941-3.
127. Savina, A., et al., *NOX2 controls phagosomal pH to regulate antigen processing during crosspresentation by dendritic cells.* Cell, 2006. **126**(1): p. 205-18.
128. Crowley, M., et al., *The cell surface of mouse dendritic cells: FACS analyses of dendritic cells from different tissues including thymus.* Cell Immunol, 1989. **118**(1): p. 108-25.
129. Allan, R.S., et al., *Epidermal viral immunity induced by CD8alpha+ dendritic cells but not by Langerhans cells.* Science, 2003. **301**(5641): p. 1925-8.
130. Hildner, K., et al., *Batf3 deficiency reveals a critical role for CD8alpha+ dendritic cells in cytotoxic T cell immunity.* Science, 2008. **322**(5904): p. 1097-100.
131. Pooley, J.L., W.R. Heath, and K. Shortman, *Cutting edge: intravenous soluble antigen is presented to CD4 T cells by CD8- dendritic cells, but cross-presented to CD8 T cells by CD8+ dendritic cells.* J Immunol, 2001. **166**(9): p. 5327-30.
132. Sung, S.S., et al., *A major lung CD103 (alphaE)-beta7 integrin-positive epithelial dendritic cell population expressing Langerin and tight junction proteins.* J Immunol, 2006. **176**(4): p. 2161-72.
133. Plantinga, M., et al., *Conventional and monocyte-derived CD11b(+) dendritic cells initiate and maintain T helper 2 cell-mediated immunity to house dust mite allergen.* Immunity, 2013. **38**(2): p. 322-35.
134. Schlitzer, A., et al., *IRF4 transcription factor-dependent CD11b+ dendritic cells in human and mouse control mucosal IL-17 cytokine responses.* Immunity, 2013. **38**(5): p. 970-83.
135. Steinman, R.M. and J. Banchereau, *Taking dendritic cells into medicine.* Nature, 2007. **449**(7161): p. 419-426.
136. Palucka, K. and J. Banchereau, *Cancer immunotherapy via dendritic cells.* Nat Rev Cancer, 2012. **12**(4): p. 265-77.
137. Sallusto, F. and A. Lanzavecchia, *Efficient presentation of soluble antigen by cultured human dendritic cells is maintained by granulocyte/macrophage colony-stimulating factor plus interleukin 4 and downregulated by tumor necrosis factor alpha.* J Exp Med, 1994. **179**(4): p. 1109-18.
138. Bachem, A., et al., *Superior antigen cross-presentation and XCR1 expression define human CD11c+CD141+ cells as homologues of mouse CD8+ dendritic cells.* J Exp Med, 2010. **207**(6): p. 1273-81.
139. Crozat, K., et al., *Comparative genomics as a tool to reveal functional equivalences between human and mouse dendritic cell subsets.* Immunol Rev, 2010. **234**(1): p. 177-98.
140. Watchmaker, P.B., et al., *Comparative transcriptional and functional profiling defines conserved programs of intestinal DC differentiation in humans and mice.* Nat Immunol, 2014. **15**(1): p. 98-108.
141. del Rio, M.L., et al., *Development and functional specialization of CD103+ dendritic cells.* Immunol Rev, 2010. **234**(1): p. 268-81.
142. Merad, M., et al., *The dendritic cell lineage: ontogeny and function of dendritic cells and their subsets in the steady state and the inflamed setting.* Annual review of immunology, 2013. **31**: p. 563-604.
143. Proietto, A.I., et al., *Dendritic cells in the thymus contribute to T-regulatory cell induction.* Proc Natl Acad Sci U S A, 2008. **105**(50): p. 19869-74.

144. Langlet, C., et al., *CD64 expression distinguishes monocyte-derived and conventional dendritic cells and reveals their distinct role during intramuscular immunization.* J Immunol, 2012. **188**(4): p. 1751-60.
145. Randolph, G.J., V. Angeli, and M.A. Swartz, *Dendritic-cell trafficking to lymph nodes through lymphatic vessels.* Nat Rev Immunol, 2005. **5**(8): p. 617-28.
146. Randolph, G.J., J. Ochando, and S. Partida-Sanchez, *Migration of dendritic cell subsets and their precursors.* Annu Rev Immunol, 2008. **26**: p. 293-316.
147. Hampton, H.R. and T. Chtanova, *Lymphatic Migration of Immune Cells.* Frontiers in immunology, 2019. **10**: p. 1168-1168.
148. Forster, R., A.C. Davalos-Misslitz, and A. Rot, *CCR7 and its ligands: balancing immunity and tolerance.* Nat Rev Immunol, 2008. **8**(5): p. 362-71.
149. Reis e Sousa, C., *Dendritic cells in a mature age.* Nat Rev Immunol, 2006. **6**(6): p. 476-83.
150. Waskow, C., et al., *The receptor tyrosine kinase Flt3 is required for dendritic cell development in peripheral lymphoid tissues.* Nat Immunol, 2008. **9**(6): p. 676-83.
151. Steinman, R.M. and Z.A. Cohn, *Identification of a novel cell type in peripheral lymphoid organs of mice. I. Morphology, quantitation, tissue distribution.* J Exp Med, 1973. **137**(5): p. 1142-62.
152. Andrés, C., et al., *HIV-1 Reservoir Dynamics after Vaccination and Antiretroviral Therapy Interruption Are Associated with Dendritic Cell Vaccine-Induced T Cell Responses.* Journal of Virology, 2015. **89**(18): p. 9189.
153. Bruno, L., *Differentiation of dendritic cell subsets from mouse bone marrow.* Methods Mol Biol, 2007. **380**: p. 47-57.
154. Alissafi, T., et al., *De novo-induced self-antigen-specific Foxp3+ regulatory T cells impair the accumulation of inflammatory dendritic cells in draining lymph nodes.* J Immunol, 2015. **194**(12): p. 5812-24.
155. Li, M., et al., *Role of dendritic cell-mediated abnormal immune response in visceral hypersensitivity.* Int J Clin Exp Med, 2015. **8**(8): p. 13243-50.
156. Tuettenberg, A., et al., *Immune regulation by dendritic cells and T cells--basic science, diagnostic, and clinical application.* Clin Lab, 2011. **57**(1-2): p. 1-12.
157. Sennikov, S.V., et al., *[Features of functional activity of dendritic cells in tumor growth].* Vopr Onkol, 2015. **61**(4): p. 556-62.
158. Steinman, R.M. and Z.A. Cohn, *Identification of a novel cell type in peripheral lymphoid organs of mice. II. Functional properties in vitro.* J Exp Med, 1974. **139**(2): p. 380-97.
159. Poltorak, M.P. and B.U. Schraml, *Fate mapping of dendritic cells.* Front Immunol, 2015. **6**: p. 199.
160. Steinman, R.M. and J. Idoyaga, *Features of the dendritic cell lineage.* Immunol Rev, 2010. **234**(1): p. 5-17.
161. Reynolds, G. and M. Haniffa, *Human and Mouse Mononuclear Phagocyte Networks: A Tale of Two Species?* Front Immunol, 2015. **6**: p. 330.
162. Guilliams, M., et al., *Dendritic cells, monocytes and macrophages: a unified nomenclature based on ontogeny.* Nat Rev Immunol, 2014. **14**(8): p. 571-8.
163. Drutman, S.B., J.C. Kendall, and E.S. Trombetta, *Inflammatory spleen monocytes can upregulate CD11c expression without converting into dendritic cells.* Journal of immunology (Baltimore, Md. : 1950), 2012. **188**(8): p. 3603-3610.
164. Hashimoto, D., J. Miller, and M. Merad, *Dendritic cell and macrophage heterogeneity in vivo.* Immunity, 2011. **35**(3): p. 323-35.
165. Murray, P.J. and T.A. Wynn, *Protective and pathogenic functions of macrophage subsets.* Nat Rev Immunol, 2011. **11**(11): p. 723-37.

166. Vermaelen, K. and R. Pauwels, *Accurate and simple discrimination of mouse pulmonary dendritic cell and macrophage populations by flow cytometry: methodology and new insights.* Cytometry A, 2004. **61**(2): p. 170-77.
167. Blasius, A.L., et al., *Development and function of murine B220+CD11c+NK1.1+ cells identify them as a subset of NK cells.* J Exp Med, 2007. **204**(11): p. 2561-8.
168. Qualai, J., et al., *Expression of CD11c Is Associated with Unconventional Activated T Cell Subsets with High Migratory Potential.* PLoS One, 2016. **11**(4): p. e0154253.
169. Rubtsov, A.V., et al., *Toll-like receptor 7 (TLR7)-driven accumulation of a novel CD11c^{+} B-cell population is important for the development of autoimmunity.* Blood, 2011. **118**(5): p. 1305-15.
170. Jersmann, H.P., *Time to abandon dogma: CD14 is expressed by non-myeloid lineage cells.* Immunol Cell Biol, 2005. **83**(5): p. 462-7.
171. Hamann, J., et al., *EMR1, the human homolog of F4/80, is an eosinophil-specific receptor.* Eur J Immunol, 2007. **37**(10): p. 2797-802.
172. Baud, V., et al., *EMR1, an unusual member in the family of hormone receptors with seven transmembrane segments.* Genomics, 1995. **26**(2): p. 334-44.
173. Hume, D.A., et al., *The mononuclear phagocyte system of the mouse defined by immunohistochemical localization of antigen F4/80. Relationship between macrophages, Langerhans cells, reticular cells, and dendritic cells in lymphoid and hematopoietic organs.* J Exp Med, 1983. **158**(5): p. 1522-36.
174. Larson, S.R., et al., *Ly6C(+) monocyte efferocytosis and cross-presentation of cell-associated antigens.* Cell Death Differ, 2016. **23**(6): p. 997-1003.
175. Pozzi, L.A., J.W. Maciaszek, and K.L. Rock, *Both dendritic cells and macrophages can stimulate naive CD8 T cells in vivo to proliferate, develop effector function, and differentiate into memory cells.* J Immunol, 2005. **175**(4): p. 2071-81.
176. Tacke, F., et al., *Immature monocytes acquire antigens from other cells in the bone marrow and present them to T cells after maturing in the periphery.* The Journal of experimental medicine, 2006. **203**(3): p. 583-597.
177. Geissmann, F., et al., *Development of monocytes, macrophages, and dendritic cells.* Science (New York, N.Y.), 2010. **327**(5966): p. 656-661.
178. Naik, S.H., et al., *Diverse and heritable lineage imprinting of early haematopoietic progenitors.* Nature, 2013. **496**(7444): p. 229-32.
179. Schraml, B.U., et al., *Genetic tracing via DNGR-1 expression history defines dendritic cells as a hematopoietic lineage.* Cell, 2013. **154**(4): p. 843-58.
180. Becher, B., et al., *High-dimensional analysis of the murine myeloid cell system.* Nat Immunol, 2014. **15**(12): p. 1181-9.
181. Gautier, E.L., et al., *Gene-expression profiles and transcriptional regulatory pathways that underlie the identity and diversity of mouse tissue macrophages.* Nat Immunol, 2012. **13**(11): p. 1118-28.
182. Miller, J.C., et al., *Deciphering the transcriptional network of the dendritic cell lineage.* Nat Immunol, 2012. **13**(9): p. 888-99.
183. Haniffa, M., et al., *Human tissues contain CD141hi cross-presenting dendritic cells with functional homology to mouse CD103+ nonlymphoid dendritic cells.* Immunity, 2012. **37**(1): p. 60-73.
184. Wu, L. and Y.-J. Liu, *Development of Dendritic-Cell Lineages.* Immunity, 2007. **26**(6): p. 741-750.
185. Thomas, M.L., et al., *gammadelta T cells lyse autologous and allogenic oesophageal tumours: involvement of heat-shock proteins in the tumour cell lysis.* Cancer Immunol Immunother, 2000. **48**(11): p. 653-9.

186. Gonzalez, H., C. Hagerling, and Z. Werb, *Roles of the immune system in cancer: from tumor initiation to metastatic progression.* Genes & development, 2018. **32**(19-20): p. 1267-1284.
187. Blankenstein, T., et al., *The determinants of tumour immunogenicity.* Nature reviews. Cancer, 2012. **12**(4): p. 307-313.
188. Boon, T., et al., *Tumor antigens recognized by T lymphocytes.* Annu Rev Immunol, 1994. **12**: p. 337-65.
189. van der Bruggen, P., et al., *A gene encoding an antigen recognized by cytolytic T lymphocytes on a human melanoma.* J Immunol, 2007. **178**(5): p. 2617-21.
190. Barry, K.C., et al., *A natural killer-dendritic cell axis defines checkpoint therapy-responsive tumor microenvironments.* Nat Med, 2018. **24**(8): p. 1178-1191.
191. Broz, M.L., et al., *Dissecting the tumor myeloid compartment reveals rare activating antigen-presenting cells critical for T cell immunity.* Cancer Cell, 2014. **26**(5): p. 638-52.
192. Ruffell, B., et al., *Macrophage IL-10 blocks CD8+ T cell-dependent responses to chemotherapy by suppressing IL-12 expression in intratumoral dendritic cells.* Cancer Cell, 2014. **26**(5): p. 623-37.
193. Steinman, R.M., *Decisions about dendritic cells: past, present, and future.* Annu Rev Immunol, 2012. **30**: p. 1-22.
194. Driessens, G., J. Kline, and T.F. Gajewski, *Costimulatory and coinhibitory receptors in anti-tumor immunity.* Immunological reviews, 2009. **229**(1): p. 126-144.
195. Wculek, S.K., et al., *Dendritic cells in cancer immunology and immunotherapy.* Nature Reviews Immunology, 2019.
196. Cornwall, S.M., et al., *Human mesothelioma induces defects in dendritic cell numbers and antigen-processing function which predict survival outcomes.* Oncoimmunology, 2016. **5**(2): p. e1082028.
197. Cornwall, S.M.J., et al., *Human mesothelioma induces defects in dendritic cell numbers and antigen-processing function which predict survival outcomes.* Oncoimmunology, 2015. **5**(2): p. e1082028-e1082028.
198. Gardner, J.K., et al., *Mesothelioma tumor cells modulate dendritic cell lipid content, phenotype and function.* PLoS One, 2015. **10**(4): p. e0123563.
199. Jackaman, C., et al., *CD8(+) cytotoxic T cell responses to dominant tumor-associated antigens are profoundly weakened by aging yet subdominant responses retain functionality and expand in response to chemotherapy.* Oncoimmunology, 2019. **8**(4): p. e1564452.
200. Busk, M., et al., *Inhibition of tumor lactate oxidation: consequences for the tumor microenvironment.* Radiother Oncol, 2011. **99**(3): p. 404-11.
201. Voelxen, N.F., et al., *Comparative metabolic analysis in head and neck cancer and the normal gingiva.* Clin Oral Investig, 2018. **22**(2): p. 1033-1043.
202. Battista, M.J., et al., *Feasibility of induced metabolic bioluminescence imaging in advanced ovarian cancer patients: first results of a pilot study.* J Cancer Res Clin Oncol, 2016. **142**(9): p. 1909-16.
203. Chang, C.H., et al., *Metabolic Competition in the Tumor Microenvironment Is a Driver of Cancer Progression.* Cell, 2015. **162**(6): p. 1229-41.
204. Pearce, E.L., et al., *Fueling immunity: insights into metabolism and lymphocyte function.* Science, 2013. **342**(6155): p. 1242454.
205. O'Neill, L.A. and D.G. Hardie, *Metabolism of inflammation limited by AMPK and pseudo-starvation.* Nature, 2013. **493**(7432): p. 346-55.
206. Pollizzi, K.N. and J.D. Powell, *Integrating canonical and metabolic signalling programmes in the regulation of T cell responses.* Nature Reviews Immunology, 2014. **14**: p. 435.

207. Diskin, C. and E.M. Pålsson-McDermott, *Metabolic Modulation in Macrophage Effector Function.* Frontiers in immunology, 2018. **9**: p. 270-270.
208. Lenzen, S., *A fresh view of glycolysis and glucokinase regulation: history and current status.* J Biol Chem, 2014. **289**(18): p. 12189-94.
209. Li, X.-B., J.-D. Gu, and Q.-H. Zhou, *Review of aerobic glycolysis and its key enzymes - new targets for lung cancer therapy.* Thoracic cancer, 2015. **6**(1): p. 17-24.
210. Altenberg, B. and K.O. Greulich, *Genes of glycolysis are ubiquitously overexpressed in 24 cancer classes.* Genomics, 2004. **84**(6): p. 1014-20.
211. Nicholls, C., H. Li, and J.P. Liu, *GAPDH: a common enzyme with uncommon functions.* Clin Exp Pharmacol Physiol, 2012. **39**(8): p. 674-9.
212. Kelly, B. and L.A.J. O'Neill, *Metabolic reprogramming in macrophages and dendritic cells in innate immunity.* Cell research, 2015. **25**(7): p. 771-784.
213. Hui, S., et al., *Glucose feeds the TCA cycle via circulating lactate.* Nature, 2017. **551**(7678): p. 115-118.
214. Oren, R., et al., *Metabolic patterns in three types of phagocytizing cells.* The Journal of cell biology, 1963. **17**(3): p. 487-501.
215. Ho, P.-C. and P.-S. Liu, *Metabolic communication in tumors: a new layer of immunoregulation for immune evasion.* Journal for immunotherapy of cancer, 2016. **4**: p. 4-4.
216. Nagy, C. and A. Haschemi, *Time and Demand are Two Critical Dimensions of Immunometabolism: The Process of Macrophage Activation and the Pentose Phosphate Pathway.* Frontiers in immunology, 2015. **6**: p. 164-164.
217. O'Neill, L.A., R.J. Kishton, and J. Rathmell, *A guide to immunometabolism for immunologists.* Nat Rev Immunol, 2016. **16**(9): p. 553-65.
218. O'Neill, L.A.J., R.J. Kishton, and J. Rathmell, *A guide to immunometabolism for immunologists.* Nature reviews. Immunology, 2016. **16**(9): p. 553-565.
219. Tannahill, G.M., et al., *Succinate is an inflammatory signal that induces IL-1beta through HIF-1alpha.* Nature, 2013. **496**(7444): p. 238-42.
220. Jha, A.K., et al., *Network integration of parallel metabolic and transcriptional data reveals metabolic modules that regulate macrophage polarization.* Immunity, 2015. **42**(3): p. 419-30.
221. Funk, J.L., et al., *Lipopolysaccharide stimulation of RAW 264.7 macrophages induces lipid accumulation and foam cell formation.* Atherosclerosis, 1993. **98**(1): p. 67-82.
222. Oiknine, J. and M. Aviram, *Increased susceptibility to activation and increased uptake of low density lipoprotein by cholesterol-loaded macrophages.* Arterioscler Thromb, 1992. **12**(6): p. 745-53.
223. Feingold, K.R., et al., *Mechanisms of triglyceride accumulation in activated macrophages.* J Leukoc Biol, 2012. **92**(4): p. 829-39.
224. Vats, D., et al., *Oxidative metabolism and PGC-1beta attenuate macrophage-mediated inflammation.* Cell Metab, 2006. **4**(1): p. 13-24.
225. Le Naour, F., et al., *Profiling changes in gene expression during differentiation and maturation of monocyte-derived dendritic cells using both oligonucleotide microarrays and proteomics.* J Biol Chem, 2001. **276**(21): p. 17920-31.
226. Ishikawa, F., et al., *The developmental program of human dendritic cells is operated independently of conventional myeloid and lymphoid pathways.* Blood, 2007. **110**(10): p. 3591-660.
227. Zaccagnino, P., et al., *An active mitochondrial biogenesis occurs during dendritic cell differentiation.* Int J Biochem Cell Biol, 2012. **44**(11): p. 1962-9.
228. Pearce, E.J. and B. Everts, *Dendritic cell metabolism.* Nature reviews. Immunology, 2015. **15**(1): p. 18-29.

229. Rehman, A., et al., *Role of fatty-acid synthesis in dendritic cell generation and function.* J Immunol, 2013. **190**(9): p. 4640-9.
230. Gao, F., et al., *Radiation-driven lipid accumulation and dendritic cell dysfunction in cancer.* Scientific Reports, 2015. **5**: p. 9613.
231. Arai, R., et al., *Lipid Accumulation in Peripheral Blood Dendritic Cells and Anticancer Immunity in Patients with Lung Cancer.* J Immunol Res, 2018. **2018**: p. 5708239.
232. Yui, S. and M. Yamazaki, *Neutral lipid accumulation in macrophages during lipid-induced macrophage growth.* J Leukoc Biol, 1989. **45**(3): p. 189-97.
233. Remmerie, A. and C.L. Scott, *Macrophages and lipid metabolism.* Cellular immunology, 2018. **330**: p. 27-42.
234. Feingold, K.R., et al., *Mechanisms of triglyceride accumulation in activated macrophages.* Journal of leukocyte biology, 2012. **92**(4): p. 829-839.
235. Gibson, M.S., N. Domingues, and O.V. Vieira, *Lipid and Non-lipid Factors Affecting Macrophage Dysfunction and Inflammation in Atherosclerosis.* Frontiers in physiology, 2018. **9**: p. 654-654.
236. Gao, F., et al., *Radiation-driven lipid accumulation and dendritic cell dysfunction in cancer.* Scientific reports, 2015. **5**: p. 9613-9613.
237. da Silva, R.F., et al., *Conversion of human M-CSF macrophages into foam cells reduces their proinflammatory responses to classical M1-polarizing activation.* Atherosclerosis, 2016. **248**: p. 170-8.
238. Jongstra-Bilen, J., et al., *Oxidized Low-Density Lipoprotein Loading of Macrophages Downregulates TLR-Induced Proinflammatory Responses in a Gene-Specific and Temporal Manner through Transcriptional Control.* J Immunol, 2017. **199**(6): p. 2149-2157.
239. Libby, P., P.M. Ridker, and G.K. Hansson, *Progress and challenges in translating the biology of atherosclerosis.* Nature, 2011. **473**(7347): p. 317-25.
240. Gardner, J.K., et al., *Mesothelioma tumor cells modulate dendritic cell lipid content, phenotype and function.* PloS one, 2015. **10**(4): p. e0123563-e0123563.
241. Coventry, B. and S. Heinzel, *CD1a in human cancers: a new role for an old molecule.* Trends Immunol, 2004. **25**(5): p. 242-8.
242. Gerlini, G., et al., *Metastatic melanoma secreted IL-10 down-regulates CD1 molecules on dendritic cells in metastatic tumor lesions.* The American journal of pathology, 2004. **165**(6): p. 1853-1863.
243. PrabhuDas, M.R., et al., *A Consensus Definitive Classification of Scavenger Receptors and Their Roles in Health and Disease.* Journal of immunology (Baltimore, Md. : 1950), 2017. **198**(10): p. 3775-3789.
244. Ingersoll, M.A., et al., *Comparison of gene expression profiles between human and mouse monocyte subsets.* Blood, 2010. **115**(3): p. e10-9.
245. Wilkinson, K. and J. El Khoury, *Microglial scavenger receptors and their roles in the pathogenesis of Alzheimer's disease.* Int J Alzheimers Dis, 2012. **2012**: p. 489456.
246. Gardner, J.K., et al., *Lipid-laden partially-activated plasmacytoid and CD4(-)CD8α(+) dendritic cells accumulate in tissues in elderly mice.* Immunity & ageing : I & A, 2014. **11**: p. 11-11.
247. Moore, K.J., F.J. Sheedy, and E.A. Fisher, *Macrophages in atherosclerosis: a dynamic balance.* Nature reviews. Immunology, 2013. **13**(10): p. 709-721.
248. Manning, L.S., et al., *Establishment and characterization of five human malignant mesothelioma cell lines derived from pleural effusions.* Int J Cancer, 1991. **47**(2): p. 285-90.
249. Jackaman, C., et al., *IL-2 intratumoral immunotherapy enhances CD8+ T cells that mediate destruction of tumor cells and tumor-associated vasculature: a novel mechanism for IL-2.* J Immunol, 2003. **171**(10): p. 5051-63.

250. Zhuang, X., et al., *Conditioned medium mimicking the tumor microenvironment augments chemotherapeutic resistance via ataxia-telangiectasia mutated and nuclear factor-κB pathways in gastric cancer cells.* Oncol Rep, 2018. **40**(4): p. 2334-2342.
251. Cohen, A.B., *The interaction of alpha-1-antitrypsin with chymotrypsin, trypsin and elastase.* Biochim Biophys Acta, 1975. **391**(1): p. 193-200.
252. Banfi, G., G.L. Salvagno, and G. Lippi, *The role of ethylenediamine tetraacetic acid (EDTA) as in vitro anticoagulant for diagnostic purposes.* Clin Chem Lab Med, 2007. **45**(5): p. 565-76.
253. Romani, N., et al., *Generation of mature dendritic cells from human blood. An improved method with special regard to clinical applicability.* J Immunol Methods, 1996. **196**(2): p. 137-51.
254. Tsuzuki, H., et al., *Lipopolysaccharide: neutralization by polymyxin B shuts down the signaling pathway of nuclear factor kappaB in peripheral blood mononuclear cells, even during activation.* J Surg Res, 2001. **100**(1): p. 127-34.
255. Mruk, D.D. and C.Y. Cheng, *Enhanced chemiluminescence (ECL) for routine immunoblotting: An inexpensive alternative to commercially available kits.* Spermatogenesis, 2011. **1**(2): p. 121-122.
256. Keane, K.N., et al., *The impact of cryopreservation on human peripheral blood leucocyte bioenergetics.* Clin Sci (Lond), 2015. **128**(10): p. 723-33.
257. Koopman, M., et al., *A screening-based platform for the assessment of cellular respiration in Caenorhabditis elegans.* Nature protocols, 2016. **11**(10): p. 1798-1816.
258. TeSlaa, T. and M.A. Teitell, *Techniques to monitor glycolysis.* Methods in enzymology, 2014. **542**: p. 91-114.
259. Traba, J., et al., *An Optimized Protocol to Analyze Glycolysis and Mitochondrial Respiration in Lymphocytes.* Journal of visualized experiments : JoVE, 2016(117): p. 54918.
260. Au - Nicholls, D.G., et al., *Bioenergetic Profile Experiment using C2C12 Myoblast Cells.* JoVE, 2010(46): p. e2511.
261. Chen, Q., et al., *Production of reactive oxygen species by mitochondria: central role of complex III.* J Biol Chem, 2003. **278**(38): p. 36027-31.
262. Agilent. Available from: https://www.agilent.com/cs/library/usermanuals/public/XF_Cell_Mito_Stress_Test_Kit_User_Guide.pdf.
263. Mohamed, W., et al., *Antibody targeting the ferritin-like protein controls Listeria infection.* Infection and immunity, 2010. **78**(7): p. 3306-3314.
264. Patik, I., et al., *Identification of novel cell-impermeant fluorescent substrates for testing the function and drug interaction of Organic Anion-Transporting Polypeptides, OATP1B1/1B3 and 2B1.* Scientific Reports, 2018. **8**(1): p. 2630.
265. Maecker, H.T. and J. Trotter, *Flow cytometry controls, instrument setup, and the determination of positivity.* Cytometry A, 2006. **69**(9): p. 1037-42.
266. Rose, S., A. Misharin, and H. Perlman, *A novel Ly6C/Ly6G-based strategy to analyze the mouse splenic myeloid compartment.* Cytometry A, 2012. **81**(4): p. 343-50.
267. Yang, H., R.M.E. Parkhouse, and T. Wileman, *Monoclonal antibodies that identify the CD3 molecules expressed specifically at the surface of porcine gammadelta-T cells.* Immunology, 2005. **115**(2): p. 189-196.
268. Assarsson, E., et al., *CD8⁺ T Cells Rapidly Acquire NK1.1 and NK Cell-Associated Molecules Upon Stimulation In Vitro and In Vivo.* The Journal of Immunology, 2000. **165**(7): p. 3673.
269. Rumin, J., et al., *The use of fluorescent Nile red and BODIPY for lipid measurement in microalgae.* Biotechnology for biofuels, 2015. **8**: p. 42.

270. Hama, Y., et al., *A comparison of the emission efficiency of four common green fluorescence dyes after internalization into cancer cells.* Bioconjugate chemistry, 2006. **17**(6): p. 1426-1431.
271. Nakano, H., M. Yanagita, and M.D. Gunn, *CD11c(+)B220(+)Gr-1(+) cells in mouse lymph nodes and spleen display characteristics of plasmacytoid dendritic cells.* J Exp Med, 2001. **194**(8): p. 1171-8.
272. Oka, S., et al., *Presence of B220 within thymocytes and its expression on the cell surface during apoptosis.* Immunology, 2000. **100**(4): p. 417-23.
273. Dannaeus, K., et al., *Flt3 ligand induces the outgrowth of Mac-1+B220+ mouse bone marrow progenitor cells restricted to macrophage differentiation that coexpress early B cell-associated genes.* Exp Hematol, 1999. **27**(11): p. 1646-54.
274. Renno, T., et al., *Peripheral T cells undergoing superantigen-induced apoptosis in vivo express B220 and upregulate Fas and Fas ligand.* The Journal of experimental medicine, 1996. **183**(2): p. 431-437.
275. Ong, C.J., et al., *Thymic CD45 tyrosine phosphatase regulates apoptosis and MHC-restricted negative selection.* J Immunol, 1994. **152**(8): p. 3793-805.
276. Watanabe, Y. and T. Akaike, *Activation signal induces the expression of B cell-specific CD45R epitope (6B2) on murine T cells.* Scand J Immunol, 1994. **39**(5): p. 419-25.
277. Torimoto, Y., et al., *Activation of T cells through a T cell-specific epitope of CD45.* Cell Immunol, 1992. **145**(1): p. 111-29.
278. Coffman, R.L. and I.L. Weissman, *B220: a B cell-specific member of th T200 glycoprotein family.* Nature, 1981. **289**(5799): p. 681-3.
279. Sandgren, K.J., et al., *Human plasmacytoid dendritic cells efficiently capture HIV-1 envelope glycoproteins via CD4 for antigen presentation.* J Immunol, 2013. **191**(1): p. 60-9.
280. Vignali, D.A.A., *CD4 on the road to coreceptor status.* Journal of immunology (Baltimore, Md. : 1950), 2010. **184**(11): p. 5933-5934.
281. Gibbings, D. and A.D. Befus, *CD4 and CD8: an inside-out coreceptor model for innate immune cells.* J Leukoc Biol, 2009. **86**(2): p. 251-9.
282. Singer, A., S. Adoro, and J.H. Park, *Lineage fate and intense debate: myths, models and mechanisms of CD4- versus CD8-lineage choice.* Nat Rev Immunol, 2008. **8**(10): p. 788-801.
283. Lynch, E.A., et al., *Cutting edge: IL-16/CD4 preferentially induces Th1 cell migration: requirement of CCR5.* J Immunol, 2003. **171**(10): p. 4965-8.
284. Winkel, K., et al., *CD4 and CD8 expression by human and mouse thymic dendritic cells.* Immunol Lett, 1994. **40**(2): p. 93-9.
285. O'Doherty, U., et al., *Dendritic cells freshly isolated from human blood express CD4 and mature into typical immunostimulatory dendritic cells after culture in monocyte-conditioned medium.* J Exp Med, 1993. **178**(3): p. 1067-76.
286. Janeway, C.A., Jr., *The T cell receptor as a multicomponent signalling machine: CD4/CD8 coreceptors and CD45 in T cell activation.* Annu Rev Immunol, 1992. **10**: p. 645-74.
287. Bierer, B.E., et al., *The biologic roles of CD2, CD4, and CD8 in T-cell activation.* Annu Rev Immunol, 1989. **7**: p. 579-99.
288. Doyle, C. and J.L. Strominger, *Interaction between CD4 and class II MHC molecules mediates cell adhesion.* Nature, 1987. **330**(6145): p. 256-9.
289. Gao, G.F. and B.K. Jakobsen, *Molecular interactions of coreceptor CD8 and MHC class I: the molecular basis for functional coordination with the T-cell receptor.* Immunol Today, 2000. **21**(12): p. 630-6.
290. Garcia, K.C., L. Teyton, and I.A. Wilson, *Structural basis of T cell recognition.* Annu Rev Immunol, 1999. **17**: p. 369-97.

291. Terry, L.A., et al., *Differential expression and regulation of the human CD8 alpha and CD8 beta chains.* Tissue Antigens, 1990. **35**(2): p. 82-91.
292. Germain, R.N., *T-cell development and the CD4-CD8 lineage decision.* Nat Rev Immunol, 2002. **2**(5): p. 309-22.
293. Ling, G.S., et al., *Integrin CD11b positively regulates TLR4-induced signalling pathways in dendritic cells but not in macrophages.* Nat Commun, 2014. **5**: p. 3039.
294. Zhou, H., et al., *CD11b/CD18 (Mac-1) is a novel surface receptor for extracellular double-stranded RNA to mediate cellular inflammatory responses.* J Immunol, 2013. **190**(1): p. 115-25.
295. Kawai, K., et al., *CD11b-mediated migratory property of peripheral blood B cells.* J Allergy Clin Immunol, 2005. **116**(1): p. 192-7.
296. Ross, G.D., *Role of the lectin domain of Mac-1/CR3 (CD11b/CD18) in regulating intercellular adhesion.* Immunol Res, 2002. **25**(3): p. 219-27.
297. van Spriel, A.B., et al., *Mac-1 (CD11b/CD18) is essential for Fc receptor-mediated neutrophil cytotoxicity and immunologic synapse formation.* Blood, 2001. **97**(8): p. 2478-86.
298. Wagner, C., et al., *The complement receptor 3, CR3 (CD11b/CD18), on T lymphocytes: activation-dependent up-regulation and regulatory function.* Eur J Immunol, 2001. **31**(4): p. 1173-80.
299. Muto, S., V. Vetvicka, and G.D. Ross, *CR3 (CD11b/CD18) expressed by cytotoxic T cells and natural killer cells is upregulated in a manner similar to neutrophil CR3 following stimulation with various activating agents.* J Clin Immunol, 1993. **13**(3): p. 175-84.
300. Ho, M.K. and T.A. Springer, *Mac-1 antigen: quantitative expression in macrophage populations and tissues, and immunofluorescent localization in spleen.* J Immunol, 1982. **128**(5): p. 2281-6.
301. Ihanus, E., et al., *Red-cell ICAM-4 is a ligand for the monocyte/macrophage integrin CD11c/CD18: characterization of the binding sites on ICAM-4.* Blood, 2007. **109**(2): p. 802-10.
302. Osugi, Y., S. Vuckovic, and D.N. Hart, *Myeloid blood CD11c(+) dendritic cells and monocyte-derived dendritic cells differ in their ability to stimulate T lymphocytes.* Blood, 2002. **100**(8): p. 2858-66.
303. Garnotel, R., et al., *Human Blood Monocytes Interact with Type I Collagen Through α_xβ₂ Integrin (CD11c-CD18, gp150-95).* The Journal of Immunology, 2000. **164**(11): p. 5928-5934.
304. Ingalls, R.R. and D.T. Golenbock, *CD11c/CD18, a transmembrane signaling receptor for lipopolysaccharide.* The Journal of experimental medicine, 1995. **181**(4): p. 1473-1479.
305. Bilsland, C.A., M.S. Diamond, and T.A. Springer, *The leukocyte integrin p150,95 (CD11c/CD18) as a receptor for iC3b. Activation by a heterologous beta subunit and localization of a ligand recognition site to the I domain.* J Immunol, 1994. **152**(9): p. 4582-9.
306. Diamond, M.S., et al., *The I domain is a major recognition site on the leukocyte integrin Mac-1 (CD11b/CD18) for four distinct adhesion ligands.* J Cell Biol, 1993. **120**(4): p. 1031-43.
307. Loike, J.D., et al., *CD11c/CD18 on neutrophils recognizes a domain at the N terminus of the A alpha chain of fibrinogen.* Proceedings of the National Academy of Sciences of the United States of America, 1991. **88**(3): p. 1044-1048.
308. Myones, B.L., et al., *Neutrophil and monocyte cell surface p150,95 has iC3b-receptor (CR4) activity resembling CR3.* J Clin Invest, 1988. **82**(2): p. 640-51.
309. Keizer, G.D., et al., *Role of p150,95 in adhesion, migration, chemotaxis and phagocytosis of human monocytes.* Eur J Immunol, 1987. **17**(9): p. 1317-22.

310. te Velde, A.A., G.D. Keizer, and C.G. Figdor, *Differential function of LFA-1 family molecules (CD11 and CD18) in adhesion of human monocytes to melanoma and endothelial cells.* Immunology, 1987. **61**(3): p. 261-267.
311. Hogg, N., et al., *The p150,95 molecule is a marker of human mononuclear phagocytes: comparison with expression of class II molecules.* Eur J Immunol, 1986. **16**(3): p. 240-8.
312. Malhotra, V., N. Hogg, and R.B. Sim, *Ligand binding by the pl50,95 antigen of U937 monocytic cells: properties in common with complement receptor type 3 (CR3).* European Journal of Immunology, 1986. **16**(9): p. 1117-1123.
313. Springer, T.A., L.J. Miller, and D.C. Anderson, *p150,95, the third member of the Mac-1, LFA-1 human leukocyte adhesion glycoprotein family.* J Immunol, 1986. **136**(1): p. 240-5.
314. Rubtsov, A.V., et al., *CD11c-Expressing B Cells Are Located at the T Cell/B Cell Border in Spleen and Are Potent APCs.* J Immunol, 2015. **195**(1): p. 71-9.
315. Rubtsov, A.V., et al., *Toll-like receptor 7 (TLR7)-driven accumulation of a novel CD11c(+) B-cell population is important for the development of autoimmunity.* Blood, 2011. **118**(5): p. 1305-15.
316. Moniuszko, M., et al., *Monocyte CD163 and CD36 expression in human whole blood and isolated mononuclear cell samples: influence of different anticoagulants.* Clinical and vaccine immunology : CVI, 2006. **13**(6): p. 704-707.
317. Huh, H.Y., et al., *Regulated expression of CD36 during monocyte-to-macrophage differentiation: potential role of CD36 in foam cell formation.* Blood, 1996. **87**(5): p. 2020-8.
318. Park, Y.M., *CD36, a scavenger receptor implicated in atherosclerosis.* Experimental &Amp; Molecular Medicine, 2014. **46**: p. e99.
319. Caux, C., et al., *Activation of human dendritic cells through CD40 cross-linking.* J Exp Med, 1994. **180**(4): p. 1263-72.
320. O'Sullivan, B. and R. Thomas, *CD40 and dendritic cell function.* Crit Rev Immunol, 2003. **23**(1-2): p. 83-107.
321. van Kooten, C. and J. Banchereau, *CD40-CD40 ligand.* J Leukoc Biol, 2000. **67**(1): p. 2-17.
322. van Kooten, C., *Immune regulation by CD40-CD40-l interactions - 2; Y2K update.* Front Biosci, 2000. **5**: p. D880-693.
323. Bourgeois, C., B. Rocha, and C. Tanchot, *A role for CD40 expression on CD8+ T cells in the generation of CD8+ T cell memory.* Science, 2002. **297**(5589): p. 2060-3.
324. Hamzah, J., et al., *Vascular targeting of anti-CD40 antibodies and IL-2 into autochthonous tumors enhances immunotherapy in mice.* J Clin Invest, 2008. **118**(5): p. 1691-9.
325. Kim, H., et al., *Direct Interaction of CD40 on Tumor Cells with CD40L on T Cells Increases the Proliferation of Tumor Cells by Enhancing TGF-β Production and Th17 Differentiation.* PLOS ONE, 2015. **10**(5): p. e0125742.
326. Munroe, M.E. and G.A. Bishop, *A Costimulatory Function for T Cell CD40.* The Journal of Immunology, 2007. **178**(2): p. 671-682.
327. Hakkarainen, T., et al., *CD40 is expressed on ovarian cancer cells and can be utilized for targeting adenoviruses.* Clin Cancer Res, 2003. **9**(2): p. 619-24.
328. Inwald, D.P., et al., *CD40 is constitutively expressed on platelets and provides a novel mechanism for platelet activation.* Circ Res, 2003. **92**(9): p. 1041-8.
329. Kotowicz, K., et al., *Biological function of CD40 on human endothelial cells: costimulation with CD40 ligand and interleukin-4 selectively induces expression of vascular cell adhesion molecule-1 and P-selectin resulting in preferential adhesion of lymphocytes.* Immunology, 2000. **100**(4): p. 441-448.

330. Hollenbaugh, D., et al., *Expression of functional CD40 by vascular endothelial cells.* J Exp Med, 1995. **182**(1): p. 33-40.
331. Paine, A., et al., *IL-2 upregulates CD86 expression on human CD4(+) and CD8(+) T cells.* J Immunol, 2012. **188**(4): p. 1620-9.
332. Sahoo, N.C., K.V. Rao, and K. Natarajan, *CD80 expression is induced on activated B cells following stimulation by CD86.* Scand J Immunol, 2002. **55**(6): p. 577-84.
333. Luque, I., H. Reyburn, and J.L. Strominger, *Expression of the CD80 and CD86 molecules enhances cytotoxicity by human natural killer cells.* Hum Immunol, 2000. **61**(8): p. 721-8.
334. Fleischer, J., et al., *Differential expression and function of CD80 (B7-1) and CD86 (B7-2) on human peripheral blood monocytes.* Immunology, 1996. **89**(4): p. 592-8.
335. Hathcock, K.S., et al., *Comparative analysis of B7-1 and B7-2 costimulatory ligands: expression and function.* J Exp Med, 1994. **180**(2): p. 631-40.
336. Tseng, S.Y., et al., *B7-DC, a new dendritic cell molecule with potent costimulatory properties for T cells.* The Journal of experimental medicine, 2001. **193**(7): p. 839-846.
337. Inaba, K., et al., *The tissue distribution of the B7-2 costimulator in mice: abundant expression on dendritic cells in situ and during maturation in vitro.* J Exp Med, 1994. **180**(5): p. 1849-60.
338. Sansom, D.M., C.N. Manzotti, and Y. Zheng, *What's the difference between CD80 and CD86?* Trends Immunol, 2003. **24**(6): p. 314-9.
339. Sansom, D.M., *CD28, CTLA-4 and their ligands: who does what and to whom?* Immunology, 2000. **101**(2): p. 169-77.
340. Peach, R.J., et al., *Both Extracellular Immunoglobin-like Domains of CD80 Contain Residues Critical for Binding T Cell Surface Receptors CTLA-4 and CD28.* Journal of Biological Chemistry, 1995. **270**(36): p. 21181-21187.
341. Linsley, P.S., et al., *Human B7-1 (CD80) and B7-2 (CD86) bind with similar avidities but distinct kinetics to CD28 and CTLA-4 receptors.* Immunity, 1994. **1**(9): p. 793-801.
342. Iacono, K.T., et al., *CD147 immunoglobulin superfamily receptor function and role in pathology.* Experimental and molecular pathology, 2007. **83**(3): p. 283-295.
343. Muramatsu, T., *Basigin (CD147), a multifunctional transmembrane glycoprotein with various binding partners.* Journal of biochemistry, 2016. **159**(5): p. 481-490.
344. Xin, X., et al., *CD147/EMMPRIN overexpression and prognosis in cancer: A systematic review and meta-analysis.* Scientific Reports, 2016. **6**: p. 32804.
345. Curtin, K.D., I.A. Meinertzhagen, and R.J. Wyman, *Basigin (EMMPRIN/CD147) interacts with integrin to affect cellular architecture.* Journal of Cell Science, 2005. **118**(12): p. 2649.
346. Trachtenberg, A., et al., *The level of CD147 expression correlates with cyclophilin-induced signalling and chemotaxis.* BMC Research Notes, 2011. **4**(1): p. 396.
347. Landsman, L., et al., *CX3CR1 is required for monocyte homeostasis and atherogenesis by promoting cell survival.* Blood, 2009. **113**(4): p. 963-72.
348. Dos Anjos Cassado, A., *F4/80 as a Major Macrophage Marker: The Case of the Peritoneum and Spleen.* Results Probl Cell Differ, 2017. **62**: p. 161-179.
349. Sahu, R., et al., *Structure and function of renal macrophages and dendritic cells from lupus-prone mice.* Arthritis & rheumatology (Hoboken, N.J.), 2014. **66**(6): p. 1596-1607.
350. Stevens, W.W., et al., *Detection and quantitation of eosinophils in the murine respiratory tract by flow cytometry.* Journal of immunological methods, 2007. **327**(1-2): p. 63-74.
351. Kuchroo, V.K., et al., *New roles for TIM family members in immune regulation.* Nat Rev Immunol, 2008. **8**(8): p. 577-80.

352. Mengshol, J.A., et al., *A Crucial Role for Kupffer Cell-Derived Galectin-9 in Regulation of T Cell Immunity in Hepatitis C Infection.* PLOS ONE, 2010. **5**(3): p. e9504.
353. Imaizumi, T., et al., *Interferon-gamma stimulates the expression of galectin-9 in cultured human endothelial cells.* J Leukoc Biol, 2002. **72**(3): p. 486-91.
354. Jayaraman, P., et al., *Tim3 binding to galectin-9 stimulates antimicrobial immunity.* The Journal of experimental medicine, 2010. **207**(11): p. 2343-2354.
355. Sehrawat, S., et al., *Galectin-9/TIM-3 interaction regulates virus-specific primary and memory CD8 T cell response.* PLoS Pathog, 2010. **6**(5): p. e1000882.
356. Zhu, C., et al., *The Tim-3 ligand galectin-9 negatively regulates T helper type 1 immunity.* Nat Immunol, 2005. **6**(12): p. 1245-52.
357. Chou, F.C., S.J. Shieh, and H.K. Sytwu, *Attenuation of Th1 response through galectin-9 and T-cell Ig mucin 3 interaction inhibits autoimmune diabetes in NOD mice.* Eur J Immunol, 2009. **39**(9): p. 2403-11.
358. Kashio, Y., et al., *Galectin-9 induces apoptosis through the calcium-calpain-caspase-1 pathway.* J Immunol, 2003. **170**(7): p. 3631-6.
359. Dardalhon, V., et al., *Tim-3/galectin-9 pathway: regulation of Th1 immunity through promotion of CD11b+Ly-6G+ myeloid cells.* J Immunol, 2010. **185**(3): p. 1383-92.
360. Li, Y., et al., *The N- and C-terminal carbohydrate recognition domains of galectin-9 contribute differently to its multiple functions in innate immunity and adaptive immunity.* Mol Immunol, 2011. **48**(4): p. 670-7.
361. Rabinovich, G.A. and M.A. Toscano, *Turning 'sweet' on immunity: galectin-glycan interactions in immune tolerance and inflammation.* Nat Rev Immunol, 2009. **9**(5): p. 338-52.
362. Matsumoto, R., et al., *Human ecalectin, a variant of human galectin-9, is a novel eosinophil chemoattractant produced by T lymphocytes.* J Biol Chem, 1998. **273**(27): p. 16976-84.
363. Barondes, S.H., et al., *Galectins: a family of animal beta-galactoside-binding lectins.* Cell, 1994. **76**(4): p. 597-8.
364. Lee, P.Y., et al., *Ly6 family proteins in neutrophil biology.* J Leukoc Biol, 2013. **94**(4): p. 585-94.
365. Wang, J.X., et al., *Ly6G ligation blocks recruitment of neutrophils via a beta2-integrin-dependent mechanism.* Blood, 2012. **120**(7): p. 1489-98.
366. Hanninen, A., et al., *Ly6C supports preferential homing of central memory CD8+ T cells into lymph nodes.* Eur J Immunol, 2011. **41**(3): p. 634-44.
367. Youn, J.I. and D.I. Gabrilovich, *The biology of myeloid-derived suppressor cells: the blessing and the curse of morphological and functional heterogeneity.* Eur J Immunol, 2010. **40**(11): p. 2969-75.
368. Egan, C.E., et al., *Understanding the multiple functions of Gr-1(+) cell subpopulations during microbial infection.* Immunol Res, 2008. **40**(1): p. 35-48.
369. Jaakkola, I., et al., *Ly6C induces clustering of LFA-1 (CD11a/CD18) and is involved in subtype-specific adhesion of CD8 T cells.* J Immunol, 2003. **170**(3): p. 1283-90.
370. Kusmartsev, S.A., Y. Li, and S.H. Chen, *Gr-1+ myeloid cells derived from tumor-bearing mice inhibit primary T cell activation induced through CD3/CD28 costimulation.* J Immunol, 2000. **165**(2): p. 779-85.
371. Fleming, T.J., M.L. Fleming, and T.R. Malek, *Selective expression of Ly-6G on myeloid lineage cells in mouse bone marrow. RB6-8C5 mAb to granulocyte-differentiation antigen (Gr-1) detects members of the Ly-6 family.* J Immunol, 1993. **151**(5): p. 2399-408.
372. Neefjes, J., et al., *Towards a systems understanding of MHC class I and MHC class II antigen presentation.* Nat Rev Immunol, 2011. **11**(12): p. 823-36.

373. Blum, J.S., P.A. Wearsch, and P. Cresswell, *Pathways of antigen processing.* Annu Rev Immunol, 2013. **31**: p. 443-73.
374. Linehan, E. and D.C. Fitzgerald, *Ageing and the immune system: focus on macrophages.* European journal of microbiology & immunology, 2015. **5**(1): p. 14-24.
375. van Beek, A.A., et al., *Metabolic Alterations in Aging Macrophages: Ingredients for Inflammaging?* Trends Immunol, 2019. **40**(2): p. 113-127.
376. Guillot, A. and F. Tacke, *Liver Macrophages: Old Dogmas and New Insights.* Hepatol Commun, 2019. **3**(6): p. 730-743.
377. Stahl, E.C., et al., *Macrophages in the Aging Liver and Age-Related Liver Disease.* Frontiers in immunology, 2018. **9**: p. 2795-2795.
378. Maeso-Diaz, R., et al., *Effects of aging on liver microcirculatory function and sinusoidal phenotype.* Aging Cell, 2018. **17**(6): p. e12829.
379. Maeso-Díaz, R., et al., *Aging Influences Hepatic Microvascular Biology and Liver Fibrosis in Advanced Chronic Liver Disease.* Aging and disease, 2019. **10**(4): p. 684-698.
380. Oishi, Y. and I. Manabe, *Macrophages in age-related chronic inflammatory diseases.* Npj Aging And Mechanisms Of Disease, 2016. **2**: p. 16018.
381. Plowden, J., et al., *Innate immunity in aging: impact on macrophage function.* Aging Cell, 2004. **3**(4): p. 161-7.
382. Murciano, C., et al., *Influence of aging on murine neutrophil and macrophage function against Candida albicans.* Pathogens and Disease, 2008. **53**(2): p. 214-221.
383. Chen, Y. and X. Zhang, *Pivotal regulators of tissue homeostasis and cancer: macrophages.* Experimental hematology & oncology, 2017. **6**: p. 23-23.
384. Fujiwara, N. and K. Kobayashi, *Macrophages in inflammation.* Curr Drug Targets Inflamm Allergy, 2005. **4**(3): p. 281-6.
385. Yang, M., et al., *Diverse Functions of Macrophages in Different Tumor Microenvironments.* Cancer Res, 2018. **78**(19): p. 5492-5503.
386. Cassetta, L. and T. Kitamura, *Targeting Tumor-Associated Macrophages as a Potential Strategy to Enhance the Response to Immune Checkpoint Inhibitors.* Frontiers in cell and developmental biology, 2018. **6**: p. 38-38.
387. Loberg, R.D., et al., *Targeting CCL2 with systemic delivery of neutralizing antibodies induces prostate cancer tumor regression in vivo.* Cancer Res, 2007. **67**(19): p. 9417-24.
388. Brana, I., et al., *Carlumab, an anti-C-C chemokine ligand 2 monoclonal antibody, in combination with four chemotherapy regimens for the treatment of patients with solid tumors: an open-label, multicenter phase 1b study.* Target Oncol, 2015. **10**(1): p. 111-23.
389. Fortin, C.F., et al., *Aging and neutrophils: there is still much to do.* Rejuvenation Res, 2008. **11**(5): p. 873-82.
390. Fulop, T., et al., *Potential role of immunosenescence in cancer development.* Ann N Y Acad Sci, 2010. **1197**: p. 158-65.
391. Koch, S., et al., *Multiparameter flow cytometric analysis of CD4 and CD8 T cell subsets in young and old people.* Immun Ageing, 2008. **5**: p. 6.
392. Spann, N.J., et al., *Regulated accumulation of desmosterol integrates macrophage lipid metabolism and inflammatory responses.* Cell, 2012. **151**(1): p. 138-152.
393. Petan, T., E. Jarc, and M. Jusović, *Lipid Droplets in Cancer: Guardians of Fat in a Stressful World.* Molecules (Basel, Switzerland), 2018. **23**(8): p. 1941.
394. Goossens, P., et al., *Membrane Cholesterol Efflux Drives Tumor-Associated Macrophage Reprogramming and Tumor Progression.* Cell Metab, 2019. **29**(6): p. 1376-1389.e4.

395. Dallagi, A., et al., *The activating effect of IFN-γ on monocytes/macrophages is regulated by the LIF-trophoblast-IL-10 axis via Stat1 inhibition and Stat3 activation.* Cellular & molecular immunology, 2015. **12**(3): p. 326-341.
396. Cotte, A.K., et al., *Lysophosphatidylcholine acyltransferase 2-mediated lipid droplet production supports colorectal cancer chemoresistance.* Nature Communications, 2018. **9**(1): p. 322.
397. Gordon, S. and P.R. Taylor, *Monocyte and macrophage heterogeneity.* Nat Rev Immunol, 2005. **5**(12): p. 953-64.
398. Stout, R.D. and J. Suttles, *Functional plasticity of macrophages: reversible adaptation to changing microenvironments.* Journal of leukocyte biology, 2004. **76**(3): p. 509-513.
399. Arnold, L., et al., *Inflammatory monocytes recruited after skeletal muscle injury switch into antiinflammatory macrophages to support myogenesis.* The Journal of experimental medicine, 2007. **204**(5): p. 1057-1069.
400. Ren, K. and R. Torres, *Role of interleukin-1beta during pain and inflammation.* Brain research reviews, 2009. **60**(1): p. 57-64.
401. Groeneveld, P.H., et al., *Relation between pro- and anti-inflammatory cytokines and the production of nitric oxide (NO) in severe sepsis.* Cytokine, 1997. **9**(2): p. 138-42.
402. Geissmann, F., S. Jung, and D.R. Littman, *Blood Monocytes Consist of Two Principal Subsets with Distinct Migratory Properties.* Immunity, 2003. **19**(1): p. 71-82.
403. Movahedi, K., et al., *Different tumor microenvironments contain functionally distinct subsets of macrophages derived from Ly6C(high) monocytes.* Cancer Res, 2010. **70**(14): p. 5728-39.
404. Mosser, D.M. and J.P. Edwards, *Exploring the full spectrum of macrophage activation.* Nat Rev Immunol, 2008. **8**(12): p. 958-69.
405. Shi, C. and E.G. Pamer, *Monocyte recruitment during infection and inflammation.* Nat Rev Immunol, 2011. **11**(11): p. 762-74.
406. Jeong, J., Y. Suh, and K. Jung, *Context Drives Diversification of Monocytes and Neutrophils in Orchestrating the Tumor Microenvironment.* Frontiers in immunology, 2019. **10**: p. 1817-1817.
407. Shi, C. and E.G. Pamer, *Monocyte recruitment during infection and inflammation.* Nature reviews. Immunology, 2011. **11**(11): p. 762-774.
408. Lee, M., et al., *Tissue-specific Role of CX(3)CR1 Expressing Immune Cells and Their Relationships with Human Disease.* Immune network, 2018. **18**(1): p. e5-e5.
409. Jacquelin, S., et al., *CX3CR1 reduces Ly6Chigh-monocyte motility within and release from the bone marrow after chemotherapy in mice.* Blood, 2013. **122**(5): p. 674-683.
410. Zheng, J., et al., *Chemokine receptor CX3CR1 contributes to macrophage survival in tumor metastasis.* Molecular Cancer, 2013. **12**(1): p. 141.
411. Kolter, J., et al., *A Subset of Skin Macrophages Contributes to the Surveillance and Regeneration of Local Nerves.* Immunity, 2019. **50**(6): p. 1482-1497.e7.
412. Zhang, J. and J.M. Patel, *Role of the CX3CL1-CX3CR1 axis in chronic inflammatory lung diseases.* International journal of clinical and experimental medicine, 2010. **3**(3): p. 233-244.
413. Li, L., et al., *The chemokine receptors CCR2 and CX3CR1 mediate monocyte/macrophage trafficking in kidney ischemia-reperfusion injury.* Kidney international, 2008. **74**(12): p. 1526-1537.
414. Ishida, Y., J.L. Gao, and P.M. Murphy, *Chemokine receptor CX3CR1 mediates skin wound healing by promoting macrophage and fibroblast accumulation and function.* J Immunol, 2008. **180**(1): p. 569-79.

415. Rose, S., A. Misharin, and H. Perlman, *A novel Ly6C/Ly6G-based strategy to analyze the mouse splenic myeloid compartment.* Cytometry. Part A : the journal of the International Society for Analytical Cytology, 2012. **81**(4): p. 343-350.
416. Italiani, P. and D. Boraschi, *From Monocytes to M1/M2 Macrophages: Phenotypical vs. Functional Differentiation.* Frontiers in immunology, 2014. **5**: p. 514-514.
417. Bain, C.C., et al., *Resident and pro-inflammatory macrophages in the colon represent alternative context-dependent fates of the same Ly6Chi monocyte precursors.* Mucosal immunology, 2013. **6**(3): p. 498-510.
418. Qian, B.Z., et al., *CCL2 recruits inflammatory monocytes to facilitate breast-tumour metastasis.* Nature, 2011. **475**(7355): p. 222-5.
419. Chittezhath, M., et al., *Molecular profiling reveals a tumor-promoting phenotype of monocytes and macrophages in human cancer progression.* Immunity, 2014. **41**(5): p. 815-29.
420. Chen, Y., et al., *Differential effects of sorafenib on liver versus tumor fibrosis mediated by stromal-derived factor 1 alpha/C-X-C receptor type 4 axis and myeloid differentiation antigen-positive myeloid cell infiltration in mice.* Hepatology, 2014. **59**(4): p. 1435-47.
421. Long, K.B., et al., *IFNγ and CCL2 Cooperate to Redirect Tumor-Infiltrating Monocytes to Degrade Fibrosis and Enhance Chemotherapy Efficacy in Pancreatic Carcinoma.* Cancer Discov, 2016. **6**(4): p. 400-413.
422. Kubo, H., et al., *Primary Tumors Limit Metastasis Formation through Induction of IL15-Mediated Cross-Talk between Patrolling Monocytes and NK Cells.* Cancer Immunol Res, 2017. **5**(9): p. 812-820.
423. Jung, K., et al., *Ly6Clo monocytes drive immunosuppression and confer resistance to anti-VEGFR2 cancer therapy.* J Clin Invest, 2017. **127**(8): p. 3039-3051.
424. Jung, K., et al., *Targeting CXCR4-dependent immunosuppressive Ly6C(low) monocytes improves antiangiogenic therapy in colorectal cancer.* Proc Natl Acad Sci U S A, 2017. **114**(39): p. 10455-10460.
425. Misharin, A.V., et al., *Nonclassical Ly6C(-) monocytes drive the development of inflammatory arthritis in mice.* Cell reports, 2014. **9**(2): p. 591-604.
426. Olingy, C.E., et al., *Non-classical monocytes are biased progenitors of wound healing macrophages during soft tissue injury.* Scientific Reports, 2017. **7**(1): p. 447.
427. Jackaman, C., et al., *Targeting macrophages rescues age-related immune deficiencies in C57BL/6J geriatric mice.* Aging Cell, 2013. **12**(3): p. 345-57.
428. Hewitt, E.W., *The MHC class I antigen presentation pathway: strategies for viral immune evasion.* Immunology, 2003. **110**(2): p. 163-169.
429. Jones, E.Y., et al., *MHC class II proteins and disease: a structural perspective.* Nat Rev Immunol, 2006. **6**(4): p. 271-82.
430. Duong, L., et al., *Macrophage Depletion in Elderly Mice Improves Response to Tumor Immunotherapy, Increases Anti-tumor T Cell Activity and Reduces Treatment-Induced Cachexia.* Front Genet, 2018. **9**: p. 526.
431. Wang, C.Q., et al., *Effect of age on marrow macrophage number and function.* Aging (Milano), 1995. **7**(5): p. 379-84.
432. Nielsen, S.R. and M.C. Schmid, *Macrophages as Key Drivers of Cancer Progression and Metastasis.* Mediators Inflamm, 2017. **2017**: p. 9624760.
433. Dandekar, R.C., A.V. Kingaonkar, and G.S. Dhabekar, *Role of macrophages in malignancy.* Annals of maxillofacial surgery, 2011. **1**(2): p. 150-154.
434. Sica, A., et al., *Macrophage polarization in tumour progression.* Semin Cancer Biol, 2008. **18**(5): p. 349-55.

435. Helm, O., et al., *M1 and M2: there is no "good" and "bad"-How macrophages promote malignancy-associated features in tumorigenesis.* Oncoimmunology, 2014. **3**(7): p. e946818-e946818.
436. Kalish, S., et al., *M3 Macrophages Stop Division of Tumor Cells In Vitro and Extend Survival of Mice with Ehrlich Ascites Carcinoma.* Medical science monitor basic research, 2017. **23**: p. 8-19.
437. Jackaman, C., et al., *Murine mesothelioma induces locally-proliferating IL-10(+)TNF-α(+)CD206(-)CX3CR1(+) M3 macrophages that can be selectively depleted by chemotherapy or immunotherapy.* Oncoimmunology, 2016. **5**(6): p. e1173299-e1173299.
438. Long, J., et al., *Lipid metabolism and carcinogenesis, cancer development.* American journal of cancer research, 2018. **8**(5): p. 778-791.
439. Collot-Teixeira, S., et al., *CD36 and macrophages in atherosclerosis.* Cardiovasc Res, 2007. **75**(3): p. 468-77.
440. Glatz, J.F.C. and J.J.F.P. Luiken, *Dynamic role of the transmembrane glycoprotein CD36 (SR-B2) in cellular fatty acid uptake and utilization.* Journal of Lipid Research, 2018.
441. Silverstein, R.L. and M. Febbraio, *CD36, a Scavenger Receptor Involved in Immunity, Metabolism, Angiogenesis, and Behavior.* Science Signaling, 2009. **2**(72): p. re3.
442. Toole, B.P., *Emmprin (CD147), a cell surface regulator of matrix metalloproteinase production and function.* Curr Top Dev Biol, 2003. **54**: p. 371-89.
443. Li, J., et al., *CD147 reprograms fatty acid metabolism in hepatocellular carcinoma cells through Akt/mTOR/SREBP1c and P38/PPARalpha pathways.* J Hepatol, 2015. **63**(6): p. 1378-89.
444. Zhu, D., et al., *The Cyclophilin A-CD147 complex promotes the proliferation and homing of multiple myeloma cells.* Nat Med, 2015. **21**(6): p. 572-80.
445. Felmlee, D.J. and T.F. Baumert, *CD147 handles lipid: a new role for anti-cancer target.* Translational Cancer Research, 2016. **5**(3): p. 238-240.
446. Martín-Orozco, N., A. Isibasi, and V. Ortiz-Navarrete, *Macrophages present exogenous antigens by class I major histocompatibility complex molecules via a secretory pathway as a consequence of interferon-gamma activation.* Immunology, 2001. **103**(1): p. 41-48.
447. Micheletti, F., et al., *The lifespan of major histocompatibility complex class I/peptide complexes determines the efficiency of cytotoxic T-lymphocyte responses.* Immunology, 1999. **96**(3): p. 411-5.
448. Wang, B., et al., *Transition of tumor-associated macrophages from MHC class IIhi to MHC class IIlow mediates tumor progression in mice.* BMC Immunology, 2011. **12**(1): p. 43.
449. Balbo, P., et al., *Differential role of CD80 and CD86 on alveolar macrophages in the presentation of allergen to T lymphocytes in asthma.* Clin Exp Allergy, 2001. **31**(4): p. 625-36.
450. Dong, L., et al., *The Activation of Macrophage and Upregulation of CD40 Costimulatory Molecule in Lipopolysaccharide-Induced Acute Lung Injury.* Journal of Biomedicine and Biotechnology, 2008. **2008**.
451. Kurotaki, D., T. Uede, and T. Tamura, *Functions and development of red pulp macrophages.* Microbiology and Immunology, 2015. **59**(2): p. 55-62.
452. Kohyama, M., et al., *Role for Spi-C in the development of red pulp macrophages and splenic iron homeostasis.* Nature, 2009. **457**(7227): p. 318-21.
453. Kurotaki, D., T. Uede, and T. Tamura, *Functions and development of red pulp macrophages.* Microbiol Immunol, 2015. **59**(2): p. 55-62.

454. Zhu, X., et al., *Penicillar arterioles of red pulp in residual spleen after subtotal splenectomy due to splenomegaly in cirrhotic patients: a comparative study.* International journal of clinical and experimental pathology, 2015. **8**(1): p. 711-718.
455. Kurotaki, D., et al., *CSF-1-dependent red pulp macrophages regulate CD4 T cell responses.* J Immunol, 2011. **186**(4): p. 2229-37.
456. Bronte, V. and M.J. Pittet, *The spleen in local and systemic regulation of immunity.* Immunity, 2013. **39**(5): p. 806-818.
457. Gordon, S., A. Plüddemann, and F. Martinez Estrada, *Macrophage heterogeneity in tissues: phenotypic diversity and functions.* Immunological reviews, 2014. **262**(1): p. 36-55.
458. Cortez-Retamozo, V., et al., *Origins of tumor-associated macrophages and neutrophils.* Proceedings of the National Academy of Sciences of the United States of America, 2012. **109**(7): p. 2491-2496.
459. Cortez-Retamozo, V., et al., *Angiotensin II drives the production of tumor-promoting macrophages.* Immunity, 2013. **38**(2): p. 296-308.
460. Luo, Q., et al., *Lipid accumulation in macrophages confers protumorigenic polarization and immunity in gastric cancer.* Cancer science, 2020. **111**(11): p. 4000-4011.
461. Pawelec, G., *Immunosenescence and cancer.* Biogerontology, 2017. **18**(4): p. 717-721.
462. Ostuni, R., et al., *Macrophages and cancer: from mechanisms to therapeutic implications.* Trends Immunol, 2015. **36**(4): p. 229-39.
463. Argyle, D. and T. Kitamura, *Targeting Macrophage-Recruiting Chemokines as a Novel Therapeutic Strategy to Prevent the Progression of Solid Tumors.* Frontiers in immunology, 2018. **9**: p. 2629-2629.
464. Cao, W., et al., *Oxidized Lipids Block Antigen Cross-Presentation by Dendritic Cells in Cancer.* The Journal of Immunology, 2014. **192**(6): p. 2920.
465. Netea-Maier, R.T., J.W.A. Smit, and M.G. Netea, *Metabolic changes in tumor cells and tumor-associated macrophages: A mutual relationship.* Cancer Letters, 2018. **413**: p. 102-109.
466. Ricciotti, E. and G.A. FitzGerald, *Prostaglandins and inflammation.* Arterioscler Thromb Vasc Biol, 2011. **31**(5): p. 986-1000.
467. Schlager, S.I., et al., *Role of macrophage lipids in regulating tumoricidal activity.* Cell Immunol, 1983. **77**(1): p. 52-68.
468. Zhang, Y., et al., *Fatty acid-binding protein E-FABP restricts tumor growth by promoting IFN-beta responses in tumor-associated macrophages.* Cancer Res, 2014. **74**(11): p. 2986-98.
469. Nickerson, J.G., et al., *Greater transport efficiencies of the membrane fatty acid transporters FAT/CD36 and FATP4 compared with FABPpm and FATP1 and differential effects on fatty acid esterification and oxidation in rat skeletal muscle.* J Biol Chem, 2009. **284**(24): p. 16522-30.
470. McFarlan, J.T., et al., *In vivo, fatty acid translocase (CD36) critically regulates skeletal muscle fuel selection, exercise performance, and training-induced adaptation of fatty acid oxidation.* J Biol Chem, 2012. **287**(28): p. 23502-16.
471. Guo, H., et al., *EMMPRIN (CD147), an inducer of matrix metalloproteinase synthesis, also binds interstitial collagenase to the tumor cell surface.* Cancer Res, 2000. **60**(4): p. 888-91.
472. Caudroy, S., et al., *EMMPRIN-mediated MMP regulation in tumor and endothelial cells.* Clin Exp Metastasis, 2002. **19**(8): p. 697-702.

473. Bougatef, F., et al., *EMMPRIN promotes angiogenesis through hypoxia-inducible factor-2alpha-mediated regulation of soluble VEGF isoforms and their receptor VEGFR-2.* Blood, 2009. **114**(27): p. 5547-56.
474. Tang, Y., et al., *Tumor-stroma interaction: positive feedback regulation of extracellular matrix metalloproteinase inducer (EMMPRIN) expression and matrix metalloproteinase-dependent generation of soluble EMMPRIN.* Mol Cancer Res, 2004. **2**(2): p. 73-80.
475. Amit-Cohen, B.-C., M.M. Rahat, and M.A. Rahat, *Tumor cell-macrophage interactions increase angiogenesis through secretion of EMMPRIN.* Frontiers in physiology, 2013. **4**: p. 178-178.
476. Walter, M., et al., *An epitope-specific novel anti-EMMPRIN polyclonal antibody inhibits tumor progression.* Oncoimmunology, 2015. **5**(2): p. e1078056-e1078056.
477. Han, Y., et al., *Tumor-Induced Generation of Splenic Erythroblast-like Ter-Cells Promotes Tumor Progression.* Cell, 2018. **173**.
478. Miluzio, A., et al., *Impairment of Cytoplasmic eIF6 Activity Restricts Lymphomagenesis and Tumor Progression without Affecting Normal Growth.* Cancer Cell, 2011. **19**(6): p. 765-775.
479. Wang, B., et al., *Transition of tumor-associated macrophages from MHC class II(hi) to MHC class II(low) mediates tumor progression in mice.* BMC immunology, 2011. **12**: p. 43-43.
480. Wei, L.J., et al., *[A case-control study on the association between serum lipid level and the risk of breast cancer].* Zhonghua Yu Fang Yi Xue Za Zhi, 2016. **50**(12): p. 1091-1095.
481. Muka, T., et al., *Dietary polyunsaturated fatty acids intake modifies the positive association between serum total cholesterol and colorectal cancer risk: the Rotterdam Study.* J Epidemiol Community Health, 2016. **70**(9): p. 881-7.
482. Kitahara, C.M., et al., *Total cholesterol and cancer risk in a large prospective study in Korea.* J Clin Oncol, 2011. **29**(12): p. 1592-8.
483. Yue, S., et al., *Cholesteryl ester accumulation induced by PTEN loss and PI3K/AKT activation underlies human prostate cancer aggressiveness.* Cell Metab, 2014. **19**(3): p. 393-406.
484. Baenke, F., et al., *Hooked on fat: the role of lipid synthesis in cancer metabolism and tumour development.* Dis Model Mech, 2013. **6**(6): p. 1353-63.
485. Shaikh, S.R., et al., *Differential effects of a saturated and a monounsaturated fatty acid on MHC class I antigen presentation.* Scandinavian journal of immunology, 2008. **68**(1): p. 30-42.
486. Herber, D.L., et al., *Lipid accumulation and dendritic cell dysfunction in cancer.* Nat Med, 2010. **16**(8): p. 880-6.
487. Veglia, F., et al., *Lipid bodies containing oxidatively truncated lipids block antigen cross-presentation by dendritic cells in cancer.* Nature Communications, 2017. **8**(1): p. 2122.
488. Rabold, K., et al., *Enhanced lipid biosynthesis in human tumor-induced macrophages contributes to their protumoral characteristics.* J Immunother Cancer, 2020. **8**(2).
489. Busse, S., et al., *Expression of HLA-DR, CD80, and CD86 in Healthy Aging and Alzheimer's Disease.* J Alzheimers Dis, 2015. **47**(1): p. 177-84.
490. Costantini, A., et al., *Age-related M1/M2 phenotype changes in circulating monocytes from healthy/unhealthy individuals.* Aging, 2018. **10**(6): p. 1268-1280.
491. Inoue, S., et al., *Persistent inflammation and T cell exhaustion in severe sepsis in the elderly.* Crit Care, 2014. **18**(3): p. R130.
492. Channappanavar, R., et al., *Advancing age leads to predominance of inhibitory receptor expressing CD4 T cells.* Mech Ageing Dev, 2009. **130**(10): p. 709-12.

493. Krummel, M.F. and J.P. Allison, *CD28 and CTLA-4 have opposing effects on the response of T cells to stimulation.* J Exp Med, 1995. **182**(2): p. 459-65.
494. Mahbub, S., C.R. Deburghgraeve, and E.J. Kovacs, *Advanced age impairs macrophage polarization.* J Interferon Cytokine Res, 2012. **32**(1): p. 18-26.
495. Stout, R.D., et al., *Macrophages sequentially change their functional phenotype in response to changes in microenvironmental influences.* J Immunol, 2005. **175**(1): p. 342-9.
496. Mahbub, S., C.R. Deburghgraeve, and E.J. Kovacs, *Advanced age impairs macrophage polarization.* Journal of interferon & cytokine research : the official journal of the International Society for Interferon and Cytokine Research, 2012. **32**(1): p. 18-26.
497. Albright, J.M., et al., *Advanced Age Alters Monocyte and Macrophage Responses.* Antioxidants & redox signaling, 2016. **25**(15): p. 805-815.
498. Glezeva, N., S. Horgan, and J.A. Baugh, *Monocyte and macrophage subsets along the continuum to heart failure: Misguided heroes or targetable villains?* J Mol Cell Cardiol, 2015. **89**(Pt B): p. 136-45.
499. Malyshev, I. and Y. Malyshev, *Current Concept and Update of the Macrophage Plasticity Concept: Intracellular Mechanisms of Reprogramming and M3 Macrophage "Switch" Phenotype.* Biomed Res Int, 2015. **2015**: p. 341308.
500. den Haan, J.M., S.M. Lehar, and M.J. Bevan, *CD8(+) but not CD8(-) dendritic cells cross-prime cytotoxic T cells in vivo.* The Journal of experimental medicine, 2000. **192**(12): p. 1685-1696.
501. Schnorrer, P., et al., *The dominant role of CD8+ dendritic cells in cross-presentation is not dictated by antigen capture.* Proc Natl Acad Sci U S A, 2006. **103**(28): p. 10729-34.
502. den Haan, J.M., S.M. Lehar, and M.J. Bevan, *CD8(+) but not CD8(-) dendritic cells cross-prime cytotoxic T cells in vivo.* J Exp Med, 2000. **192**(12): p. 1685-96.
503. Maldonado-López, R., et al., *CD8alpha+ and CD8alpha- subclasses of dendritic cells direct the development of distinct T helper cells in vivo.* The Journal of experimental medicine, 1999. **189**(3): p. 587-592.
504. Shortman, K. and S.H. Naik, *Steady-state and inflammatory dendritic-cell development.* Nat Rev Immunol, 2007. **7**(1): p. 19-30.
505. Vremec, D., et al., *CD4 and CD8 expression by dendritic cell subtypes in mouse thymus and spleen.* J Immunol, 2000. **164**(6): p. 2978-86.
506. Edwards, A.D., et al., *Relationships among murine CD11c(high) dendritic cell subsets as revealed by baseline gene expression patterns.* J Immunol, 2003. **171**(1): p. 47-60.
507. Martin, P., et al., *Characterization of a new subpopulation of mouse CD8alpha+ B220+ dendritic cells endowed with type 1 interferon production capacity and tolerogenic potential.* Blood, 2002. **100**(2): p. 383-90.
508. Zheng, D., et al., *Lipopolysaccharide-pretreated plasmacytoid dendritic cells ameliorate experimental chronic kidney disease.* Kidney Int, 2012. **81**(9): p. 892-902.
509. Audiger, C., et al., *The Importance of Dendritic Cells in Maintaining Immune Tolerance.* Journal of immunology (Baltimore, Md. : 1950), 2017. **198**(6): p. 2223-2231.
510. Ali, S., et al., *Sources of Type I Interferons in Infectious Immunity: Plasmacytoid Dendritic Cells Not Always in the Driver's Seat.* Frontiers in immunology, 2019. **10**: p. 778-778.
511. Nakano, H., M. Yanagita, and M.D. Gunn, *CD11c(+)B220(+)Gr-1(+) cells in mouse lymph nodes and spleen display characteristics of plasmacytoid dendritic cells.* The Journal of experimental medicine, 2001. **194**(8): p. 1171-1178.

512. Steger, M.M., C. Maczek, and B. Grubeck-Loebenstein, *Morphologically and functionally intact dendritic cells can be derived from the peripheral blood of aged individuals.* Clin Exp Immunol, 1996. **105**(3): p. 544-50.
513. van Dommelen, S.L.H., et al., *Regeneration of dendritic cells in aged mice.* Cellular & molecular immunology, 2010. **7**(2): p. 108-115.
514. Zacca, E.R., et al., *Aging Impairs the Ability of Conventional Dendritic Cells to Cross-Prime CD8+ T Cells upon Stimulation with a TLR7 Ligand.* PLoS One, 2015. **10**(10): p. e0140672.
515. Wong, C.P., K.R. Magnusson, and E. Ho, *Aging is associated with altered dendritic cells subset distribution and impaired proinflammatory cytokine production.* Exp Gerontol, 2010. **45**(2): p. 163-9.
516. Chougnet, C.A., et al., *Loss of Phagocytic and Antigen Cross-Presenting Capacity in Aging Dendritic Cells Is Associated with Mitochondrial Dysfunction.* Journal of immunology (Baltimore, Md. : 1950), 2015. **195**(6): p. 2624-2632.
517. Jiang, J., et al., *Limited expansion of virus-specific CD8 T cells in the aged environment.* Mech Ageing Dev, 2009. **130**(11-12): p. 713-21.
518. Lages, C.S., et al., *Partial restoration of T-cell function in aged mice by in vitro blockade of the PD-1/ PD-L1 pathway.* Aging Cell, 2010. **9**(5): p. 785-98.
519. Shurin, G.V., et al., *Regulation of dendritic cell expansion in aged athymic nude mice by FLT3 ligand.* Exp Gerontol, 2004. **39**(3): p. 339-48.
520. Hadrup, S., M. Donia, and P. Thor Straten, *Effector CD4 and CD8 T cells and their role in the tumor microenvironment.* Cancer microenvironment : official journal of the International Cancer Microenvironment Society, 2013. **6**(2): p. 123-133.
521. Melief, C.J., *Tumor eradication by adoptive transfer of cytotoxic T lymphocytes.* Adv Cancer Res, 1992. **58**: p. 143-75.
522. Chomarat, P., et al., *IL-6 switches the differentiation of monocytes from dendritic cells to macrophages.* Nat Immunol, 2000. **1**(6): p. 510-4.
523. Pahne-Zeppenfeld, J., et al., *Cervical cancer cell-derived interleukin-6 impairs CCR7-dependent migration of MMP-9-expressing dendritic cells.* Int J Cancer, 2014. **134**(9): p. 2061-73.
524. Huang, L.-Y., et al., *IL-12 Induction by a Th1-Inducing Adjuvant In Vivo: Dendritic Cell Subsets and Regulation by IL-10.* The Journal of Immunology, 2001. **167**(3): p. 1423.
525. Yang, A.S. and E.C. Lattime, *Tumor-induced interleukin 10 suppresses the ability of splenic dendritic cells to stimulate CD4 and CD8 T-cell responses.* Cancer Res, 2003. **63**(9): p. 2150-7.
526. Thomas, A., et al., *Distinctive clinical characteristics of malignant mesothelioma in young patients.* Oncotarget, 2015. **6**(18): p. 16766-16773.
527. Gardner, J.K., et al., *The Regulatory Status Adopted by Lymph Node Dendritic Cells and T Cells During Healthy Aging Is Maintained During Cancer and May Contribute to Reduced Responses to Immunotherapy.* Front Med (Lausanne), 2018. **5**: p. 337.
528. Ramakrishnan, R., et al., *Oxidized lipids block antigen cross-presentation by dendritic cells in cancer.* J Immunol, 2014. **192**(6): p. 2920-31.
529. Mohammadyani, D., et al., *Molecular speciation and dynamics of oxidized triacylglycerols in lipid droplets: Mass spectrometry and coarse-grained simulations.* Free Radic Biol Med, 2014. **76**: p. 53-60.
530. Tyurin, V.A., et al., *Mass-spectrometric characterization of peroxidized and hydrolyzed lipids in plasma and dendritic cells of tumor-bearing animals.* Biochem Biophys Res Commun, 2011. **413**(1): p. 149-53.
531. Hammerschmidt, S.I., et al., *CRISPR/Cas9 Immunoengineering of Hoxb8-Immortalized Progenitor Cells for Revealing CCR7-Mediated Dendritic Cell Signaling and Migration Mechanisms in vivo.* Frontiers in Immunology, 2018. **9**(1949).

532. Mencarelli, A., et al., *Calcineurin-mediated IL-2 production by CD11chighMHCII+ myeloid cells is crucial for intestinal immune homeostasis.* Nature Communications, 2018. **9**(1): p. 1102.
533. Wang, H., et al., *Role of bone marrow-derived CD11c(+) dendritic cells in systolic overload-induced left ventricular inflammation, fibrosis and hypertrophy.* Basic research in cardiology, 2017. **112**(3): p. 25-25.
534. Gardner, J., et al., *Lipid-laden partially-activated plasmacytoid and CD4−CD8α+ dendritic cells accumulate in tissues in elderly mice.* Immunity & ageing : I & A, 2014. **11**: p. 11.
535. Hong, S., et al., *B Cells Are the Dominant Antigen-Presenting Cells that Activate Naive CD4(+) T Cells upon Immunization with a Virus-Derived Nanoparticle Antigen.* Immunity, 2018. **49**(4): p. 695-708.e4.
536. van Leeuwen-Kerkhoff, N., et al., *Human Bone Marrow-Derived Myeloid Dendritic Cells Show an Immature Transcriptional and Functional Profile Compared to Their Peripheral Blood Counterparts and Separate from Slan+ Non-Classical Monocytes.* Frontiers in Immunology, 2018. **9**(1619).
537. Yanagihara, S., et al., *EBI1/CCR7 is a new member of dendritic cell chemokine receptor that is up-regulated upon maturation.* J Immunol, 1998. **161**(6): p. 3096-102.
538. Hirao, M., et al., *CC chemokine receptor-7 on dendritic cells is induced after interaction with apoptotic tumor cells: critical role in migration from the tumor site to draining lymph nodes.* Cancer Res, 2000. **60**(8): p. 2209-17.
539. Pham, W., J. Xie, and J.C. Gore, *Tracking the migration of dendritic cells by in vivo optical imaging.* Neoplasia (New York, N.Y.), 2007. **9**(12): p. 1130-1137.
540. Komatsubara, S., B. Cinader, and S. Muramatsu, *Functional competence of dendritic cells of ageing C57BL/6 mice.* Scand J Immunol, 1986. **24**(5): p. 517-25.
541. Tesar, B.M., et al., *Murine [corrected] myeloid dendritic cell-dependent toll-like receptor immunity is preserved with aging.* Aging Cell, 2006. **5**(6): p. 473-86.
542. Shen, H., et al., *Aging impairs recipient T cell intrinsic and extrinsic factors in response to transplantation.* PloS one, 2009. **4**(1): p. e4097-e4097.
543. Mir, M.A., *Chapter 2 - Concept of Reverse Costimulation and Its Role in Diseases*, in *Developing Costimulatory Molecules for Immunotherapy of Diseases*, M.A. Mir, Editor. 2015, Academic Press. p. 45-81.
544. Zacca, E.R., et al., *Aging Impairs the Ability of Conventional Dendritic Cells to Cross-Prime CD8+ T Cells upon Stimulation with a TLR7 Ligand.* PLOS ONE, 2015. **10**(10): p. e0140672.
545. Emens, L.A., *Breast cancer immunobiology driving immunotherapy: vaccines and immune checkpoint blockade.* Expert Rev Anticancer Ther, 2012. **12**(12): p. 1597-611.
546. Weng, N.P., A.N. Akbar, and J. Goronzy, *CD28(-) T cells: their role in the age-associated decline of immune function.* Trends Immunol, 2009. **30**(7): p. 306-12.
547. Vallejo, A.N., *CD28 extinction in human T cells: altered functions and the program of T-cell senescence.* Immunol Rev, 2005. **205**: p. 158-69.
548. Effros, R.B., *Loss of CD28 expression on T lymphocytes: a marker of replicative senescence.* Dev Comp Immunol, 1997. **21**(6): p. 471-8.
549. Warrington, K.J., et al., *CD28 loss in senescent CD4+ T cells: reversal by interleukin-12 stimulation.* Blood, 2003. **101**(9): p. 3543-9.
550. Sansom, D.M., *CD28, CTLA-4 and their ligands: who does what and to whom?* Immunology, 2000. **101**(2): p. 169-177.
551. Gao, F., et al., *Radiation-driven lipid accumulation and dendritic cell dysfunction in cancer.* Scientific Reports, 2015. **5**(1): p. 9613.

552. Arai, R., et al., *Lipid Accumulation in Peripheral Blood Dendritic Cells and Anticancer Immunity in Patients with Lung Cancer.* Journal of immunology research, 2018. **2018**: p. 5708239-5708239.
553. Cumberbatch, M. and I. Kimber, *Tumour necrosis factor-alpha is required for accumulation of dendritic cells in draining lymph nodes and for optimal contact sensitization.* Immunology, 1995. **84**(1): p. 31-35.
554. Halliday, G.M., V.E. Reeve, and R.S. Barnetson, *Langerhans cell migration into ultraviolet light-induced squamous skin tumors is unrelated to anti-tumor immunity.* J Invest Dermatol, 1991. **97**(5): p. 830-4.
555. Kuwahara, M., et al., *Transforming growth factor beta production by spontaneous malignant mesothelioma cell lines derived from Fisher 344 rats.* Virchows Arch, 2001. **438**(5): p. 492-7.
556. Imai, K., et al., *Inhibition of dendritic cell migration by transforming growth factor-β1 increases tumor-draining lymph node metastasis.* Journal of experimental & clinical cancer research : CR, 2012. **31**(1): p. 3-3.
557. Hirao, M., et al., *CC Chemokine Receptor-7 on Dendritic Cells Is Induced after Interaction with Apoptotic Tumor Cells: Critical Role in Migration from the Tumor Site to Draining Lymph Nodes.* Cancer Research, 2000. **60**(8): p. 2209.
558. Maddaluno, L., et al., *The adhesion molecule L1 regulates transendothelial migration and trafficking of dendritic cells.* The Journal of experimental medicine, 2009. **206**(3): p. 623-635.
559. Agrawal, A. and S. Gupta, *Impact of aging on dendritic cell functions in humans.* Ageing research reviews, 2011. **10**(3): p. 336-345.
560. Linton, P.J., et al., *Intrinsic versus environmental influences on T-cell responses in aging.* Immunol Rev, 2005. **205**: p. 207-19.
561. Agrawal, A., et al., *Increased reactivity of dendritic cells from aged subjects to self-antigen, the human DNA.* J Immunol, 2009. **182**(2): p. 1138-45.
562. Lee, H.W., et al., *Tracking of dendritic cell migration into lymph nodes using molecular imaging with sodium iodide symporter and enhanced firefly luciferase genes.* Scientific Reports, 2015. **5**(1): p. 9865.
563. Zong, J., et al., *Tumor-derived factors modulating dendritic cell function.* Cancer Immunol Immunother, 2016. **65**(7): p. 821-33.
564. Conejo-Garcia, J.R., M.R. Rutkowski, and J.R. Cubillos-Ruiz, *State-of-the-art of regulatory dendritic cells in cancer.* Pharmacol Ther, 2016. **164**: p. 97-104.
565. Tang, M., J. Diao, and M.S. Cattral, *Molecular mechanisms involved in dendritic cell dysfunction in cancer.* Cell Mol Life Sci, 2017. **74**(5): p. 761-776.
566. Diamond, M.S., et al., *Type I interferon is selectively required by dendritic cells for immune rejection of tumors.* The Journal of experimental medicine, 2011. **208**(10): p. 1989-2003.
567. Fuertes, M.B., et al., *Host type I IFN signals are required for antitumor CD8+ T cell responses through CD8{alpha}+ dendritic cells.* J Exp Med, 2011. **208**(10): p. 2005-16.
568. Diamond, M.S., et al., *Type I interferon is selectively required by dendritic cells for immune rejection of tumors.* J Exp Med, 2011. **208**(10): p. 1989-2003.
569. McDonnell, A., et al., *CD8??+ DC are not the sole subset cross-presenting cell-associated tumor antigens from a solid tumor.* European journal of immunology, 2010. **40**: p. 1617-27.
570. Gardner, J.K., et al., *Mesothelioma Tumor Cells Modulate Dendritic Cell Lipid Content, Phenotype and Function.* PLOS ONE, 2015. **10**(4): p. e0123563.
571. Roper, R.L., *Antigen presentation assays to investigate uncharacterized immunoregulatory genes.* Methods in molecular biology (Clifton, N.J.), 2012. **890**: p. 259-271.

572. Rehm, K.E., et al., *Vaccinia virus A35R inhibits MHC class II antigen presentation.* Virology, 2010. **397**(1): p. 176-186.
573. Campos-Neto, A., et al., *Cutting Edge: CD40 Ligand Is Not Essential for the Development of Cell-Mediated Immunity and Resistance to <em>Mycobacterium tuberculosis</em&gt.* The Journal of Immunology, 1998. **160**(5): p. 2037.
574. Tran Janco, J.M., et al., *Tumor-Infiltrating Dendritic Cells in Cancer Pathogenesis.* The Journal of Immunology, 2015. **194**(7): p. 2985.
575. Swiecki, M. and M. Colonna, *Accumulation of plasmacytoid DC: Roles in disease pathogenesis and targets for immunotherapy.* European journal of immunology, 2010. **40**(8): p. 2094-2098.
576. Hoeffel, G., et al., *Antigen crosspresentation by human plasmacytoid dendritic cells.* Immunity, 2007. **27**(3): p. 481-92.
577. Sapoznikov, A., et al., *Organ-dependent in vivo priming of naive CD4+, but not CD8+, T cells by plasmacytoid dendritic cells.* J Exp Med, 2007. **204**(8): p. 1923-33.
578. Abdalla, D.R., et al., *Bone marrow-derived dendritic cells under influence of experimental breast cancer and physical activity.* Oncology letters, 2017. **13**(3): p. 1406-1410.
579. Lamberti, M.J., et al., *Dendritic Cells and Immunogenic Cancer Cell Death: A Combination for Improving Antitumor Immunity.* Pharmaceutics, 2020. **12**(3): p. 256.
580. Salmon, H., et al., *Expansion and Activation of CD103(+) Dendritic Cell Progenitors at the Tumor Site Enhances Tumor Responses to Therapeutic PD-L1 and BRAF Inhibition.* Immunity, 2016. **44**(4): p. 924-38.
581. Sánchez-Paulete, A.R., et al., *Cancer Immunotherapy with Immunomodulatory Anti-CD137 and Anti-PD-1 Monoclonal Antibodies Requires BATF3-Dependent Dendritic Cells.* Cancer Discov, 2016. **6**(1): p. 71-9.
582. Chudnovskiy, A., G. Pasqual, and G.D. Victora, *Studying interactions between dendritic cells and T cells in vivo.* Current opinion in immunology, 2019. **58**: p. 24-30.
583. Pittet, M.J., et al., *Recording the wild lives of immune cells.* Science immunology, 2018. **3**(27): p. eaaq0491.
584. Zipfel, W.R., R.M. Williams, and W.W. Webb, *Nonlinear magic: multiphoton microscopy in the biosciences.* Nat Biotechnol, 2003. **21**(11): p. 1369-77.
585. Pittet, M.J. and R. Weissleder, *Intravital imaging.* Cell, 2011. **147**(5): p. 983-991.
586. Domogalla, M.P., et al., *Tolerance through Education: How Tolerogenic Dendritic Cells Shape Immunity.* Frontiers in immunology, 2017. **8**: p. 1764-1764.
587. Wculek, S.K., et al., *Metabolic Control of Dendritic Cell Functions: Digesting Information.* Frontiers in immunology, 2019. **10**: p. 775-775.
588. Wu, J., et al., *Critical role of integrin CD11c in splenic dendritic cell capture of missing-self CD47 cells to induce adaptive immunity.* Proceedings of the National Academy of Sciences, 2018. **115**(26): p. 6786.
589. Pearce, E.L., et al., *Fueling immunity: insights into metabolism and lymphocyte function.* Science (New York, N.Y.), 2013. **342**(6155): p. 1242454-1242454.
590. Pollizzi, K.N. and J.D. Powell, *Integrating canonical and metabolic signalling programmes in the regulation of T cell responses.* Nat Rev Immunol, 2014. **14**(7): p. 435-46.
591. Everts, B. and E.J. Pearce, *Metabolic control of dendritic cell activation and function: recent advances and clinical implications.* Frontiers in immunology, 2014. **5**: p. 203-203.
592. Zhao, Y., E.B. Butler, and M. Tan, *Targeting cellular metabolism to improve cancer therapeutics.* Cell Death Dis, 2013. **4**(3): p. e532.

593. Krawczyk, C.M., et al., *Toll-like receptor-induced changes in glycolytic metabolism regulate dendritic cell activation.* Blood, 2010. **115**(23): p. 4742-4749.
594. Dong, H. and T.N.J. Bullock, *Metabolic influences that regulate dendritic cell function in tumors.* Frontiers in immunology, 2014. **5**: p. 24-24.
595. Perrin-Cocon, L., et al., *TLR4 antagonist FP7 inhibits LPS-induced cytokine production and glycolytic reprogramming in dendritic cells, and protects mice from lethal influenza infection.* Scientific reports, 2017. **7**: p. 40791-40791.
596. Perrin-Cocon, L., et al., *Toll-like Receptor 4-Induced Glycolytic Burst in Human Monocyte-Derived Dendritic Cells Results from p38-Dependent Stabilization of HIF-1alpha and Increased Hexokinase II Expression.* J Immunol, 2018. **201**(5): p. 1510-1521.
597. O'Neill, L.A.J. and E.J. Pearce, *Immunometabolism governs dendritic cell and macrophage function.* The Journal of Experimental Medicine, 2016. **213**(1): p. 15.
598. Abdi, K., N.J. Singh, and P. Matzinger, *Lipopolysaccharide-activated dendritic cells: "exhausted" or alert and waiting?* Journal of immunology (Baltimore, Md. : 1950), 2012. **188**(12): p. 5981-5989.
599. Everts, B., et al., *Commitment to glycolysis sustains survival of NO-producing inflammatory dendritic cells.* Blood, 2012. **120**(7): p. 1422-1431.
600. Perrin-Cocon, L., et al., *Toll-like Receptor 4–Induced Glycolytic Burst in Human Monocyte-Derived Dendritic Cells Results from p38-Dependent Stabilization of HIF-1α and Increased Hexokinase II Expression.* The Journal of Immunology, 2018. **201**(5): p. 1510-1521.
601. Tan, B., et al., *The profiles of mitochondrial respiration and glycolysis using extracellular flux analysis in porcine enterocyte IPEC-J2.* Animal Nutrition, 2015. **1**(3): p. 239-243.
602. Langston, P.K., M. Shibata, and T. Horng, *Metabolism Supports Macrophage Activation.* Frontiers in immunology, 2017. **8**: p. 61-61.
603. Chang, C.-H., et al., *Metabolic Competition in the Tumor Microenvironment Is a Driver of Cancer Progression.* Cell, 2015. **162**(6): p. 1229-1241.
604. Frisard, M.I., et al., *Low levels of lipopolysaccharide modulate mitochondrial oxygen consumption in skeletal muscle.* Metabolism: clinical and experimental, 2015. **64**(3): p. 416-427.
605. Rose, S., et al., *Oxidative stress induces mitochondrial dysfunction in a subset of autism lymphoblastoid cell lines in a well-matched case control cohort.* PloS one, 2013. **31**(1): p. e85436-e85436.
606. Malinarich, F., et al., *High mitochondrial respiration and glycolytic capacity represent a metabolic phenotype of human tolerogenic dendritic cells.* J Immunol, 2015. **194**(11): p. 5174-86.
607. Sim, W.J., P.J. Ahl, and J.E. Connolly, *Metabolism Is Central to Tolerogenic Dendritic Cell Function.* Mediators of Inflammation, 2016. **2016**: p. 10.
608. Mookerjee, S.A., D.G. Nicholls, and M.D. Brand, *Determining Maximum Glycolytic Capacity Using Extracellular Flux Measurements.* PLOS ONE, 2016. **11**(3): p. e0152016.
609. Solaini, G., G. Sgarbi, and A. Baracca, *Oxidative phosphorylation in cancer cells.* Biochimica et Biophysica Acta (BBA) - Bioenergetics, 2011. **1807**(6): p. 534-542.
610. Kornberg, M.D., et al., *Dimethyl fumarate targets GAPDH and aerobic glycolysis to modulate immunity.* Science, 2018. **360**(6387): p. 449.
611. Agnello, M., G. Morici, and A.M. Rinaldi, *A method for measuring mitochondrial mass and activity.* Cytotechnology, 2008. **56**(3): p. 145-149.
612. Suliman, H.B., et al., *Lipopolysaccharide stimulates mitochondrial biogenesis via activation of nuclear respiratory factor-1.* J Biol Chem, 2003. **278**(42): p. 41510-8.

613. Xiao, B., et al., *Flow Cytometry-Based Assessment of Mitophagy Using MitoTracker.* Frontiers in cellular neuroscience, 2016. **10**: p. 76-76.
614. Satapati, S., et al., *Elevated TCA cycle function in the pathology of diet-induced hepatic insulin resistance and fatty liver.* Journal of lipid research, 2012. **53**(6): p. 1080-1092.
615. Liu, Y., et al., *Effect of various freezing solutions on cryopreservation of mesenchymal stem cells from different animal species.* Cryo Letters, 2011. **32**(5): p. 425-35.
616. Lauterboeck, L., et al., *Xeno-Free Cryopreservation of Bone Marrow-Derived Multipotent Stromal Cells from Callithrix jacchus.* Biopreserv Biobank, 2016. **14**(6): p. 530-538.
617. Demetrius, L., *Of mice and men. When it comes to studying ageing and the means to slow it down, mice are not just small humans.* EMBO reports, 2005. **6 Spec No**(Suppl 1): p. S39-S44.
618. Vijayan, V., et al., *Human and murine macrophages exhibit differential metabolic responses to lipopolysaccharide - A divergent role for glycolysis.* Redox biology, 2019. **22**: p. 101147-101147.
619. Mestas, J. and C.C.W. Hughes, *Of Mice and Not Men: Differences between Mouse and Human Immunology.* The Journal of Immunology, 2004. **172**(5): p. 2731.
620. Hilkens, C.M. and J.D. Isaacs, *Tolerogenic dendritic cell therapy for rheumatoid arthritis: where are we now?* Clin Exp Immunol, 2013. **172**(2): p. 148-57.
621. Benner, B., et al., *Generation of monocyte-derived tumor-associated macrophages using tumor-conditioned media provides a novel method to study tumor-associated macrophages in vitro.* Journal for immunotherapy of cancer, 2019. **7**(1): p. 140-140.
622. Zhao, F., et al., *Paracrine Wnt5a-beta-Catenin Signaling Triggers a Metabolic Program that Drives Dendritic Cell Tolerization.* Immunity, 2018. **48**(1): p. 147-160.e7.
623. Zheng, J., *Energy metabolism of cancer: Glycolysis versus oxidative phosphorylation (Review).* Oncology letters, 2012. **4**(6): p. 1151-1157.
624. Warburg, O., F. Wind, and E. Negelein, *THE METABOLISM OF TUMORS IN THE BODY.* The Journal of general physiology, 1927. **8**(6): p. 519-530.
625. Sbarra, A.J. and M.L. Karnovsky, *The biochemical basis of phagocytosis. I. Metabolic changes during the ingestion of particles by polymorphonuclear leukocytes.* J Biol Chem, 1959. **234**(6): p. 1355-62.
626. Hard, G.C., *Some biochemical aspects of the immune macrophage.* British journal of experimental pathology, 1970. **51**(1): p. 97-105.
627. Newsholme, P., et al., *Metabolism of glucose, glutamine, long-chain fatty acids and ketone bodies by murine macrophages.* Biochem J, 1986. **239**(1): p. 121-5.
628. Pantel, A., et al., *Direct type I IFN but not MDA5/TLR3 activation of dendritic cells is required for maturation and metabolic shift to glycolysis after poly IC stimulation.* PLoS Biol, 2014. **12**(1): p. e1001759.
629. Palsson-McDermott, E.M. and L.A. O'Neill, *The Warburg effect then and now: from cancer to inflammatory diseases.* Bioessays, 2013. **35**(11): p. 965-73.
630. Pearce, E.L. and E.J. Pearce, *Metabolic pathways in immune cell activation and quiescence.* Immunity, 2013. **38**(4): p. 633-43.
631. Zhuo, B., et al., *PI3K/Akt signaling mediated Hexokinase-2 expression inhibits cell apoptosis and promotes tumor growth in pediatric osteosarcoma.* Biochem Biophys Res Commun, 2015. **464**(2): p. 401-6.
632. Andrejeva, G. and J.C. Rathmell, *Similarities and Distinctions of Cancer and Immune Metabolism in Inflammation and Tumors.* Cell Metab, 2017. **26**(1): p. 49-70.
633. Bauerfeld, C.P., et al., *TLR4-mediated AKT activation is MyD88/TRIF dependent and critical for induction of oxidative phosphorylation and mitochondrial transcription*

factor A in murine macrophages. Journal of immunology (Baltimore, Md. : 1950), 2012. **188**(6): p. 2847-2857.
634. Kornberg, M.D., et al., *Dimethyl fumarate targets GAPDH and aerobic glycolysis to modulate immunity.* Science (New York, N.Y.), 2018. **360**(6387): p. 449-453.
635. Everts, B., et al., *TLR-driven early glycolytic reprogramming via the kinases TBK1-IKKvarepsilon supports the anabolic demands of dendritic cell activation.* Nat Immunol, 2014. **15**(4): p. 323-32.
636. Du, X., N.M. Chapman, and H. Chi, *Emerging Roles of Cellular Metabolism in Regulating Dendritic Cell Subsets and Function.* Front Cell Dev Biol, 2018. **6**: p. 152.
637. Rethi, B., *Disarmed by density AU - Nasi, Aikaterini.* OncoImmunology, 2013. **2**(12): p. e26744.
638. Abbott, R.D., et al., *Joint distribution of lipoprotein cholesterol classes. The Framingham study.* Arteriosclerosis, 1983. **3**(3): p. 260-72.
639. Leifer, C.A., et al., *Macrophage lipid accumulation is regulated by substrate stiffness.* The Journal of Immunology, 2016. **196**(1 Supplement): p. 57.5.
640. Gomez, C.R., et al., *Innate immunity and aging.* Experimental Gerontology, 2008. **43**(8): p. 718-728.
641. Lloberas, J. and A. Celada, *Effect of aging on macrophage function.* Experimental Gerontology, 2002. **37**(12): p. 1325-1331.
642. Makinodan, T. and M.M.B. Kay, *Age Influence on the Immune System*, in *Advances in Immunology*, H.G. Kunkel and F.J. Dixon, Editors. 1980, Academic Press. p. 287-330.
643. Sondell, K., et al., *The role of sex and age in yeast cell phagocytosis by monocytes from healthy blood donors.* Mechanisms of Ageing and Development, 1990. **51**(1): p. 55-61.
644. Aprahamian, T., et al., *Ageing is associated with diminished apoptotic cell clearance in vivo.* Clinical & Experimental Immunology, 2008. **152**(3): p. 448-455.
645. Swift, M.E., et al., *Age-Related Alterations in the Inflammatory Response to Dermal Injury.* Journal of Investigative Dermatology, 2001. **117**(5): p. 1027-1035.
646. *Advanced Age Impairs Macrophage Polarization.* Journal of Interferon & Cytokine Research, 2012. **32**(1): p. 18-26.
647. Yoon, P., et al., *Macrophage hypo-responsiveness to interferon-γ in aged mice is associated with impaired signaling through Jak-STAT.* Mechanisms of Ageing and Development, 2004. **125**(2): p. 137-143.
648. Herrero, C., et al., *IFN-gamma-dependent transcription of MHC class II IA is impaired in macrophages from aged mice.* J Clin Invest, 2001. **107**(4): p. 485-93.
649. Franceschi, C., et al., *Inflammaging and 'Garb-aging'.* Trends Endocrinol Metab, 2017. **28**(3): p. 199-212.
650. Sambrano, G.R. and D. Steinberg, *Recognition of oxidatively damaged and apoptotic cells by an oxidized low density lipoprotein receptor on mouse peritoneal macrophages: role of membrane phosphatidylserine.* Proceedings of the National Academy of Sciences, 1995. **92**(5): p. 1396.
651. Shaw, T.N., et al., *Tissue-resident macrophages in the intestine are long lived and defined by Tim-4 and CD4 expression.* The Journal of Experimental Medicine, 2018. **215**(6): p. 1507.
652. Schyns, J., F. Bureau, and T. Marichal, *Lung Interstitial Macrophages: Past, Present, and Future.* J Immunol Res, 2018. **2018**: p. 5160794.
653. Rőszer, T., *Understanding the Mysterious M2 Macrophage through Activation Markers and Effector Mechanisms.* Mediators of Inflammation, 2015. **2015**: p. 816460.

654. Kalish, S., et al., *M3 Macrophages Stop Division of Tumor Cells In Vitro and Extend Survival of Mice with Ehrlich Ascites Carcinoma.* Med Sci Monit Basic Res, 2017. **23**: p. 8-19.
655. Williams, K.C. and W.K. Kim, *Editorial: Identification of in vivo markers for human polarized macrophages: a need that's finally met.* J Leukoc Biol, 2015. **98**(4): p. 449-50.
656. Ruddle, N.H. and E.M. Akirav, *Secondary Lymphoid Organs: Responding to Genetic and Environmental Cues in Ontogeny and the Immune Response.* The Journal of Immunology, 2009. **183**(4): p. 2205.
657. Cortez-Retamozo, V., et al., *Origins of tumor-associated macrophages and neutrophils.* Proceedings of the National Academy of Sciences, 2012. **109**(7): p. 2491.
658. Franceschi, C., et al., *Inflamm-aging. An evolutionary perspective on immunosenescence.* Ann N Y Acad Sci, 2000. **908**: p. 244-54.
659. Michaud, M., et al., *Proinflammatory Cytokines, Aging, and Age-Related Diseases.* Journal of the American Medical Directors Association, 2013. **14**(12): p. 877-882.
660. Xia, S., et al., *An Update on Inflamm-Aging: Mechanisms, Prevention, and Treatment.* Journal of immunology research, 2016. **2016**: p. 8426874-8426874.
661. Yue, H.H., et al., *Expression of CD147 on phorbol-12-myris-tate-13-acetate (PMA)-treated U937 cells differentiating into foam cells.* Archives of Biochemistry and Biophysics, 2009. **485**(1): p. 30-34.
662. Li, J., et al., *CD147 reprograms fatty acid metabolism in hepatocellular carcinoma cells through Akt/mTOR/SREBP1c and P38/PPARα pathways.* Journal of Hepatology, 2015. **63**(6): p. 1378-1389.
663. Grass, G.D. and B.P. Toole, *How, with whom and when: an overview of CD147-mediated regulatory networks influencing matrix metalloproteinase activity.* Bioscience reports, 2015. **36**(1): p. e00283-e00283.
664. Baba, M., et al., *Blocking CD147 induces cell death in cancer cells through impairment of glycolytic energy metabolism.* Biochemical and Biophysical Research Communications, 2008. **374**(1): p. 111-116.
665. Mauris, J., et al., *Loss of CD147 results in impaired epithelial cell differentiation and malformation of the meibomian gland.* Cell Death & Disease, 2015. **6**(4): p. e1726-e1726.
666. Voloshyna, I., et al., *Macrophage lipid accumulation in the presence of immunosuppressive drugs mycophenolate mofetil and cyclosporin A.* Inflammation Research, 2019. **68**(9): p. 787-799.
667. Tabas, I. and K.E. Bornfeldt, *Macrophage Phenotype and Function in Different Stages of Atherosclerosis.* Circ Res, 2016. **118**(4): p. 653-67.
668. Jeong, S.J., M.N. Lee, and G.T. Oh, *The Role of Macrophage Lipophagy in Reverse Cholesterol Transport.* Endocrinology and metabolism (Seoul, Korea), 2017. **32**(1): p. 41-46.
669. Panda, A., et al., *Age-associated decrease in TLR function in primary human dendritic cells predicts influenza vaccine response.* J Immunol, 2010. **184**(5): p. 2518-27.
670. Prakash, S., et al., *Dendritic cells from aged subjects contribute to chronic airway inflammation by activating bronchial epithelial cells under steady state.* Mucosal Immunol, 2014. **7**(6): p. 1386-94.
671. Agrawal, A., et al., *Increased Reactivity of Dendritic Cells from Aged Subjects to Self-Antigen, the Human DNA.* Journal of immunology (Baltimore, Md. : 1950), 2009. **182**: p. 1138-45.
672. Chistiakov, D.A., et al., *Plasmacytoid dendritic cells: development, functions, and role in atherosclerotic inflammation.* Frontiers in physiology, 2014. **5**: p. 279-279.

673. Bialecki, E., et al., *Spleen-resident CD4+ and CD4- CD8α- dendritic cell subsets differ in their ability to prime invariant natural killer T lymphocytes.* PloS one, 2011. **6**(10): p. e26919-e26919.
674. Grolleau-Julius, A., et al., *Impaired dendritic cell function in aging leads to defective antitumor immunity.* Cancer research, 2008. **68**(15): p. 6341-6349.
675. Leung, C.S.K., *Endogenous Antigen Presentation of MHC Class II Epitopes through Non-Autophagic Pathways.* Frontiers in immunology, 2015. **6**: p. 464-464.
676. Pereira, L.F., et al., *Impaired in vivo CD4+ T cell expansion and differentiation in aged mice is not solely due to T cell defects: Decreased stimulation by aged dendritic cells.* Mechanisms of Ageing and Development, 2011. **132**(4): p. 187-194.
677. Canaday, D.H., et al., *Age-dependent changes in the expression of regulatory cell surface ligands in activated human T-cells.* BMC immunology, 2013. **14**: p. 45-45.
678. van der Merwe, P.A., et al., *CD80 (B7-1) binds both CD28 and CTLA-4 with a low affinity and very fast kinetics.* J Exp Med, 1997. **185**(3): p. 393-403.
679. Ikemizu, S., et al., *Structure and dimerization of a soluble form of B7-1.* Immunity, 2000. **12**(1): p. 51-60.
680. Stamper, C.C., et al., *Crystal structure of the B7-1/CTLA-4 complex that inhibits human immune responses.* Nature, 2001. **410**(6828): p. 608-11.
681. Taub, D.D. and D.L. Longo, *Insights into thymic aging and regeneration.* Immunol Rev, 2005. **205**: p. 72-93.
682. Palmer, D.B., *The effect of age on thymic function.* Frontiers in immunology, 2013. **4**: p. 316-316.
683. Hale, J.S., et al., *Thymic output in aged mice.* Proc Natl Acad Sci U S A, 2006. **103**(22): p. 8447-52.
684. Flores, K.G., et al., *Analysis of the human thymic perivascular space during aging.* The Journal of clinical investigation, 1999. **104**(8): p. 1031-1039.
685. Pinchuk, L.M. and N.M. Filipov, *Differential effects of age on circulating and splenic leukocyte populations in C57BL/6 and BALB/c male mice.* Immunity & Ageing, 2008. **5**(1): p. 1.
686. Aw, D., et al., *Phenotypical and morphological changes in the thymic microenvironment from ageing mice.* Biogerontology, 2009. **10**(3): p. 311-322.
687. Sempowski, G.D., et al., *T cell receptor excision circle assessment of thymopoiesis in aging mice.* Mol Immunol, 2002. **38**(11): p. 841-8.
688. Ferrando-Martínez, S., et al., *Age-related deregulation of naive T cell homeostasis in elderly humans.* Age (Dordr), 2011. **33**(2): p. 197-207.
689. Goronzy, J.J., W.W. Lee, and C.M. Weyand, *Aging and T-cell diversity.* Exp Gerontol, 2007. **42**(5): p. 400-6.
690. Lazuardi, L., et al., *Age-related loss of naïve T cells and dysregulation of T-cell/B-cell interactions in human lymph nodes.* Immunology, 2005. **114**(1): p. 37-43.
691. Fagnoni, F.F., et al., *Shortage of circulating naive CD8+ T cells provides new insights on immunodeficiency in aging.* Blood, 2000. **95**(9): p. 2860-2868.
692. Pahlavani, M.A. and A. Richardson, *The effect of age on the expression of interleukin-2.* Mech Ageing Dev, 1996. **89**(3): p. 125-54.
693. Whisler, R.L., L. Beiqing, and M. Chen, *Age-related decreases in IL-2 production by human T cells are associated with impaired activation of nuclear transcriptional factors AP-1 and NF-AT.* Cell Immunol, 1996. **169**(2): p. 185-95.
694. Pieren, D.K.J., et al., *Response kinetics reveal novel features of ageing in murine T cells.* Scientific Reports, 2019. **9**(1): p. 5587.
695. Adolfsson, O., B.T. Huber, and S.N. Meydani, *Vitamin E-Enhanced IL-2 Production in Old Mice: Naive But Not Memory T Cells Show Increased Cell Division Cycling and IL-2-Producing Capacity.* The Journal of Immunology, 2001. **167**(7): p. 3809.

696. Li, M., et al., *Age related human T cell subset evolution and senescence.* Immunity & Ageing, 2019. **16**(1): p. 24.
697. Garrido, F., et al., *Implications for immunosurveillance of altered HLA class I phenotypes in human tumours.* Immunology Today, 1997. **18**(2): p. 89-95.
698. Marincola, F.M., et al., *Escape of human solid tumors from T-cell recognition: molecular mechanisms and functional significance.* Adv Immunol, 2000. **74**: p. 181-273.
699. Garrido, F. and I. Algarra, *MHC antigens and tumor escape from immune surveillance.* Adv Cancer Res, 2001. **83**: p. 117-58.
700. Seliger, B., et al., *HLA class I antigen abnormalities and immune escape by malignant cells.* Semin Cancer Biol, 2002. **12**(1): p. 3-13.
701. Zinger, A., W.C. Cho, and A. Ben-Yehuda, *Cancer and Aging - the Inflammatory Connection.* Aging and disease, 2017. **8**(5): p. 611-627.
702. Wu, C., Q. Hua, and L. Zheng, *Generation of Myeloid Cells in Cancer: The Spleen Matters.* Frontiers in immunology, 2020. **11**: p. 1126-1126.
703. Kopp, H.G., C.A. Ramos, and S. Rafii, *Contribution of endothelial progenitors and proangiogenic hematopoietic cells to vascularization of tumor and ischemic tissue.* Curr Opin Hematol, 2006. **13**(3): p. 175-81.
704. Kaplan, R.N., et al., *VEGFR1-positive haematopoietic bone marrow progenitors initiate the pre-metastatic niche.* Nature, 2005. **438**(7069): p. 820-7.
705. Dolcetti, L., et al., *Hierarchy of immunosuppressive strength among myeloid-derived suppressor cell subsets is determined by GM-CSF.* Eur J Immunol, 2010. **40**(1): p. 22-35.
706. Travelli, C., et al., *Nicotinamide Phosphoribosyltransferase Acts as a Metabolic Gate for Mobilization of Myeloid-Derived Suppressor Cells.* Cancer Res, 2019. **79**(8): p. 1938-1951.
707. Hiratsuka, S., et al., *Tumour-mediated upregulation of chemoattractants and recruitment of myeloid cells predetermines lung metastasis.* Nat Cell Biol, 2006. **8**(12): p. 1369-75.
708. McAllister, S.S., et al., *Systemic endocrine instigation of indolent tumor growth requires osteopontin.* Cell, 2008. **133**(6): p. 994-1005.
709. Elkabets, M., et al., *Human tumors instigate granulin-expressing hematopoietic cells that promote malignancy by activating stromal fibroblasts in mice.* J Clin Invest, 2011. **121**(2): p. 784-99.
710. Al Sayed, M.F., et al., *T-cell-Secreted TNFα Induces Emergency Myelopoiesis and Myeloid-Derived Suppressor Cell Differentiation in Cancer.* Cancer Res, 2019. **79**(2): p. 346-359.
711. Gabrilovich, D.I., et al., *Production of vascular endothelial growth factor by human tumors inhibits the functional maturation of dendritic cells.* Nat Med, 1996. **2**(10): p. 1096-103.
712. Yang, L., et al., *Cancer-associated immunodeficiency and dendritic cell abnormalities mediated by the prostaglandin EP2 receptor.* J Clin Invest, 2003. **111**(5): p. 727-35.
713. Serafini, P., et al., *High-dose granulocyte-macrophage colony-stimulating factor-producing vaccines impair the immune response through the recruitment of myeloid suppressor cells.* Cancer Res, 2004. **64**(17): p. 6337-43.
714. Shurin, G.V., et al., *Neuroblastoma-derived gangliosides inhibit dendritic cell generation and function.* Cancer Res, 2001. **61**(1): p. 363-9.
715. Sharma, S., et al., *T cell-derived IL-10 promotes lung cancer growth by suppressing both T cell and APC function.* J Immunol, 1999. **163**(9): p. 5020-8.
716. Ratta, M., et al., *Dendritic cells are functionally defective in multiple myeloma: the role of interleukin-6.* Blood, 2002. **100**(1): p. 230-7.

717. Alleva, D.G., T.M. Walker, and K.D. Elgert, *Induction of macrophage suppressor activity by fibrosarcoma-derived transforming growth factor-beta 1: contrasting effects on resting and activated macrophages.* J Leukoc Biol, 1995. **57**(6): p. 919-28.
718. Hegmans, J.P.J.J., et al., *Mesothelioma environment comprises cytokines and T-regulatory cells that suppress immune responses.* European Respiratory Journal, 2006. **27**(6): p. 1086.
719. Rabold, K., et al., *Enhanced lipid biosynthesis in human tumor-induced macrophages contributes to their protumoral characteristics.* Journal for ImmunoTherapy of Cancer, 2020. **8**(2): p. e000638.
720. Wieczorek, M., et al., *Major Histocompatibility Complex (MHC) Class I and MHC Class II Proteins: Conformational Plasticity in Antigen Presentation.* Frontiers in immunology, 2017. **8**: p. 292-292.
721. Bandola-Simon, J. and P.A. Roche, *Dysfunction of antigen processing and presentation by dendritic cells in cancer.* Mol Immunol, 2019. **113**: p. 31-37.
722. Maher, J. and E.T. Davies, *Targeting cytotoxic T lymphocytes for cancer immunotherapy.* British journal of cancer, 2004. **91**(5): p. 817-821.
723. Liu, K., *Role of apoptosis resistance in immune evasion and metastasis of colorectal cancer.* World journal of gastrointestinal oncology, 2010. **2**(11): p. 399-406.
724. Narasimhan, S.R., et al., *Resistance of pleural mesothelioma cell lines to apoptosis: relation to expression of Bcl-2 and Bax.* Am J Physiol, 1998. **275**(1): p. L165-71.
725. O'Connell, J., *Fas ligand and the fate of antitumour cytotoxic T lymphocytes.* Immunology, 2002. **105**(3): p. 263-266.
726. Stewart, J.H., et al., *Induction of apoptosis in malignant pleural mesothelioma cells by activation of the Fas (Apo-1/CD95) death-signal pathway.* The Journal of Thoracic and Cardiovascular Surgery, 2002. **123**(2): p. 295-302.
727. Zeytun, A., et al., *Fas-Fas Ligand–Based Interactions Between Tumor Cells and Tumor-Specific Cytotoxic T Lymphocytes: A Lethal Two-Way Street.* Blood, 1997. **90**(5): p. 1952-1959.
728. Beloribi-Djefaflia, S., S. Vasseur, and F. Guillaumond, *Lipid metabolic reprogramming in cancer cells.* Oncogenesis, 2016. **5**: p. e189.
729. Cubillos-Ruiz, J.R., S.E. Bettigole, and L.H. Glimcher, *Tumorigenic and Immunosuppressive Effects of Endoplasmic Reticulum Stress in Cancer.* Cell, 2017. **168**(4): p. 692-706.
730. Cubillos-Ruiz, J.R., et al., *ER Stress Sensor XBP1 Controls Anti-tumor Immunity by Disrupting Dendritic Cell Homeostasis.* Cell, 2015. **161**(7): p. 1527-38.
731. den Brok, M.H., et al., *Lipid Droplets as Immune Modulators in Myeloid Cells.* Trends Immunol, 2018. **39**(5): p. 380-392.
732. Schumann, T., et al., *Deregulation of PPARbeta/delta target genes in tumor-associated macrophages by fatty acid ligands in the ovarian cancer microenvironment.* Oncotarget, 2015. **6**(15): p. 13416-33.
733. Veglia, F., et al., *Lipid bodies containing oxidatively truncated lipids block antigen cross-presentation by dendritic cells in cancer.* Nat Commun, 2017. **8**(1): p. 2122.
734. Pearce, E.L., et al., *Enhancing CD8 T-cell memory by modulating fatty acid metabolism.* Nature, 2009. **460**(7251): p. 103-107.
735. Pearce, E.L. and E.J. Pearce, *Metabolic pathways in immune cell activation and quiescence.* Immunity, 2013. **38**(4): p. 633-643.
736. Maroof, A., et al., *Developing dendritic cells become 'lacy' cells packed with fat and glycogen.* Immunology, 2005. **115**(4): p. 473-83.
737. Bougnères, L., et al., *A role for lipid bodies in the cross-presentation of phagocytosed antigens by MHC class I in dendritic cells.* Immunity, 2009. **31**(2): p. 232-244.

738. Bougneres, L., et al., *A role for lipid bodies in the cross-presentation of phagocytosed antigens by MHC class I in dendritic cells.* Immunity, 2009. **31**(2): p. 232-44.
739. Houten, S.M., et al., *The Biochemistry and Physiology of Mitochondrial Fatty Acid beta-Oxidation and Its Genetic Disorders.* Annu Rev Physiol, 2016. **78**: p. 23-44.
740. Oberkampf, M., et al., *Mitochondrial reactive oxygen species regulate the induction of CD8+ T cells by plasmacytoid dendritic cells.* Nature Communications, 2018. **9**(1): p. 2241.
741. Ferreira, G.B., et al., *Vitamin D3 Induces Tolerance in Human Dendritic Cells by Activation of Intracellular Metabolic Pathways.* Cell Rep, 2015. **10**(5): p. 711-725.

Supplementary Figures for chapter 3

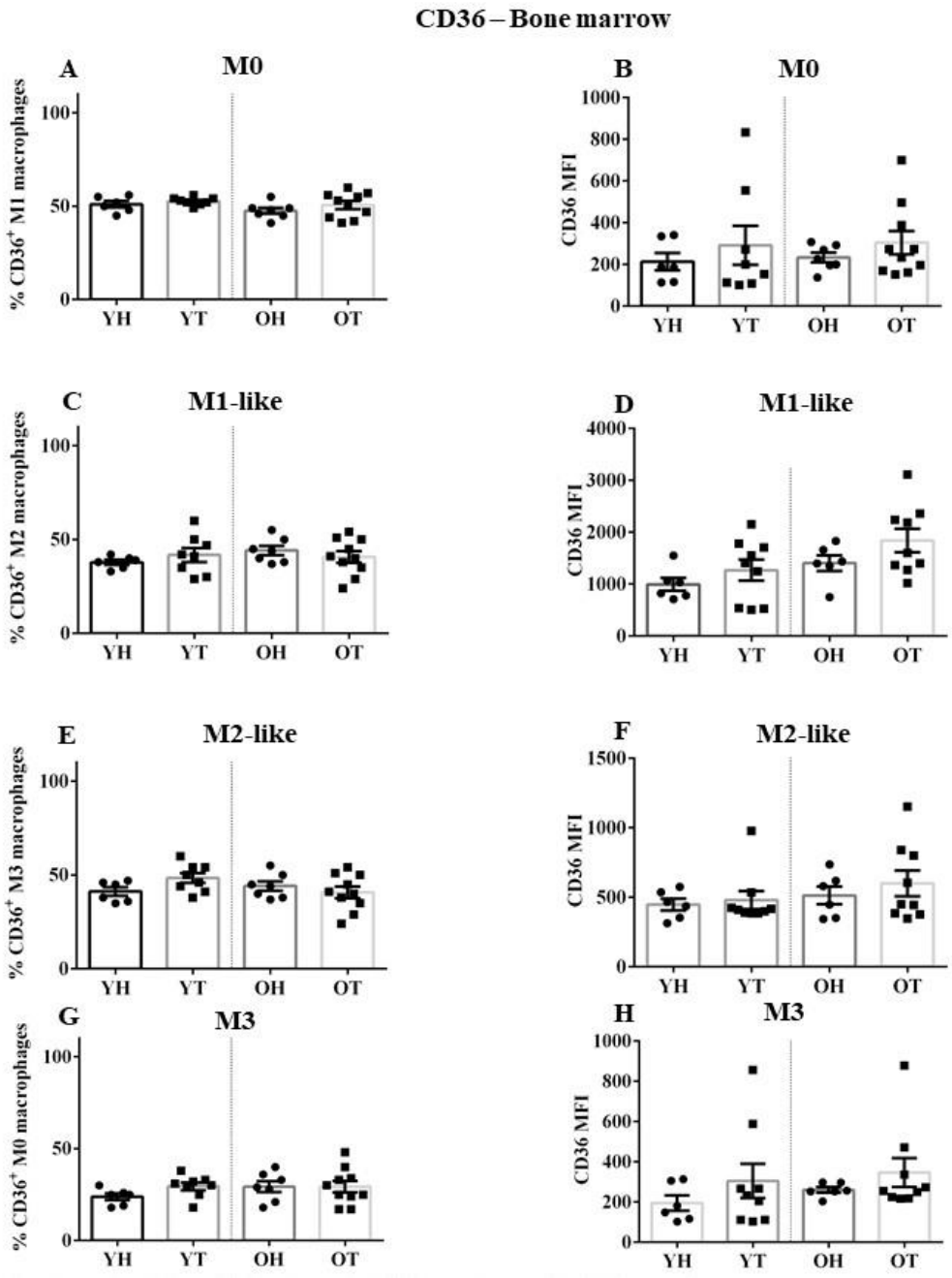

Figure 3.1: No change in CD36 was observed in BM macrophages

BM macrophages from YH, YT, OH and OT mice were stained with CD36 which is a member of class B scavenger receptor family and imports fatty acids inside the cells. Percentages of $CD36^+$ cells in $Ly6C^-CX3CR1^-$ (M0) macrophages **(A)**, $Ly6C^+CX3CR1^-$ (M1-like) macrophages (**C**), $Ly6C^-CX3CR1^+$ (M2-like) macrophages **(E)**, and $Ly6C^+CX3CR1^+$ (M3) macrophages **(G)** and expression levels of CD36 (MFI) in M0 macrophages **(B)**, M1-like macrophages (**D**), M2-like macrophages **(F)**, and M3 macrophages **(H)** were measured. Data shown as mean ± SEM, n = 10-11 mice/group. * = $p<0.05$, ** = $p<0.005$. Statistical significance assessed by Kruskal-Wallis test followed by post hoc Dunn's test.

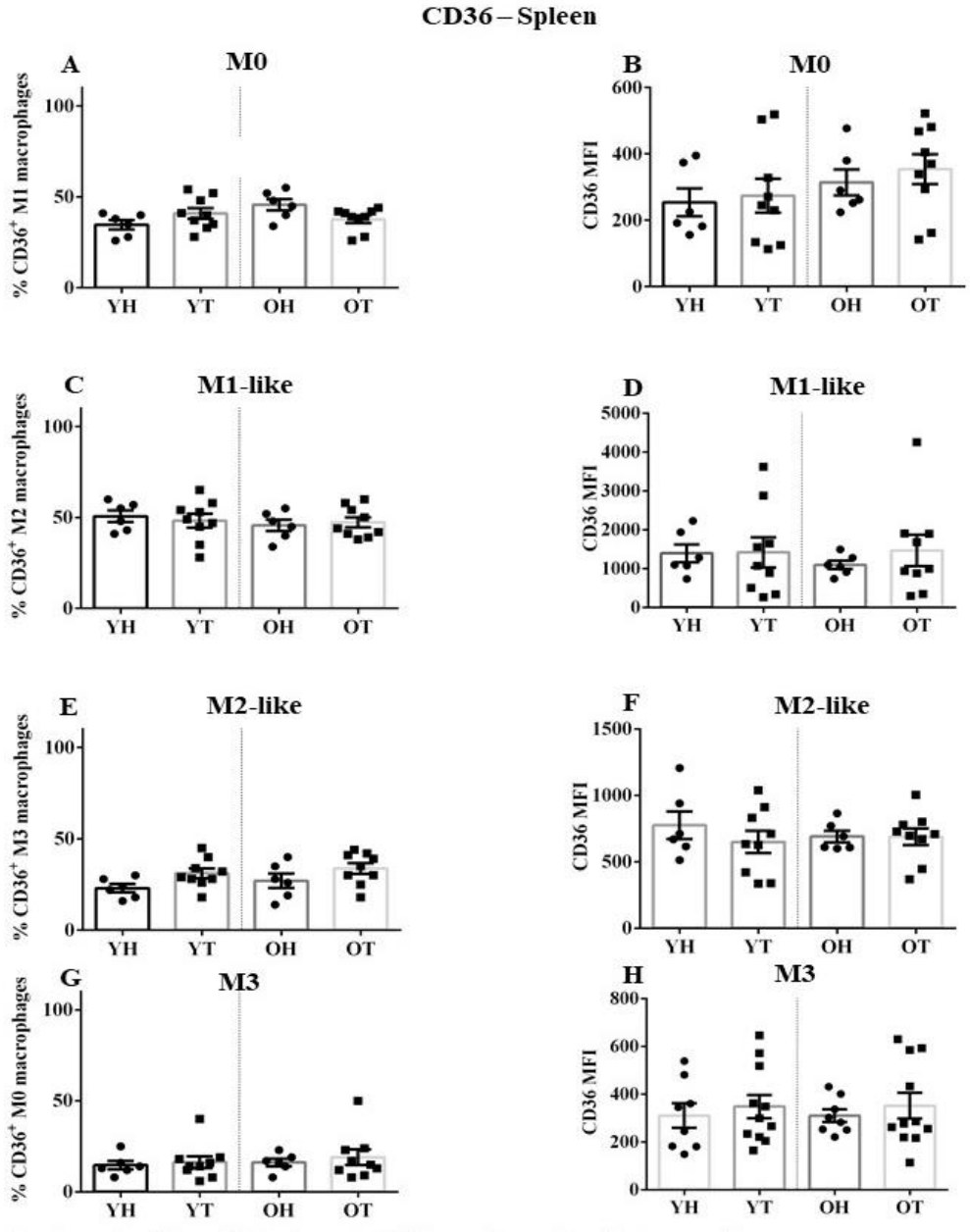

Figure 3.2: No change in CD36 was observed in splenic macrophages

Splenic macrophages from YH, YT, OH and OT mice were stained with CD36 which is a member of class B scavenger receptor family and imports fatty acids inside the cells. Percentages of $CD36^+$ cells in $Ly6C^-CX3CR1^-$ (M0) macrophages **(A)**, $Ly6C^+CX3CR1^-$ (M1-like) macrophages (**C)**, $Ly6C^-CX3CR1^+$ (M2-like) macrophages **(E)**, and $Ly6C^+CX3CR1^+$ (M3) macrophages **(G)** and expression levels of CD36 (MFI) in M0 macrophages **(B)**, M1-like macrophages (**D)**, M2-like macrophages **(F)**, and M3 macrophages **(H)** were measured. Data shown as mean ± SEM, n = 10-11 mice/group. * = $p<0.05$, ** = $p<0.005$. Statistical significance assessed by Kruskal-Wallis test followed by post hoc Dunn's test.

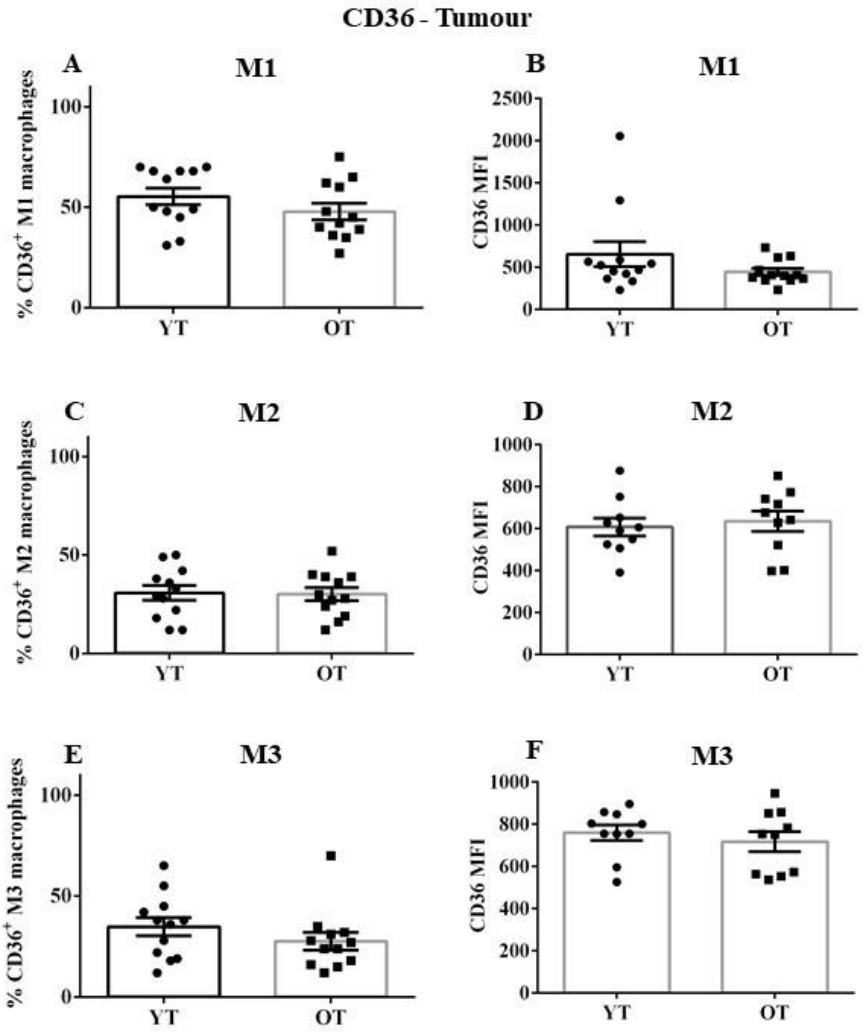

Figure 3.3: No change in CD36 was observed in TAMs

Tumour macrophages from young tumour bearing mice (YT) and old tumour bearing mice (OT) were stained with CD36 which is a member of class B scavenger receptor family and imports fatty acids inside the cells. Percentages of $CD36^+$ cells in $Ly6C^+CX3CR1^-$ (M1-like) macrophages (**A)**, $Ly6C^-CX3CR1^+$ (M2-like) macrophages **(C)**, and $Ly6C^+CX3CR1^+$ (M3) macrophages **(E)** and expression levels of CD36 (MFI) in M1-like macrophages (**B)**, M2-like macrophages **(D)**, and M3 macrophages **(F)** were measured. Data shown as mean ± SEM, n = 10-11 mice/group. * = $p<0.05$, ** = $p<0.005$. Statistical significance assessed by Kruskal-Wallis test followed by post hoc Dunn's test.

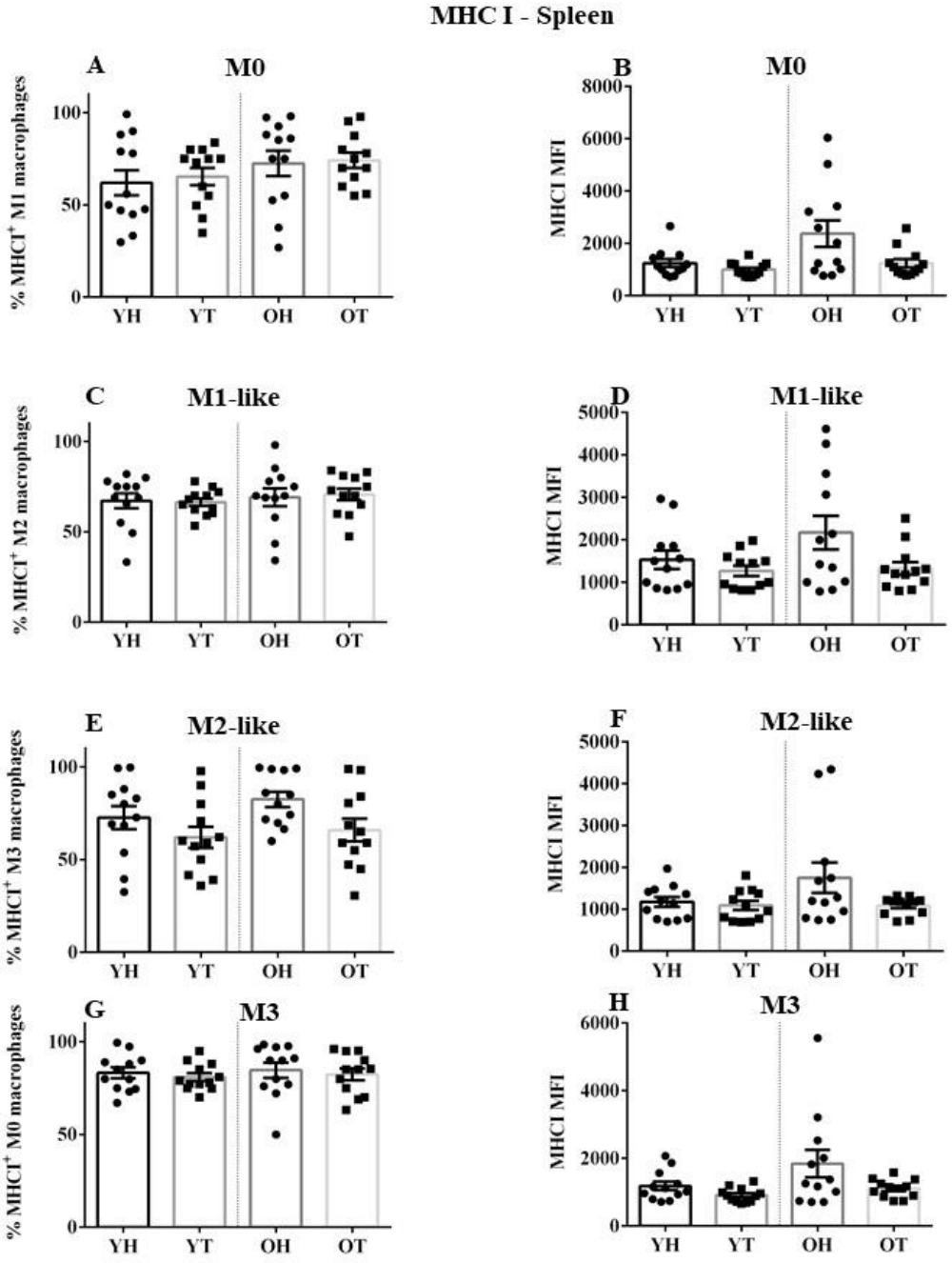

Figure 3.4: No change in MHC-I was observed in splenic macrophages

Splenic macrophages from YH, YT, OH and OT mice were stained for MHC-I expression and analysed by flow cytometry. Percentages of MHC-I$^+$ cells in Ly6C$^-$CX3CR1$^-$ (M0) macrophages **(A)**, Ly6C$^+$CX3CR1$^-$ (M1-like) macrophages (**C)**, Ly6C$^-$CX3CR1$^+$ (M2-like) macrophages **(E)**, and Ly6C$^+$CX3CR1$^+$ (M3) macrophages **(G)** plus expression levels of MHCI I (MFI) in the same macrophage subpopulations were measured. Data shown as mean ± SEM, n = 10-11 mice/group. * = $p<0.05$, ** = $p<0.005$. Statistical significance assessed by Kruskal-Wallis test followed by post hoc Dunn's test.

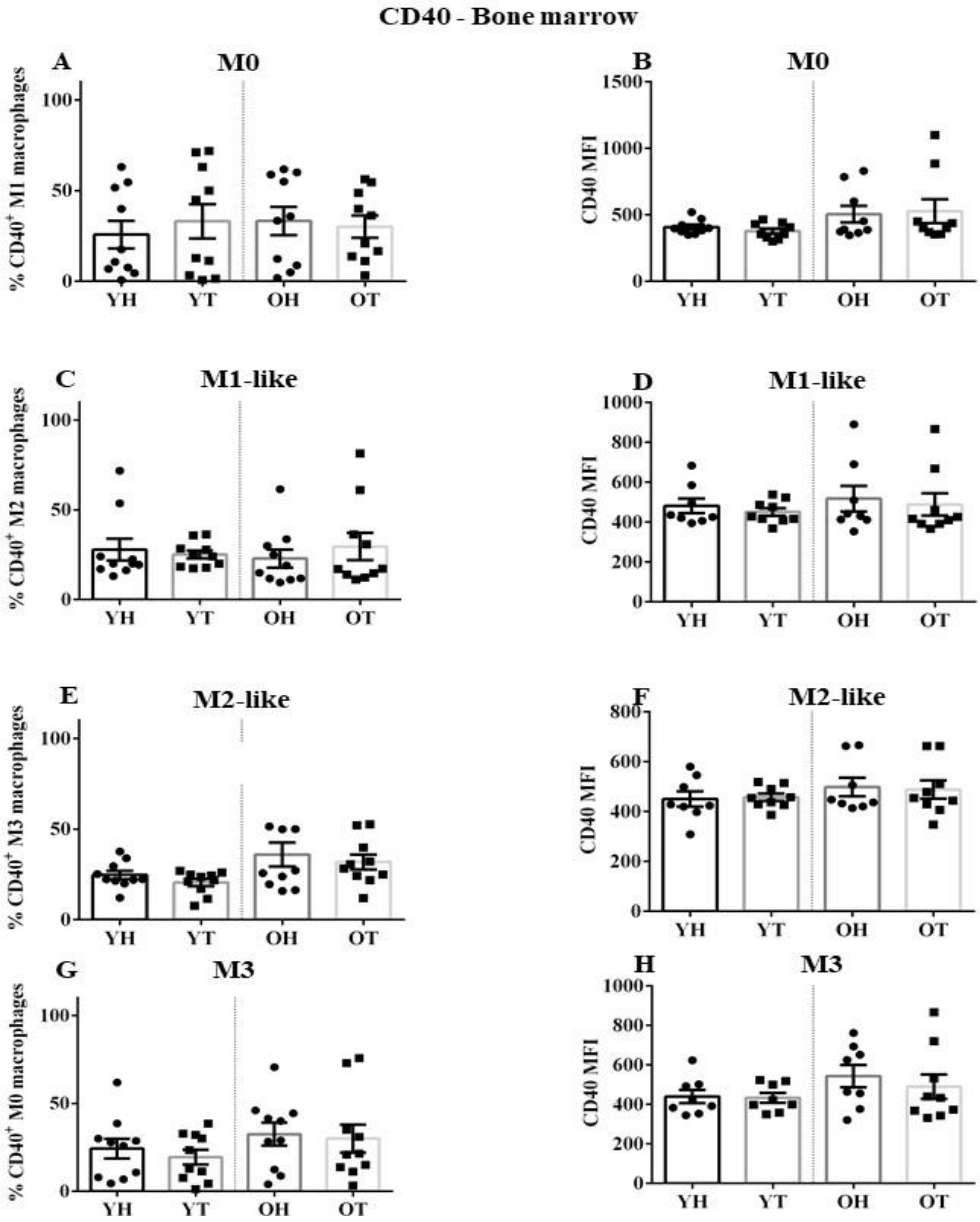

Figure 3.5: No change in CD40 was observed in BM macrophages

BM macrophages from YH, YT, OH and OT mice were stained with CD40 which is a co-stimulatory molecule that binds with CD40L expressed on antigen specific CD4+ T cells providing a strong maturation stimulus driving DCs to become potent APCs. Percentages of $CD40^+$ cells in $Ly6C^-CX3CR1^-$ (M0) macrophages **(A)**, $Ly6C^+CX3CR1^-$ (M1-like) macrophages (**C**), $Ly6C^-CX3CR1^+$ (M2-like) macrophages **(E)**, and $Ly6C^+CX3CR1^+$ (M3) macrophages **(G)** and expression levels of CD40 (MFI) in M0 macrophages **(B)**, M1-like macrophages (**D)**, M2-like macrophages **(F)**, and M3 macrophages **(H)** were measured. Data shown as mean ± SEM, n = 10-11 mice/group. * = $p<0.05$, ** = $p<0.005$. Statistical significance assessed by Kruskal-Wallis test followed by post hoc Dunn's test.

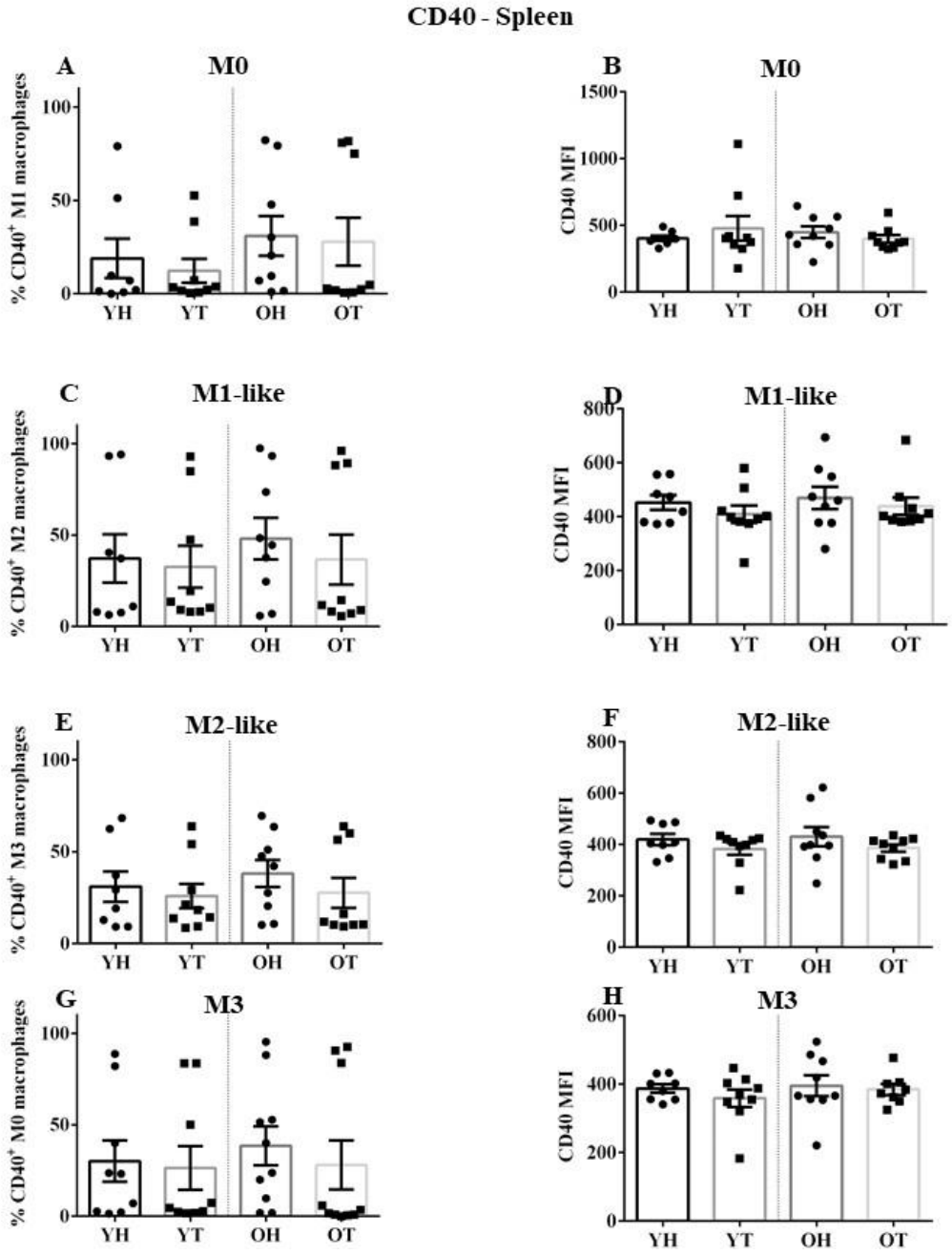

Figure 3.6: No change in CD40 was observed in splenic macrophages

Splenic macrophages from YH, YT, OH and OT mice were stained with CD40 which is a co-stimulatory molecule that binds with CD40L expressed on antigen specific CD4+ T cells providing a strong maturation stimulus driving DCs to become potent APCs. Percentages of $CD40^+$ cells in $Ly6C^-CX3CR1^-$ (M0) macrophages **(A)**, $Ly6C^+CX3CR1^-$ (M1-like) macrophages (**C**), $Ly6C^-CX3CR1^+$ (M2-like) macrophages **(E)**, and $Ly6C^+CX3CR1^+$ (M3) macrophages **(G)** and expression levels of CD40 (MFI) in M0 macrophages **(B)**, M1-like macrophages (**D)**, M2-like macrophages **(F)**, and M3 macrophages **(H)** were measured. Data shown as mean ± SEM, n = 10-11 mice/group. * = $p<0.05$, ** = $p<0.005$. Statistical significance assessed by Kruskal-Wallis test followed by post hoc Dunn's test.

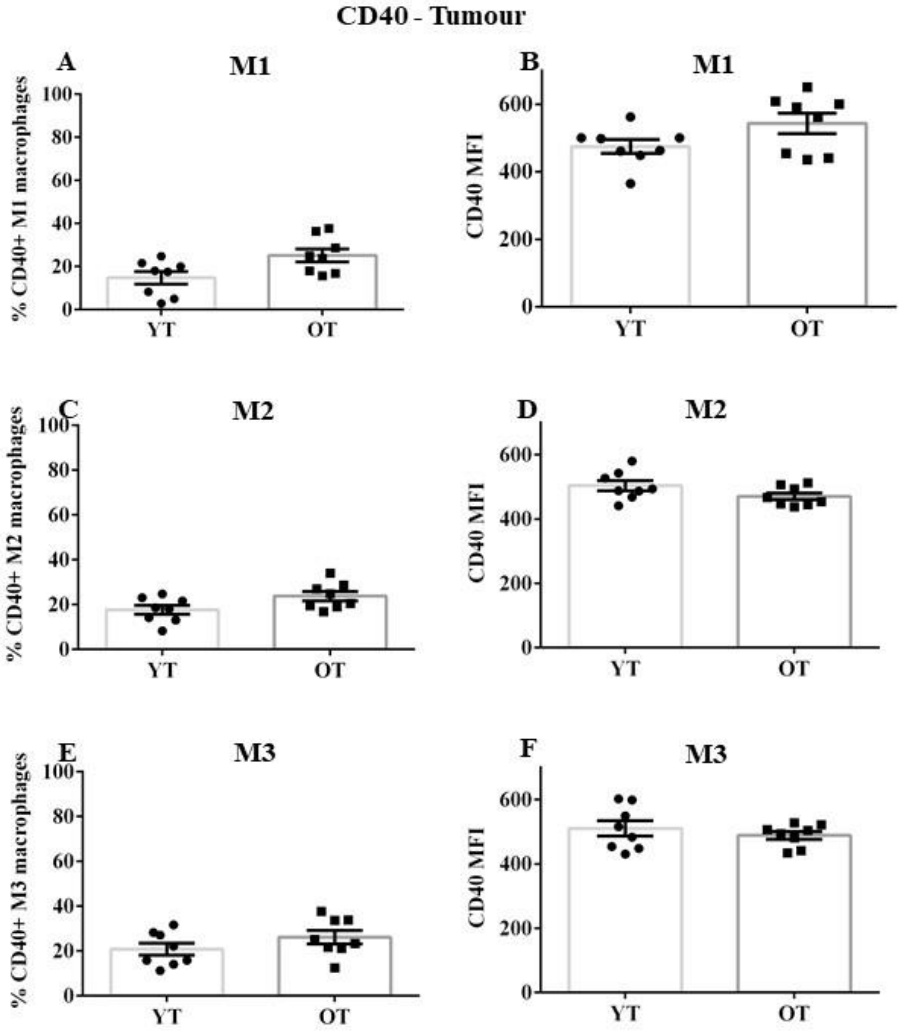

Figure 3.7: No change in CD40 was observed in TAMs

Tumour macrophages from YT and OT mice were stained with CD40 which is a co-stimulatory molecule that binds with CD40L expressed on antigen specific $CD4^+$ T cells providing a strong maturation stimulus driving DCs to become potent APCs. Percentages of $CD40^+$ cells in $Ly6C^+CX3CR1^-$ (M1-like) macrophages (**A)**, $Ly6C^-CX3CR1^+$ (M2-like) macrophages **(C)**, and $Ly6C^+CX3CR1^+$ (M3) macrophages **(E)** and expression levels of CD40 (MFI) M1-like macrophages (**B)**, M2-like macrophages **(D)**, and M3 macrophages **(F)** were measured. Data shown as mean ± SEM, n = 10-11 mice/group. * = $p<0.05$, ** = $p<0.005$. Statistical significance assessed by Mann-Whitney test .

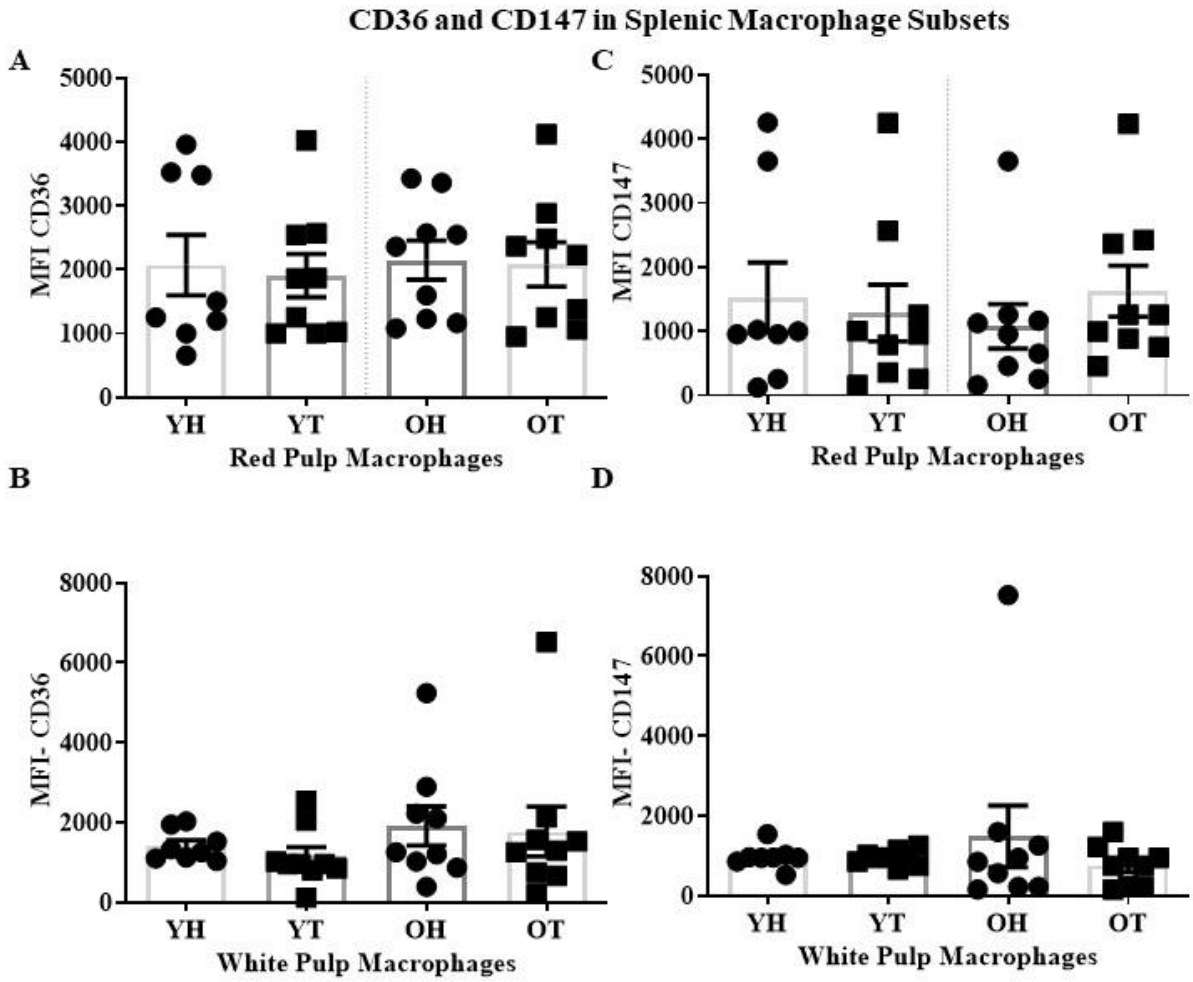

Figure 3.8: No change in CD36 or CD147 was observed in splenic red/white pulp macrophages

Splenic macrophages from YH, YT, OH and OT mice were stained with CD36 and CD147. **MFI expression of CD36 (A)red pulp, (B) white pulp and MFI expression levels of CD147 (C) red pulp and (D) white pulp macrophages** were measured. Data shown as mean ± SEM, n = 10-11 mice/group. * = $p<0.05$, ** = $p<0.005$. Statistical significance assessed by Kruskal Wallis test followed by ad hoc Dunn's Test.

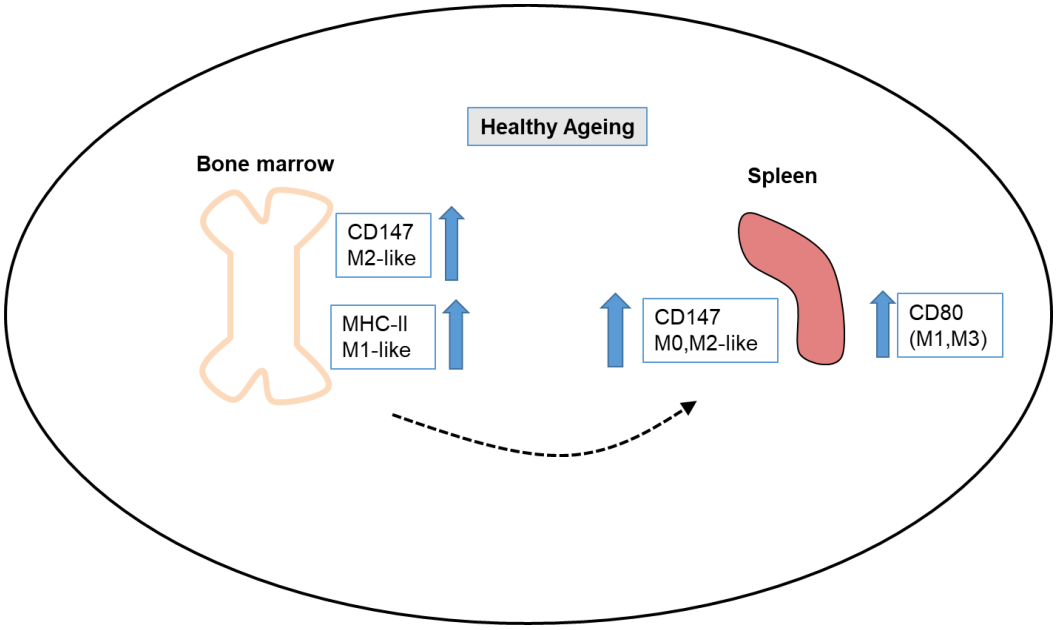

Figure 3.9 Effect of healthy ageing on macrophages

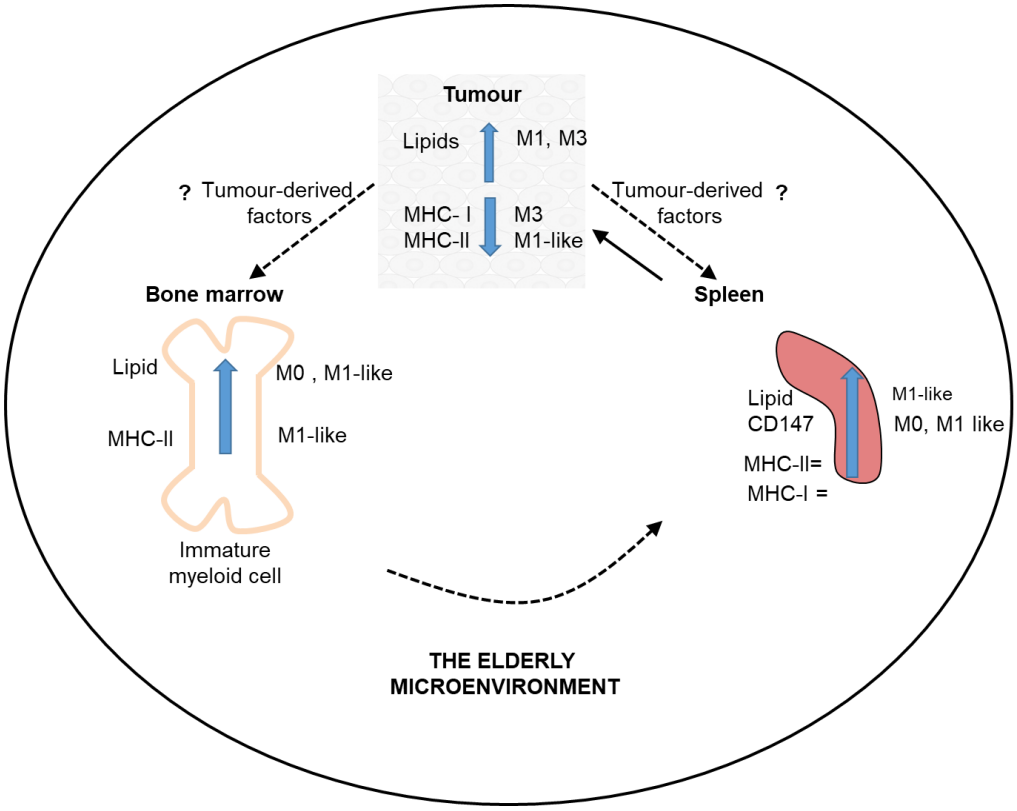

Figure 3.10 Effect of mesothelioma and ageing on macrophages

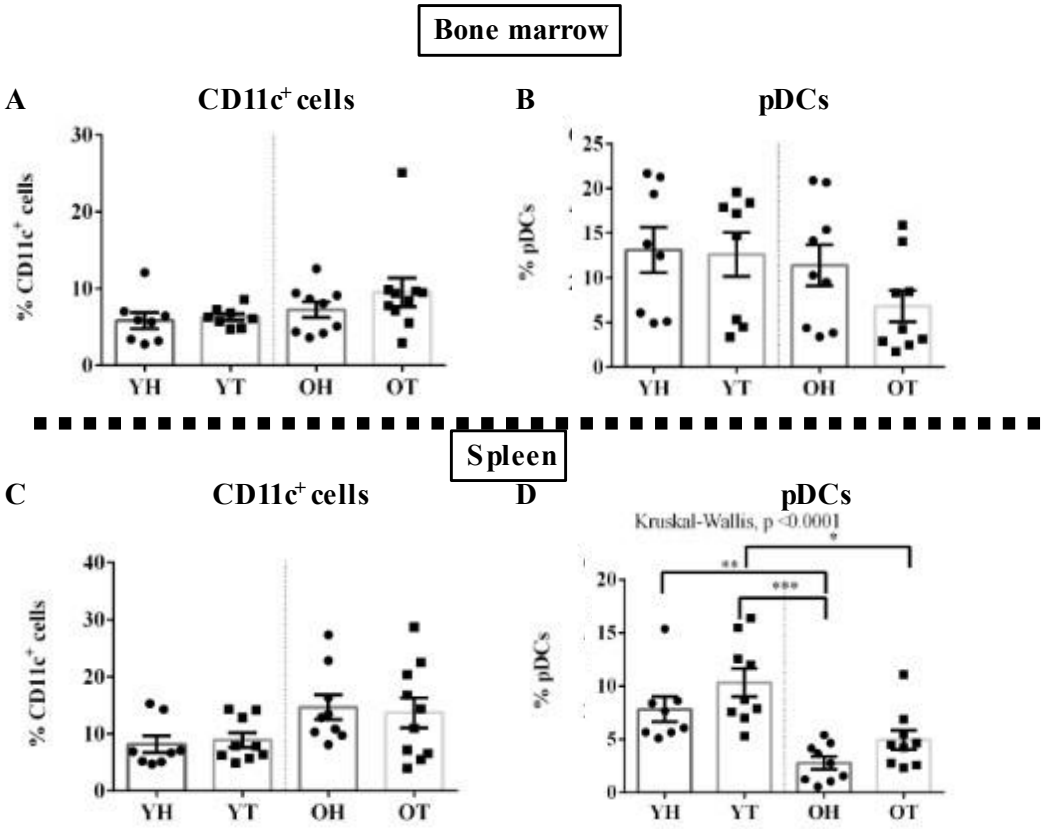

Figure 4.1 No change in CD11c$^+$ cell proportions observed in BM and spleens

Bone marrow (BM) and spleens from young healthy (YH), young tumour-bearing (YT), old healthy (OH) and old tumour-bearing mice (OT) were stained with CD11c and DCs selected as described in Figure 4.2. The proportion of CD11c$^+$ cells and pDCs in BM **(A,B)** and spleens **(C,D)** are shown as mean ± SEM, n = 10-11 mice in each group. * = $p<0.05$, ** = $p<0.005$, *** = $p<0.0005$. Statistical significance assessed by Kruskal-Wallis Test followed by post-hoc Dunn's Test.

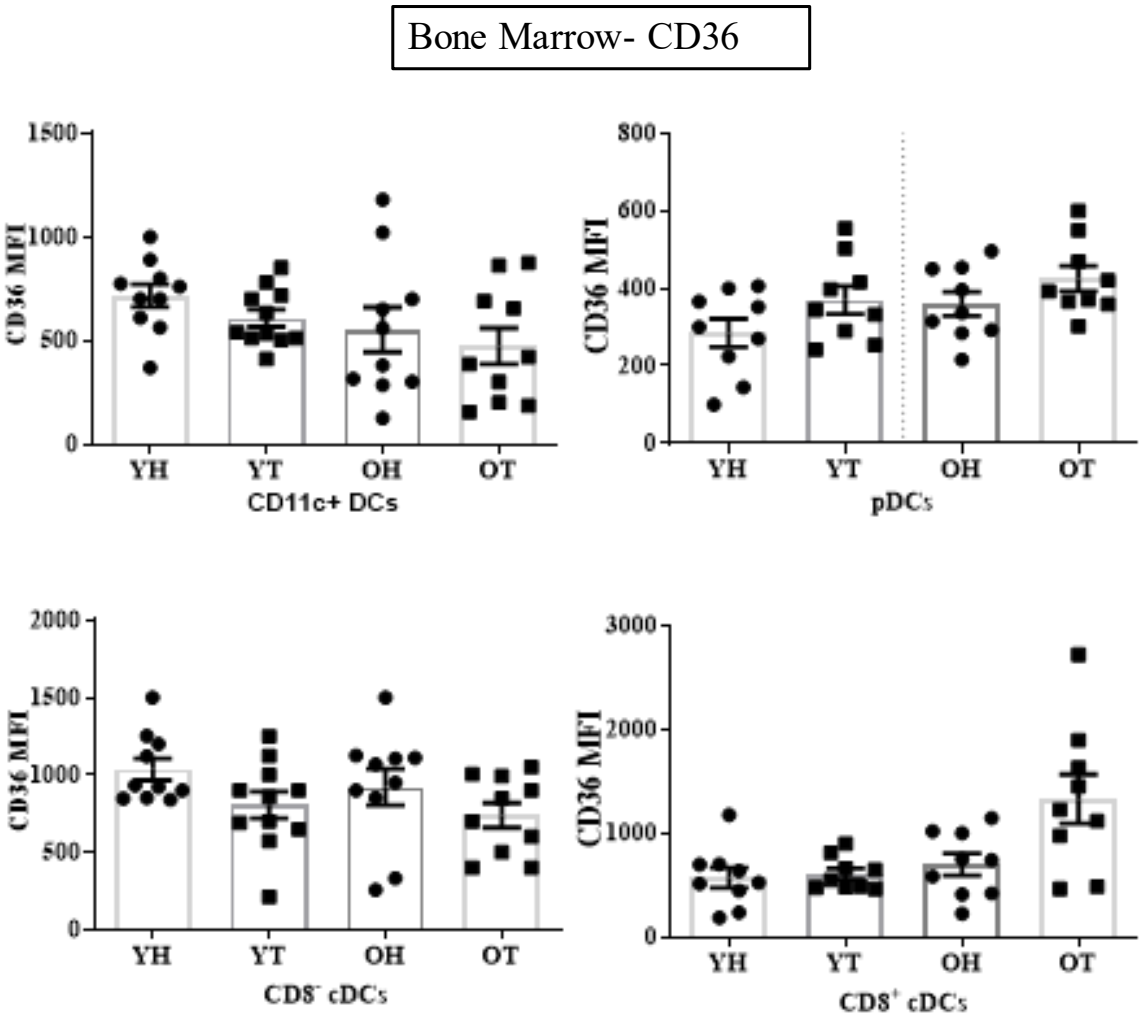

Figure 4.2: No change in CD36 was observed in BM DCs with healthy ageing

BM DCs from YH, YT, OH and OT mice were stained with CD36 which is a member of class B scavenger receptor family and imports fatty acids inside the cells. Expression levels of CD36 (measured as MFI) in **CD11c$^+$ cells(A), pDCs (B), CD11b$^+$CD8$^-$cDCs (C), CD11b$^+$CD8$^+$cDCs (D)** were measured. Data shown as mean ± SEM, n = 10-11 mice/group. * = p<0.05, ** = p<0.005, *** = p<0.0005, **** =p<0.0001. Statistical significance assessed by Kruskal-Wallis Test, followed by post-hoc Dunn's s test..

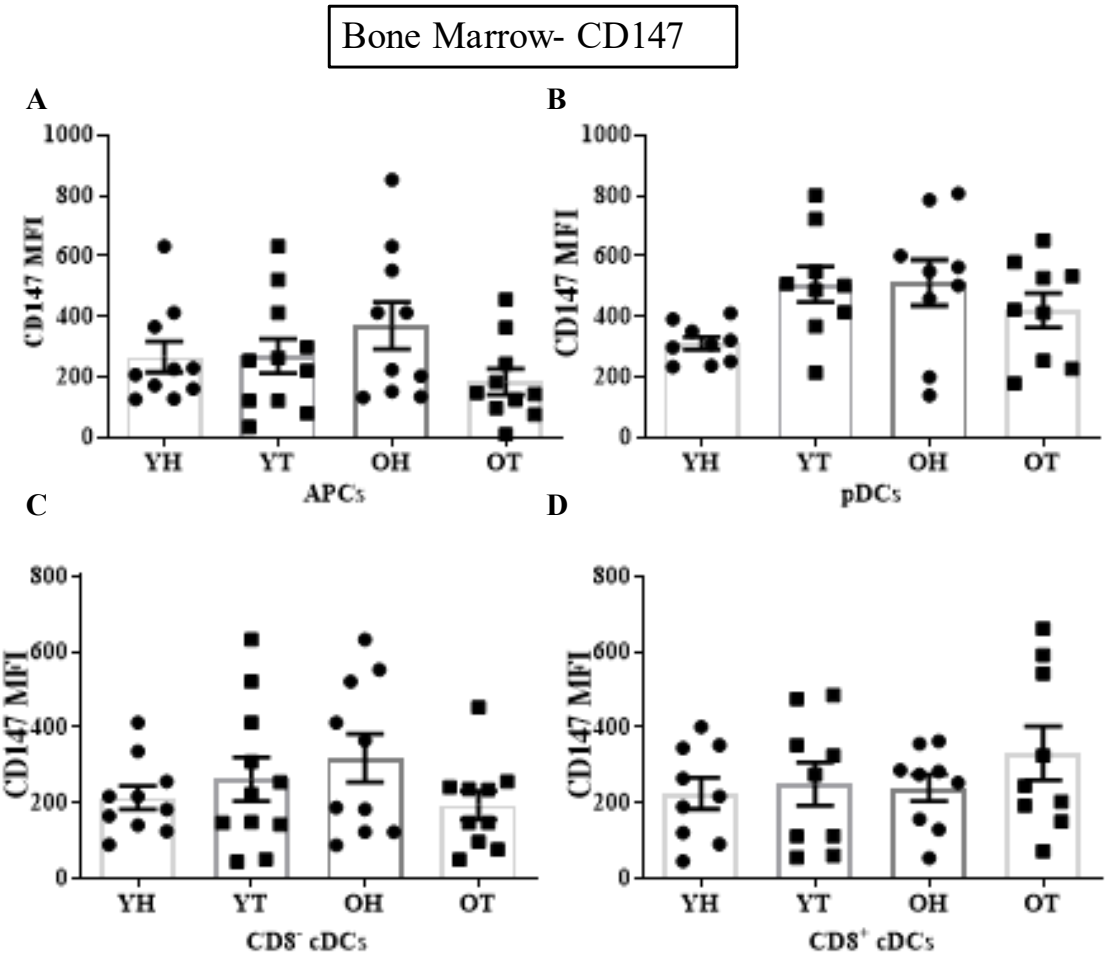

Figure 4.3: No change in CD147 with healthy ageing or tumour

Splenic DCs from YH, YT, OH and OT mice were stained with CD147. Expression levels of CD147 (measured as MFI) in **CD11c$^+$ cells(A), pDCs (B), CD11b$^+$CD8$^-$cDCs (C), CD11b$^+$CD8$^+$cDCs (D)** were measured. Data shown as mean ± SEM, n = 10-11 mice/group. * = p<0.05, ** = p<0.005, *** = p<0.0005, **** =p<0.0001. Statistical significance assessed by Kruskal-Wallis Test, followed by post-hoc Dunn's s test..

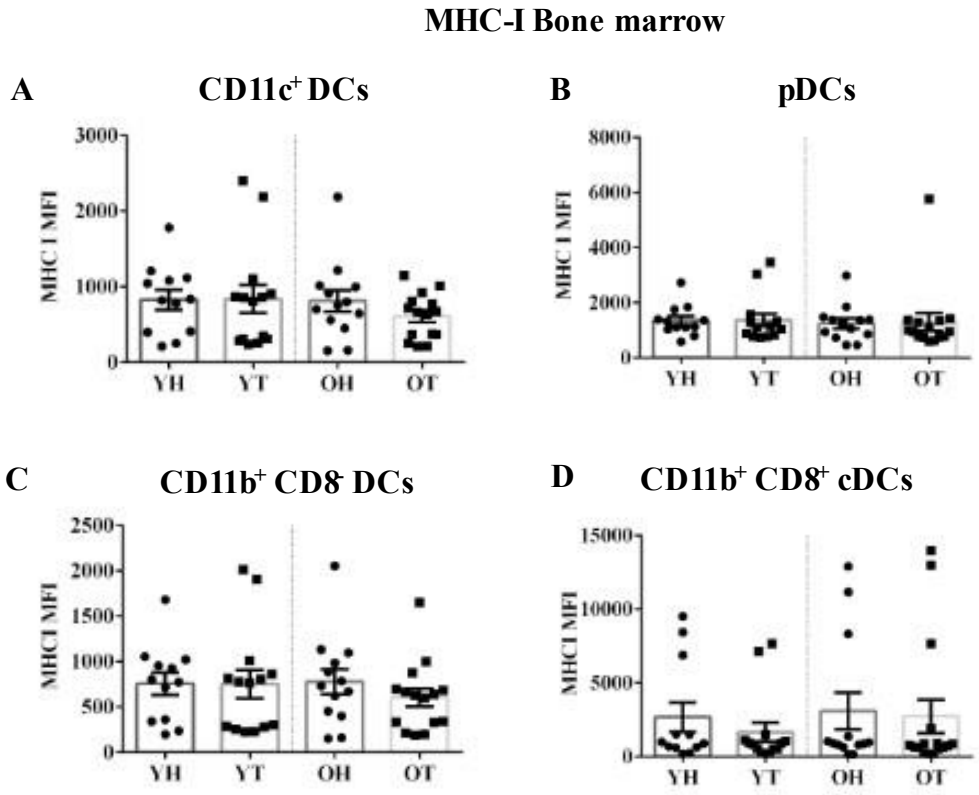

Figure 4.4: No change in MHC-I expression in BM DCs

BM DCs from YH, YT, OH and OT mice were stained with MHC-I. Expression levels of MHC-I (measured as MFI) in **$CD11c^+$ cells (APCs) (A), pDCs (B), $CD11b^+CD8^-$cDCs (C), $CD11b^+CD8^+$cDCs (D)** were measured. Data shown as mean ± SEM, n = 10-11 mice/group. * = $p<0.05$, ** = $p<0.005$, *** = $p<0.0005$, **** =$p<0.0001$. Statistical significance assessed by Kruskal-Wallis Test, followed by post-hoc Dunn's s test..

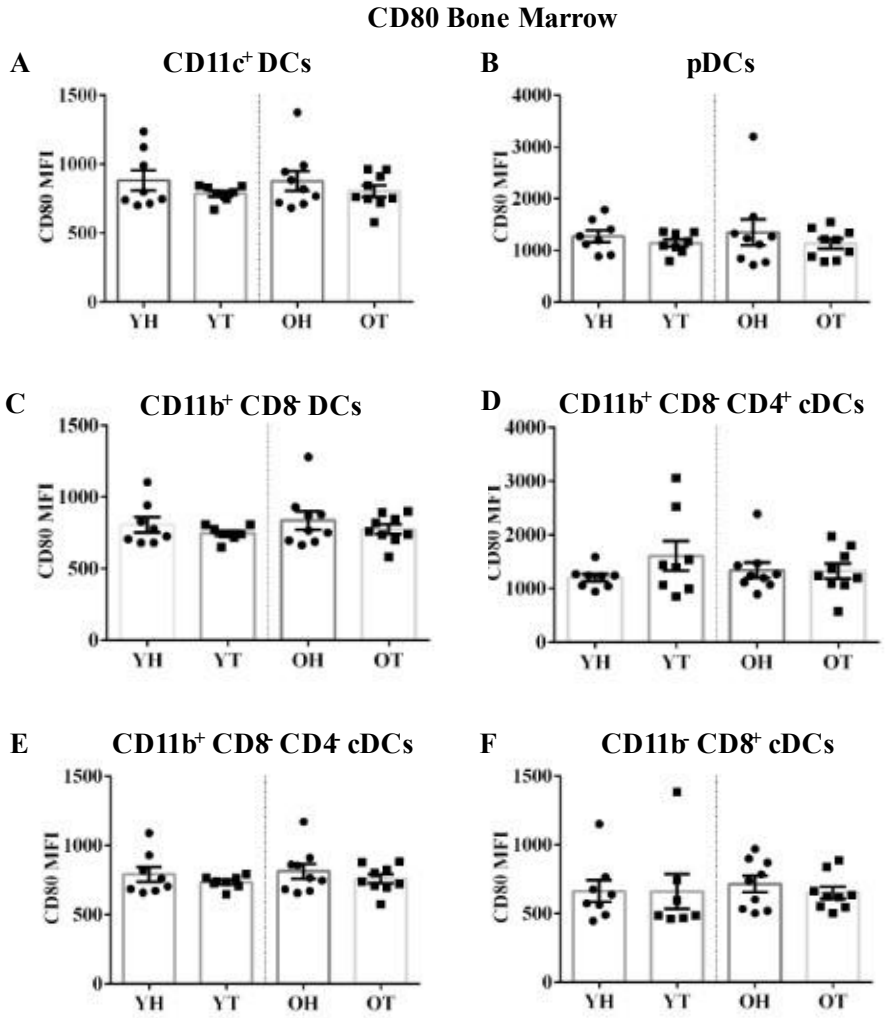

Figure 4.5: No change in CD80 expression was observed in BM DCs with healthy ageing

BM DCs from YH, YT, OH and OT mice were stained with CD80. Expression levels of CD80 (measured as MFI) in **CD11c$^+$ cells(A), pDCs (B), CD11b$^+$CD8$^-$cDCs (C), CD11b$^+$CD8$^-$CD4$^+$cDCs (D), CD11b$^+$CD8$^-$CD4$^-$cDCs (E) and CD11b$^+$CD8$^+$cDCs (F)** were measured. Data shown as mean ± SEM, n = 10-11 mice/group. * = p<0.05, ** = p<0.005, *** = p<0.0005, **** =p<0.0001. Statistical significance assessed by Kruskal-Wallis Test, followed by post-hoc Dunn's s test..

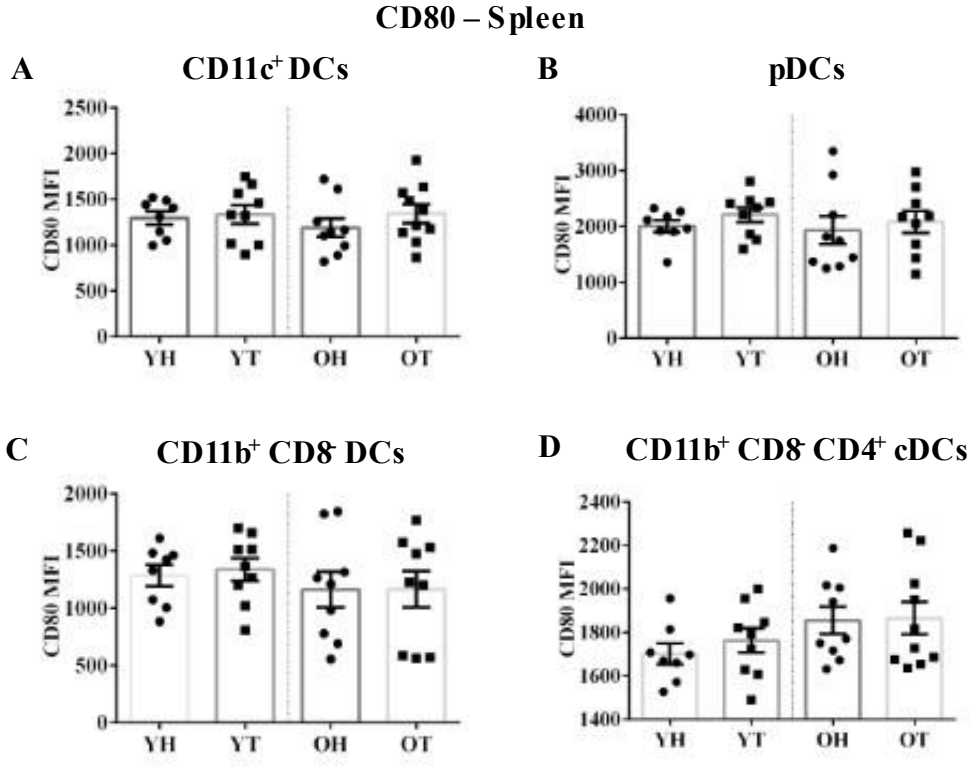

Figure 4.6: No change in CD80 expression was observed in splenic DCs with healthy ageing

Splenic DCs from YH, YT, OH and OT mice were stained with CD80. Expression levels of CD80 (measured as MFI) in **CD11c$^+$ cells(A), pDCs (B), CD11b$^+$CD8$^-$cDCs (C), CD11b$^+$CD8$^+$cDCs (D)** were measured. Data shown as mean ± SEM, n = 10-11 mice/group. * = p<0.05, ** = p<0.005, *** = p<0.0005, **** =p<0.0001. Statistical significance assessed by Kruskal-Wallis Test, followed by post-hoc Dunn's s test..

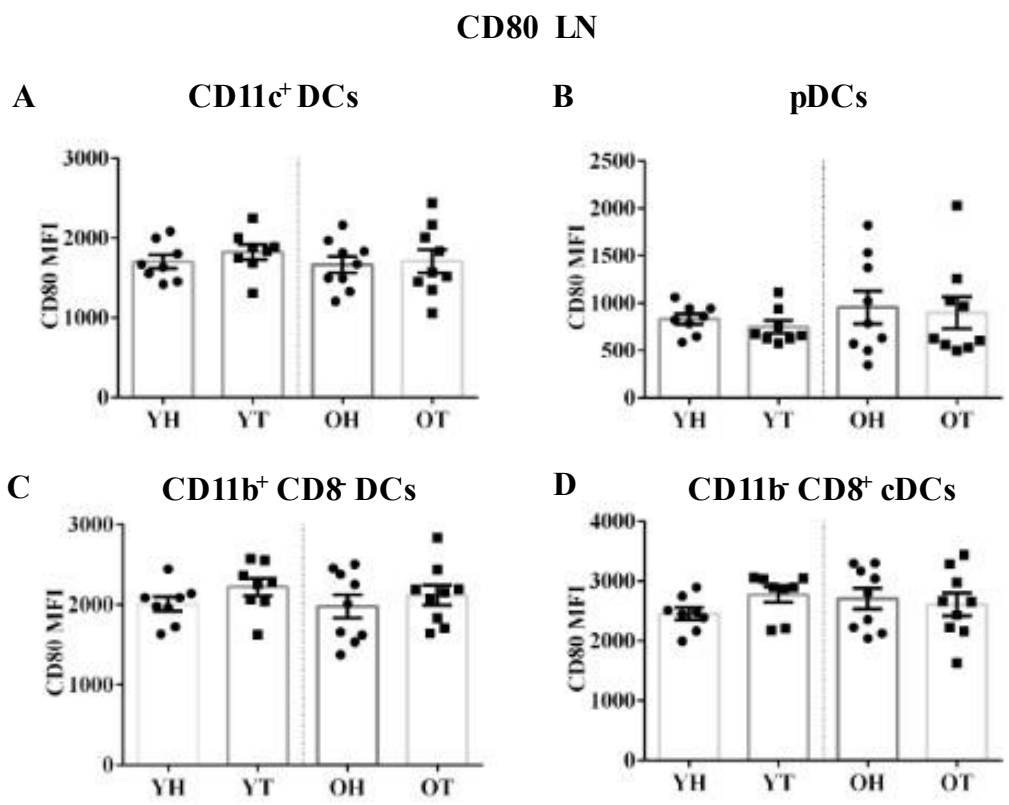

Figure 4.7: No change in CD80 expression was observed in LN DCs with healthy ageing

LN DCs from YH, YT, OH and OT mice were stained with CD80. Expression levels of CD80 (measured as MFI) in **CD11c$^+$ cells(A), pDCs (B), CD11b$^+$CD8$^-$cDCs (C), CD11b$^+$CD8$^+$cDCs (D)** were measured. Data shown as mean ± SEM, n = 10-11 mice/group. * = p<0.05, ** = p<0.005, *** = p<0.0005, **** =p<0.0001. Statistical significance assessed by Kruskal-Wallis Test, followed by post-hoc Dunn's s test..

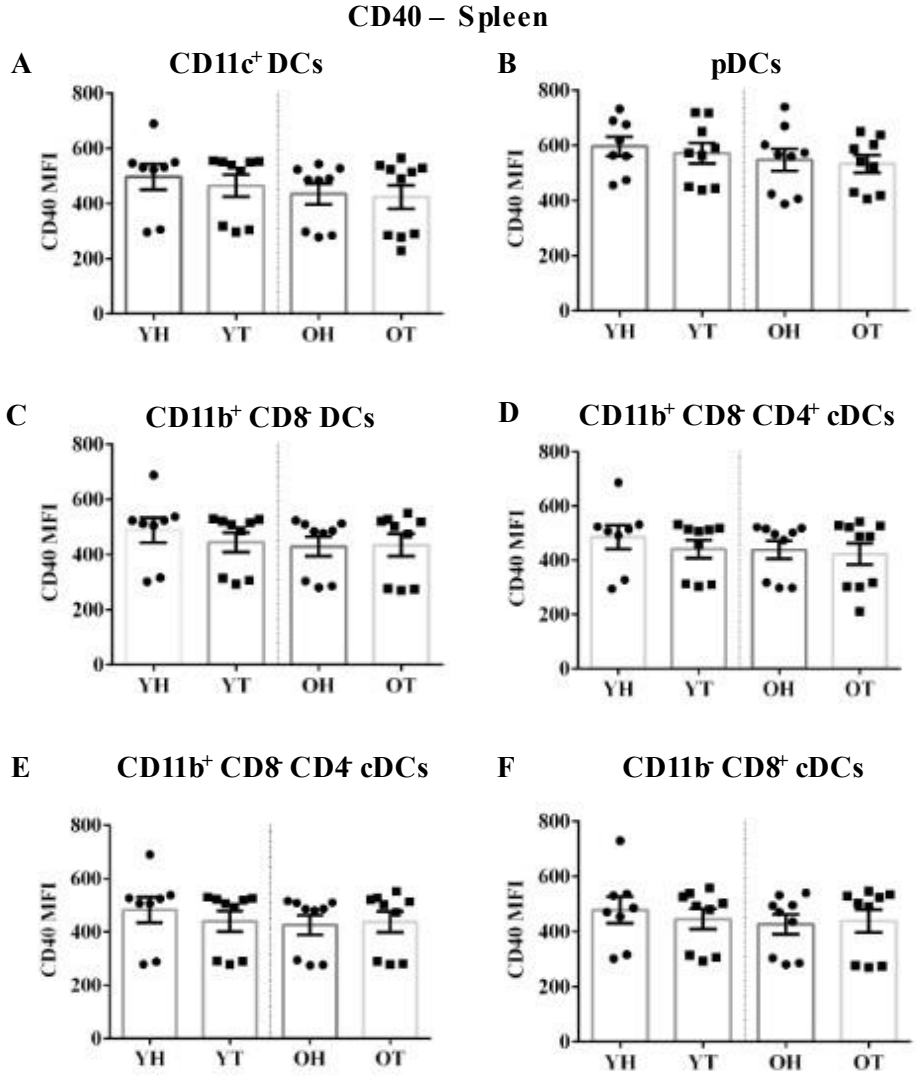

Figure 4.8: No change in CD40 expression was observed in splenic DCs with healthy ageing

Splenic DCs from YH, YT, OH and OT mice were stained with CD40. Expression levels of CD40 (measured as MFI) in **CD11c$^+$ cells(A), pDCs (B), CD11b$^+$CD8$^-$cDCs (C), CD11b$^+$CD8$^-$CD4$^+$cDCs (D), CD11b$^+$CD8$^-$CD4$^-$cDCs (E) and CD11b$^+$CD8$^+$cDCs (F)** were measured. Data shown as mean ± SEM, n = 10-11 mice/group. * = p<0.05, ** = p<0.005, *** = p<0.0005, **** =p<0.0001. Statistical significance assessed by Kruskal-Wallis Test, followed by post-hoc Dunn's s test.

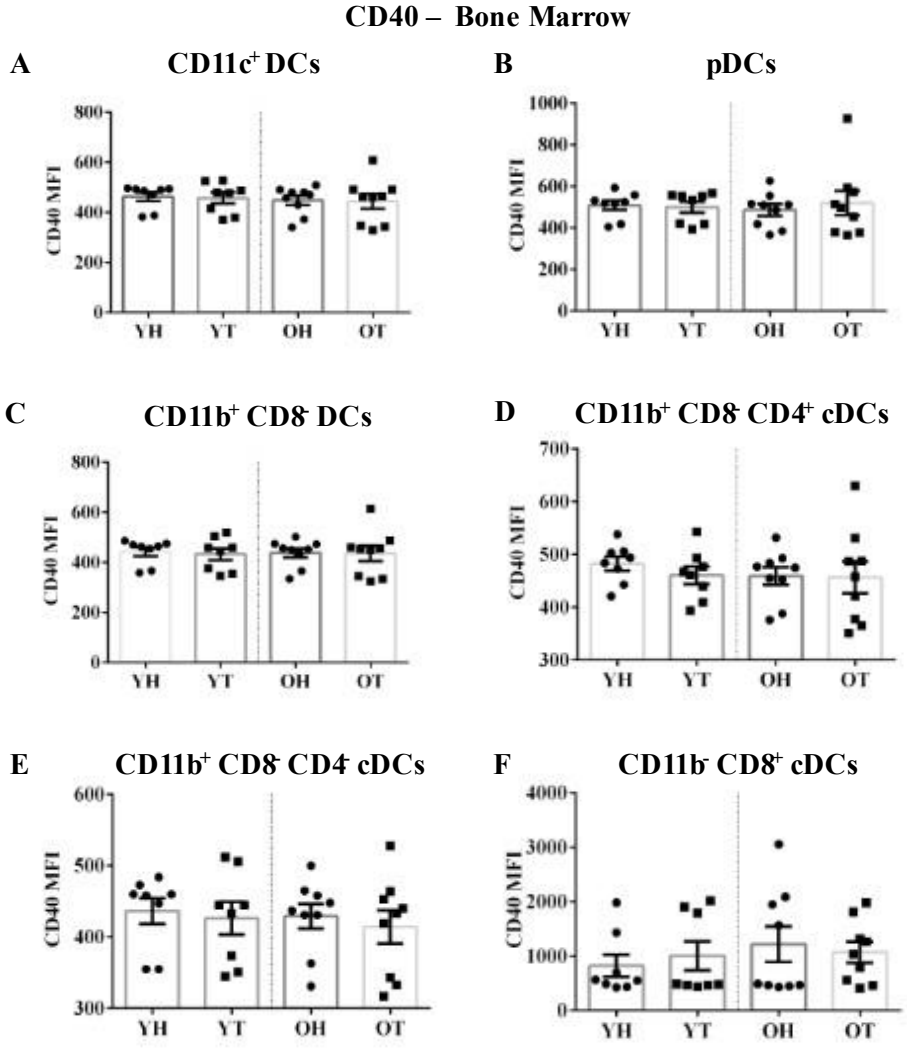

Figure 4.9: No change in CD40 expression was observed in BM DCs with healthy ageing

BM DCs from YH, YT, OH and OT mice were stained with CD40. Expression levels of CD40 (measured as MFI) in **CD11c$^+$ cells(A), pDCs (B), CD11b$^+$CD8$^-$cDCs (C), CD11b$^+$CD8$^-$CD4$^+$cDCs (D), CD11b$^+$CD8$^-$CD4$^-$cDCs (E) and CD11b$^+$CD8$^+$cDCs (F)** were measured. Data shown as mean ± SEM, n = 10-11 mice/group. * = p<0.05, ** = p<0.005, *** = p<0.0005, **** =p<0.0001. Statistical significance assessed by Kruskal-Wallis Test, followed by post-hoc Dunn's s test..

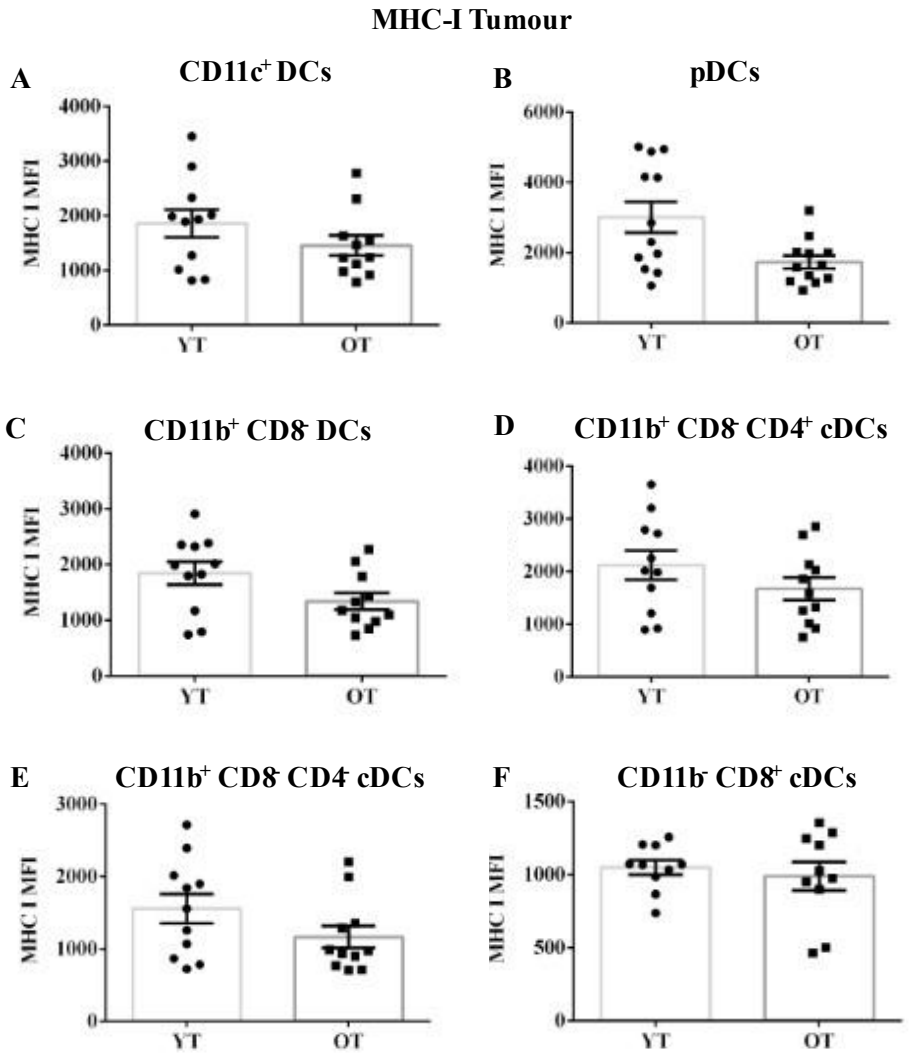

Figure 4.10: No change in MHC-I in TADCs

Tumour DCs from YH, YT, OH and OT mice were stained with MHC-I which is a member of class B scavenger receptor family and imports fatty acids inside the cells. Expression levels of MHC-I (measured as MFI) in **CD11c$^+$ cells(A), pDCs (B), CD11b$^+$CD8$^-$cDCs (C), CD11b$^+$CD8$^-$CD4$^+$cDCs (D), CD11b$^+$CD8$^-$CD4$^-$cDCs (E) and CD11b$^+$CD8$^+$cDCs (F)** were measured. Data shown as mean ± SEM, n = 10-11 mice/group. * = p<0.05, ** = p<0.005, *** = p<0.0005, **** =p<0.0001. Statistical significance assessed by Kruskal-Wallis Test, followed by post-hoc Dunn's s test..

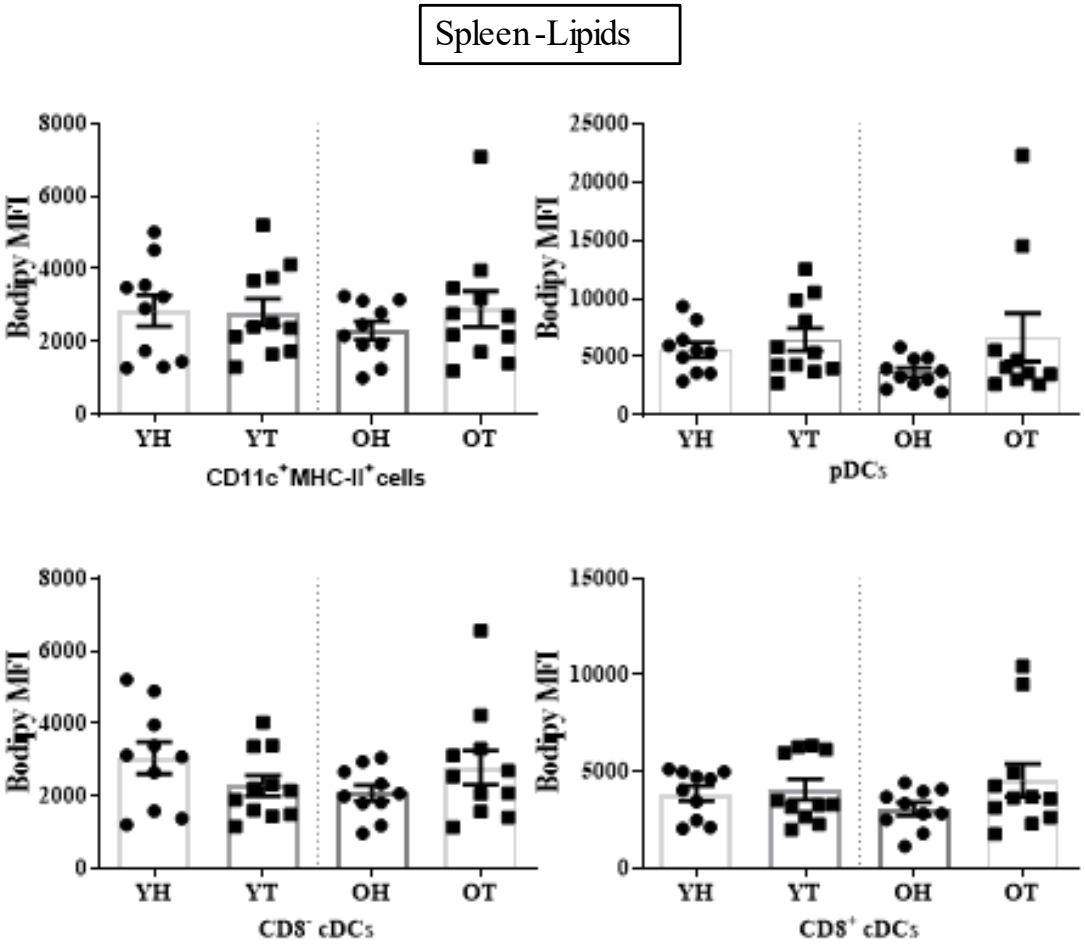

Figure 4.11: Lipid levels remain unchanged in different DC subsets

Splenic DCs from young healthy (YH), young tumour-bearing (YT), old healthy (OH) and old tumour-bearing mice (OT) were stained for Bodipy and analysed by flow cytometry. Expression levels of Bodipy (measured as MFI) in APCs (**$CD11c^+$ MHC-II+ cells(A), pDCs (B), $CD11b^+CD8^-$cDCs (C), $CD11b^+CD8^+$cDCs (D)** were measured. Data shown as mean ± SEM, n = 10-11 mice/group. * = $p<0.05$, ** = $p<0.005$, *** = $p<0.0005$, **** =$p<0.0001$. Statistical significance assessed by Kruskal-Wallis Test, followed by post-hoc Dunn's s test.

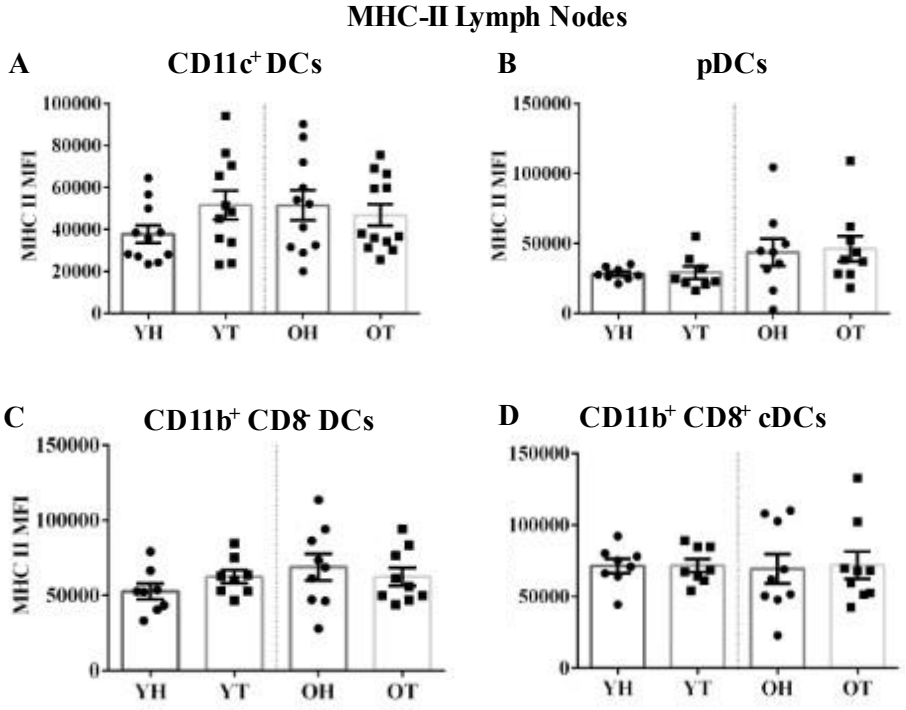

Figure 4.12: MHC-II levels remain unchanged in different DC subsets

Splenic DCs from young healthy (YH), young tumour-bearing (YT), old healthy (OH) and old tumour-bearing mice (OT) were stained for MHC-II and analysed by flow cytometry. Expression levels of MHc-I (measured as MFI) in **$CD11c^+$ cells(A), pDCs (B), $CD11b^+CD8^-$cDCs (C), $CD11b^+CD8^+$cDCs (D)** were measured. Data shown as mean ± SEM, n = 10-11 mice/group. * = $p<0.05$, ** = $p<0.005$, *** = $p<0.0005$, **** =$p<0.0001$. Statistical significance assessed by Kruskal-Wallis Test, followed by post-hoc Dunn's s test.

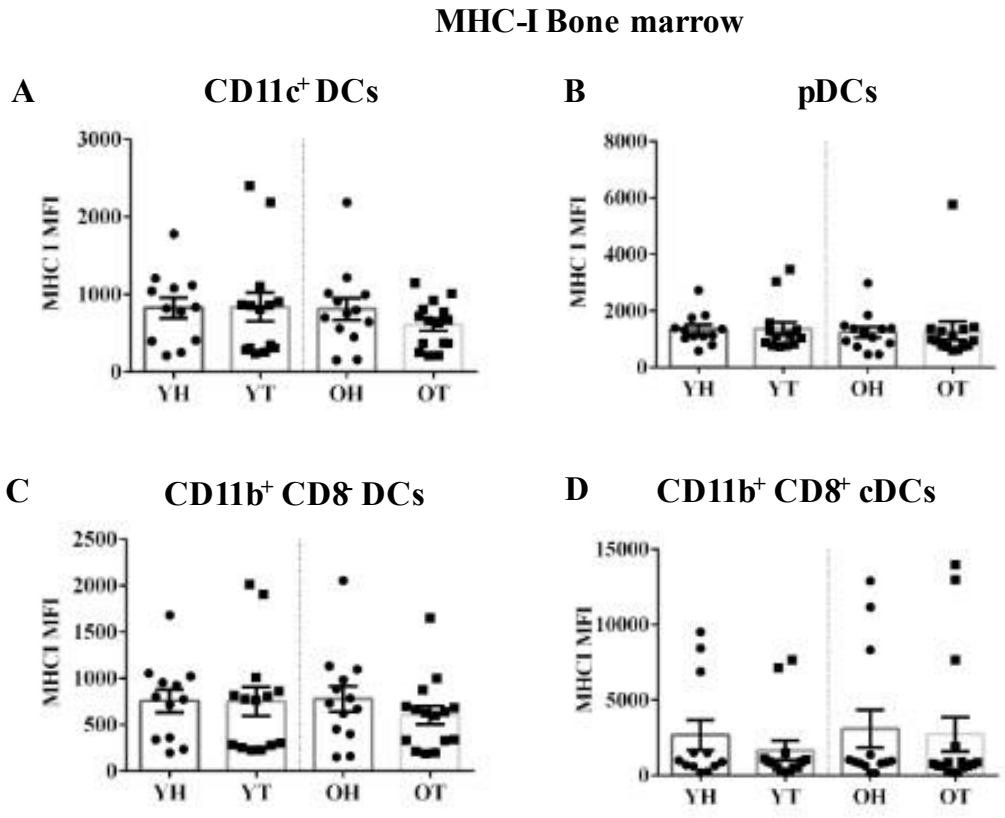

Figure 4.13: MHC-I levels remain unchanged in different DC subsets

BM DCs from young healthy (YH), young tumour-bearing (YT), old healthy (OH) and old tumour-bearing mice (OT) were stained for MHC-I and analysed by flow cytometry. Expression levels of MHC-I (measured as MFI) in **CD11c$^+$ cells(A), pDCs (B), CD11b$^+$CD8$^-$cDCs (C), CD11b$^+$CD8$^+$cDCs (D)** were measured. Data shown as mean ± SEM, n = 10-11 mice/group. * = p<0.05, ** = p<0.005, *** = p<0.0005, **** =p<0.0001. Statistical significance assessed by Kruskal-Wallis Test, followed by post-hoc Dunn's s test.

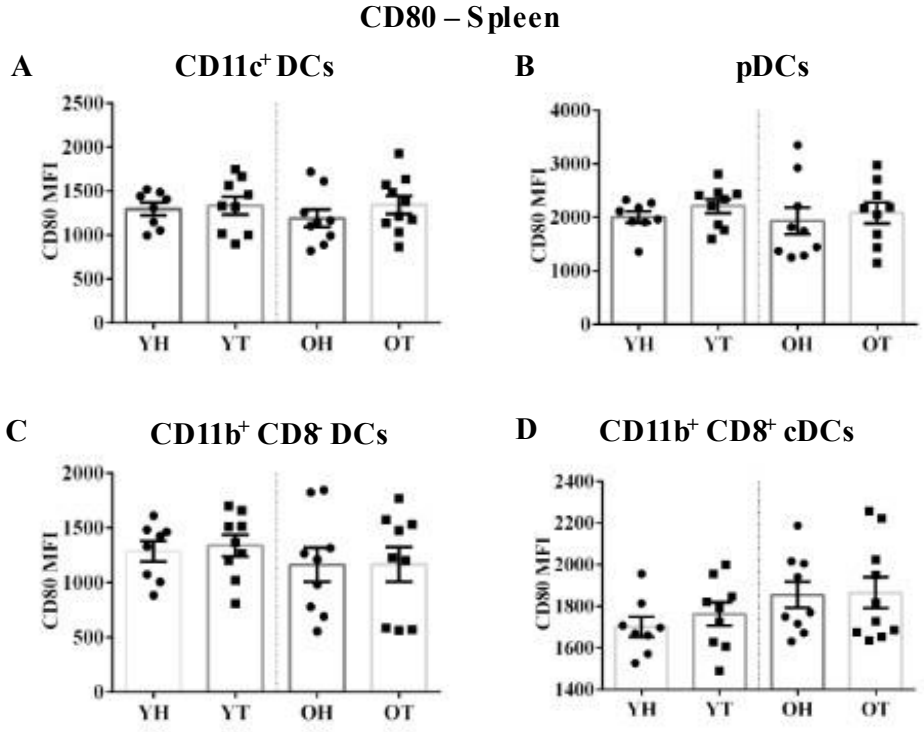

Figure 4.14: CD80 levels remain unchanged in different DC subsets

Splenic DCs from young healthy (YH), young tumour-bearing (YT), old healthy (OH) and old tumour-bearing mice (OT) were stained for CD80 and analysed by flow cytometry. Expression levels of CD80 (measured as MFI) in **$CD11c^+$ cells(A), pDCs (B), $CD11b^+CD8^-$cDCs (C), $CD11b^+CD8^+$cDCs (D)** were measured. Data shown as mean ± SEM, n = 10-11 mice/group. * = $p<0.05$, ** = $p<0.005$, *** = $p<0.0005$, **** =$p<0.0001$. Statistical significance assessed by Kruskal-Wallis Test, followed by post-hoc Dunn's s test.

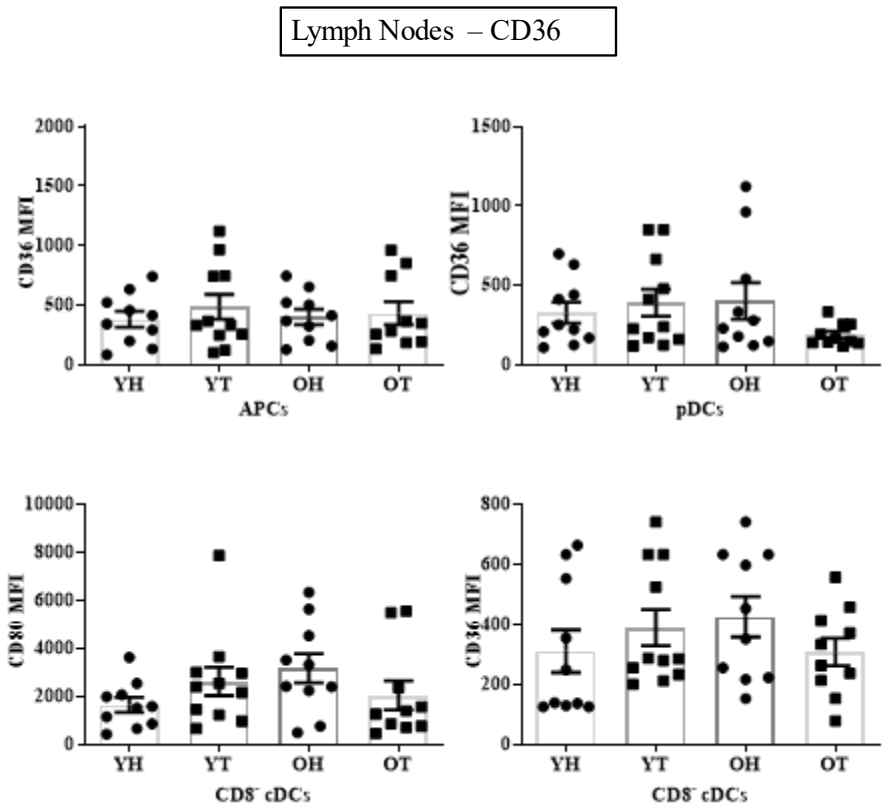

Figure 4.15: CD36 levels remain unchanged in different LN DC subsets

LN DCs from young healthy (YH), young tumour-bearing (YT), old healthy (OH) and old tumour-bearing mice (OT) were stained for CD36 and analysed by flow cytometry. Expression levels of CD36 (measured as MFI) in APCs(**$CD11c^+$ MHC-II+ cells(A), pDCs (B), $CD11b^+CD8^-$cDCs (C), $CD11b^+CD8^+$cDCs (D)** were measured. Data shown as mean ± SEM, n = 10-11 mice/group. * = $p<0.05$, ** = $p<0.005$, *** = $p<0.0005$, **** =$p<0.0001$. Statistical significance assessed by Kruskal-Wallis Test, followed by post-hoc Dunn's s test.

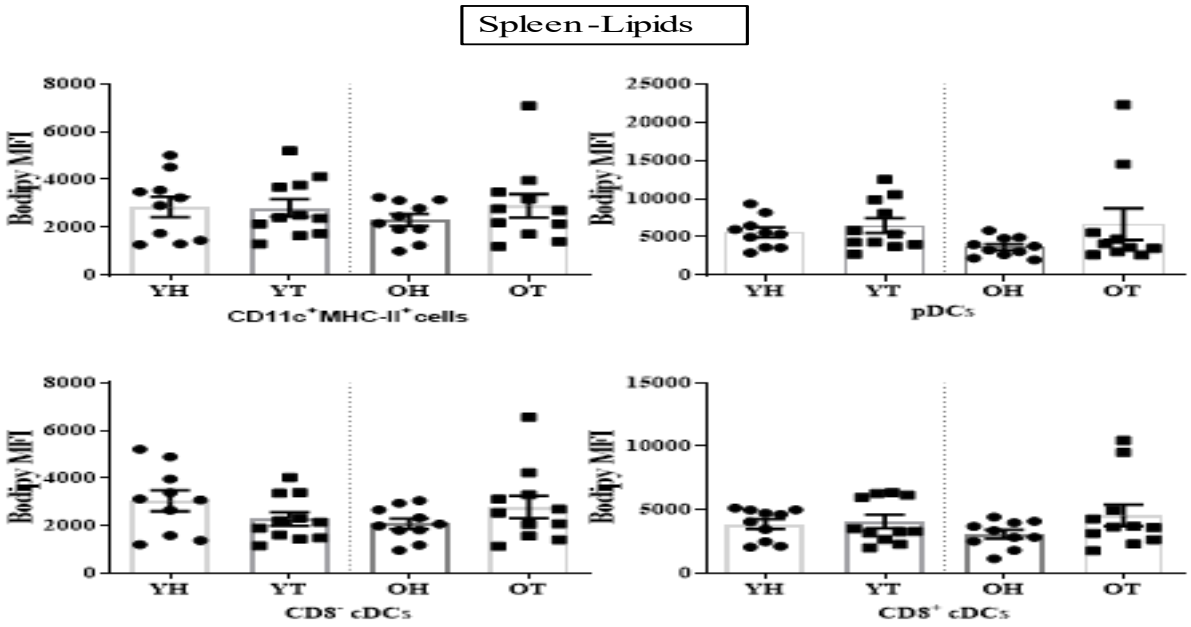

Figure 4.16: Lipid levels remain unchanged in different splenic subsets
Splenic DCs from young healthy (YH), young tumour-bearing (YT), old healthy (OH) and old tumour-bearing mice (OT) were stained for Bodipy and analysed by flow cytometry. Expression levels of Bodipy (measured as MFI) in APCs (**CD11c$^+$ MHC-II+ cells(A), pDCs (B), CD11b$^+$CD8$^-$cDCs (C), CD11b$^+$CD8$^+$cDCs (D)** were measured. Data shown as mean ± SEM, n = 10-11 mice/group. * = p<0.05, ** = p<0.005, *** = p<0.0005, **** =p<0.0001. Statistical significance assessed by Kruskal-Wallis Test, followed by post-hoc Dunn's s test..

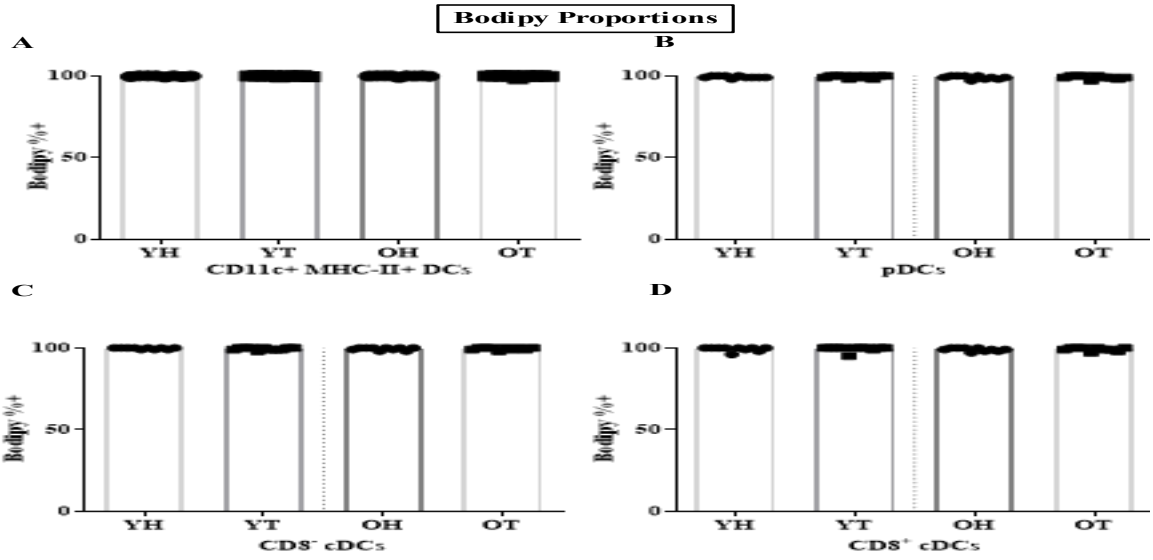

Figure 4.17: All BM DC subsets shows 100% Bodipy percent positive
BM DCs from young healthy (YH), young tumour-bearing (YT), old healthy (OH) and old tumour-bearing mice (OT) were stained for Bodipy and analysed by flow cytometry. Proportion of Bodipy+ in APCs(**CD11c$^+$ MHC-II+ cells(A), pDCs (B), CD11b$^+$CD8$^-$cDCs (C), CD11b$^+$CD8$^+$cDCs (D)** were measured. Data shown as mean ± SEM, n = 10-11 mice/group. * = p<0.05, ** = p<0.005, *** = p<0.0005, **** =p<0.0001. Statistical significance assessed by Kruskal-Wallis Test, followed by post-hoc Dunn's s test..

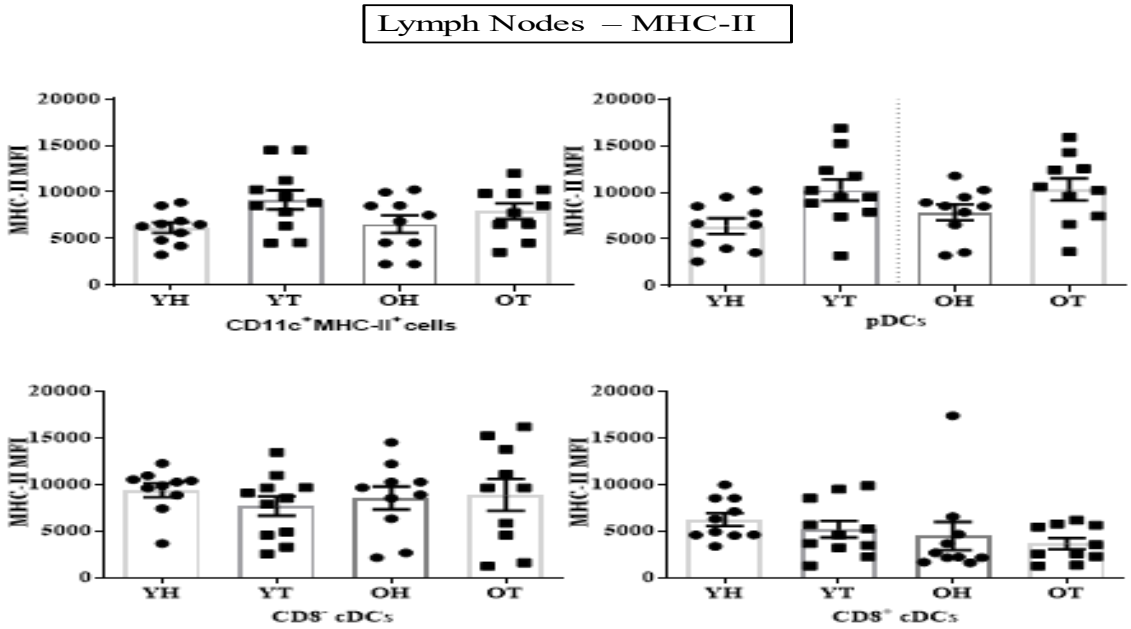

Figure 4.18: No changes in MHC-II in LN DC subsets

LN DCs from young healthy (YH), young tumour-bearing (YT), old healthy (OH) and old tumour-bearing mice (OT) were stained for MHC-II and analysed by flow cytometry. Expression of MHC-II in APCs(**$CD11c^+$ MHC-II+ cells(A), pDCs (B), $CD11b^+CD8^-$cDCs (C), $CD11b^+CD8^+$cDCs (D)** were measured. Data shown as mean ± SEM, n = 10-11 mice/group. * = p<0.05, ** = p<0.005, *** = p<0.0005, **** =p<0.0001. Statistical significance assessed by Kruskal-Wallis Test, followed by post-hoc Dunn's s test..

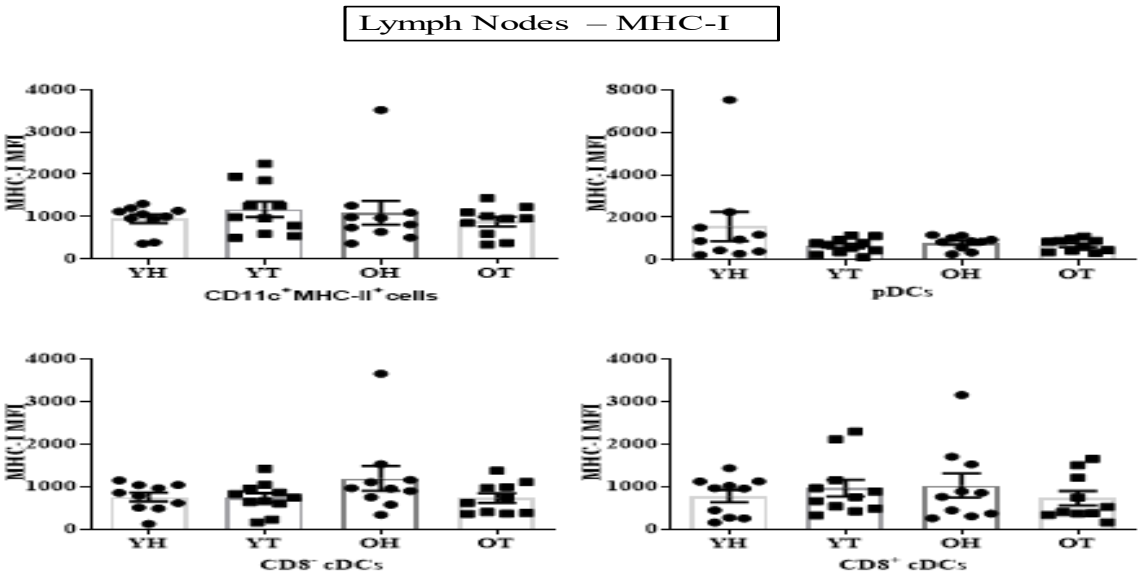

Figure 4.19: No changes in MHC-I in LN DC subsets

LN DCs from young healthy (YH), young tumour-bearing (YT), old healthy (OH) and old tumour-bearing mice (OT) were stained for MHC-I and analysed by flow cytometry. Expression of MHC-I in APCs(**$CD11c^+$ MHC-II+ cells(A), pDCs (B), $CD11b^+CD8^-$cDCs (C), $CD11b^+CD8^+$cDCs (D)** were measured. Data shown as mean ± SEM, n = 10-11 mice/group. * = p<0.05, ** = p<0.005, *** = p<0.0005, **** =p<0.0001. Statistical significance assessed by Kruskal-Wallis Test, followed by post-hoc Dunn's s test..

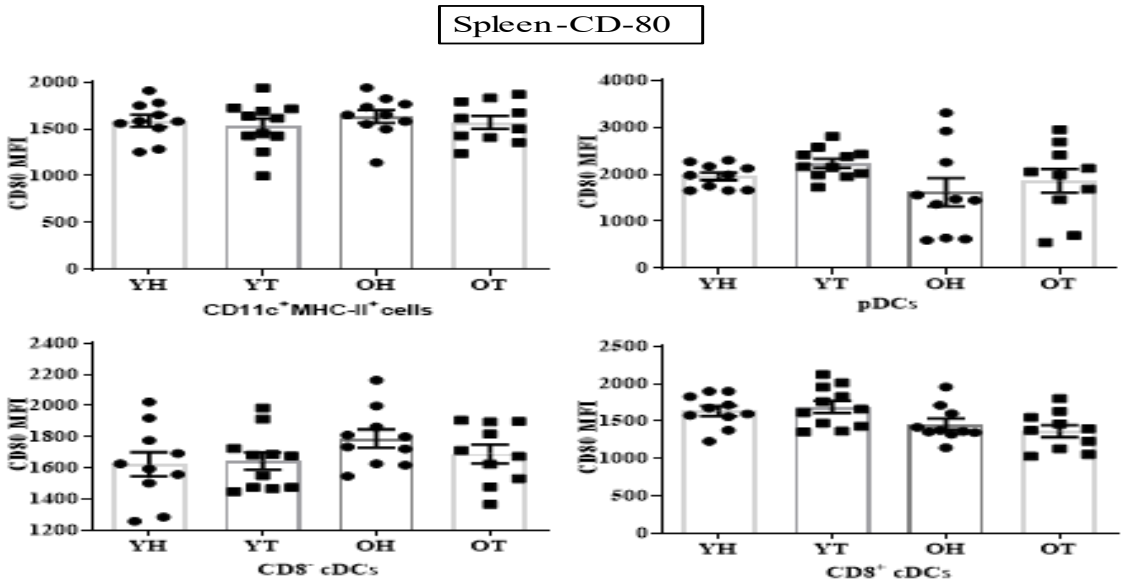

Figure 4.20: No change in CD80 in DC subsets

Splenic DCs from young healthy (YH), young tumour-bearing (YT), old healthy (OH) and old tumour-bearing mice (OT) were stained for CD80 and analysed by flow cytometry. Expression levels of CD80 (measured as MFI) in APCs (**$CD11c^+$ MHC-II+ cells(A), pDCs (B), $CD11b^+CD8^-$cDCs (C), $CD11b^+CD8^+$cDCs (D)** were measured. Data are shown as mean ± SEM, n = 10-11 mice/group. * = p<0.05, ** = p<0.005, *** = p<0.0005, **** =p<0.0001. Statistical significance assessed by Kruskal-Wallis Test.

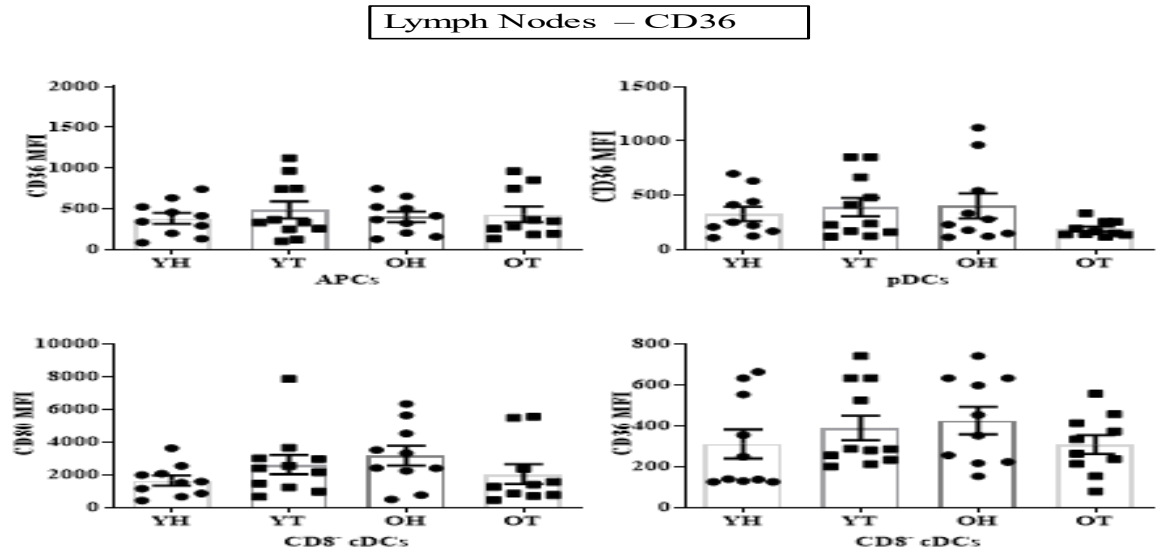

Figure 4.21: No change in CD36 in LN DC subsets

LN DCs from young healthy (YH), young tumour-bearing (YT), old healthy (OH) and old tumour-bearing mice (OT) were stained for CD36 and analysed by flow cytometry. Expression levels of CD36(measured as MFI) in APCs (**$CD11c^+$ MHC-II+ cells(A), pDCs (B), $CD11b^+CD8^-$cDCs (C), $CD11b^+CD8^+$cDCs (D)** were measured. Data are shown as mean ± SEM, n = 10-11 mice/group. * = p<0.05, ** = p<0.005, *** = p<0.0005, **** =p<0.0001. Statistical significance assessed by Kruskal-Wallis Test.

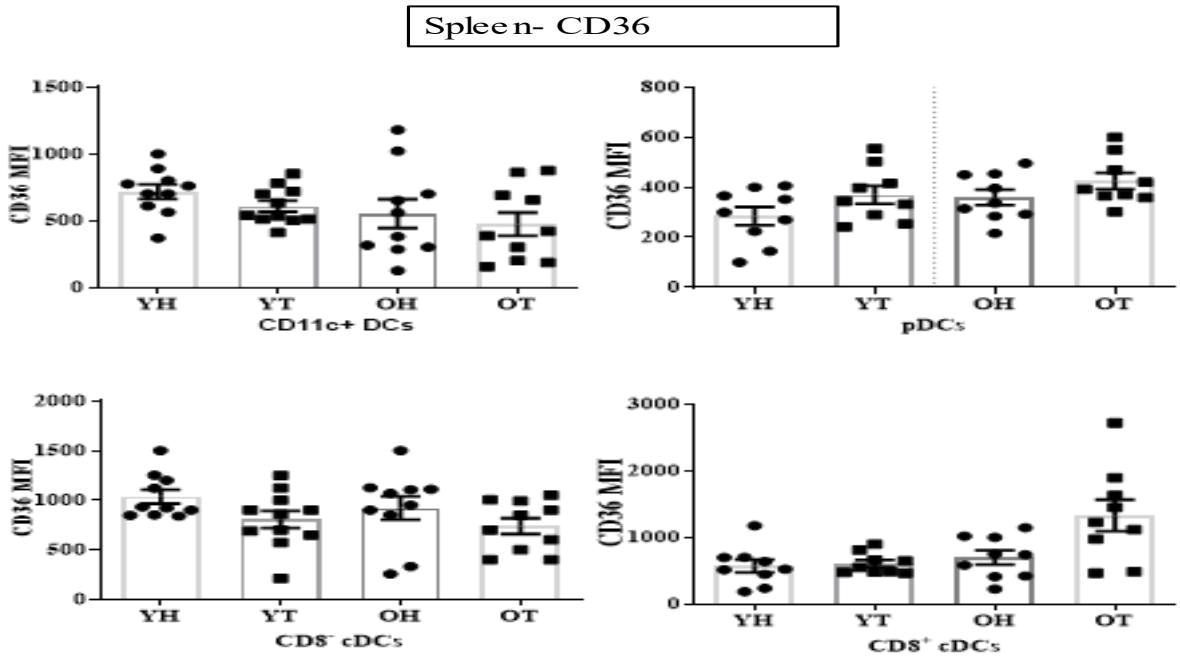

Figure 4.22: No change in CD36 in splenic DC subsets

Splenic DCs from young healthy (YH), young tumour-bearing (YT), old healthy (OH) and old tumour-bearing mice (OT) were stained for CD36 and analysed by flow cytometry. Expression levels of CD36 (measured as MFI) in APCs **CD11c$^+$ MHC-II+ cells(A), pDCs (B), CD11b$^+$CD8$^-$cDCs (C), CD11b$^+$CD8$^+$cDCs (D)** were measured. Data are shown as mean ± SEM, n = 10-11 mice/group. * = p<0.05, ** = p<0.005, *** = p<0.0005, **** =p<0.0001. Statistical significance assessed by Kruskal-Wallis Test.

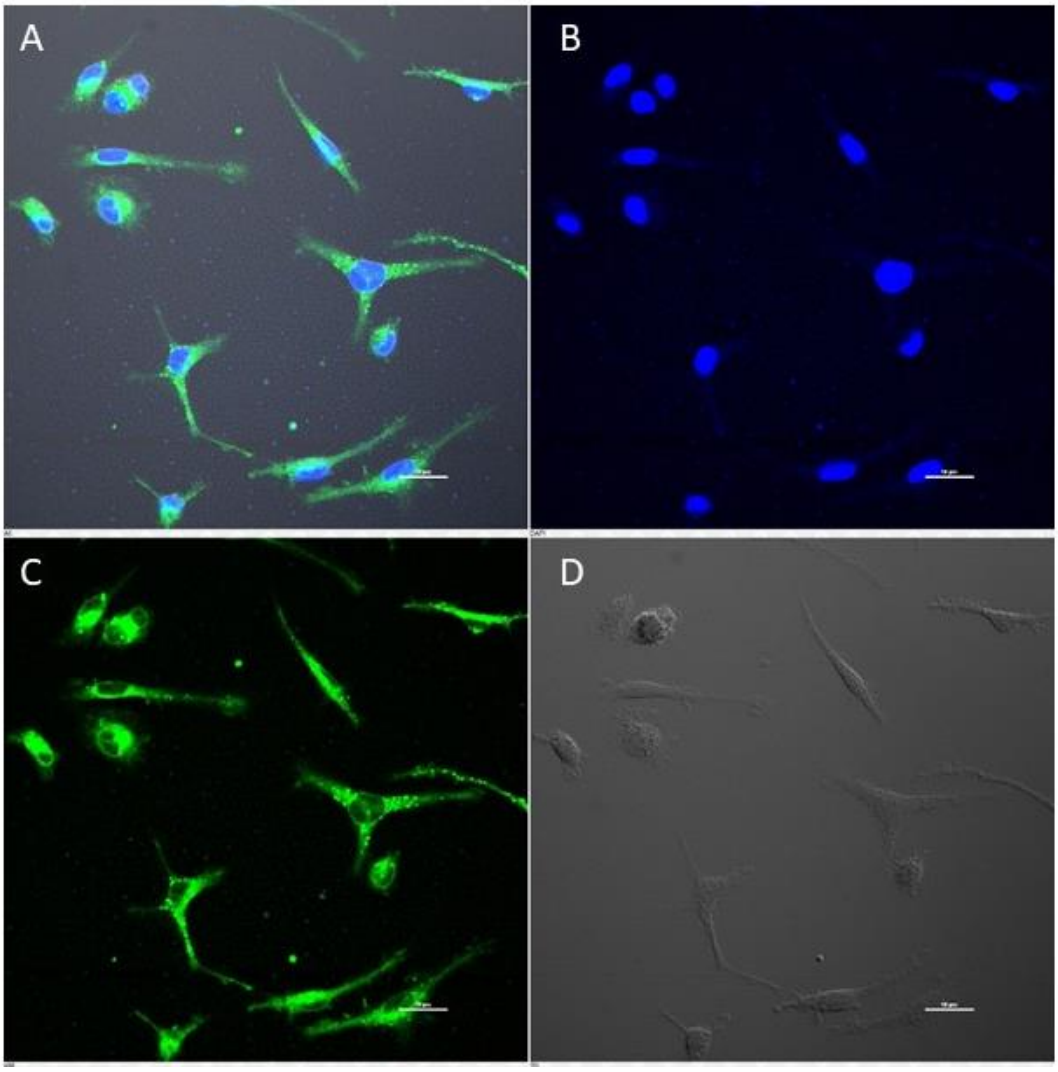

Figure 4.23: Shows confocal microscopy imaging of mesothelioma-exposed DCs. DCs were cultured on glass bottom plates. Overlay of Bodipy, DAPI and phase contrast is shown in [A], DAPI (nucleus, blue) [B] Bodipy (lipids, green) [C] and, phase contrast [D].

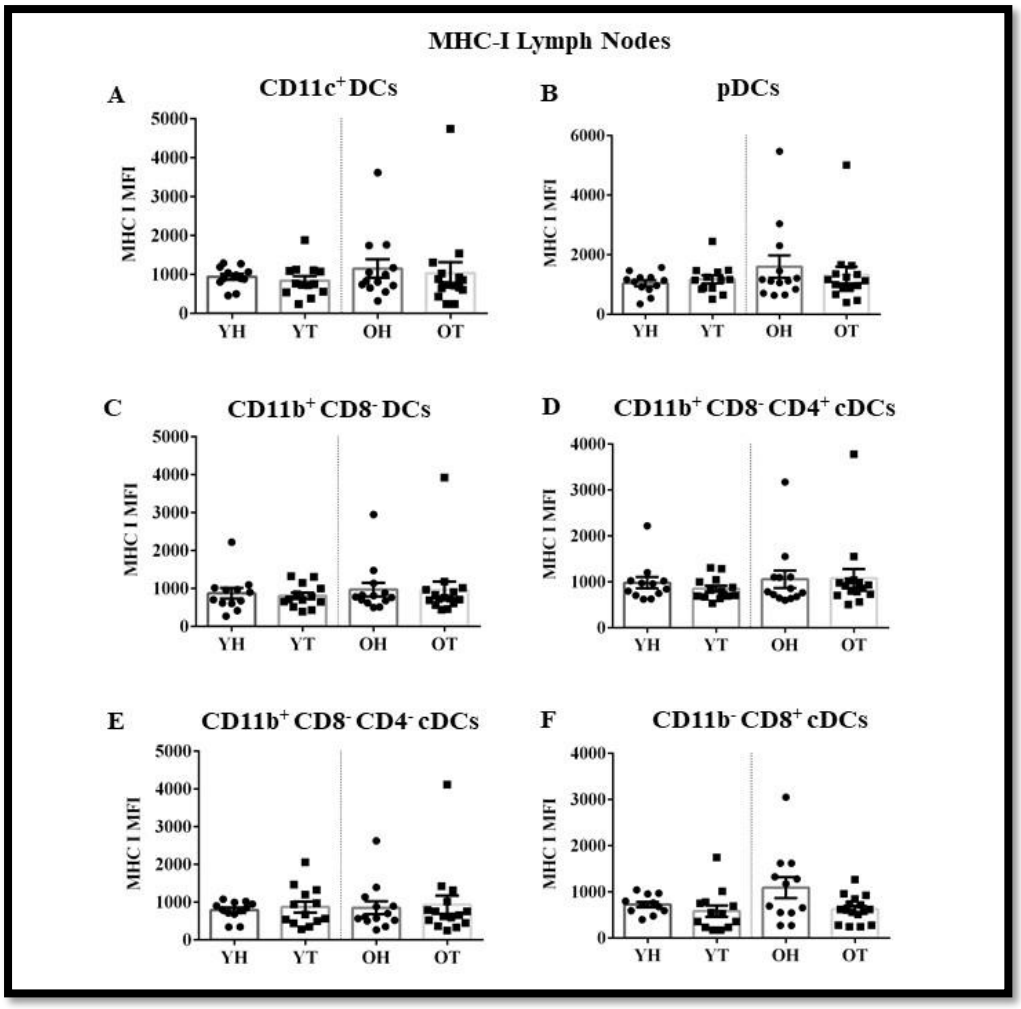

Figure 4.24: No change in MHC-I on LN DCs

LN DCs from young healthy (YH), young tumour-bearing (YT), old healthy (OH) and old tumour-bearing mice (OT) were stained for MHC-I and analysed by flow cytometry. Expression levels of MHC-I (measured as geometric mean fluorescence intensity; MFI in different subpopulations of dendritic cells $CD11c^+$ DCs (A), pDCs (B), $CD11b^+CD8^-$ DCs (C), $CD11b^+CD8^-CD4^+$ cDCs (D), $CD11b^+CD8^-CD4^-$ cDCs (E), $CD11b^-CD8^+$ cDCs (F) were measured. Data are shown as mean ± SEM, n = 10-11 mice/group. Statistical significance assessed by Kruskal Wallis Test.

Supplementary data for chapter 5

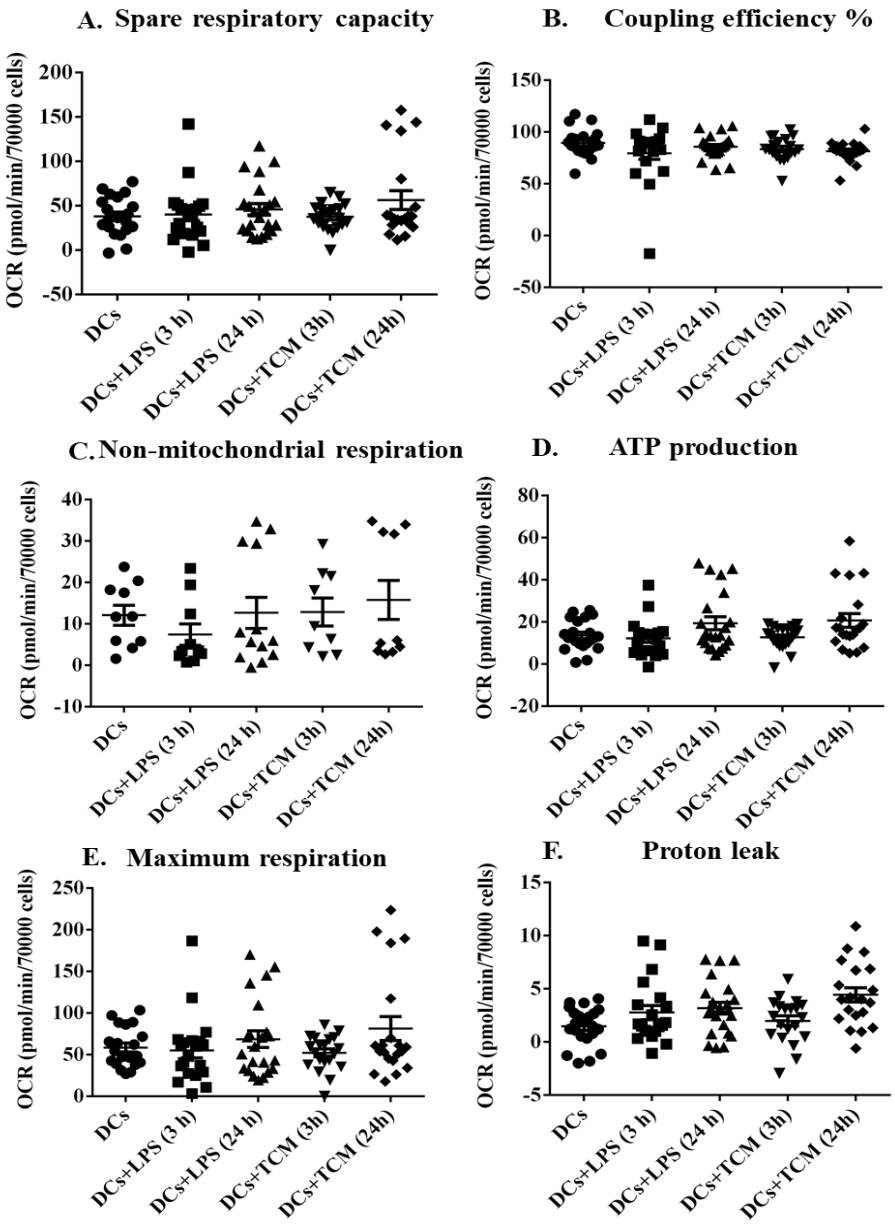

Supplementary Figure 5.1 No changes in individual mitochondrial parameters

Individual parameters for spare respiratory capacity **(A),** coupling efficiency **(B),** non-mitochondrial respiration (**C),** ATP production **(D),** maximal respiration **(E)**, proton leak **(F)** were measured. Spare respiratory capacity is the difference between the maximum and basal respiration. Coupling efficiency is the ATP production rate divided by the basal respiration. Non-mitochondrial respiration is the minimum rate measurement after rotenone/antimycin injection. ATP production is the difference in OCR before and after oligomycin. Maximal respiration is the OCR after carbonyl cyanide m-chlorophenylhydrazone (CCCP) injection and antimycin A/rotenone. Proton leak is the difference in oxygen consumption rate (OCR) after oligomycin injection and antimycin A/rotenone. The data are represented as mean SEM.

Healthy Volunteer Questionnaire (ID code:)

1. Age _____years
2. Gender Male ☐ Female ☐
3. Date of Birth ___/___/___

4. Have you ever been diagnosed with any of the following conditions?

☐ Heart problems
☐ High blood fats
☐ High blood pressure
☐ Stroke
☐ Easy bleeding
☐ Allergy
☐ Asthma
☐ Rheumatoid arthritis
☐ Diabetes
☐ Other autoimmune diseases (e.g. Lupus, MS)
☐ Cancer of _____ _____
☐ Other _____ _____

5. Statement of present health (please tick the box)

Excellent ☐ Good ☐ Fair ☐ Poor ☐
Please Explain
_____
_____

6. Are you currently taking any steroid medicines?

☐ Cortisone
☐ Corticosteroids
☐ Cortisone acetate
☐ Prednisone
☐ Prednisolone
☐ Dexamethasone
☐ Decadron
☐ Hydrocortisone
☐ Solumedrol
☐ Other _____

7. Are you currently taking any anticoagulant (blood thinning) medicines?

☐ Warfarin ☐ Fondaparinux

☐ Heparin ☐ Aspirin

☐ Clexane ☐ Other _____

☐ Fragmin

8. Are you currently taking any medicines for lowering blood fats?

☐ Atorvastatin (Lipitor) ☐ Gemfibrozil

☐ Simvastatin (Zocor) ☐ Fenofibrate

☐ Rosuvastatin (Crestor) ☐ Other _____

☐ Pravastatin (Pravachol)

9. Have you been prescribed anti-inflammatory medicines?

☐ Ibuprofen (Nurofen) ☐ Other _____

☐ Celecoxib

10. Please list all prescription medication currently being taken

_____
_____
_____

11. Please list all non-prescription medication currently being taken

_____
_____
_____

12. Do you currently smoke tobacco (cigarette, cigar or pipe)?

☐ Yes, on most or all days ☐ Only occasionally ☐ No

13. Have you been knowingly exposed to asbestos? E.g. Brake pads, asbestos fencing, shipbuilding industry, etc.

☐ Yes ☐ No